PROTEIN-BASED DRUG DELIVERY SYSTEMS

A thesis
submitted in partial fulfilment
of the requirements for the degree
of
Doctor of Philosophy in Chemistry
at the
University of Canterbury

Marie A. Squire

UNIVERSITY OF CANTERBURY
Te Whare Wānanga o Waitaha
CHRISTCHURCH NEW ZEALAND

2004

"...There's jasmine! Alcohol there! Bergamont there! Storax there! Grenouille went on crowing, and at each name he pointed to a different spot in the room, although it was so dark that at best you could only surmise the shadows of the cupboards filled with bottles."
(Patrick Süsskind, *Perfume*)

The only lifelong, reliable motivations are those that come from within, and one of the strongest of those is the joy and pride that grow from knowing that you've just done something as well as you can do it.
(Lloyd Dobens and Clare Crawford-Mason, *Thinking About Quality*)

ACKNOWLEDGEMENTS

I would first like to thank my supervisors, Professor Murray Munro and Professor John Blunt, for their encouragement, guidance and support throughout my time at Canterbury.

The Chemistry Department, University of Canterbury, has been a brilliant environment to work in. I would like to thank the academic and technical staff for their open and friendly expertise and assistance. In particular, I am indebted to Bruce Clark for his countless hours of teaching, repairing, and helping me with my mass spectrometric analyses. I would also like to thank Gill Ellis for her help and support and the biological assays. Special thanks go to past and present members of the Marine Chemistry group, and to the Action Packed Mentallists, Dean Stark Naked, Mixed Muppets, and the Beer O'clock team. You have all been wonderfully supportive, helpful, hilariously entertaining and full of gossip. Thank you all for making my time at Canterbury a wonderful and unforgettable experience.

I am very grateful to Dr Michael Boyd and Dr Barry O'Keefe, for the collaborative agreement to undertake this project, and for the wonderful opportunity to join them and the rest of the team at the MTDP, NCI-Frederick, USA. I thank you all; for your wonderful hospitality, your supervision, input and assistance, putting up with the Kiwi and her accent, and making me feel right at home.

I gratefully acknowledge the financial assistance that I have received from the Evans Fund Travel Scholarship, NZIC Canterbury Branch Travel Award, Sadie Balkind Scholarship, New Zealand Federation of University Women, National Cancer Institute - USA, Royal Society of New Zealand (Science and Technology Award), Royal Society of New Zealand Canterbury Branch, 5th International Symposium on Polymer Therapeutics (Welsh School of Pharmacy, Cardiff University), and most importantly, the University of Canterbury Doctoral Scholarship.

To Kate, Kyriakos, Kristina, Louise, Breckon, Giles, and the rest of the 'lads', I thank you for your constant reminder that there is life other than chemistry. And yes, I am finally finishing school Kyri!

Thank you to Liz, Peter, Helen and David for their supportive pep talks, and Indian dinners.

'Ra' and 'Rina' deserve special mention. They have been right there when I needed it; in pink, and with chocolate! Thank you. Still working on that Country Club plan....

I appreciate the ongoing support of all my family. In particular, I would like to thank Mum, Dad, Craig and Glenn, for loving me and putting up with me during all the PhD madness.

The biggest thank you is reserved for Chris Fitchett. Thank you for believing that I really would finish 'soon'! No more sleeps! I totally appreciate your continual love and support.

ABSTRACT

The targeted delivery of drugs is one of the most actively pursued goals in anti-HIV and anti-cancer chemotherapy. This project takes a proof-of-concept approach to the development of protein-based drug delivery systems – delivery systems that would package, target, and deliver cytotoxins to diseased cells.

Primarily, this project explores the use of the potent anti-HIV protein, cyanovirin-N (CV-N), to actively target and deliver cytotoxic natural products to HIV-infected cells. This project also investigates the use of human serum albumin (HSA), a 66 kDa protein, as a macromolecular carrier to passively target and deliver cytotoxic natural products to cancerous cells.

To facilitate release of the toxin within infected cells, an enzymatically-cleavable tetrapeptide was incorporated in the conjugates. Maleimido-activated tetrapeptide toxin constructs were prepared in readiness for selective reaction with proteins carrying thiol functionalities. Release of the toxin, norhomohalichondrin B, was demonstrated *in vitro*.

Native CV-N conjugates were prepared by thiolation of the lysine ε-amino groups, and the subsequent reaction with maleimido-activated compounds. Reaction across all lysine residues was demonstrated. A singly-substituted tyrosinamide conjugate of CV-N was prepared. Two recombinantly produced mutant CV-N proteins allowed for the production of selectively modified, double- and single-norhomohalichondrin B conjugates of CV-N. The conjugates retained the anti-HIV activity of the parent protein.

Homohalichondrin B, doxorubicin, and tyrosinamide conjugates of HSA were prepared. The syntheses exploited the availability of a free thiol moiety at cysteine-34 of HSA, and the specific and selective reaction of this thiol with the maleimido-activated tetrapeptide derivatives.

All toxin conjugates demonstrate excellent cell toxicity. Further research to investigate whether this is targeted toxicity is currently underway.

CONTENTS

CHAPTER ONE INTRODUCTION

REFERENCES

ABBREVIATIONS

Å	angstrom(s)
Ab	antibodies
AIDS	acquired immune deficiency syndrome
BSA	bovine serum albumin
CIGAR	constant time inverse-detected gradient accordion rescaled long-range heteronuclear multiple bond correlation (in NMR)
COSY	correlation spectroscopy
Cys	cysteine
CV-N	cyanovirin-N
d	doublet (NMR)
Da	daltons (in mass spectrometry)
DCC	dicyclohexylcarbodiimide
DCE	dichloroethane
DCM	dichloromethane
DNA	deoxyribonucleic acid
°C	degrees Celsius
δ	chemical shift in parts per million (NMR)
DIPEA	diisopropylethylamine
DMAP	4-(dimethylamino)pyridine
DMF	dimethylformamide
DTT	dithiothreitol
EC	effective concentration
EDTA	ethylenediaminetetraacetic acid
ELISA	enzyme linked immunosorbent assay
EPR	enhanced permeability and retention
ESI	electrospray ionisation
Fmoc	9-fluorenylmethoxycarbonyl

Gly	glycine
gp	glycoprotein
HAART	highly active anti-retroviral therapy
HBTU	*O*-benzotriazol-1-yl-tetramethyluronium hexafluorophosphate
HIV	human immunodeficiency virus
HOBt	1-hydroxybenzotriazole
HPLC	high-performance liquid chromatography
HR	high-resolution (in mass spectrometry)
HSA	human serum albumin
HSQC	heteronuclear single quantum coherence (in NMR)
Hz	hertz
IC	inhibition concentration
IPA	isopropyl alcohol
2-IT	2-iminothiolane
J	coupling constant (in NMR)
K	lysine
LC MS	liquid chromatography mass spectrometry
LDL	low-density lipoprotein
Leu	leucine
Lys	lysine
m	multiplet (NMR) or milli
m/z	mass to charge ratio (mass spectrometry)
MALDI	matrix-assisted laser desorption ionisation
MaxEnt	maximum entropy
MS	mass spectrometry
MW	molecular weight
NHS	*N*-hydroxysuccinimide
NMR	nuclear magnetic resonance
p	pentuplet (in NMR)
PBS	phosphate buffered saline

Phe	phenylalanine
ppm	parts per million (NMR)
R	arginine
RNA	ribonucleic acid
RT	room temperature
s	singlet (NMR)
SIV	simian immunodeficiency virus
SPPS	solid phase peptide synthesis
t	triplet (NMR)
TES	triethylsilane
TFA	trifluoroacetic acid
THF	tetrahydrofuran
TIC	total ion current (in MS)
TOCSY	total correlation spectroscopy
TLC	thin layer chromatography
TPCK	L-1-tosylamido-2-phenylethylchloromethylketone
UV	ultraviolet
V_0	void volume

1 INTRODUCTION

INTRODUCTION

1.1 Human Immunodeficiency Virus

1.1.1 The Global HIV/AIDS Epidemic

AIDS – acquired immunodeficiency syndrome – was first reported in the United States in 1981 and has since become a worldwide epidemic. AIDS is caused by the human immunodeficiency virus (HIV). By destroying or damaging the cells of the body's immune system, HIV progressively destroys its ability to fight infections and certain cancers.[1]

In 2003, New Zealand had a record 188 newly identified HIV cases.[2] An estimated 1,400 people are living with HIV/AIDS in New Zealand in 2004.[2]

As of the end of 2003, an estimated 40 million people worldwide - 37 million adults and 2.5 million children younger than 15 years - were living with HIV/AIDS. Approximately two-thirds of these people live in Sub-Saharan Africa; another 18 percent live in Asia and the Pacific. An estimated five million new HIV infections occurred worldwide during 2003; that is, approximately 14,000 infections each day. More than 95 percent of these new infections occurred in developing countries, and nearly 50 percent were among females. In 2003 alone, HIV/AIDS-associated illnesses caused the deaths of approximately three million people worldwide.[3]

HIV is primarily a bloodborne and sexually transmitted disease. The chief routes of HIV transmission are by exposure to contaminated blood or blood products, insertive or receptive sexual intercourse, and vertical transmission from mother-to-child.[2,3]

1.1.2 Overview

HIV disease is characterised by gradual deterioration of immune function. Most notably, crucial immune cells called CD4+ cells are disabled and killed during the typical course of infection. These cells, sometimes called "T-helper cells", play a central role in the immune response, signaling other cells in the immune system to perform their functions.[4-7]

A healthy, uninfected person usually has 800 to 1,200 CD4+ T-cells per cubic millimeter (mm^3) of blood. During HIV infection, the number of these cells in a person's blood progressively declines. When a CD4+ T-cell count falls below 200 mm^{-3}, he or she becomes particularly vulnerable to the opportunistic infections and cancers that typify AIDS, the end stage of HIV disease.[6] People with AIDS often suffer infections of the lungs, intestinal tract, brain, eyes and other organs, as well as debilitating weight loss, diarrhoea, neurological conditions and cancers such as Kaposi's sarcoma and certain types of lymphomas.[6,8]

1.1.3 Classification of HIV

The human immunodeficiency virus (HIV) is a member of the *Retroviridae* family. Retroviruses such as HIV are RNA-containing viruses that replicate through a DNA intermediate by virtue of a viral-coded RNA-directed DNA polymerase, also called reverse transcriptase. Within the retrovirus family, HIV is classified as a lentivirus, having genetic and morphologic similarities to animal lentiviruses such as those infecting cats, sheep, goats, and non-human primates.[9] Electron microscopy reveals the most prominent morphological characteristic, a cylindrical or cone shaped capsid (as illustrated in Figure **1.1**) in the mature virion. Like HIV in humans, the animal lentiviruses primarily infect cells of the immune system, including T-lymphocytes and macrophages.[6-8]

HIV is subdivided into two distantly related types, HIV-1 and HIV-2. HIV-1 is the predominant worldwide isolate from individuals with AIDS, or at high risk for the development of AIDS. HIV-2 is endemic among people in West Africa.[6]

1.1.4 Origins of HIV

Debate around the origin of HIV has sparked considerable interest and controversy since the beginning of the epidemic. There is now clear evidence that the origins of HIV-1 and HIV-2 represent cross-species (zoonotic) infections. All HIV-1 strains are closely related phylogenetically to a strain of SIV (simian immunodeficiency virus) that naturally infects a subspecies of chimpanzee (*Pan troglodytes*), whose habitat corresponds to regions in West Africa, in which human HIV-1 infection is endemic.[10,11] A primate reservoir of HIV-2 has also been identified.[11]

In human populations there are three major groups of HIV-1, named M, N and O. Group M has given rise to the worldwide pandemic, diverging into various subtypes, A-K. HIV-1 groups O and N, are largely confined to Gabon, Cameroon and neighbouring countries close to the natural habitat of *Pan troglodytes*.[12]

1.1.5 The HIV Virion

The mature HIV virion (Figure **1.1**) is a roughly spherical (actually icosahedral) particle with a diameter of ~110 nanometers.[7] The central core contains four viral proteins (p24 - the major capsid protein, p17- a matrix protein, p9, and p6), two copies of the HIV RNA genome, and three viral enzymes (reverse transcriptase, integrase, and protease) essential for viral replication.[6,7]

The outer envelope is acquired during virion budding and is studded with approximately 72 knobs formed by the two major viral-envelope glycoproteins (gp120 and gp41). The envelope structures are derived from a 160 kDa precursor, gp160, which is cleaved into a gp120 external surface protein and a gp41 transmembrane protein.[6,13] Electron microscopy and X-ray crystal structures suggest that these proteins are organised into trimers.[14] Both proteins are extensively glycosylated.[13,15]

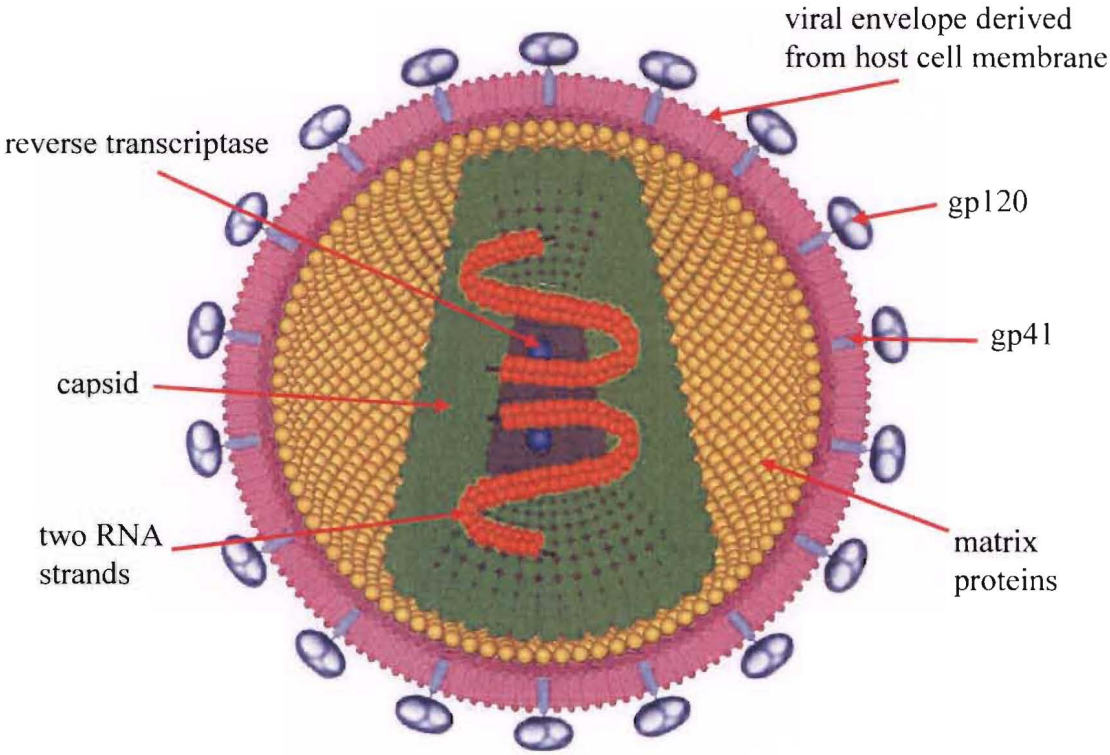

Figure 1.1: *Stylised Human Immunodeficiency Virus structure.*

Increasing knowledge about HIV-1 (hereafter referred to as HIV) has permitted the characterisation of this virus in considerable detail, including the mechanisms whereby it infects cells and becomes cytopathic to them. A key to the development of drug intervention strategies is a knowledge of the viral life cycle (Figure **1.2**).

1.1.6 The Life Cycle of HIV

CD4 is a membrane glycoprotein and plays a central role in orchestrating immune responses.[6] The chief target cells for HIV infection are human CD4+ T-lymphocytes and macrophages. The CD4 moiety is also found at the surface of monocytes, endothelial cells, and microglial cells.[6,16,17] An infection is initiated by binding of the virion envelope gp120 to the CD4 receptor on the host cell. The CD4–gp120 interaction occurs with high affinity and is an obligate step of the virus life cycle.[14,15,18-20] Upon binding to CD4, gp120 undergoes a conformational change that enables it to bind to a co-receptor molecule, such as the chemokine receptors CCR5 and CXCR4,[21] which act as fusion co-

receptors.[14,15,21-23] The structure of the ternary complex, containing a portion of HIV-1 gp120 bound to CD4 and a neutralising monoclonal antibody, was determined by X-ray crystallography.[15] This structural analysis was fundamental in advancing the understanding of the HIV infection process.

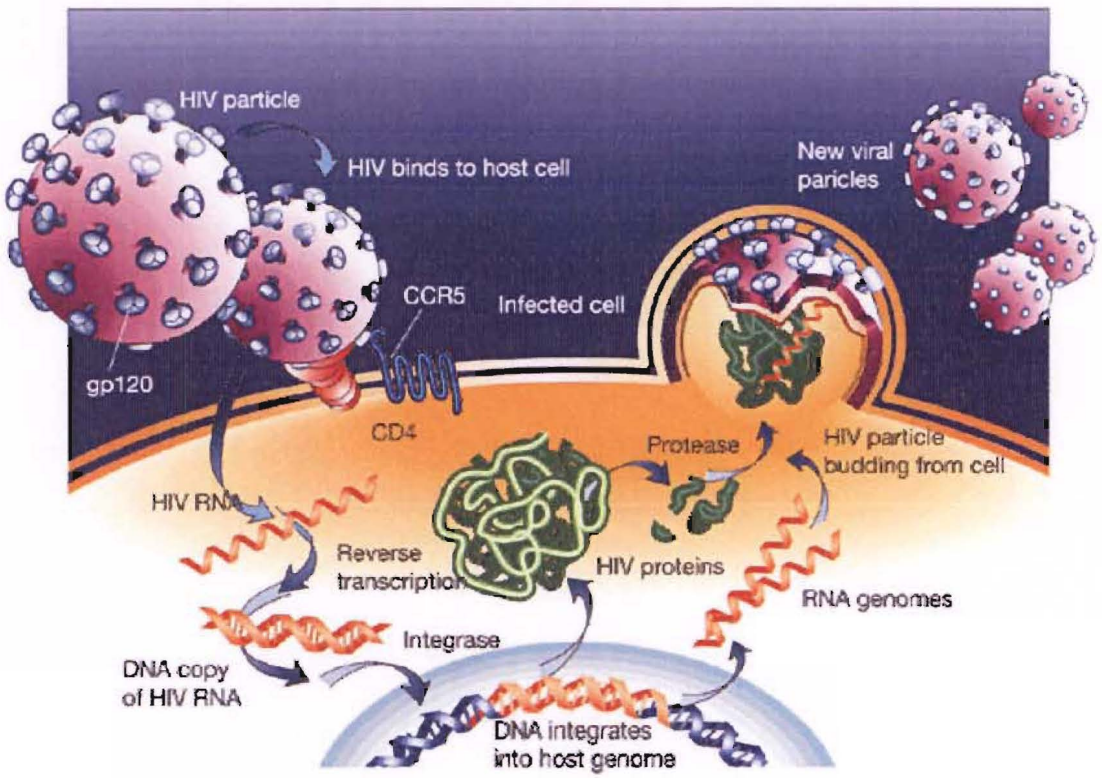

Figure 1.2: *The HIV Replication Cycle.* (Reproduced with permission from Professor Robin Weiss, Department of Immunology and Molecular Pathology, University College London, London. Copyright permission from *Nature Publishing Group*)

The interaction of gp120 with CD4 and co-receptor initiates conformational changes in the transmembrane protein gp41, which mediates fusion of the viral and cellular membranes. The essential parts of this protein are an N-terminal fusion peptide, and N-terminal heptad repeat and a C-terminal heptad repeat. Current models show gp41 adopting a 'pre-hairpin' conformation that places the fusion peptide near to or in the target cell membrane. Intramolecular interactions between the C- and N-heptad repeats results in a hairpin conformation that leads to a juxtaposition of the host cell and viral membranes, followed by fusion.[19,20,24]

Conceptually, the use of agents to block viral entry is an attractive target in the treatment of HIV infection. Unfortunately, this area of drug development has had limited success. A

number of inhibitors are showing promising results and several of these will be reviewed below. The focus of this thesis has been the development of a proof-of-concept approach to an anti-HIV therapeutic. The research has taken advantage of the specific delivery opportunities offered by cyanovirin-N (CV-N), an 11kDa protein that binds specifically to the HIV envelope protein gp120.[25]

The proteins that surround the viral nucleic acid are digested away, leaving the genome exposed to the cytoplasm of the cell. The viral genome is composed of two identical segments of single-stranded RNA, which are complexed with the enzyme known as RNA-dependent DNA polymerase or reverse transcriptase. The viral reverse transcriptase converts viral RNA into first single- and then double-stranded DNA.[7,20,26] The viral reverse transcriptase is, in some sense, the most logical target for antiviral chemotherapy, since human cells do not possess this enzyme. This enzyme is the target of many anti-retroviral drugs that are now in clinical use. Importantly, the HIV reverse transcriptase is very error-prone, and the resulting nucleotide mismatches introduce a high mutation rate in the viral genome.[26] As will be noted later, the genotypic and phenotypic diversity of HIV is a major factor in pathogenicity, in circumventing host defence, and in developing resistance to antiretroviral drugs.

The proviral DNA duplex is transported to the cell nucleus where it is inserted (integrated) by the virally encoded enzyme integrase, into the host cell genome. Proviral DNA, once integrated, is the equivalent of cellular DNA. No method has yet been devised to excise proviral DNA from cells.[7,20,26] The integrase enzyme provides yet another target for drug activity, and development of integrase inhibitors is ongoing.

Once integrated into the host cell genome, HIV can establish a virus-producing infection or a latent infection depending upon critical host factors, particularly whether the infected cell is in an activated or resting state.[27] In a permissive cellular environment, cellular replication will now include the duplication of the proviral DNA segments. These segments can be transcribed by host cell RNA polymerases to yield viral messenger RNA (mRNA), which in turn, can be translated into viral proteins. Final maturation of the virion proteins, mediated by protease, takes place, and these newly made viral proteins ultimately assemble with viral RNA molecules at the plasma membrane to yield

infectious viral progeny that bud out from the cell.[6,7,20,26] Inhibitors of the protease enzyme make up a large number of the anti-HIV treatments currently in clinical use.

An analogous mechanism to the one discussed above mediates cell-cell fusion between HIV envelope-expressing (productively infected cells) and CD4-expressing cells.[6]

By contrast, with a latently infected cell, the HIV provirus DNA is not expressed as viral RNA, viral proteins or virions, but is replicated as DNA by the host cell DNA polymerase, as are other cellular genes, and is transmitted to progeny cells by cell division. Without expression or surface adherence of HIV proteins, such latently infected cells are not affected by anti-HIV immune mechanisms. Further, a latently infected cell, such as a $CD4^+$ T-lymphocyte, can be activated by antigens, mitogens, certain cytokines, and other viral gene products, to initiate transcription and translation of the HIV provirus DNA and the production and spread of infectious virus.[7,27,28] Complete viral eradication is dependent on elimination of the latent reservoir.

1.1.7 The Course of HIV Infection

Although the course of HIV infection may vary somewhat among individual patients, a common pattern of development has been recognised (Figure **1.3**).[29-32] The pattern is characterised by three phases: the acute or primary infection (first viremia), the asymptomatic, and the symptomatic (AIDS) phase.

The overall effect of HIV on the immune system is to gradually lower its ability to mount an immune response. From the original infection, there is usually a period of 8-10 years before the clinical manifestations of AIDS occur; however this may be two years or less.[5]

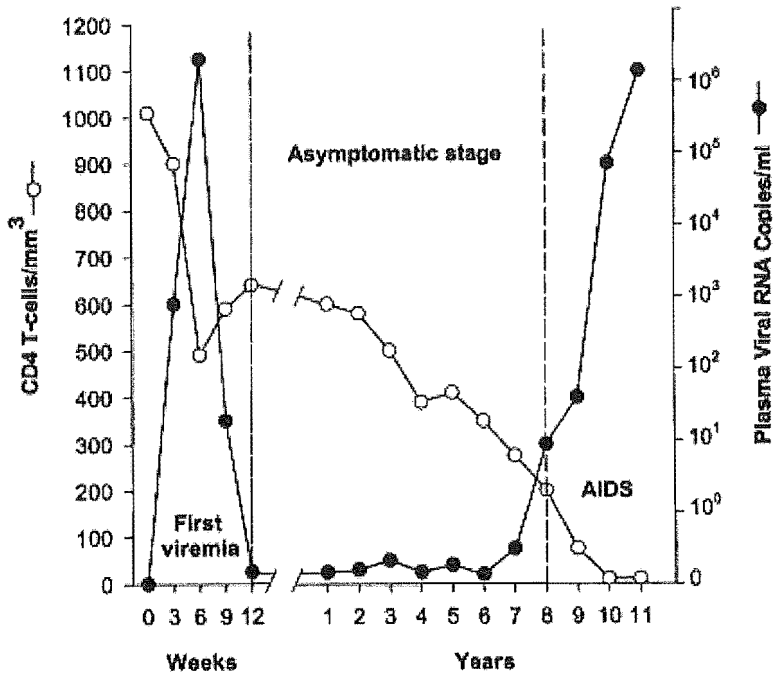

Figure 1.3: *The Typical Course of HIV infection.* (Reproduced with permission from Dr Robert Wallace,[29] Department of Biology, City College of New York, New York and Dr Anthony Fauci,[32] Laboratory of Immunoregulation, NIH, USA)

Primary infection, which generally lasts for two to eight weeks, is typically associated with high levels of virus.[30,32] The patient often experiences fever, rash, and swollen lymph glands.[30] The result is an initial fall in $CD4^+$ cells.[30,32]

With the emergence of anti-retroviral immune responses, and in particular of specific cytotoxic T lymphocyte response, levels of plasma HIV-RNA decline precipitously. After about three months of infection, plasma HIV-RNA levels stabilise and remain relatively constant during the asymptomatic phase.[30,32] Studies show that during this clinically latent phase of disease, there is a very dynamic process of viral production and clearance.[28]

The asymptomatic phase is characterised by a slow, gradual depletion of CD4+ T lymphocytes. Eventually the immune system collapses, mirrored by a return to high-level virus production. The inevitable outcome of the progressive deterioration of the immune system is clinically apparent disease or an acquired immunodeficiency syndrome (AIDS) defining illness. Even with treatment, death usually occurs within two years.[30,32]

1.1.8 Treatment Strategies

The development of potent anti-retroviral drugs is central to the control of HIV infection and the prevention of disease. In recent years significant progress has been made towards the chemotherapy of HIV. The current armamentarium for the treatment of HIV infections consists of nineteen formally approved drugs.[33] A representative sample of these compounds can be seen in Figure **1.4**.

The drugs licensed for clinical use fall into one of the following five categories: a) nucleoside reverse transcriptase inhibitors; and b) nucleotide reverse transcriptase inhibitors, that, following phosphorylation steps, act as chain terminators at the substrate binding site of the reverse transcriptase[33,34] (for example zidovudine (**1**), abacavir (**2**) and tenofovir disoproxil (**3**)); c) non-nucleoside reverse transcriptase inhibitors, that interact with the reverse transcriptase at an allosteric, non-substrate binding site[33,34] (for example nevirapine (**4**) and delavirdine (**5**)); d) protease inhibitors, that specifically inhibit, as peptidomimetics, the virus associated protease[33,34] (for example ritonavir (**6**)); and e) the viral entry inhibitor, enfuvirtide (**7**), that inhibits virus-cell fusion through an interaction with its homologous region in gp41.[33,35]

a) Nucleoside Reverse Transcriptase Inhibitors

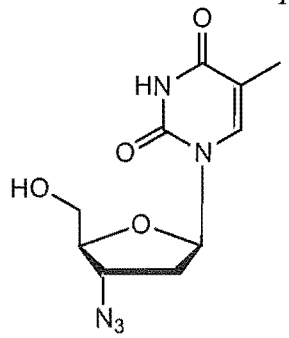

zidovudine (**1**)

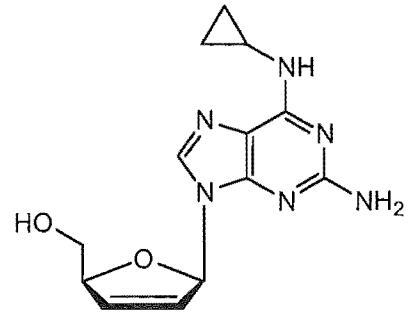

abacavir (**2**)

b) Nucleotide Reverse Transcriptase Inhibitors

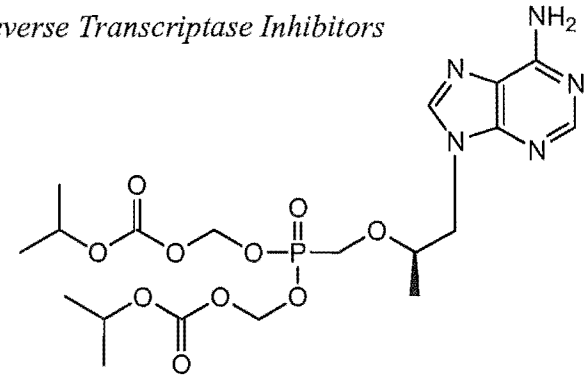

tenofovir disoproxil (**3**)

c) Non-Nucleoside Reverse Transcriptase Inhibitors

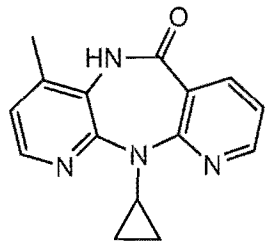

nevirapine (**4**)

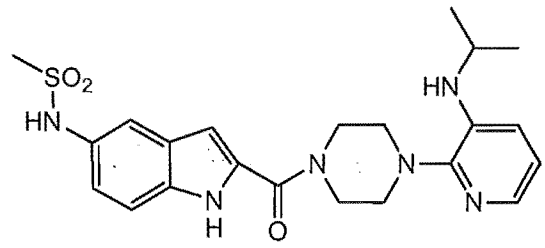

delavirdine (**5**)

d) Protease Inhibitors

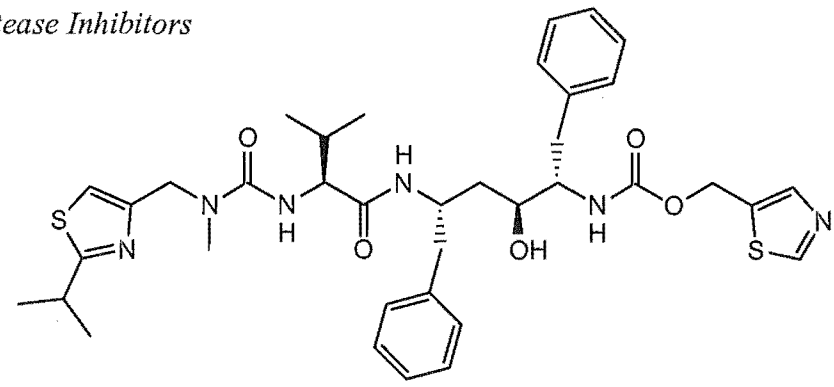

ritonavir (**6**)

e) Viral Entry Inhibitors

YTSLIHSLIEESQNQQEKNEQELLELDKWASLWNWF

enfuvirtide (**7**)

Figure 1.4: *A Selection of Licensed Anti-HIV Drugs.*

In addition to the anti-HIV compounds that are currently available, there are a large number that are presently under preclinical or clinical development. Some examples include the virus adsorption inhibitors (for example, cosalane derivatives, cyanovirin-N); CXCR4 and CCR5 antagonists (AMD3100 (**8**), TAK-779 (**9**)); nucleoside/nucleotide reverse transcriptase inhibitors (for example, amdoxovir (**10**)); integrase inhibitors (for example, S-1360 (**11**)); and peptidomimetic (for example, TMC-126 (**12**)) and non-peptidomimetic (for example, tipranavir (**13**)) protease inhibitors.[33,35,36]

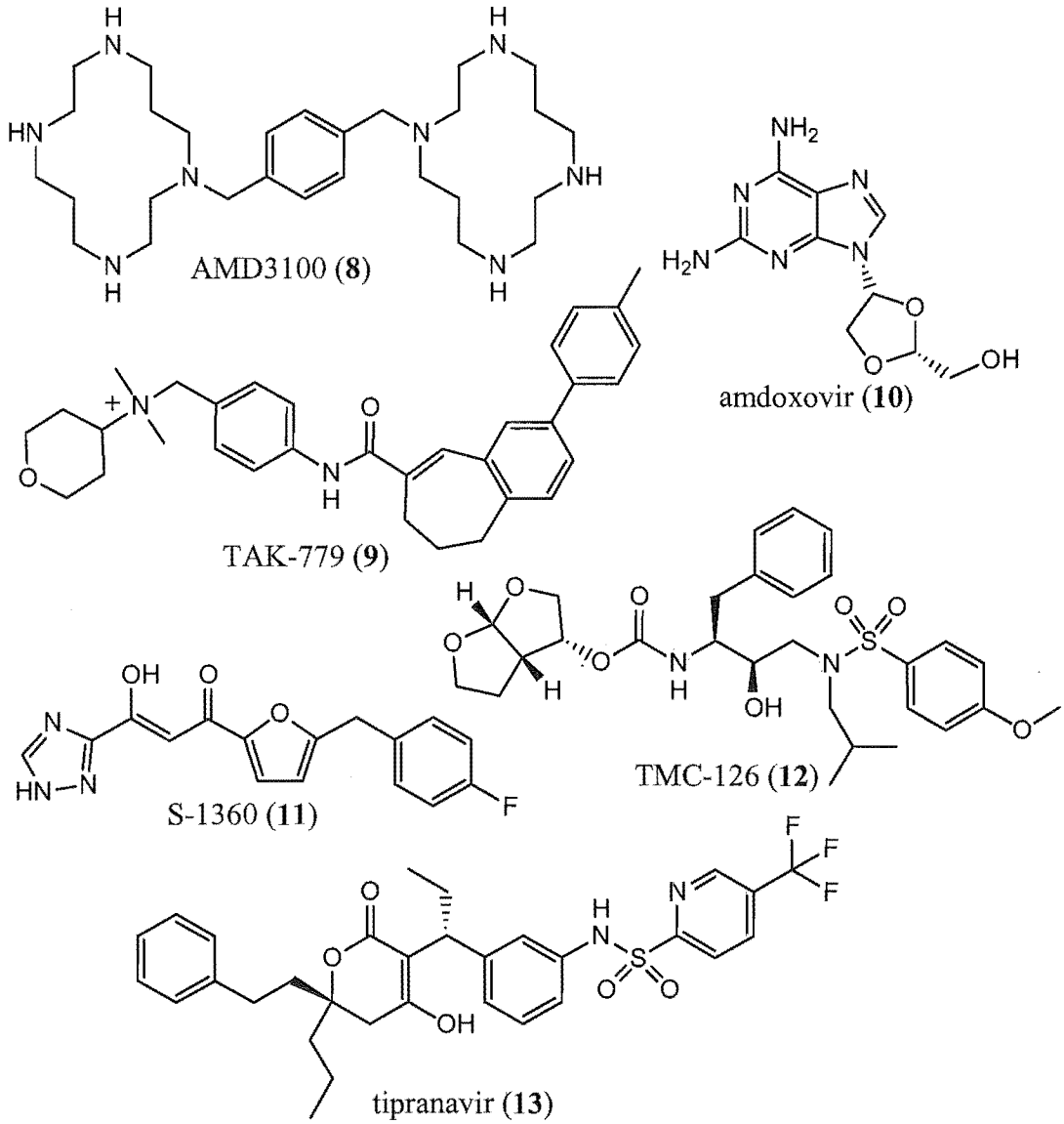

Figure 1.5: *Anti-HIV drugs under development.*

Highly active anti-retroviral therapy (HAART)[37-40] refers to a broad category of treatment regimes usually comprised of three or more anti-retroviral drugs used concurrently. The

goal of this approach is to reduce the viral load to below detection levels, to limit disease progression, and to delay the occurrence of resistant mutants that would compromise its therapeutic efficacy. Most HAART regimes include drugs from at least two of the categories mentioned above.

HIV reverse transcriptase lacks proof reading capability, so the mutation rate is high (1 in 10^4 to 1 in 10^5 nucleotide mutations per replication cycle).[41] An important benefit of the multi-drug therapy is that drug resistance develops more slowly with HAART than with older monotherapy regimens. This is a result of fewer absolute viral replication cycles, resulting in a decreased probability of resistance mutations emerging.[38,42]

The use of HAART has reduced HIV viremia in many patients to undetectable levels[38,43] and substantially delays the onset of AIDS by halting the progressive loss of CD4+ T-lymphocytes.[43,44] HIV infection has changed (at least in the western countries[40]), from a progressive disease that ultimately results in death from opportunistic infection or malignancy, to a chronic condition with slow disease progression that requires life-long therapy.

However, these clinical benefits of HAART still hold limitations. First, the high cost and limited availability of drugs used in HAART make the clinical benefits largely available only to persons in developed countries.[34,40] Second, HAART regimens require patients to take many tablets per day.[45] Third, the potential side effects[45] and the risk of developing HIV resistant to any of the anti-retroviral compounds makes long-term maintenance on HAART unrealistic.[40,44,45] Lastly, the initial hope that prolonged suppression of HIV by current HAART regimens could result in the clearance and eradication of virus from an individual has been shown to be improbable.[45]

Given that the latent reservoir for HIV appears to represent a major barrier to virus eradication,[6,27,28,46,47] a good deal of research is exploring approaches for eliminating this reservoir. One strategy involves activating latently infected cells and "flushing out" the reservoir.[27,46] The goal is to promote viral transcription and replication in cells that harbour latent virus. Virus produced from these cells should be unable to infect other cells due to the presence of anti-retroviral agents.[27]

Viral gene expression in latently infected cells can be reactivated by a wide variety of signals including cytokines, such as interleukin-2, tumour necrosis factor, antigens, bacterial infections and lipopolysaccharides.[27,28,45,47] A number of studies of combination regimes of HAART and interleukin-2 have been undertaken and show positive results but have not been successful in eradicating infection.[45]

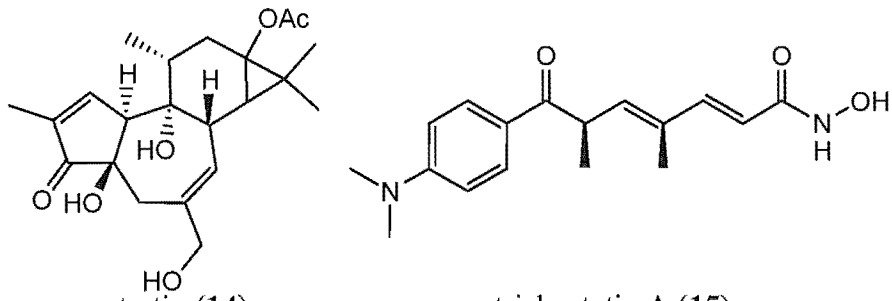

prostratin (**14**) trichostatin A (**15**)

Figure 1.6: *Clearing the Latent Reservoir. Prostratin and trichostatin A.*

Also, compounds like the plant-derived prostratin (**14**),[27] a number of other non-tumour promoting phorbol esters,[46] and the deacetylase inhibitor trichostatin A (**15**)[48] have been found to potently induce latent virus from quiescent T-cells *in vitro*. The preliminary results with prostratin are encouraging, but its clinical potential is hampered by low potency.[27,46]

1.1.9 Vaccine Development

A safe, effective and readily available vaccine remains the ultimate goal for the containment of HIV. The appeal of a vaccine encompasses both preventative and therapeutic considerations.[49] In addition to their ability to inhibit infection, vaccines against HIV may also boost immune responses that control viral replication. To date, no vaccine has been accepted for standard treatment of infected individuals, but the concept of vaccination remains a goal for future treatment of the disease.[49-53]

Three main types of therapeutic vaccines have been clinically tested to date.

1) Subunit vaccines containing HIV-1 proteins:

Recombinant envelope glycoproteins (rgp160/rgp120) have advanced in clinical trials.[49,52] These reflect the preventative vaccine effort, based on the fact that neutralising antibodies are directed primarily against these proteins.[49] Vaccines of HIV immunogen (whole inactivated HIV, depleted of gp160 and gp120 proteins) and other viral proteins and peptides have also been developed.[52]

2) Recombinant viral vectors encoding viral proteins:

Live viral vectors, primarily recombinant poxviruses (for example, canarypox) are able to carry large sequences of foreign DNA and, by mimicking microbial infection, induce immune responses to these antigens *in vivo*.[49,52]

3) DNA vaccines:

Use of plasmid DNA enables vaccination with select sequences of genetic material that express immunogenic HIV proteins with the goal of eliciting long-lived humoral and cellular responses.[49,50,52]

Candidate HIV vaccines have been evaluated in over 70 phase I trials, in more than 3,500 patients, with only one progressing on to phase III trials.[54]

The most extensively studied vaccine candidate, AIDSVAX B/B, contains recombinant forms of HIV gp120 from two subtype B strains.[51,52,55] In late 2002 this vaccine became the first to finish phase III clinical trials. However, results were disappointing with AIDSVAX B/B not inducing broad neutralising antibodies or T-cell responses, and failing to protect against infection with a vaccine efficacy of 3.8%.[51,55]

Phase I and II trials are in progress for a further 20 vaccines.[51]

Clinical trials of the anti-retroviral drugs have employed viral load as a marker to detect clinical efficacy. No immunological endpoint has been identified which correlates to survival in a similar manner for the testing of vaccines.[52] All of the therapeutic vaccines investigated have been safe and well tolerated.[49] Many have demonstrated immunogenicity, as measured with a variety of immunological parameters (for example, cytotoxic T-lymphocytes and antibodies).[49]

No vaccines have yet demonstrated clinical benefit.[49]

Despite these factors, there is hope for a vaccine against HIV. Two cohorts of people who possess natural immunity to infection by HIV have been described.[54] Firstly, individuals who are homozygous for a 32-base pair deletion in the CCR5 receptor remain uninfected, despite multiple exposures to HIV. It is not clear whether this genetically-based resistance to infection can be utilised in a vaccine strategy. The second group of individuals who appear to possess immunity from infection are a number of African prostitutes who remain HIV negative despite multiple exposures. The immune correlate or protection is unknown, although it has been noted that they show a detectable CD8+ cytotoxic T-lymphocyte response.[54]

Jon Cohen aptly describes the quest for a vaccine in his 2001 book, "Shots in the Dark: The Wayward Search for an HIV Vaccine."[56] It is likely that the eventual HIV vaccine will involve a combination of multiple vaccine ideas and technologies and it will take a concerted effort from the scientific, commercial and political communities to develop, test, licence and deliver.

1.2 Natural Products

For thousands of years mankind has known about the benefit of drugs from nature. The curative powers of certain compounds have been discovered by various means: from folk remedies to targeted research, and from serendipitous accidents to systematic investigations. Throughout recorded history and in all societies, the identification of substances effective against illness and disease has been an important activity.[57] In the fourth century B.C., Hippocrates described a 'tea' made by boiling willow bark in water. The concoction was used as a treatment for fevers. Over the centuries that folk remedy ultimately led to the synthesis of aspirin, a true "wonder drug" that has aided millions, arguably billions, of people.[58]

Williams *et al.*[59] define a natural product, or a secondary metabolite, as "*a substance that has no known role in the internal economy of the producing organism*". There are many hypotheses as to why natural products are produced. Williams *et al.* argue that the ability to synthesise secondary metabolites, which may repel or attract other organisms, has evolved as one aspect of an organism's strategy for survival.

1.2.1 Marine Natural Products

Among the least explored of the planet's organisms are the invertebrates, algae, fungi, and bacteria of the marine environment. The majority of phyla and more than 90% of all classes of organisms are represented in the marine environment.[60] With oceans covering more than 70% of our planet's surface, the marine environment is composed of a tremendous variety of habitats. These habitats differ markedly in salinity, temperature, pressure and light.

For more than two decades, there has been an ongoing quest to discover new drugs from the sea. There is little doubt that marine biodiversity is a source of chemical diversity. It has proved to be a rich reservoir of biologically active natural products. Over 14,000 compounds have now been described.[61]

Considering the diversity of chemical structures found in nature with the narrow spectrum of structural variation of even the largest combinatorial library, natural products will continue to play an important role in drug discovery. Despite achievements in synthetic chemistry and advances towards rational drug design, natural products will continue to be essential in providing medicinal compounds and as starting points for the development of synthetic analogues.

Below is a brief overview of two species of marine organisms that have been responsible for producing the natural products central to this thesis.

1.2.2 Blue-green Algae (Cyanobacteria)

Blue-green algae or cyanobacteria are a remarkable group of simple photosynthetic microorganisms. In evolutionary terms they represent a link between bacteria and green plants. Their cellular organisation (prokaryotic), is characterised by the lack of membrane-bound organelles such as a nucleus, mitochondria or chloroplasts, and resembles that found in bacteria. Their principal mode of nutrition, oxygen-evolving photosynthesis, however, is similar to that which operates in all other eukaryotic algae and in green plants.[62]

Cyanobacteria are, perhaps, the most primitive things living on earth. Their fossilised remains have been found in sediments from the Early Precambrian period.[63] It seems likely that some 3 billion years ago, they were responsible for changing the earth's atmosphere to one rich in oxygen that could support plants and animals.[62]

Blue-green algae are found widely in various environments, from the intertidal zone of marine shores, to damp rocks and salt marshes, freshwater lakes and the glass walls of aquariums. Cyanobacteria are found not only in aquatic samples, but also in soils, animals, and higher plants. [62]

Cyanobacteria have proven to be a source of biologically active and structurally unique natural products. The structures of two representative compounds are shown below.

Anatoxin-a (**16**) is an alkaloid neurotoxin,[64] and the cyclic depsipeptide, cryptophycin-1 (**17**), acts as a microtubule depolymerising agent.[65]

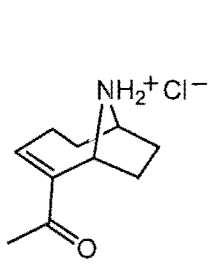

anatoxin-a (**16**)

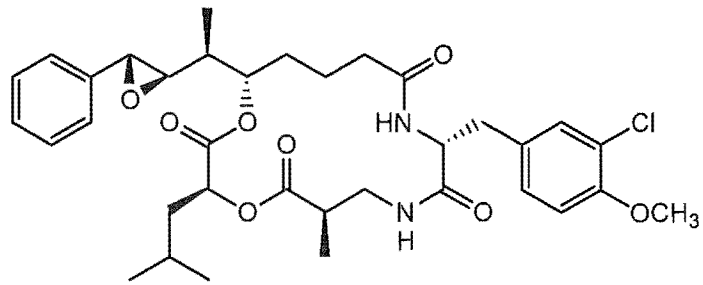

cryptophycin-1 (**17**)

Figure 1.7: *Two representative natural products isolated from cyanobacteria.*

The focus of this thesis is an 11 kDa protein, cyanovirin-N, isolated from cultures of the blue-green alga *Nostoc ellipsosporum*. This protein will be reviewed in depth in the following chapters.

Little experimental evidence exists to establish the full ecological significance of cyanobacterial metabolites. Secondary metabolite production is often sensitive to environmental factors and current research shows that some compounds produced by marine cyanobacteria kill off or discourage fish and invertebrate grazers and denude the local populations of algae and other cyanobacteria that might compete for the same nutrients.[64]

1.2.3 Sponges

Sponges are a common and diverse group of about 10,000 multi-cellular animals belonging to the phylum Porifera. They lack true tissue and organs and therefore have a level of structural organisation that is intermediate between other invertebrate groups and the protozoans.[66]

Sponges are specially adapted for a stationary filter-feeding life. Water containing food particles is drawn into the internal cavity of the sponge through numerous pores. The water is strained of food and expelled.[66]

These invertebrates are benthic organisms and are widely distributed in both fresh and salt water, and at all depths and latitudes.[66]

Sponges have provided a diverse array of bioactive metabolites. Four interesting compounds are discussed here. In 1955, Bergman isolated unusual nucleosides named spongouridine (**18**) and spongothymidine (**19**) from a Caribbean sponge. Further biological and synthetic studies led to the development of compounds such as acyclovir (**20**) with potent antiviral activity.[67,68] Calyculin A (**21**), a cytotoxic polyketide is a selective inhibitor of protein phosphatase 1 and 2A and is widely used as a research tool in life science fields.[68] Homohalichondrin B (**22**) is a polyether macrolide which is an exceedingly potent tubulin-binding antimitotic agent with *in vivo* activity against a number of pre-clinical models.[67] This project has investigated harnessing the potency of homohalichondrin B.

Marine invertebrates are sessile organisms that lack a developed immune system. They are prone to predation, fouling or the overgrowth by other organisms. The production of biologically active natural products is proposed to act as a chemical defence against these types of invasive and life threatening events. In some cases, microorganisms are known or suspected to be the biosynthetic source of marine invertebrate natural products.[69]

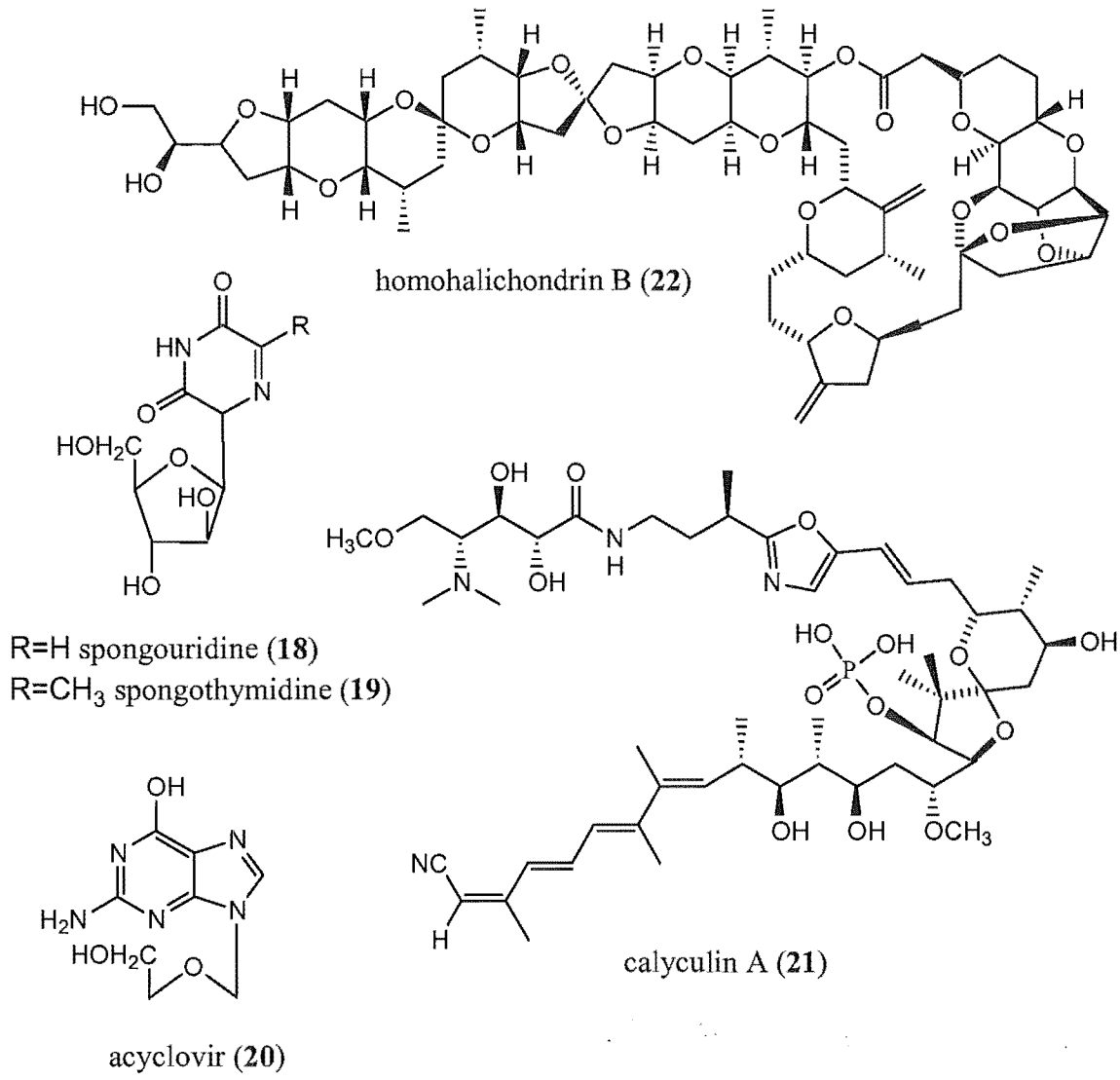

Figure 1.8: *A selection of natural products isolated from marine sponges, and the synthetically developed anti-viral compound, acyclovir.*

1.2.4 The Marine Chemistry Group

The Marine Chemistry Group at the University of Canterbury was formed in 1975. The prime objective of the Group is the isolation and identification of biologically active marine natural products. Historically, work has concentrated on natural products from marine invertebrates. In 1983 a large-scale collection programme was initiated with marine invertebrates collected from around New Zealand waters, and from McMurdo Sound in Antartica. From these specimens a large number of novel natural products have been isolated and their structures determined.

More recently, the Marine Chemistry Group has turned to the investigation of marine fungi as a new source of novel and exciting bioactive natural products.

The Marine Chemistry Group is also exploring new drug delivery approaches, polymer therapeutics, and protein conjugates, as a means of enhancing the value of marine toxins.

1.3 The Halichondrins

1.3.1 Discovery and Isolation

The attention of Hirata and Uemura was caught by the remarkable *in vivo* anti-tumour activity exhibited by an extract of the marine sponge *Halichondria okadai* Kadota.[70,71] Bioassay against B-16 melanoma cells guided the isolation of a class of complex polyether macrolides. This extremely bioactive group of compounds were named the halichondrins.[70,71] Subsequently, the halichondrins have been isolated from a variety of marine sponges including *Axinella* sp.,[72,73] *Phakellia carteri*,[74,75] and *Lissodendryx* sp.[76,77]

To date the structures of 14 halichondrin and three closely related halistatin congeners have been reported. The structures of three representative halichondrins are shown in Figure **1.9**.

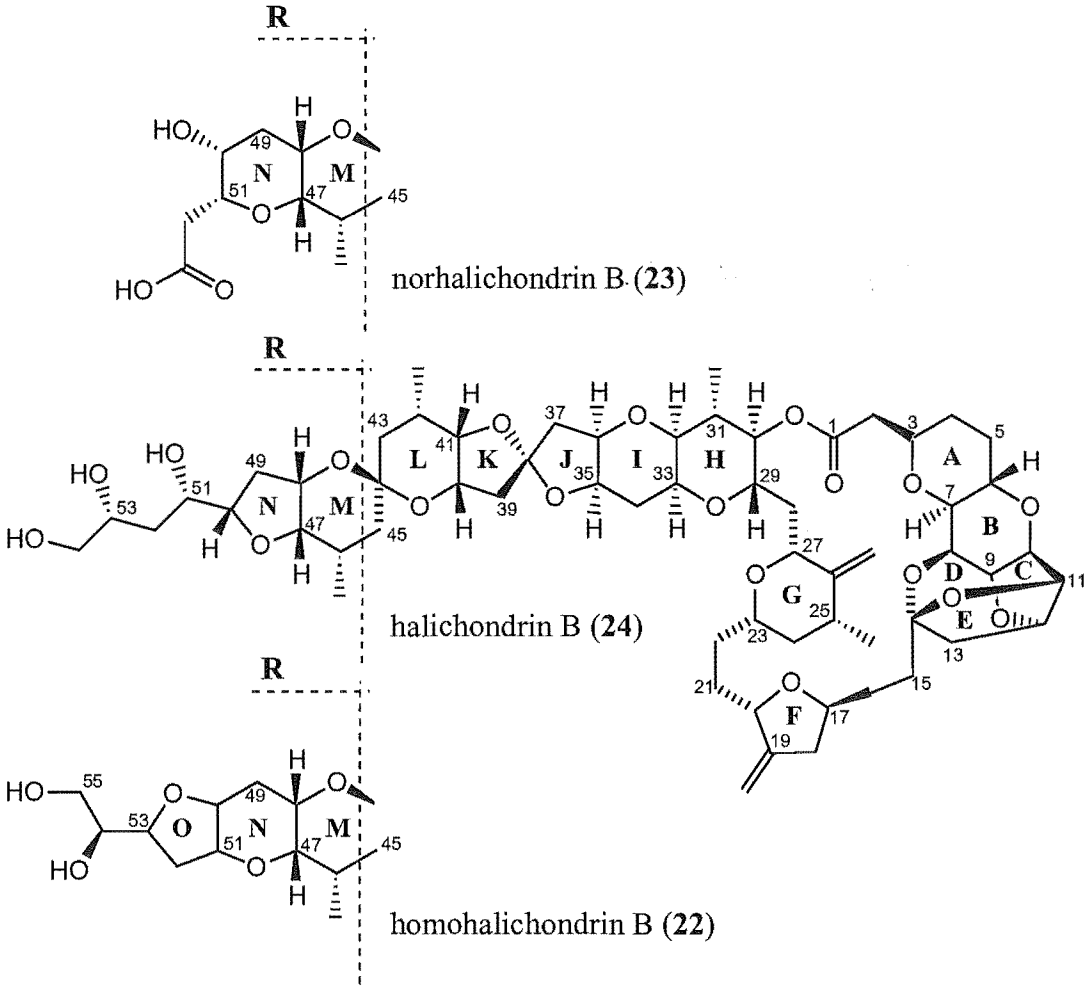

Figure 1.9: *Norhalichondrin B, halichondrin B and homohalichondrin B.*

The structures are characterised by a novel 2,6,9-trioxatricyclo[3.3.2.$0^{3,7}$]-decane system (rings C-E), a 22-membered lactone ring (C1-C30), two exocyclic olefinic groups and several pyranose and furanose rings.[70,78] The halichondrins are divided into three families, A, B and C, distinguished by the degree of oxygenation at C12 and C13 (Figure **1.10**). Within each family variation occurs beyond the C45 position as seen in Figure **1.9**. (halichondrin, homohalichondrin or norhomohalichondrin).[70,78]

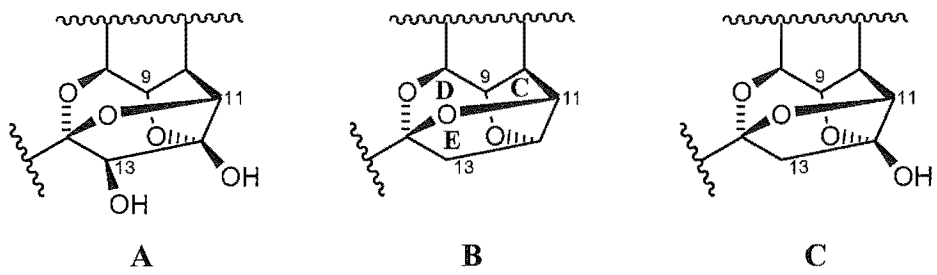

Figure 1.10: *The three families of halichondrins.*

The structure of norhalichondrin A was unambiguously established by X-ray analysis.[71] The absolute configurations of halichondrin B (**24**), norhalichondrin B (**23**), and homohalichondrin B (**22**) were proven by total synthesis.[79,80]

Comparison of the cytotoxicity of the halichondrins isolated against the *in vitro* B-16 melanoma cell-line (Table **1.1**) showed that halichondrin B (**24**) was the most cytotoxic. Halichondrins with B-type C-E rings and homo- or hali-type terminal moieties gave the most potent results.

Compound	**IC_{50}[a] (ng/mL)**
Homohalichondrin A	0.26
Norhalichondrin A	5.2
Halichondrin B (**24**)	0.093
Homohalichondrin B (**22**)	0.1
Norhalichondrin B (**23**)	NR[b]
Halichondrin C	0.35

[a] Inhibition Concentration. (Concentration at which the growth of cells is 50% of the control value for untreated cells.)
[b] Data not reported (NR) but result inferior to that for halichondrin B (**24**).

Table 1.1: *Cytotoxicity against B-16 Melanoma cells (ng/mL).*[70]

A number of hemi-synthetic derivatives of the halichondrins have been investigated to establish the structural and conformational features essential for the high levels of biological activity.[77,81] The halichondrins are sensitive to exposure to acid conditions[81] and the products of this degradation (C38 epimer, and cleavage of the ether links between 8,14 and 9,12) showed significant decreases in cytotoxicity. Opening of the lactone C1-C30 ring, and modification of the olefinic groups at C9 and C26, demonstrated similar results.[77] Modification beyond C47 did not result in significant changes in the biological activity of the resulting halichondrins.[77]

Hirata *et al.* investigated the anti-tumour activities of halichondrin B (**24**) and homohalichondrin B (**22**) by *in vivo* testing on mice with B-16 melanoma, P388 leukaemia and L-1210 leukaemia tumours.[70] A 300% increase in life expectancy of the afflicted mice was reported, relative to the control, for both compounds. By 1992 the NCI had also demonstrated that halichondrin B (**24**) and homohalichondrin B (**22**) were active *in vivo* against a variety of tumour types.[82]

1.3.2 Mechanism of Action

An evaluation of the differential activity (mean-graph profile) of halichondrin B (**24**) against the NCI 60 human tumour cell line panel using the COMPARE[83] algorithm demonstrated that the halichondrin pattern closely resembled those of tubulin-binding compounds like vincristine.[84] Bai *et al.*[84] confirmed that halichondrin B was an extremely potent anti-mitotic agent. Halichondrin B (**24**) inhibits *in vitro* polymerisation of purified tubulin and microtubule assembly dependent on microtubule associated proteins. It was shown to be a non-competitive inhibitor of the binding of vinblastine to tubulin and to inhibit nucleotide exchange on tubulin.

1.3.3 Further Development

In 1992, the NCI Decision Network Committee selected halichondrin B (**24**) for pre-clinical anti-cancer drug development (DNIIA status). Two factors, in particular, have mitigated against any further development of halichondrin B (**24**) at the NCI.

The most important problem is that of supply of the halichondrins. It has been estimated that 1-5 kg/annum of halichondrin B (**24**) would be required for the compound to be marketed as a commercial drug.[78] A variety of supply options are being investigated.

The natural supply of the highest yielding of the halichondrin containing sponges, *Lissodendoryx* sp., is limited to an exclusive site off the Kaikoura Peninsula of New Zealand. It has been established unambiguously that the halichondrins could never be supplied on a commercial scale by collection from the wild.[78,85]

Aquaculture feasibility trials have shown some initial encouraging results.[78]

There is some thought that a symbiont could be responsible for the production of the halichondrins. Preliminary cell separation studies are currently being undertaken by National Institute of Water and Atmospheric Research (NIWA) and the University of Canterbury Marine Chemistry Group. Identification of the producing organism raises the possibility of fermentation of the microorganism, or transfer of relevant portion(s) of the genome to a vector appropriate for fermentation.[78]

The scarcity of the halichondrins, their potent cytotoxicity, and their academically challenging structures, has encouraged considerable synthetic effort in this area. The total synthesis of halichondrin B (**24**) and norhalichondrin B (**23**) was achieved by Kishi and coworkers in 1992.[79] Significant improvements have been made to the syntheses but they still entail over 100 synthetic steps.[86] With such an extensive synthetic route, a commercially cost effective supply of the halichondrins is unlikely by total synthesis. The groups of Salomon, Horita and Yonemitsu, and Burke have also made noteworthy contributions to the synthesis of halichondrin B (**24**).[87] The synthesis of the right-half diol (**25**) was reported by Stamos *et al.*[86] This diol (**25**) exhibits the same activity pattern

pattern as the parent halichondrin B (**24**), with a reported cytotoxicity within one order of magnitude of the parent compound.[86] This discovery has concentrated synthetic efforts on the right-half segment of halichondrin B.

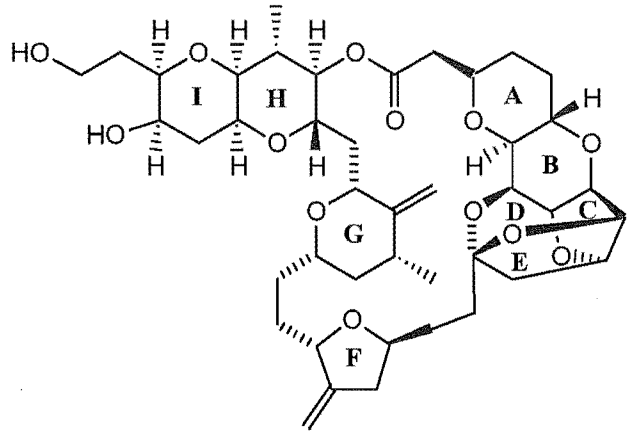

right-half diol (**25**)

Figure 1.11: *The right-half diol from halichondrin B.*

The existence of a synthetic route for halichondrin B (**24**) and the knowledge that its activity resides in the macrocyclic lactone C1-C38 moiety has permitted development of structurally simplified synthetic analogues that retain the exceptional activity of the parent.[88] The macrocyclic ketone analogues, ER-076349 (**26**) and ER-086526 (**27**), (Figure **1.12**) have been synthesised by Towle *et al.*,[88] and have highly potent activities *in vitro* and *in vivo*.

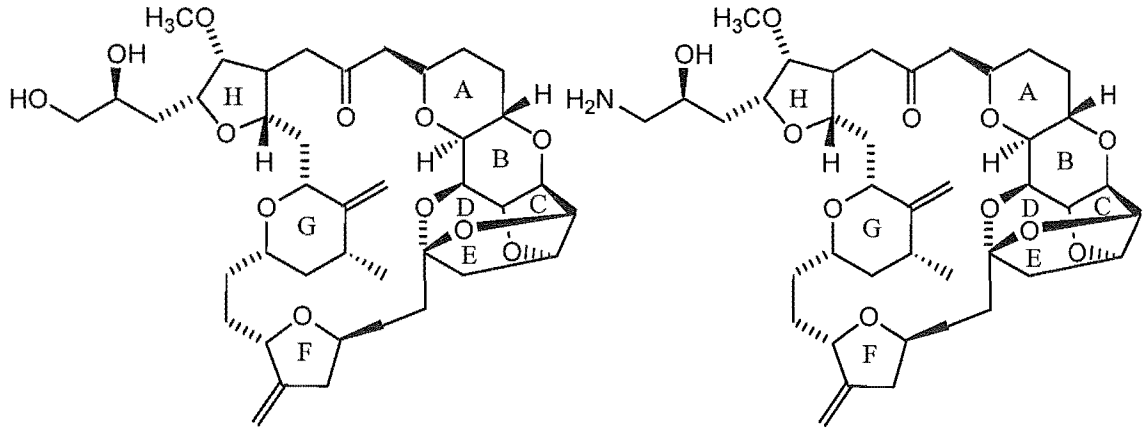

ER-076349 (**26**) ER-086526 (**27**)

Figure 1.12: *Structures of the macrocyclic ketone analogues ER-076349 and ER-086526.*

Retention of the extraordinary *in vitro* and *in vivo* activity of halichondrin B (**24**) in structurally simplified, fully synthetic analogues establishes the feasibility of developing commercially viable halichondrin-based agents as highly effective, novel cytotoxic drugs.

The second factor preventing further drug development relates to the potent cytotoxicity of the halichondrin series of compounds and their non-selectivity for diseased cells. This problem can be addressed by focusing on delivery methods (see below). The Marine Chemistry Group at the University of Canterbury have worked in collaboration with the NCI, the London School of Pharmacy and the Welsh School of Pharmacy on the development of polymer therapeutics[89] and conjugates of CV-N[90] based on the homohalichondrin B (**22**) skeleton.

1.4 Cyanovirin-N

1.4.1 Discovery and Isolation

The pharmaceutical industry has, as already alluded to, depended heavily on the process of empirically screening large numbers of pure organic compounds or crude natural product extracts to provide new leads.

In 1988, the United States National Cancer Institute (NCI) began a comprehensive pre-clinical drug development program. As part of this agenda, a broad screening program was conducted to evaluate synthetic and natural products for anti-HIV activity. In part, this screening program focused on extracts from unusual microorganisms, including cyanobacteria.[91]

The Laboratory of Drug Discovery Research and Development (LDDRD) selected an aqueous cellular extract of a cultured cyanobacterium *Nostoc ellipsosporum* for detailed investigation. This decision was based on the extract's strong inhibition of HIV in an empirical screen, and because there were preliminary indications that the active constituent was a protein, and not due to the presence of sulfolipids, sulfated polysaccharides or any other known anti-HIV chemical class.[25,91]

In 1997, anti-HIV bioassay guided fractionation of the extract led to the isolation and purification of a unique protein, Cyanovirin-N (CV-N, **28**).[25,91] A 101 amino acid sequence (Figure **1.13**) was deduced by N-terminal Edman degradation of the intact protein and peptide fragments produced by endoproteinase digestions. Amino acid analysis confirmed the sequence. CV-N (**28**) contains four cysteines that form two intrachain disulfide bonds. The positions of these disulfide linkages were established by fast atom bombardment mass spectral studies of peptide fragments generated by enzymatic digestion of CV-N (**28**). No amino acid residues undergo post-translational modification. Electrospray ionisation mass spectrometry (ESI MS) showed molecular ions for the native protein with mass-to-charge ratios consistent with the calculated molecular weight of 11,009 Da.[25,91]

CV-N (**28**) is a highly potent virucidal protein that irreversibly inactivates diverse primary clinical isolates and laboratory adapted strains of HIV-1, HIV-2, and simian immunodeficiency virus. EC_{50} values are generally in the 1-10 nM range. CV-N (**28**) prevents *in vitro* fusion and transmission of HIV-1 between infected and uninfected cells.[25,91] This protein is not toxic to host cells or peripheral blood lymphocytes, even at concentrations as high as 9 μM.[25]

The physiological role of CV-N within the cyanobacterium is presently unknown.[92]

CV-N (**28**) is extremely resistant to physico-chemical denaturation and can withstand multiple freeze-thaw cycles, dissolution in organic solvents such as acetonitrile and methanol, treatment with denaturants, detergents, and heat (up to 100°C) with no significant loss of anti-viral activity.[25,91]

1.4.2 Recombinant Production

The use of genetically engineered organisms for the large-scale production of proteins can provide a ready source of material for further development and investigation. There must be an abundant supply of CV-N (**28**) for it to make any progress as an anti-HIV prophylactic and/or therapeutic.

A DNA coding sequence corresponding to the chemically deduced protein sequence was synthesised by Mori et al.[25] A recombinant protein indistinguishable from natural CV-N (**28**) can be successfully expressed in *Escherichia coli* using a variety of expression vectors.[25,93]

A number of CV-N mutant proteins have also been produced by recombinant methods to explore functional domains, sequence requirements for activity,[93,94] and to facilitate the development of CV-N conjugates that may be useful therapeutics in the future.[95]

1.4.3 Primary Structure of Cyanovirin-N

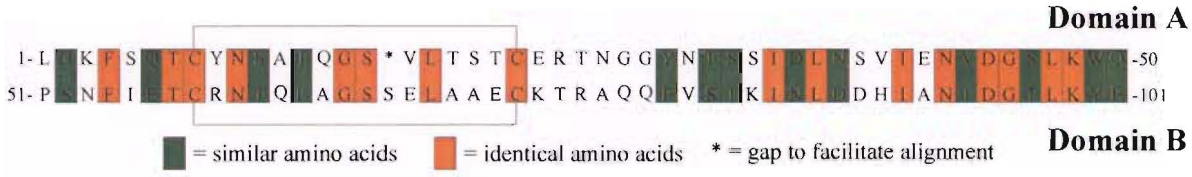

cyanovirin-N (CV-N, **28**)

Figure 1.13: *Amino acid sequence of CV-N.*

Searches of available databases did not reveal any homologies of greater than eight contiguous amino acids or >20% total sequence homology between CV-N (**28**) and any amino acid sequences of known proteins.[25,91] Internally, however, the sequence shows a high degree of homology. Figure **1.13** shows the amino acid sequence of CV-N (**28**). To faciliate visualisation of the internal sequence homology, the sequence has been separated into two portions. The upper portion of the sequence represents amino acids 1-50 (Domain A) and the lower portion of the sequence represents amino acids 51-101 (Domain B). Two intramolecular disulfide bonds are indicated by linking cysteine residues, and are essential for the structural stability and anti-HIV activity of the native protein. Sequence comparison between Domain A and Domain B show high sequence similarity (32% identity and 26% conservative changes, thus 58% overall homology) suggesting that the cyanobacterial gene coding for CV-N (**28**) might have arisen through tandem gene duplication.[25,91]

1.4.4 Three-Dimensional Structure of Cyanovirin-N

Bewley et al. reported the solution structure of CV-N (**28**) in 1998.[96] (Figure **1.14**) The structure was determined using double and triple resonance multidimensional heteronuclear nuclear magnetic resonance (NMR) spectroscopy, making use of uniformly ^{15}N- and $^{15}N/^{13}C$ labelled protein. The elucidation involved extensive use of dipolar couplings that provided long-range structural information.

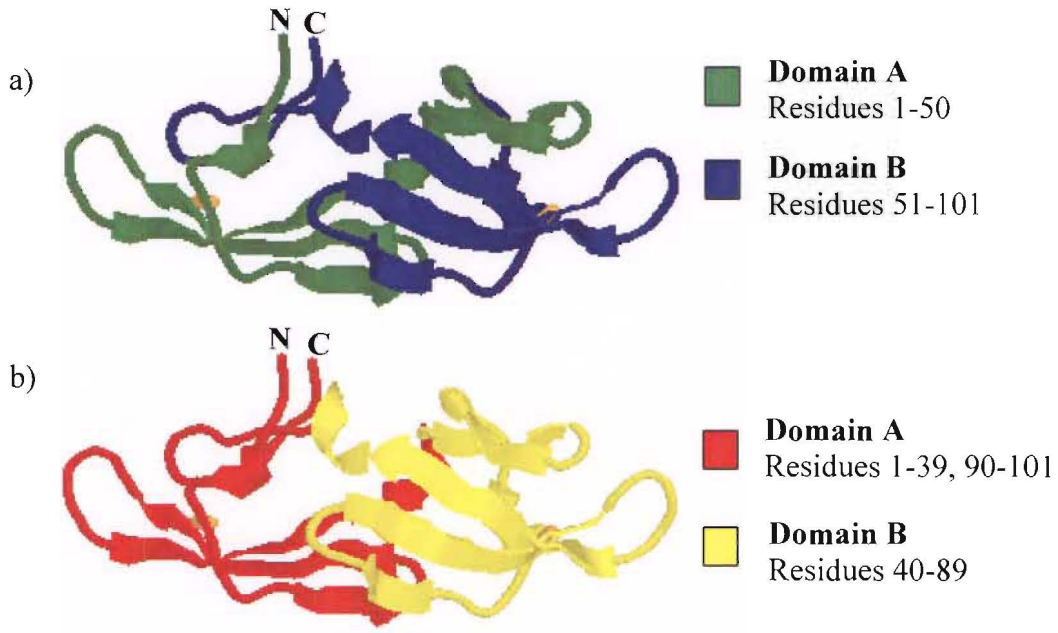

Figure 1.14: *Solution structure of CV-N as determined by NMR spectroscopy.*[96] ***a)*** *sequential domains highlighted.* ***b)*** *structural domains highlighted. The diagrams were produced with Protein Explorer from the RCSB PDB, entry 2ezn.*

CV-N (**28**) is an elongated protein with a length of ~55 Å in length with a maximum width of ~25 Å. The secondary structure elements comprise ten β-strands and four short helical turns. The protein displays internal two-fold pseudosymmetry due to the two sequence domains mentioned above. The two repeats, however, do not form separate domains since the overall fold is dependent on numerous contacts between them. Rather, two symmetrically related structural domains are formed by strand exchange between the two repeats.[96] (Figure **1.14**)

The crystal structure of CV-N (**28**) (Figure **1.15**) was solved by Yang *et al.* in 1998,[97] and was found to consist of a dimer of two molecules of CV-N (**28**). This dimer represents an unusual and unexpected case of an almost symmetric domain swapping and consists of two quasi-monomers, with one made up of residues 1-50 (Domain A) and 51'-101' (Domain B') and the other of 51-101 (Domain B) and 1-50 (Domain A'). The domain-swapped crystal structure shows a flexible linker, or hinge, extending between residues 49 and 54. The two sequence-based domains are therefore moving around the hinge, forming either a monomer by intramolecular interactions or a dimer by intermolecular interactions.[97] The domain swapping occurs under non-physiological conditions, demonstrated structurally by NMR spectroscopy[98] and X-ray crystallography.[97]

Specifically, the dimer occurs following purification by reversed phase HPLC at low pH, and also under crystallisation conditions. The dimer can be converted through to the thermodynamically more stable monomer by incubation at pH>5 at 38°C.[92]

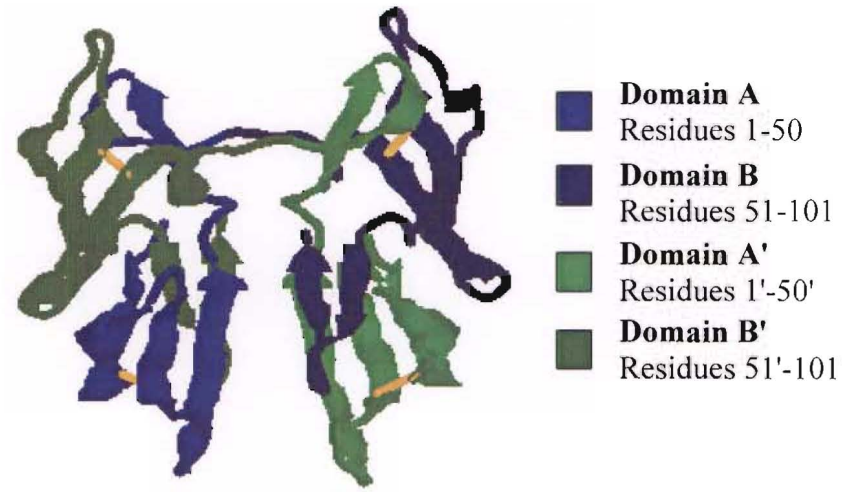

Figure 1.15: *Crystal structure of the domain-swapped CV-N.[97] The diagram was produced with Protein Explorer from the RCSB PDB, entry 115b.*

1.4.5 Mechanism of Action

Early studies revealed that CV-N (**28**) bound with high affinity to the HIV surface glycoprotein gp120.[25] Biochemical studies addressing the mechanism behind the potent anti-viral activity of CV-N (**28**) have included binding,[99,100] hybridisation,[101] mutagenesis[94] studies, and investigations into the activity of CV-N (**28**) at discrete steps along the HIV-1 envelope-mediated fusion pathway.[102] All of these studies confirm the initial findings that CV-N (**28**) interacts with gp120 (and not with CD4 or chemokine receptors) with high affinity and that these interactions are responsible for its potent anti-viral activity at least by preventing the requisite interactions between gp120 and cellular receptors from occurring.[99,101,102] CV-N appears to bind to unique regions of gp120 (as yet to be determined) which are involved in essential fusion event(s), independent of and/or subsequent to the initial interactions with CD4, preceding viral entry.[99]

Gp120 is one of the most highly glycosylated viral proteins known, with a carbohydrate component constituting approximately 50% of the total molecular weight.[103] CV-N (**28**)

was found to bind to non-glycosylated gp120 with considerably less affinity than to glycosylated gp120.[25] It was subsequently reported that the anti-viral activity of CV-N (**28**) is mediated through specific interactions with the HIV envelope glycoproteins, gp120, and possibly gp41.[100] Further investigations have indicated that CV-N (**28**) binds to these proteins through unique interactions with the high mannose oligosaccharides oligomannose-8 and -9 (Man-8 and Man-9 respectively) present in both glycoproteins.[100,103,104] NMR titration experiments with the disaccharide Manα1-2Manα demonstrated the presence on CV-N (**28**) of two binding sites of differing affinities, which mapped to opposite ends of the molecule (Figure **1.16**).[105] Manα1-2Manα represents the terminal accessible disaccharide present in Man-8 and Man-9. The NMR solution structure of CV-N complexed with Manα1-2Manα has also been reported (Figure **1.16**).[105,106] This revealed that the high-affinity site (S2) consists of a deep pocket where the disaccharide is almost completely buried and involved in an extensive hydrogen-bonding network. The low-affinity site (S1) consists of a cleft that only partially surrounds the Manα1-2Manα structure.[106]

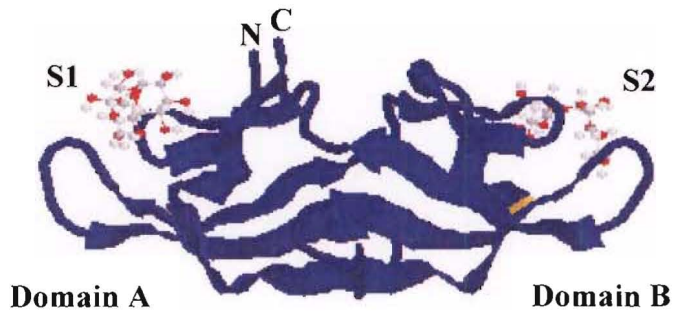

Figure 1.16: *Solution NMR structure of the CVN:Manα1-2Manα complex.[105,106] The protein is depicted as a ribbon with the N- and C-termini labelled. The bound ligands, Manα1-2Manα, are shown in ball and stick representation. The high-affinity binding site is labelled as S2 and the low-affinity binding site as S1. The two structural domains, A and B, are indicated. The diagram was produced with Protein Explorer from the RCSB PDB, entry 1IIY.*

Recently, Chang Leng *et al.* published results that showed that only a single high affinity carbohydrate-binding site, that is, a monovalent CV-N carbohydrate interaction, is required for inhibition of HIV fusion.[107]

In addition to the interactions with specific oligosaccharides, the data from a thermodynamic analysis indicates that discrete protein-protein interactions may play an important ancillary role in the tight binding of CV-N (**28**).[104] The data from a crystal structure of a domain swapped CV-N dimer with Man-9,[108] and the recent identification and characterisation of peptides that bind to CV-N (**28**),[109] further supports the possibility of protein-protein interactions in the binding of gp120 and CV-N (**28**).

1.4.6 Applications of Cyanovirin-N

CV-N (**28**) has also demonstrated inhibition of fusion and/or infection of human herpesvirus 6 and measles virus.[102] Very recently CV-N (**28**) has been shown to have highly potent anti-viral activity against the influenza virus[110] and the Ebola virus.[111] The activity against Ebola is particularly exciting as there are currently no effective therapies for this virus. These studies broaden the range of viruses known to be inhibited by CV-N (**28**), and highlights potential clinical utility. The broad-spectrum anti-viral activity against diverse enveloped viruses further implicates carbohydrate moieties on viral surface proteins as common viral molecular targets for CV-N (**28**).

A high throughput screen has been developed based on the interaction of the HIV gp41 ectodomain with CV-N (**28**). This has resulted in the isolation of new compounds that can bind competitively to gp41 in a manner similar to CV-N (**28**), therefore providing new anti-viral leads.[112]

Boyd et al. propose the use of CV-N (**28**) as method of inducing an immune response in animals.[113,114] The generation of anti-CV-N antibodies with an internal image of gp120 has been demonstrated by administering CV-N (**28**) to rabbits.[113,114] This raises the possibility of using either CV-N (**28**) or anti-CV-N antibodies to prevent or treat a viral infection in an animal.

Another approach to the application of CV-N (**28**) is to immobilise the protein on a solid matrix in order to screen for and exclude HIV from blood or plasma. Biotinylated CV-N was coupled to streptavidin coated magnetic beads to provide sessile CV-N.[115] When

reacted with a primary isolate of HIV the sessile CV-N removed a fraction of the infectious virions but left behind a larger fraction of replication-incompetent virions. The latter fraction could be used as a vaccine for HIV.[113,115]

HIV can be transmitted by vaginal and rectal sexual intercourse. An effective microbicide is one strategy that could significantly reduce the spread of HIV infection. The *in vitro* and *in vivo* efficacy of CV-N (**28**) has been studied in vaginal transmission models. CV-N (**28**) was found to have no adverse effects and was a highly active infection-blocking agent in the model systems.[116] Similar results have been demonstrated with a CV-N gel as a topical microbicide for the prevention of rectal transmission of a pathogenic chimeric simian/HIV-1 virus.[117] *In vitro* studies indicate that CV-N (**28**) is fully active against representative strains of all known HIV subgroups and no CV-N-resistant virus has emerged after numerous tests.[116] Together these results suggest that CV-N (**28**) is a promising agent for development as a topical microbicide for the prevention of sexual transmission of HIV infection.

An effective microbicide may require a system that delivers and maintains an effective concentration of the drug at the mucosal sites of entry of HIV. Giomarelli *et al.* have been exploring the feasibility of endogenous production of CV-N (**28**) at mucosal surfaces by a colonizing commensal bacterium such as *Streptococcus gordonii*. The initial results are positive with *S. gordonii* expressing CV-N (**28**) in a biologically active form.[118]

In addition to direct virucidal applications, CV-N (**28**) has been used in creating a recombinant chimeric toxin molecule in which the translocation and cytotoxic domains of *Pseudomonas* exotoxin A are linked to CV-N (**28**).[95] In the resulting molecule, CV-N (**28**) serves as the targeting moiety that binds to HIV-infected cells expressing gp120. The chimeric molecule demonstrates enhanced cytotoxicity for HIV infected H9 cells compared with uninfected H9 cells, although with the diminution of the overall gp120 binding activity.[95] These results highlight the potential for a similar application of CV-N (**28**) – one that attached low molecular weight, non-proteinaceous cytotoxic agents to CV-N (**28**) – that would not diminish its gp120 binding activity. This concept provides the foundation for the work presented in this thesis.

1.5 Drug Delivery

The development of drugs is often hampered by a poor therapeutic index.[119,120] The therapeutic index is the relationship between the concentration of a drug that results in treatment efficacy, and the concentration that causes toxicity. Ideally, medications should have a high therapeutic index so that they can exert their beneficial effects without causing harm to the patient. A major disadvantage of many clinically established drugs, and of newly isolated compounds showing promising cytotoxicity, is their lack of selectivity for infected tissue, causing systemic toxicity and severe side effects. They are often of low molecular weight and readily gain access to the cells by rapid passage across the plasma membrane.[121,122] The high potency of many compounds, like the halichondrins for example, only serves to exacerbate the problem. Thus, in order to increase the therapeutic index of these agents, drug delivery systems are required which target the drug, through both passive and active mechanisms, to the site of infection. To achieve site specific targeting, it is necessary to identify unique features of affected cell biology that will concentrate the drug within a particular region. In addition, delivery systems can address and correct problems related to the physical characteristic of a drug, including solubility and stability.[123]

One approach that has been found to alter the pharmacokinetic behaviour and overcome the toxicity of cytotoxic compounds to healthy tissue – thereby increasing the therapeutic index of these agents – is to attach the cytotoxic compounds to soluble macromolecules.[121,124] In recent years, such conjugates have been extensively studied as drug carriers facilitating site-specific delivery of immunosuppressants and anti-cancer drugs. Numerous pre-clinical studies have shown that macromolecules such as antibodies, serum proteins, polysaccharides, poly(amino acids), or synthetic polymers are taken up by tumour tissue.[125] These polymers accumulate in solid tumours due to the passive mechanism of the enhanced permeability and retention (EPR) effect.[121,122,126] The entry of macromolecules into tumours is mediated by a 'leaky' blood supply to the tumour. This is in contrast to normal tissue where a continuous layer of endothelial cells allows diffusion of small compounds but not macromolecules. In general, solid tumour tissue does not have a lymphatic drainage system, resulting in retention and accumulation of macromolecules.

Polymer therapeutics is a rapidly growing field in the development of drugs. The basic design of a polymer therapeutic[121,127] (Figure **1.17**) attaches the toxin to a water-soluble polymer (synthetic or biological) so that it can be transported through the blood stream. This attachment is *via* a small biodegradable biolinker. This biolinker acts as a spacer between the drug and the polymer, and, more importantly, can be specifically designed to resist cleavage during circulation in the body but be amenable to enzymatic or hydrolytic cleavage after entry into a diseased cell.[128,129] Drug conjugation to a macromolecule limits cellular uptake to the mechanism of endocytosis. This provides an ideal opportunity to control the rate of drug liberation by careful tailoring of the drug-polymer linker. A targeting residue attached independently to the polymer is the key to targeting receptors found predominantly on cells of interest.

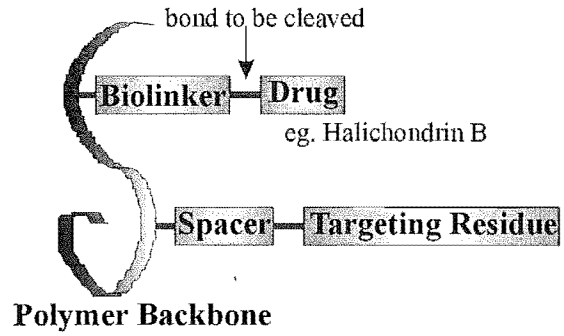

Figure 1.17: *Schematic diagram of the basic features of a soluble polymer therapeutic*[121,127]

Blood proteins, serum albumin, transferrin, and low-density lipoprotein (LDL), have attracted attention regarding their potential as drug delivery systems for improved chemotherapy. These endogenous proteins are suitable as drug carriers for a number of reasons:

- They are readily available in a pure form and exhibit good biological stability.
- They are biodegradable, non-toxic, and non-immunogenic.[119]
- They exhibit a preferential uptake in tumour tissue by the EPR effect.[130,131]
- Tumour cells express high amounts of specific transferrin or LDL receptors on their cell surface.[132,133] Numerous examples of cytotoxic agents have been developed as conjugates with the proteins above in an effort to improve selectivity and toxicity profiles. Promising results have been obtained.[119,134-136]

Drugs that actively target affected cells are sought after for treatments of cancer and HIV. As mentioned briefly above, transferrin and LDL are potential carrier proteins for the targeted delivery of toxic drugs to tumour cells due to receptors on the cell surface. CV-N (**28**) linked to the cytotoxic domains of *Pseudomonas* exotoxin A showed targeted delivery to HIV-infected cells because of its affinity to gp120.[95] Monoclonal antibodies have attracted enormous interest as targeted therapeutics. A variety of antibody-toxin conjugates are showing therapeutic potential as tumour-specific[137] or HIV-specific targeted agents.[138,139] In particular, an anti-HIV molecular conjugate containing the effector domains of the *Pseudomonas* exotoxin A linked to a single chain antibody, with specificity for the highly conserved CD4 binding site of gp120, has been produced. This conjugate is able to kill cells productively infected with diverse strains of HIV while sparing uninfected cells *in vivo*.[27]

The research of the last few decades has resulted in a number of polymer-based products that are now on the market or have entered clinical trial. One approach of particular note involving soluble macromolecular drug carriers is SMANCS. In the clinical formulation, neocarcinostatin (NCS) is conjugated to two chains of a styrene-maleic anhydride copolymer (SMA). SMANCS is marketed in Japan for the treatment of hepatocellular carcinoma.[140]

Polyethylene glycol (PEG)-modified adenosine deaminase (ADAGEN®) and PEG-L-asparaginase (ONCASPAR®) were the first PEG modified enzymes on the market in the early 1990s. PEG-ADA is used for the treatment of ADA-deficient Severe Combine Immunodeficiency Syndrome, and PEG-L-asparaginase is used to treat lymphocytic leukemia and malignant lymphosarcoma. PEG-modification resulted in a prolonged plasma clearance of the enzymes. Both products are in clinical use today.[140]

An anti-HIV hybrid protein toxin, CD4-PE40 (soluble CD4 linked to the translocation and toxic domains of *Pseudomonas* exotoxin A), has been developed to selectively target and kill cells expressing the HIV-envelope glycoproteins.[39,138,139] The genetically engineered protein displays high potency and specificity for killing HIV-1 infected cells *in vitro* and *in vivo* animal models. Disappointingly, the conjugate has demonstrated little

evidence of anti-HIV efficacy in initial Phase I clinical trials. It is believed however, that this drug should be reconsidered in combination with HAART.[39]

PK1 and PK2 are both derivatives of HPMA copolymer with the anti-tumour agent doxorubicin linked onto it *via* the peptidyl spacer Gly-Phe-Leu-Gly. PK2 also contains galactose as a targeting group to facilitate liver targeting.[141] PK1 is currently undergoing Phase II evaluation for treatment of breast, colon and non-small-cell lung cancer. Phase I results revealed that PK1 displayed greatly reduced toxicity with maintained anti-tumour efficacy compared with free doxorubicin.[142] The maximum tolerated dose of PK1 is about four times higher than the usual clinical dose of free doxorubicin.[142] PK2 has entered Phase I clinical testing.[143]

These positive results demonstrate that the coupling of cytotoxic agents to suitable macromolecules is a promising approach of circumventing the toxic side effects of these agents to normal cells, and of improving their efficacy towards infected cells. Primarily, this thesis explores the use of the 11 kDa protein, CV-N, to **actively** target and deliver cytotoxic natural products to HIV-infected cells. This project also investigates the use of human serum albumin, a 66 kDa protein, as a macromolecular carrier to **passively** target and deliver cytotoxic natural products to cancerous cells.

1.6 Project Aims

1.6.1 Anti-HIV Therapeutics

Mori *et al.* created a chimeric molecule in which the cytotoxic domain of *Pseudomonas* exotoxin A is linked to CV-N (**28**) (Section **1.4.6**).[95] The conjugate demonstrates enhanced cytotoxicity for HIV infected H9 cells compared with uninfected H9 cells. As a result of the large proteinaceous toxin, however, it shows a diminution of the overall gp120 binding activity.[95]

The primary aim of this project was to design and follow a synthetic strategy that attached low molecular weight, cytotoxic agents to CV-N (**28**) that would not diminish its gp120 binding activity. The resultant conjugates would be fully chemically characterised. Their selective cytotoxicity to HIV-infected cells and gp120 binding activity would also be assessed. Previous work by Scott Bringans[90] established the viability of this approach by synthesising fluorescently-labeled conjugates of native CV-N (**28**). Biological testing of these derivatives showed no interference with the anti-HIV activity of the protein.

A number of factors needed to be taken into consideration in the development of a CV-N-toxin conjugate:

- Firstly, the modifications made to CV-N (**28**) must not interfere with the binding capabilities of the protein to gp120.
- Secondly, ideally the toxin would behave under a prodrug strategy until the conjugate was internalised and the "active" drug was released within the infected cell. However, any synthetic modifications to the toxins must still allow the toxin to retain its inherent biological activity.
- Thirdly, with limited toxin and protein supply, synthetic steps must be carefully planned and as high yielding as possible.
- Finally, a protein-conjugate must be internalised before it can function to kill a cell. Most virologists believe that retroviral envelope proteins found on the cell surface are in the process of leaving the cell *via* viral budding. However, Pincus *et al.*[138] showed that, at least a portion of the cell-surface envelope protein is

reinternalised. Their studies demonstrated that there is a recirculating pool of envelope protein, and that the rates of internalisation were subject to regulatory influences. These results demonstrate the feasibility of creating a CV-N-toxin conjugate as an anti-HIV therapeutic.

The focus of this project has been on the development of a proof-of-concept approach to an anti-HIV therapeutic. The aim was to take advantage of the specific, targeted, delivery opportunity offered by CV-N, and the bioactivity of several natural products, to develop novel anti-HIV therapeutics with high specificity and high toxicity towards HIV infected cells.

1.6.2 Anti-Cancer Therapeutics

Section **1.5** introduced the phenomenon of macromolecules accumulating in solid tumors. The plasma protein, human serum albumin (HSA), exhibits a significant uptake in tumour tissue as demonstrated by Matsumura *et al.*[131] and Sinn *et al.*[130] A number of conjugates in which anti-cancer drugs, for example chlorambucil[134] or doxorubicin,[144] have been bound to albumin through acid-sensitive linkages have been developed. The positive *in vitro* and *in vivo* anticancer activity demonstrated by these conjugates encouraged a second aim of this project. This would investigate the use of human serum albumin as a macromolecular carrier, to passively target and deliver selected cytotoxic natural products to cancerous cells. The chemistry developed in Section **1.6.1** would be utilised to attach low-molecular-weight, cytotoxic agents to HSA.

2 STRATEGY DEVELOPMENT

STRATEGY DEVELOPMENT

2.1 Introduction

As outlined in the previous chapter, the primary aim of this project was to develop an anti-HIV therapeutic agent, by attaching low-molecular-weight cytotoxic compounds to CV-N (**28**). The target structure is shown schematically in Figure **2.1**. The rationale was that CV-N (**28**) would target and deliver the drug to infected cells. Selective cleavage of the biolinker, within diseased cells, would release the drug and the inherent cytoxicity. This strategy was adapted from the polymer therapeutic model proposed by Ringsdorf in 1975.[127]

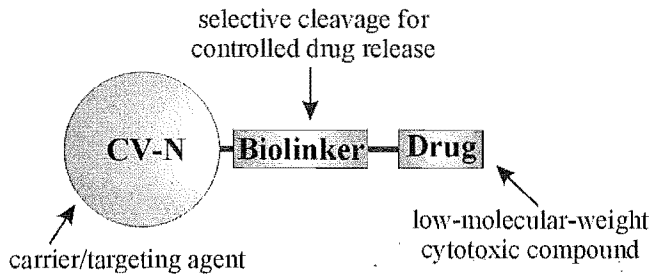

Figure 2.1: *Schematic of a CV-N-drug conjugate.*

In the development of this strategy, attention needed to be focused on each of the individual components of the conjugate in Figure **2.1**. This chapter describes:

1) The selection of an appropriate biolinker that would allow controlled release of a drug within HIV-infected cells.
2) The selection of a synthetic method by which the biolinker unit could be covalently coupled to CV-N (**28**).
3) The establishment of a synthetic route to prepare an activated biolinker that could participate in the coupling strategy planned in 2).

4) The selection of appropriate cytotoxic drugs, and hemi-synthetic modification of these compounds, so that they could be functionalised in such a way as to be covalently attached to the biolinker.
5) Proof-of-principle of the conjugation strategy in 2) with a model protein and a model biolinker-toxin construct. This objective provided the opportunity to develop purification methods and establish approaches for evaluating the structures of the conjugates.

2.2 Biolinker Development

Careful tailoring of the protein-drug biolinker is essential to the creation of a "prodrug" that is stable during transport but allows drug liberation at an appropriate rate intracellularly. Acid labile, pH-dependent hydrazone and acetal linkages[145] have been fashionable for drug conjugation. The proton pump present in the endosomal and lysosomal membranes creates an acidic intravesicular environment (typically pH 6.5 – 5.5) so drug liberation is triggered following internalisation of the conjugate.[141,145] Peptidyl linkers were popularised by the successful design of anti-cancer HPMA copolymer-Gly-Phe-Leu-Gly-doxorubicin conjugates.[146,147] The tetrapeptide linker, Gly-Phe-Leu-Gly, was shown to be stable in bloodstream circulation,[148] but be cleaved by the cathepsin enzymes following endocytic uptake of the conjugate from the tumour interstitium.[149,150]

Macromolecules, particularly proteins, can be taken up by the cell *via* endocytosis, transported in the form of endosomes and finally directed to degradation by fusion of these vesicles with lysosomes.[141,145,151] Lysosomes are organelles which form by pinching off from the Golgi apparatus and which contain a multitude of hydrolytic enzymes, including proteases, esterases and glycosidases.[145] The term "cathepsin" is used to refer to intracellular proteases, mostly localised in the lysosomes, which are active at weakly acidic pH values (approximately pH 5.0).[151] Most of the lysosomal proteases are cysteine, or thiol dependent proteases. Cathepsin B has been the most extensively investigated. Various physiological roles have been ascribed to this enzyme, including degradation of defective or damaged proteins within cell lysosomes, endosomal processing of exogenous proteins and participation in bone remodelling.[151,152] Cathepsin B also shows enhanced expression in tumours. The enzyme is believed to be involved in degradation of the extra-cellular matrix, enabling cancer growth and invasion.[152,153]

The tetrapeptide, Gly-Phe-Leu-Gly, shown in Figure **2.2**, has been designed as a substrate for the cathepsin enzymes,[149,150] and in particular, has been shown to be degraded *in vitro* by cathepsin B.[128,146,147] The success of the HPMA copolymer-Gly-Phe-Leu-Gly-doxorubicin conjugates (PK1 and PK2), both *in vitro* and within Phase I/II clinical

evaluation,[141-143] made the tetrapeptide an attractive biolinker option for the protein therapeutic model being developed in this project.

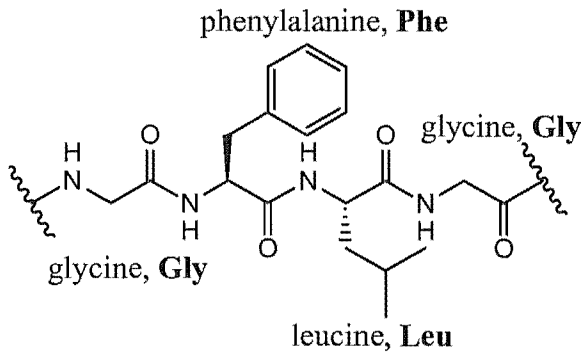

Figure 2.2: *Biolinker; tetrapeptide Gly-Phe-Leu-Gly, a substrate for the cathepsin enzymes.*

2.3 Coupling Method

Bioconjugation involves the linking of two or more molecules to form a novel complex having the combined properties of its individual components. Natural or synthetic compounds with their individual activities can be combined to create unique substances possessing carefully engineered characteristics. Modification and conjugation techniques are dependent on two interrelated chemical functionalities: the reactive functional groups that are present on the derivatising reagents and the functional groups that are present on the target macromolecules to be modified. Without both types of functional groups being available and chemically congruent, the process of conjugation would be impossible.

The technology of bioconjugation has affected nearly every discipline in the life sciences, serving research, diagnostics and therapeutic markets. The development of this field has resulted in an arsenal of reagent systems and conjugation strategies[154] to select from in the design of unique applications.

Several factors needed to be taken into consideration in the development of a CV-N-toxin conjugate. Firstly, the bond between biolinker and protein must be sufficiently stable so as to resist cleavage in circulation of the body. And secondly, there is the requirement to attach toxin molecules to CV-N (**28**), without affecting the tenuous relationship between amino acid functionality and the three-dimensional folding of the polypeptide chain. CV-N (**28**) must retain its ability to bind to gp120, and hence retain the unique anti-HIV activity. Scott Bringans[90] synthesised fluorescently-labeled conjugates of native CV-N (**28**). These conjugates had been prepared by activating a fluorescent compound with an *N*-hydroxysuccinimide (NHS) ester. NHS ester-containing compounds react with nucleophiles, with a marked preference for *N*-based nucleophiles, with release of the NHS leaving group to form an acylated product. The alternative reaction of such esters with a sulfhydryl or hydroxyl group does not yield stable conjugates, forming thioesters or ester linkages, respectively. Both of these bonds hydrolyse in aqueous environments.[154] Thus, in protein molecules, NHS ester reagents couple principally with the ε- and N-terminal amines.[154] Biological testing of the CV-N derivatives prepared in this manner, demonstrated that modification of the amine functionalities of CV-N (**28**) created conjugates with good retention of the native anti-HIV activity.[90] The NHS ester reagent

hydrolysed rapidly in the aqueous environment. An alternative 'modifier' of the amines was sought that would eliminate this hydrolysis problem at the start of the bioconjugation process.

Traut's reagent, 2-iminothiolane (2-IT, **29**), has been used previously as a protein cross-linking agent,[155,156] and is also being developed by Kratz and Beyer[135,157] as a strategy for conjugating the transferrin protein to natural products, such as chlorambucil. The cyclic imidothioester reacts with primary amines in a ring-opening reaction that generates a free thiol (Figure **2.3**). 2-IT (**29**) has been shown to react preferentially with exposed lysine ε-amino groups and at the N-terminal α-amino group.[158] Traut's reagent (**29**) is fully water-soluble and reacts with primary amines in the pH range 7 – 10. The cyclic imidothioester is stable to hydrolysis at acid pH values, but its half-life in solution decreases as the pH increases beyond neutrality. At high pH (10), 2-IT (**29**) is also reactive with aliphatic and aromatic hydroxyl groups, although the rate of reaction is only about 0.01 that of primary amines.[154]

Maleimide derivatives can then be selectively bound to the introduced sulfhydryl groups on the carrier protein. The sulfhydryl functionality adds to the double bond of a maleimide group in a fast and selective Michael reaction forming a stable thioether bond. Maleimide reactions are specific for sulfhydryl groups in the pH range 6.5 – 7.5.[154] At pH 7, the reaction of the maleimide with sulfhydryls proceeds at a rate of 1000 times greater than its reaction with amines while at higher pH values some cross-reactivity of amino groups can take place.[154] Figure **2.3** depicts the use of this methodology to produce a CV-N-drug conjugate. CV-N has six primary amino groups that can be thiolated, and hence up to six equivalents of a maleimido-activated drug construct could be conjugated to the protein. The thioether linkage is stable in blood circulation.[157]

Owing to the highly selective nature of the thiolation reaction, followed by the preferential and rapid binding of the sulfhydryl to a maleimido derivative, the synthetic strategy in Figure **2.3** was selected to produce CV-N drug conjugates.

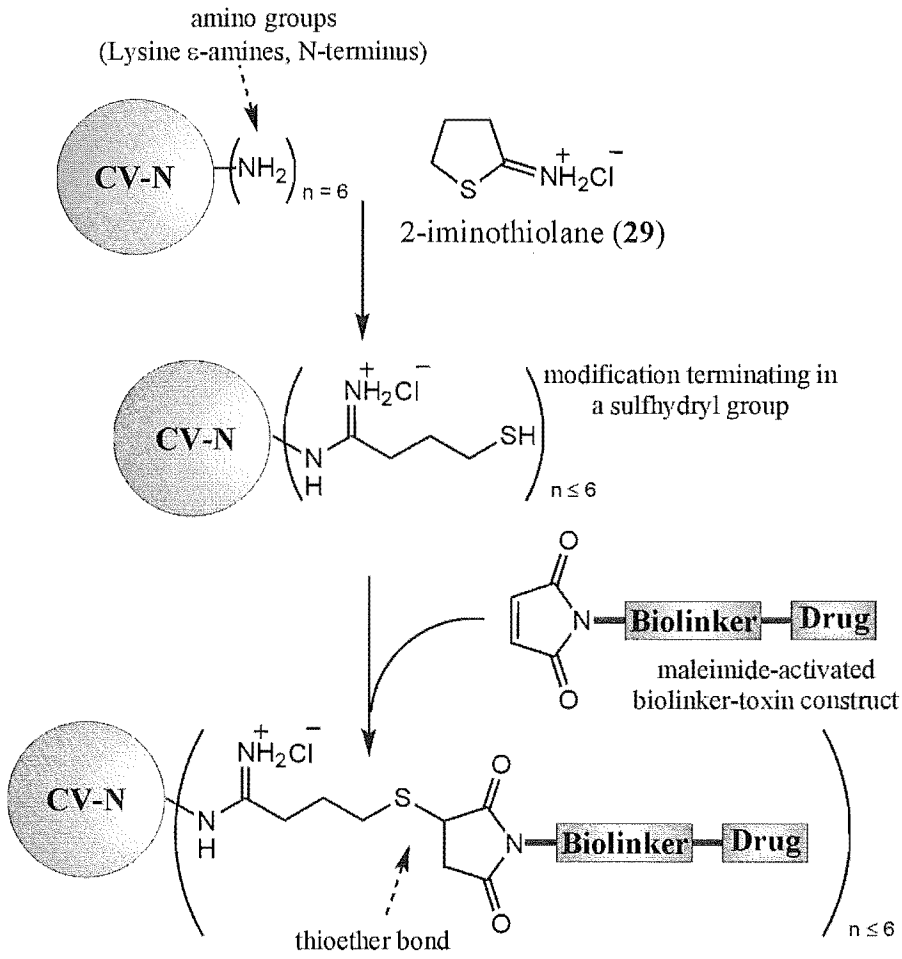

Figure 2.3: *Synthesis of a CV-N-drug conjugate using thioether bond formation.*

2.4 Synthetic Route to an Activated Biolinker

Based on the considerations outlined in Sections **2.2** and **2.3**, γ-maleimidobutyric-Gly-Phe-Leu-Gly-OH (**30**) was selected as the target maleimido-activated biolinker. This compound could then be subsequently coupled to chosen toxin derivatives.

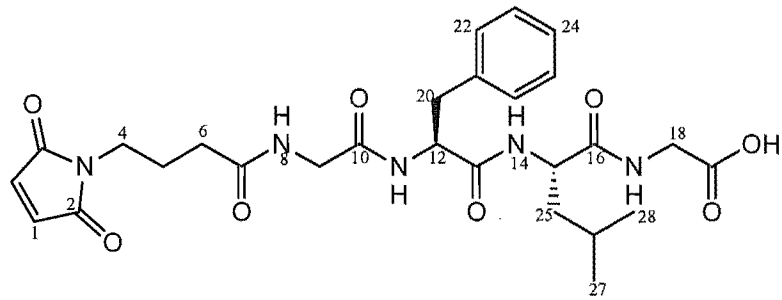

γ-maleimidobutyric-Gly-Phe-Leu-Gly-OH (**30**)

Figure 2.4: *The target maleimido-activated biolinker:* γ-maleimidobutyric-Gly-Phe-Leu-Gly-OH (**30**)

2.4.1 Solid Phase Peptide Synthesis

The importance of peptides in biological processes is beyond doubt. Their wide spectrum of activity marks them out as a class of compounds of significant interest in areas from medicinal chemistry through to molecular biology. It is therefore not surprising that there has been a constant drive to develop new and improved strategies for peptide synthesis.

Solid Phase Peptide Synthesis (SPPS) was first introduced by Merrifield in 1963,[159] and has dominated synthetic peptide research since. The concept of SPPS is illustrated in Figure **2.5**. SPPS is based on sequential addition of α-amino and side chain protected amino acid residues to an insoluble solid support. The base-labile fluorenylmethoxycarbonyl (Fmoc)-group is often used for N-α-protection. After removal of this group, the next protected amino acid is added using either a coupling reagent or a pre-activated protected amino acid derivative. The resulting peptide is attached to the resin, *via* a linker, through its C-terminus and may be cleaved to yield a peptide acid or amide depending on the linking agent used. The revolutionary principle behind SPPS is that if the peptide is bound to an insoluble support then any unreacted reagents left at the

end of any synthetic step can be removed by a simple wash procedure, greatly decreasing the time required for synthesis.[159-161]

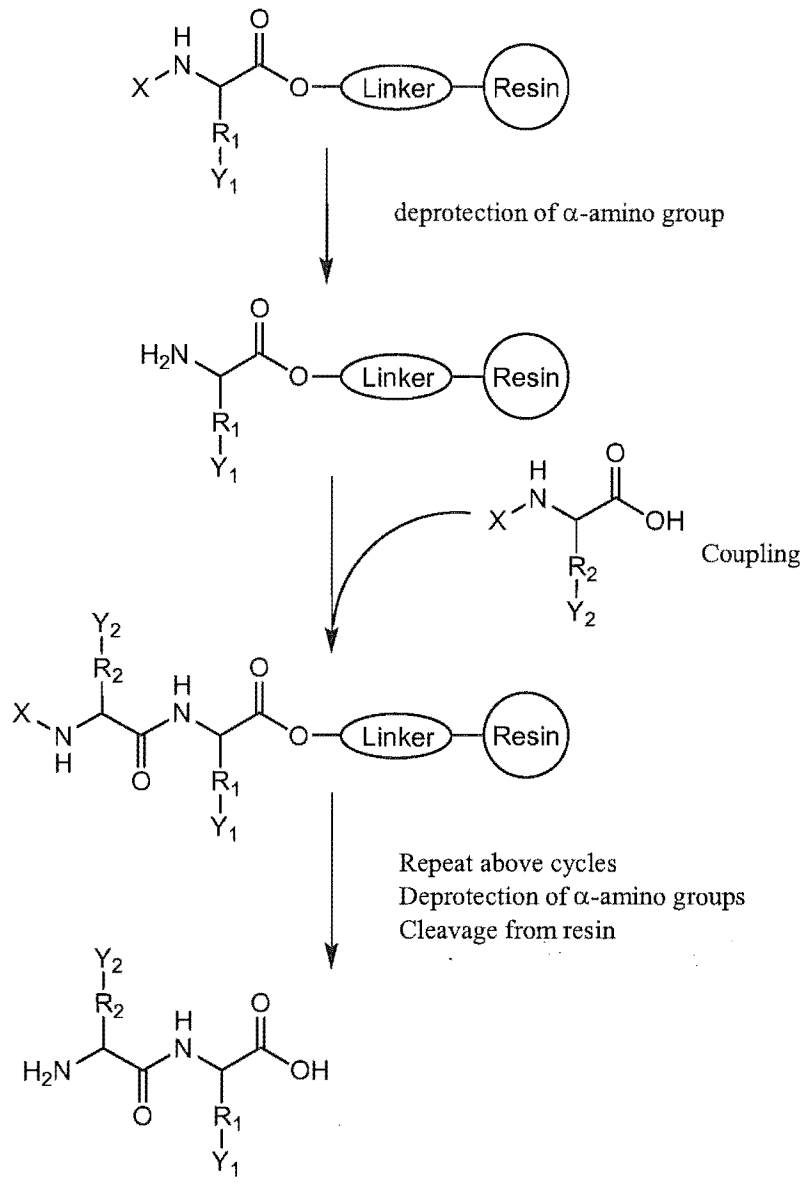

Figure 2.5: *Schematic of Solid Phase Peptide Synthesis. R: side chains. X: temporary α-amino protecting group. Y: side chain protecting groups.*

The maleimido-tetrapeptide derivative, **30**, was synthesised on solid phase, with the maleimide introduced in the final step, at the N-terminal position of the tetrapeptide.

Although several types of polystyrene-based resins have been used for synthesis of peptides using the Fmoc strategy, the most successful and widely used resin is that of Wang.[162] The resin consists of a polystyrene bead onto which an acid-labile linker has been attached. Attachment of the first amino acid to Wang resin has often been

accomplished using dicyclohexylcarbodiimide (DCC) and 4-dimethylaminopyridine (DMAP). This method is fraught with the problem of racemisation of the amino acids (though not a problem in this case, with the first amino acid being glycine) and formation of dipeptides (through premature loss of Fmoc) due to the basic nature of DMAP.[163] For this reason, the esterification of glycine to the hydroxyl group on the resin followed the method described by Sieber.[163] This esterification method is a good alternative, requiring longer loading times, but virtually eliminating racemisation and dipeptide formation. Wang resin (2 g, 3 mmol hydroxymethyl groups) and 1.1 equivalents Fmoc-Gly-OH were shaken in DMF at RT for 15 minutes. Pyridine (6.9 equivalents) and 2,6-dichlorobenzoyl chloride (3.5 equivalents) were added successively and the suspension was shaken for 15 hours. After washing, any remaining hydroxyl groups of the resin were benzoylated with four equivalents benzoyl chloride and six equivalents of pyridine in dichloroethane.

The extent of functionalisation of the resin was measured by UV determination of the 9-fluorenylmethylpiperidine after cleavage of the Fmoc-group with piperidine. A small amount of resin (0.5 – 1 mg) was weighed into two quartz cuvettes. A piperidine/DMF solution was dispensed into each cuvette along with a third that was used as a solvent blank. A UV spectrum of each sample taken after five minutes. The loading of the resin was determined on the basis of a linear relationship between absorbance at 290 nm and quantity of Fmoc amino acid present. One mmol of Fmoc-amino acid gives an absorbance of 1.650. An average loading of 0.873 mmol Fmoc/g resin, and hence 0.873 mmol glycine/g resin, was determined.

The glycine-loaded resin was subsequently used in a batch-wise synthesis of the tetrapeptide. The peptide resin was contained in a filter reaction vessel, to allow bubbling of the resin with nitrogen gas from below, and removal of solvent and excess reagents by vacuum after each step. The glycine-resin (2 g, 0.873 meq/g) was bubbled in DMF for 30 minutes to preswell the resin. Thus, the reactions occur not on the surface of a rigid particle, but within the support of a solvated gel which permits easy access to the growing peptide chain. The glycine residue was then deprotected by subjecting it to mild base treatment using piperidine (20% piperidine/DMF, 20 mL) for ten minutes. The reaction mixture was filtered by suction and washed with DMF and IPA. The completion of the deprotection was monitored to ensure the success of the SPPS. The qualitative ninhydrin-

based Kaiser test[164] (Section **8.1.6**) was used to determine the presence or absence of free amino groups. A positive result was recorded with the expected dark blue colour typical of free amines, so the synthesis continued. Two equivalents of Fmoc-Leu-OH were combined with two equivalents of the *in situ* coupling reagent, HBTU, two equivalents of HOBt, to prevent racemisation, and four equivalents of the base, DIPEA, for two minutes. This solution was then bubbled with the glycine-resin for one hour. The beads were washed with DMF and IPA before being reanalysed with the Kaiser test. A negative result confirmed that the coupling procedure was complete. The steps described to this point completed one cycle; the peptide chain was lengthened by one amino acid residue. Further cycles were carried out in the same way by alternating deprotecting and coupling with the remaining amino acids, Fmoc-Phe-OH and Fmoc-Gly-OH, and the maleimido-acid, γ-maleimidobutyric acid. The sample was left to dry overnight in the presence of P_2O_5 under vacuum, before the completed maleimido-tetrapeptide was liberated from the resin by treatment with a TFA solution (95% TFA, 2.5% TES and 2.5% water) for 20 minutes. The solution was drained and the resin was rinsed with further TFA. The acidic fractions were combined and alternately concentrated under vacuum and precipitated with water to remove TFA from the solution.

The crude peptide product was purified by semipreparative reverse phase HPLC. A solvent gradient comprising the following steps was used: an isocratic hold on 15% CH_3CN/H_2O (0.05% TFA) for two minutes; a linear gradient to 50% CH_3CN/H_2O over 20 minutes; a return to 15% CH_3CN/H_2O over one minute; and finally an isocratic hold on 15% CH_3CN/H_2O for two minutes. The system was monitored at 213 nm and a peak eluting at 15.6 minutes was collected manually and the solvent removed under nitrogen gas flow to give **30**.

2.4.2 Characterisation of γ-maleimidobutyric-Gly-Phe-Leu-Gly-OH (**30**)

The ^1H NMR (Figure **2.6**) and ^{13}C NMR spectra of **30** were readily assignable with reference to COSY, HSQC and CIGAR 2D NMR experiments. Determination of connectivity between spin systems within the same amino acid allowed the identification

of individual amino acid residues, while heteronuclear couplings across the peptide bond were used for elucidation and confirmation of the sequence.

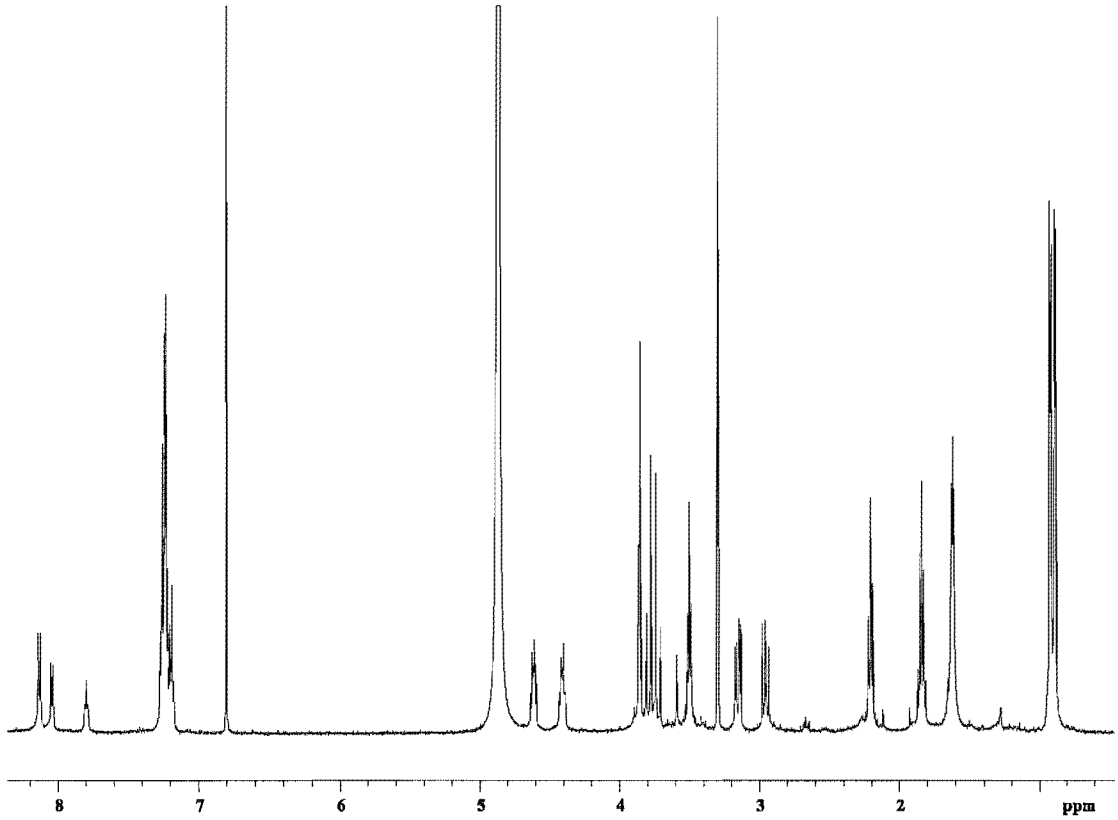

Figure 2.6: *^{1}H NMR spectrum of γ-maleimidobutyric-Gly-Phe-Leu-Gly-OH (**30**)(500 MHz, CD_3OD)*

The chemical shift assignments for the ^{1}H and ^{13}C NMR spectra are shown in Table **2.1**, with the structure and major CIGAR correlations shown in Figure **2.7**.

NMR analysis was carried out in CD_3OD. This resulted in a loss of the proton signals beyond 7.80 ppm over time. This was due to the exchange of the amide protons by the ionisable deuterium atom of the solvent. For this reason the amide protons were not assigned. All expected HSQC correlations were present in the spectra, therefore allowing immediate assignment of ^{1}H chemical shifts to their ^{13}C counterparts. A useful starting point for the structural elucidation was the readily assigned lone proton of the maleimide, the singlet at 6.80 ppm. A CIGAR correlation connected the ketone at position C2. A CIGAR correlation from the proton multiplet at 3.50 ppm back to C2 linked the alkyl chain to the maleimide functionality. With H4 now established, the assignment of H5 and H6 was also possible due to COSY correlations. H5 was correlated to both H4 and H6, and was placed in the centre of the alkyl chain. This order of assignment was confirmed

with a correlation from H6 into the carbonyl at position C7. The first glycine residue was connected to the maleimide entity, C7, due to CIGAR correlations through the amide bond from the two α-protons at 3.80 ppm and 3.72 ppm respectively. In turn, these α-protons established the assignment of the carbonyl at C10 with further CIGAR correlations. The phenylalanine residue was subsequently linked into the peptide via a CIGAR correlation from the α-proton multiplet at 4.62 ppm to the carbonyl, C10. Access into the aromatic ring of phenylalanine was gained through CIGAR correlations from H12 to C20 and C21. The phenylalanine carbonyl, C13, was confirmed with CIGAR correlations from both the α- and β-phenylalanine protons. A further CIGAR correlation from the leucine α-proton linked the leucine residue into the peptide chain. The leucine α-proton also fed important CIGAR correlations into the branched leucine alkyl side-chain, allowing assignment of positions 25 to 28. Finally, the second glycine residue completed the tetrapeptide, with CIGAR correlations from the α-proton at position H18, across the amide bond into C16, and into the carboxylic acid at C19. An HSQC correlation confirmed the chemical shift of C18.

Atom No.	^{1}H δ (ppm)[a]	^{13}C δ (ppm)[b]	Atom No.	^{1}H δ (ppm)[a]	^{13}C δ (ppm)[b]
1	6.80 (s)	134.3	15	4.41 (m)	51.9
2	–	171.5	16	–	171.5
3	–	–	17	–	–
4	3.50 (m)	36.6	18	3.86 (s)	40.6
5	1.84 (m)	24.1	19	–	173.6
6	2.21 (t, 7.5)	32.2	20α	3.15 (dd, 8.5, 13.5)	37.0
7	–	174.4	20β	2.96 (dd, 8.5, 13.5)	37.0
8	–	–	21	–	137.2
9α	3.80 (d, 16.5)	42.5	22	7.19 (m)	129.1
9β	3.72 (d, 16.5)	42.5	23	7.25 (m)	128.3
10	–	171.0	24	7.22 (m)	126.7
11	–	–	25	1.62 (m)	40.4
12	4.62 (m)	55.0	26	1.62 (m)	24.5
13	–	172.4	27	0.93 (d, 6.5)	22.3
14	–	–	28	0.89 (d, 6.5)	20.5

Table 2.1: *^{1}H and ^{13}C NMR data for γ-maleimidobutyric-Gly-Phe-Leu-Gly-OH (**30**). Recorded at 500 MHz in CD_3OD.*

[a] ^{1}H chemical shift values (δ ppm and referenced to $CD_2\mathbf{H}OD$, δ_H 3.31) followed by multiplicity and coupling constant (J/Hz). The amides were only partially observed in the ^{1}H spectrum but had exchanged before characterisation by other experiments could take place.

[b] ^{13}C chemical shift values (δ ppm) as determined from HSQC experiments.

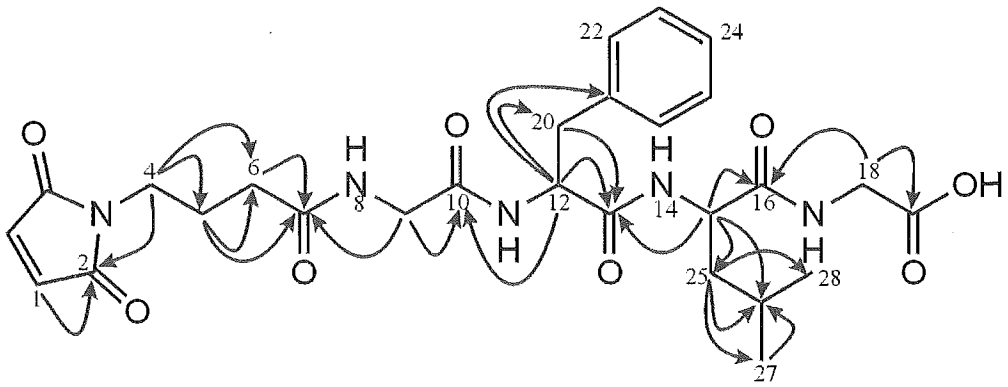

Figure 2.7: *Important CIGAR correlations for γ-maleimidobutyric-Gly-Phe-Leu-Gly-OH (**30**)*

γ-Maleimidobutyric-Gly-Phe-Leu-Gly-OH (**30**) was subsequently reacted with the toxin derivatives. This is discussed below.

2.5 Cytotoxin Development

There is already a plethora of natural compounds that have the potential to be effective as anti-HIV or anti-tumour agents (Chapter **1**). Many of these compounds possess non-specific toxicity restricting their efficacy *in vivo*. One of the main limitations can be viewed simply as an inability to deliver therapeutic agents properly to diseased cells. Early clinical studies with HPMA copolymer conjugates have shown, unequivocally, that drug conjugation can significantly decrease non-specific toxicity while maintaining anti-tumour activity.[142,143] It is clear that if designed correctly, protein- or polymer-drug conjugates could provide an ideal 'package' for compounds whose therapeutic potential has been overshadowed by unacceptable toxicity. Attaching hydrophobic compounds to hydrophilic proteins or polymers also provides the possibility of circumventing the problems associated with poor drug solubility.[165]

There needed to be a careful selection of an appropriate cytotoxin(s) to complete the model in Figure **2.1**. The prospective compound needs to be amenable to derivatisation, and attachment to the biolinker, while still retaining an inherent cytotoxicity. This is, after all, the essential warhead of the conjugate.

The tetrapeptide, Gly-Phe-Leu-Gly, was chosen as a biolinker based on its ability to act as a substrate for the cathepsin enzymes (Section **2.2**). Because of the peptide nature of this linker, the strategy was to attach the cytotoxin to the peptide *via* a peptide bond. The amide linkage serves as the basic unit from which all proteins are made, and resists hydrolysis in circulation of the body. Following endocytosis of the conjugate, hydrolysis by the cathepsin enzymes would release the cytotoxin within diseased cells. Release of the cytotoxin would be in a specific and controlled manner. The biolinker carries a free carboxylic acid, so it follows that the toxin must be functionalised with an amine moiety, in order for amide conjugation to occur.

2.5.1 Homohalichondrin B (**22**)

Homohalichondrin B (**22**) was selected from the library of potent cytotoxic compounds isolated by the Marine Chemistry Group at the University of Canterbury. There was no doubt that this compound showed potential as a pharmaceutical based on its potent *in vitro* and *in vivo* cytotoxicity (Section **1.3**) As outlined in Section **1.3.3** further development of this compound has been hampered by supply issues. However, even with a ready supply of homohalichondrin B (**22**), the critical issue of this compound's high potency and lack of selectivity for infected tissue must be addressed. Homohalichondrin B (**22**) was an ideal candidate to attach to CV-N (**28**), or HSA, in the hope that the therapeutic profile of the cytotoxin could be improved. Homohalichondrin B (**22**) was also chosen because there was an extensive in-house knowledge of the chemistry of the halichondrins. Synthetic methods have already been devised by Rachel Lill[89] and Scott Bringans[90] that have led to the successful production of norhomohalichondrin B amine (**31**). This amine derivative of homohalichondrin B could be subsequently attached to the biolinker *via* a peptide bond.

2.5.1.1 Preparation of norhomohalichondrin B amine (**31**)

Based on the previous discussions, the target maleimide-activated biolinker-halichondrin B construct was γ-maleimidobutyric-Gly-Phe-Leu-Gly-norhomohalichondrin B (**32**).

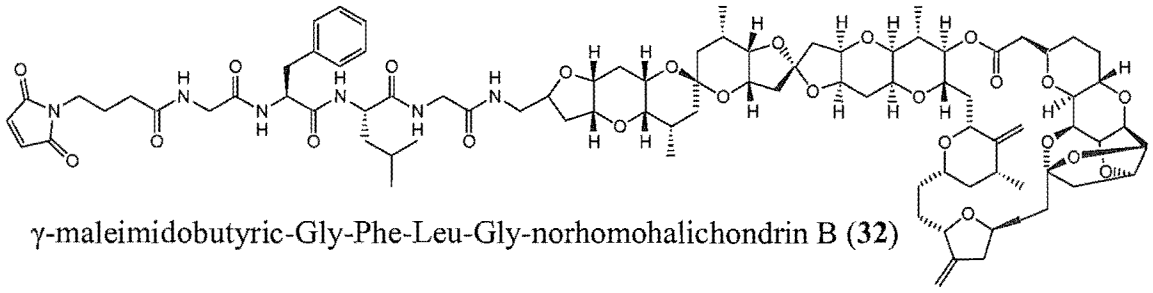

γ-maleimidobutyric-Gly-Phe-Leu-Gly-norhomohalichondrin B (**32**)

Figure 2.8: *The target maleimido-activated biolinker-homohalichondrin B.*

Homohalichondrin B (**22**) first needed to be functionalised with an amine moiety, and then further conjugated with the maleimido-biolinker prepared in Section **2.4**.

Rachel Lill completed the series of reactions outlined in Figure **2.9**. These steps present the synthetic route that she took to convert homohalichondrin B (**22**) to norhomohalichondrin B amine (**31**).[89]

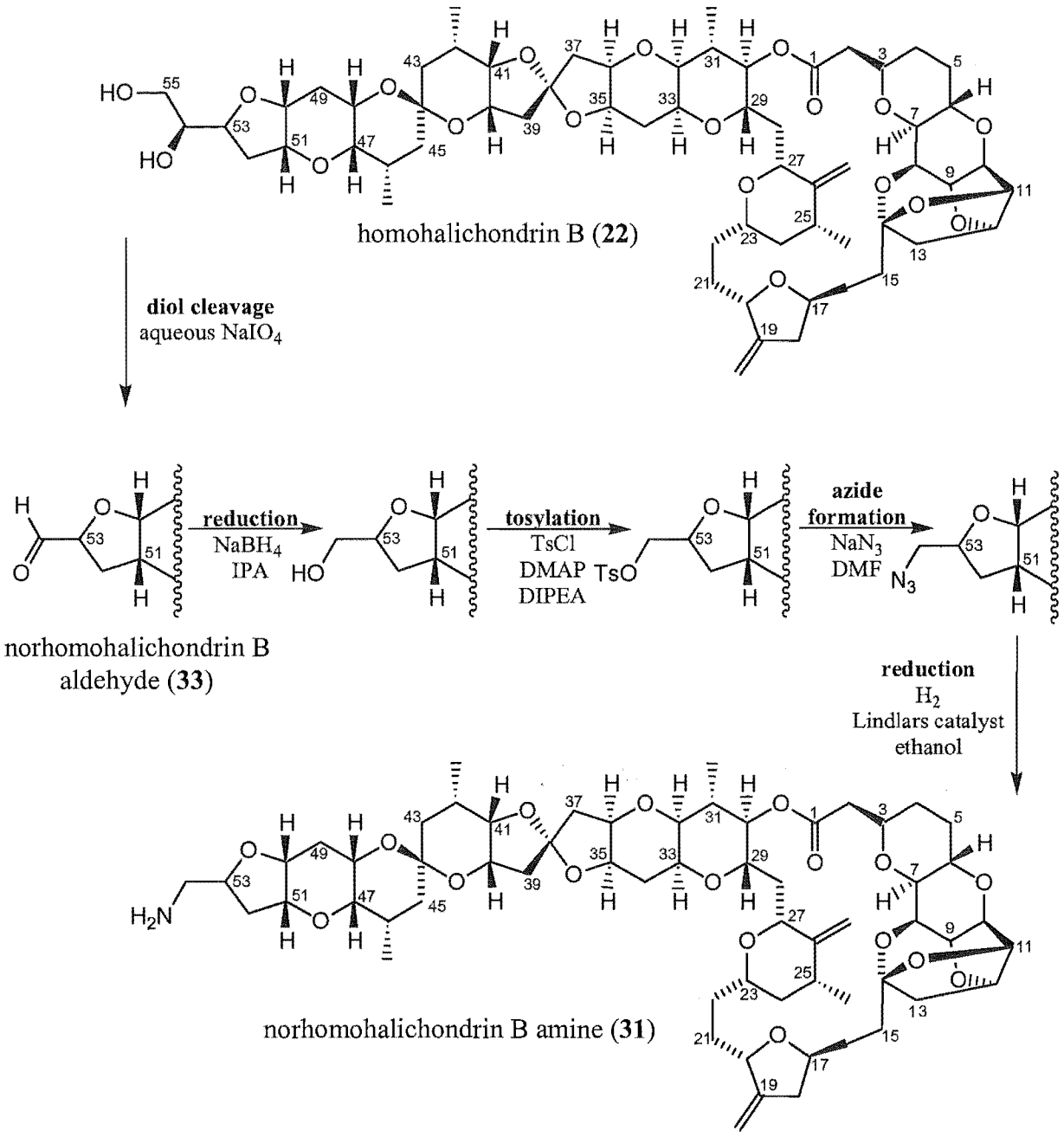

Figure 2.9: *A five-step conversion of homohalichondrin B (22) to norhomohalichondrin B amine (31).*[89]

The scheme in Figure **2.9** shows initial oxidation of the diol (**22**) to an aldehyde (**33**) with subsequent reduction back to the primary alcohol. Tosylation with tosyl chloride was then followed by the formation of the azido norhomohalichondrin B derivative. The final step involved hydrogenation of the azide to the amino-derivative, with Lindlar's catalyst.

Although these reactions were ultimately successful in achieving the desired end amino product, the synthetic scheme was time consuming, purification difficulties were experienced at each stage, and the number of manipulations resulted in significant compound loss over the five steps.

Scott Bringans pursued a different route[90] adapted from a method developed for the conversion of 17-formyl-normycalamide A to 17-amino-normycalamide A by Sean Devenish.[166]

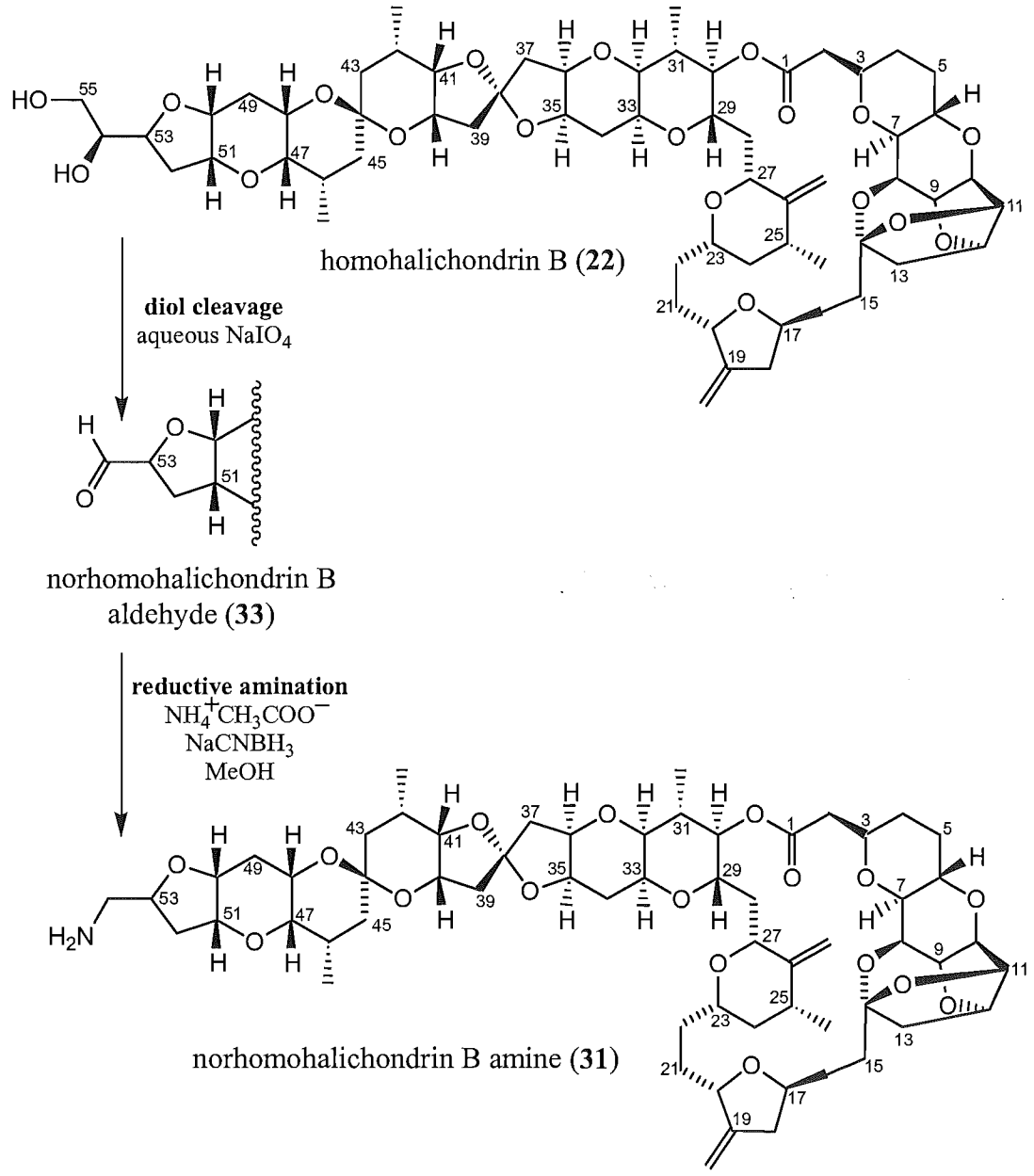

Figure 2.10: *A simple two-step conversion of homohalichondrin B (22) to norhomohalichondrin B amine (31).*[90]

This strategy (Figure **2.10**) bypassed the need for a five step synthetic scheme by forming norhomohalichondrin B amine (**31**) in two simple quantitative steps from homohalichondin B (**22**). It was therefore the method of choice for the generation of an amino derivative of homohalichondrin B that could be subsequently attached to the biolinker.

Homohalichondrin B (**22,** 2 mg) was stirred with an aqueous solution of sodium periodate (30 mM) at room temperature for 24 hours. The aqueous reaction mixture was extracted with ethyl acetate, and the organic fractions were combined and taken to dryness. The ^{1}H NMR spectrum (Figure **2.11**) matched a spectrum for norhomohalichondrin B aldehyde (**33**) produced by Rachel Lill.[89] Of particular interest was the distinctive doublet peak for the aldehyde resonance (H54) at 9.71 ppm, and the readily visible proton peaks representing H53 and H50 of the 'O' ring, at 4.52 ppm and 3.97 ppm, respectively.

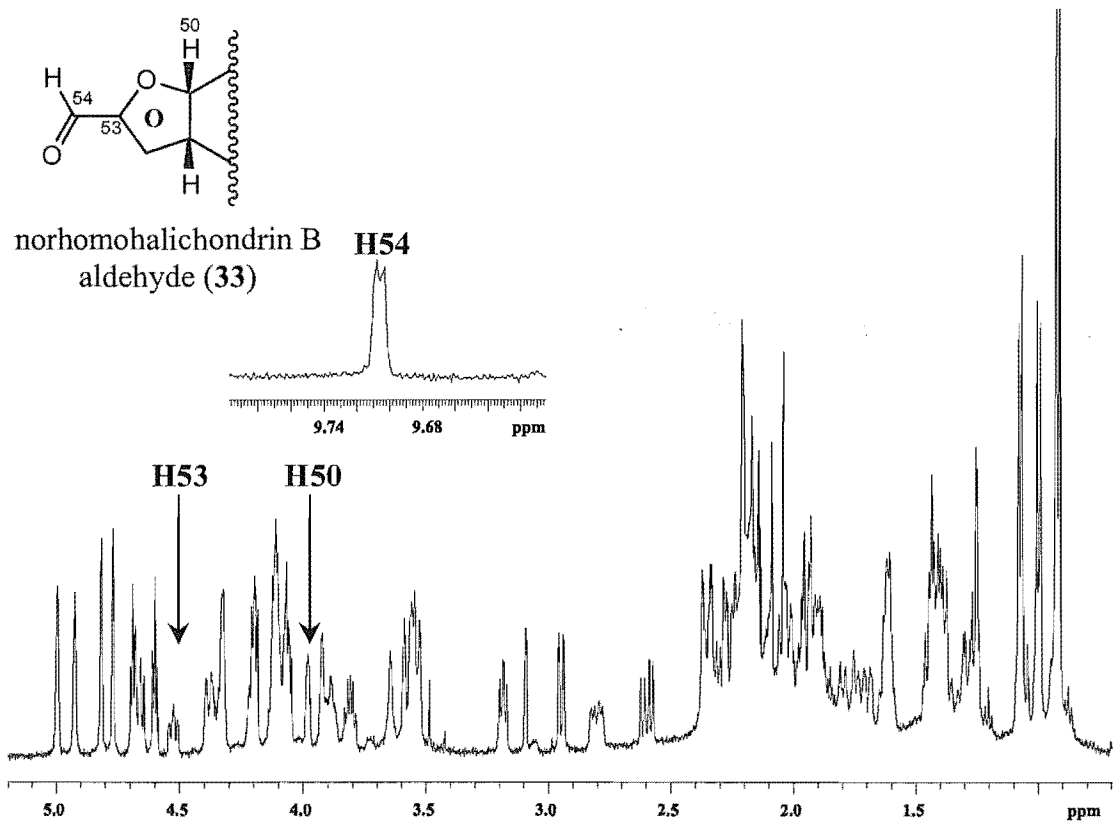

Figure 2.11: *^{1}H NMR spectrum of norhomohalichondrin B aldehyde (33)(500 MHz, CD_3OD).*

Final confirmation that **33** had been prepared was sought through MS analysis. Initially, in both ESI and FAB analyses, no product was observed as only a peak isobaric with the

parent homohalichondrin B diol (**22**) was present. The sample had been prepared in methanol. Comparatively, when the sample was prepared in acetonitrile, the expected molecular ion of norhomohalichondrin B aldehyde (**33**) (MH^+ 1091.5607, $C_{60}H_{83}O_{18}$ requires 1091.5579) was seen. Presumably methanol had been acting as a nucleophile and adding to the aldehyde (**33**), forming a hemiacetal that was isobaric with the diol (**22**). This reaction was reversible.

The preparation of norhomohalichondrin B amine (**31**) involved the reductive amination of norhomohalichondrin B aldehyde (**33**) with ammonia. A solution of **31** (1.7 mg), 100 equivalents of ammonium acetate, and crushed 3 Å molecular sieves, in dry methanol (saturated with ammonium carbonate) was stirred for 30 minutes. The molecular sieves were employed to promote imine formation by absorbing water, thus driving the dehydration to completion. The methanol was saturated with ammonium carbonate to maintain the pH of the reaction, removing any acetic acid that was produced in the process. Sodium cyanoborohydride (five equivalents) was added in ammonium carbonate-saturated dry methanol. Sodium cyanoborohydride was utilised as it allows for selective reduction of carbon-nitrogen double bonds.[167,168] The reaction progress was monitored by TLC (SiO_2), with the disappearance of **31** and the appearance of a ninhydrin active spot near the baseline after 12 hours indicating that the reaction was complete. The reaction solution was diluted in water and passed through a C18 cartridge, washed with further water, and then eluted with methanol. The ^{1}H NMR spectrum (Figure **2.12**) of the methanol fraction was shown to contain norhomohalichondrin B amine (**31**) by comparison to the spectrum of an amine previously produced by Rachel Lill.[89] Notably, the aldehyde resonance at δ 9.71 ppm was no longer present, and the resonances of H53 and H50 of the aldehyde (present in Figure **2.11**) had moved. Rachel Lill had not been able to complete the assignment of the 'O' ring of the amine due to severe overlap in the 2D NMR spectra.[89] HRESIMS provided further confirmation that the amine, **31**, had been prepared. Norhomohalichondrin B amine (**31**) was acylated with the maleimido-tetrapeptide, **30**, without further purification.

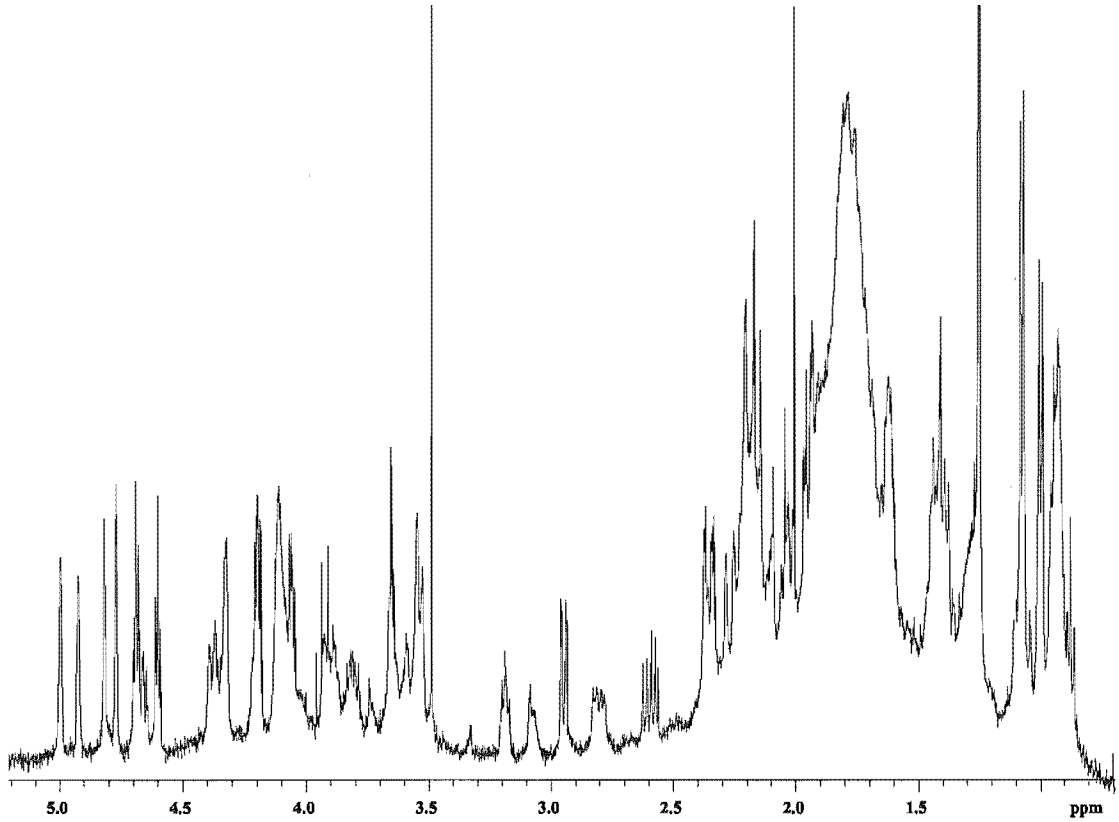

Figure 2.12: *^{1}H NMR spectrum of norhomohalichondrin B amine (**31**)(500 MHz, CD_3OD).*

2.5.1.2 γ-Maleimidobutyric-Gly-Phe-Leu-Gly-norhomohalichondrin B (**32**)

The carboxyl functionality of the maleimido-tetrapeptide (**30**, 858 μg) was activated by conversion to a succinimidyl ester by stirring with *N*-hydroxysuccinimide (NHS, 1.8 equivalents) and dicyclohexylcarbodiimide (DCC, 1.8 equivalents) in dry THF, for two minutes under nitrogen atmosphere. Norhomohalichondrin B amine (**31**, 0.9 equivalents) was added to the reaction system in dry THF, and the reaction was stirred under an inert atmosphere. An excess of **30** to the amine **31**, ensured complete reaction of the toxin. The toxin is more precious than the readily synthesised peptide biolinker. The reaction was visualised by analytical reverse phase HPLC after 60 hours, showing the disappearance of the amine **31**, and the appearance of a less polar peak. Collection of this peak, and subsequent ESI MS analysis, confirmed that it represented the coupled product **32**. To achieve sufficient purity for conjugation to the protein, **32** was purified by analytical HPLC (C18). A 50-minute method was developed (Section **8.2.7**) without an acid additive in the solvent system. This avoided acid-catalysed degradation of

norhomohalichondrin B as discussed in Section **1.3.1**. The peak eluting at 33.7 minutes was collected. Insufficient sample (0.4 mg) was obtained for NMR analysis, but HRESIMS analysis confirmed the preparation of γ-maleimidobutyric-Gly-Phe-Leu-Gly-norhomohalichondrin B (**32**).

2.5.2 Doxorubicin (**34**)

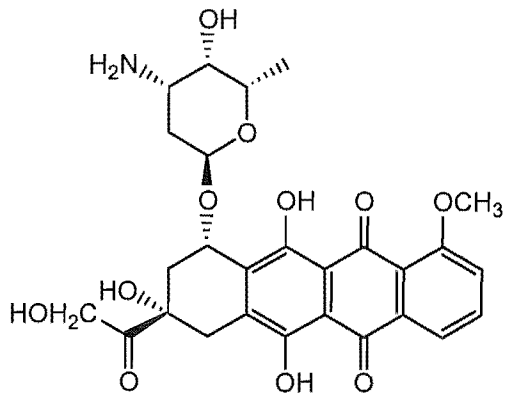

doxorubicin (**34**)

Figure 2.13: *The anthracycline antibiotic, doxorubicin (34).*

Doxorubicin (**34**) is an anthracycline antibiotic with potent cytotoxicity.[169] It is currently used in cancer chemotherapy, but the therapeutic index of doxorubicin is compromised by its dose-related side effects, notably cumulative cardiotoxicity, myleosuppression and development of drug resistance.[169,170] One approach that has been taken to overcome the toxicity of this drug to normal tissue – thereby increasing the therapeutic index of this agent – is the attachment of doxorubicin to a carrier polymer that exhibits significant uptake in tumour cells. PK1 is a synthetic *N*-(2-hydroxypropyl)methylacrylamide copolymer-doxorubicin conjugate currently undergoing Phase II evaluation in the United Kingdom.[171] PK1 has shown promising antitumour activity, and is essentially non-toxic *in vitro* until lysosomal proteases release free doxorubicin from the drug, within the cell. Doxorubicin is linked through its amine functionality to the polymer *via* a peptidyl spacer. PK1 is essentially allowing doxorubicin to act as a pro-drug, designed to be inactive until it is released at a specific point.[171]

Doxorubicin (**34**) was chosen as a complementary toxin to homohalichondrin B (**22**) for several reasons. Firstly, the strategy of attaching doxorubicin to CV-N could achieve site-

specific delivery of doxorubicin to HIV-infected cells, increasing the therapeutic effect and minimising the side-toxicity of the drug. Conjugation to HSA, would create a protein equivalent to PK1 that could be targeted at tumour cells. Secondly, as an important design issue, doxorubicin (**34**) already contains a free amine on the glycoside moiety. This reduces synthetic steps to the maleimido activated-tetrapeptide-conjugate, and avoids extra manipulations and consequential losses of the precious toxin. Thirdly, as mentioned above, attachment of a peptide to the aminoglycoside abolishes doxorubicin's cytotoxic activity.[171,172] The administration of a prodrug of doxorubicin, through attachment of the maleimido-tetrapeptide (**30**), to the glycoside, would allow selective activation by HIV infected cells, or tumours, and would reduce general systemic exposure to the active drug. This would thereby increase the therapeutic index of doxorubicin (**34**). Invariably, drug-delivery systems have been designed around the anthracycline as the compound has been one of the most widely used chemotherapeutics.[144,172-174] Many of these systems are showing therapeutic promise.[171] The conjugates of doxorubicin (**34**) proposed in this thesis could be compared to those already prepared in the literature, and would provide a basis of comparison to the unique homohalichondrin derivatives prepared in this project of work.

The commercial supply of doxorubicin (**34**) is as the hydrochloride salt. This results in the amine being unavailable for coupling to the tetrapeptide construct. Therefore the doxorubicin sample must first be converted to the free base. A reversed phase C18 cartridge was pre-equilibrated with 0.05% NH_4OH/H_2O. Doxorubicin hydrochoride (3 mg) was dissolved in 0.05% NH_4OH/H_2O, resulting in a dark purple solution that was immediately loaded onto the cartridge. The cartridge was washed with five column volumes 0.05% NH_4OH/H_2O. Washing with acetone (five column volumes) eluted **34** in quantitative yield after drying under $N_{2(g)}$. The ^1H NMR spectrum in CD_3OD was identical to that previously reported.[175]

2.5.2.1 γ-Maleimidobutyric-Gly-Phe-Leu-Gly-doxorubicin (**35**)

The target maleimide-activated biolinker-doxorubicin counterpart construct to **32** was γ-maleimidobutyric-Gly-Phe-Leu-Gly-doxorubicin (**35**).

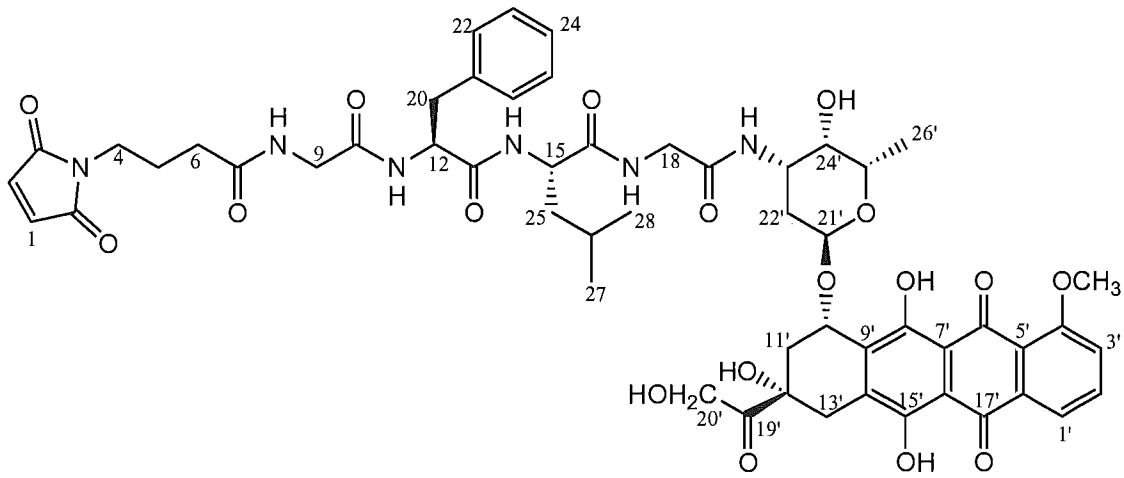

γ-maleimidobutyric-Gly-Phe-Leu-Gly-doxorubicin (**35**)

Figure 2.14: *The target maleimido-activated biolinker-doxorubicin.*

The maleimido-tetrapeptide (**30**, 2.26 mg) was coupled with 0.9 equivalents of doxorubicin (**34**) in the manner described for the norhomohalichondrin B amine (**31**) example described in Section **2.5.1.2**. The reaction was left to stir under nitrogen atmosphere for 24 hours at which time analytical HPLC established the reaction had gone to completion, with consumption of the amine **34**. A short 13-minute solvent gradient (Section **8.2.9**), on an analytical reverse phase HPLC system, was utilised to purify compound **35** from the reaction mixture. A peak with an absorbance at 480 nm eluting at 4.3 minutes was collected and the solvent removed under nitrogen gas flow to give **35** as a red solid. The ^{1}H NMR spectrum in CD_3OD (Figure **2.15**) was assigned as far as possible through comparison with the spectra of **30** (Section **2.5.1.2**) and **34**.[175] Figure **2.15** displays the assigned peaks. Insufficient mass was obtained to carry out 2D NMR experiments. Notable was the obvious disappearance of the glycine α-proton resonance at 3.86 ppm upon the coupling of the tetrapeptide and the aminoglycoside. Ultimately, however, HRESIMS was essential to confirming that γ-maleimidobutyric-Gly-Phe-Leu-Gly-doxorubicin (**35**) had been prepared. (MNa^+ 1105.4034 ($C_{54}H_{62}N_6O_{18}Na$ requires 1105.4018).

Both doxorubicin (**34**) and γ-maleimidobutyric-Gly-Phe-Leu-Gly-doxorubicin (**35**) proved difficult to handle, adsorbing onto the glass surfaces of the vials and NMR tubes that they were contained in. This did result in loss of product, so transfer of **34** and **35** from their respective containments was kept to a minimum.

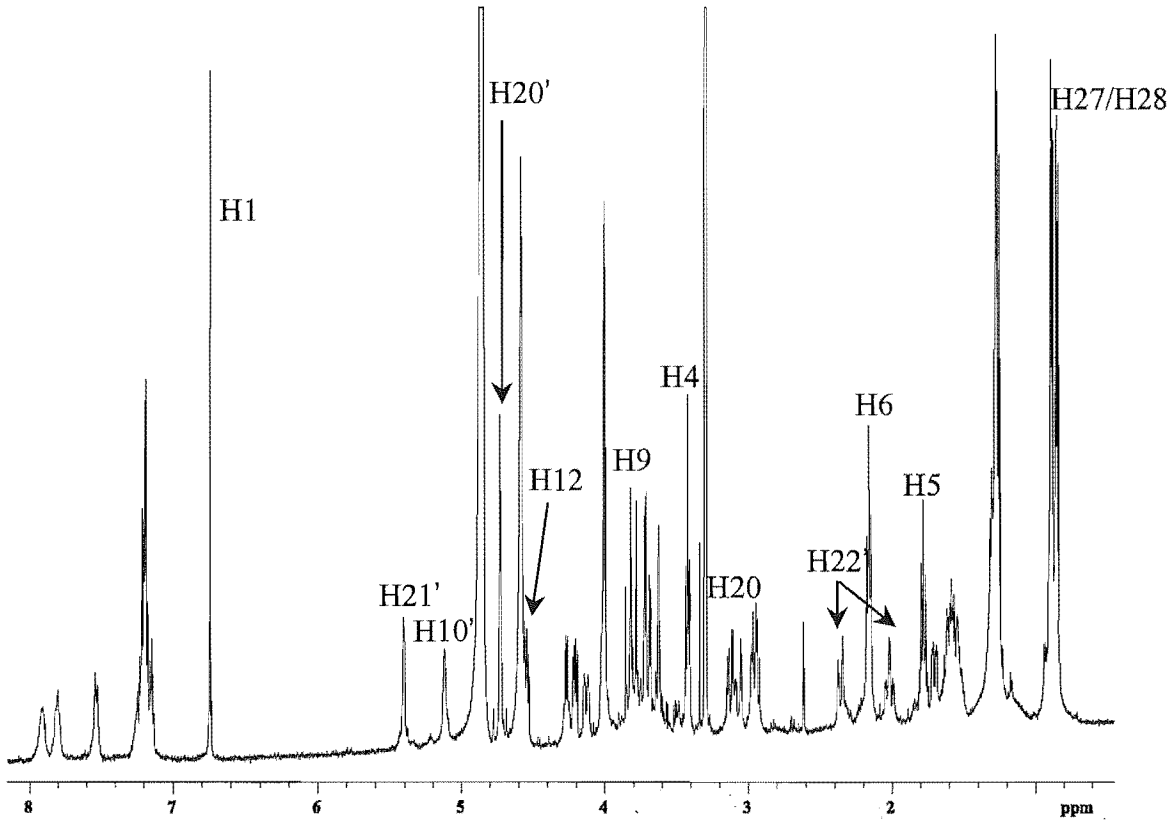

Figure 2.15: *^1H NMR* spectrum of γ-maleimidobutyric-Gly-Phe-Leu-Gly-doxorubicin (**35**) (500 *MHz, CD_3OD).*

2.5.3 Tyrosinamide (**36**)

Tyrosinamide (**36**), was included in the complement of toxins to be conjugated to HSA and CV-N (**28**) because it is capable of incorporating a radiolabel tracer. This would allow cellular and body distribution studies to be carried out in the future. Tyrosinamide (**36**) can be radioiodinated utilising chloramine T and sodium [^{125}I]iodide (Figure **2.16**).[176]

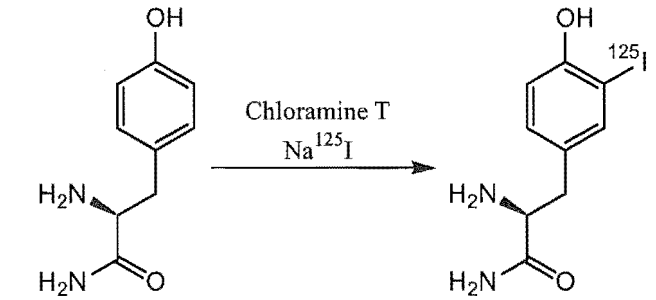

tyrosinamide (**36**)

Figure 2.16: *Radioiodination of tyrosinamide.*

2.5.3.1 γ-Maleimidobutyric-Gly-Phe-Leu-Gly-tyrosinamide (**37**)

Like doxorubicin, tyrosinamide (**36**) was particularly attractive as it had a free amine available for incorporation into an amide bond. The target compound is illustrated in Figure **2.18**. The primary amine is more nucleophilic than the primary amide, so coupling with the tetrapeptide will occur exclusively at the primary amine.

The maleimido-tetrapeptide (**30**, 3 mg) was activated as a succinimidyl ester and coupled with tyrosinamide (**36**, 0.9 equivalents) in the same manner as for the halichondrin (Section **2.5.1.2**) and doxorubicin (Section **2.5.2.1**) examples. The reaction was left to stir under argon atmosphere for 24 hours. Compound **37** was purified from the reaction mixture using a semi-preparative reverse phase HPLC system and a 25-minute solvent gradient (Section **8.2.10**) at a flow rate of 5 mL/min. The system was monitored at 213 nm and a peak eluting at 13.8 minutes was collected to give **37**.

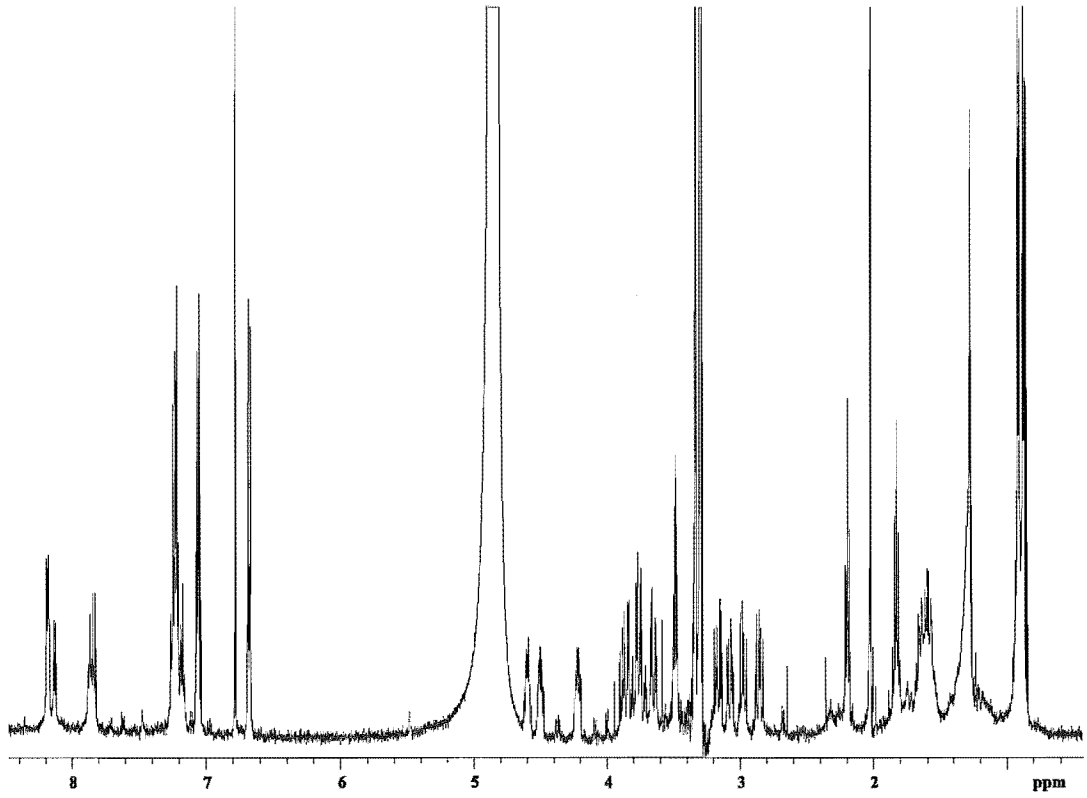

Figure 2.17: *^{1}H NMR* spectrum of γ-maleimidobutyric-Gly-Phe-Leu-Gly-tyrosinamide (**37**) (500 *MHz, CD_3OD).*

The ^{1}H NMR (Figure **2.17**) and ^{13}C NMR spectra of **37** were readily assignable in conjunction with TOCSY and HSQC 2D NMR experiments. The assigned ^{1}H and ^{13}C NMR spectral data are tabulated in Table **2.2**. HRESIMS provided final confirmation that γ-maleimidobutyric-Gly-Phe-Leu-Gly-tyrosinamide (**37**) had been prepared.

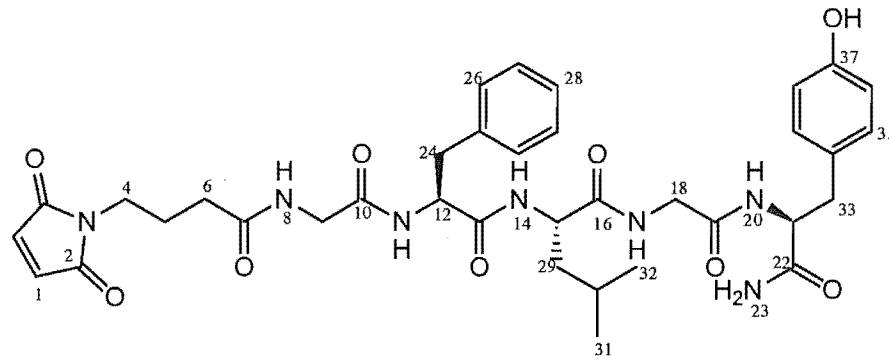

γ-maleimidobutyric-Gly-Phe-Leu-Gly-tyrosinamide (**37**)

Figure 2.18: *The target maleimido-activated biolinker-tyrosinamide.*

Atom No.	^{1}H δ (ppm)[a]	^{13}C δ (ppm)[b]	Atom No.	^{1}H δ (ppm)[a]	^{13}C δ (ppm)[b]
1	6.79 (s)	134.5	20	–	–
2	–	–	21	4.50 (dd, 5.0, 9.3)	55.2
3	–	–	22	–	–
4	3.49 (m, 2.3, 6.7, 9.0)	36.6	23	–	–
5	1.83 (m)	25.0	24α	2.98 (dd, 9.0, 14.3)	36.8
6	2.20 (t, 7.2)	32.1	24β	3.16 (dd, 5.4, 14.2)	36.8
7	–	–	25	–	–
8	–	–	26	7.23 (m)	129.1
9α*	3.65 (d, 16.5)	42.5	27	7.23 (m)	128.4
9β*	3.86 (d, 16.5)	42.5	28	7.23 (m)	126.8
10	–	–	29	1.28 (m)	29.4
11	–	–	30	1.61 (m)	27.3
12	4.60 (dd, 5.6, 9.1)	55.2	31	0.92 (d, 6.2)	22.3
13	–	–	32	0.88 (d, 6.2)	20.5
14	–	–	33α	2.85 (dd, 9.0, 14.0)	36.7
15	4.22 (dd, 4.8, 10.2)	52.8	33β	3.08 (dd, 5.1, 13.8)	36.7
16	–	–	34	–	–
17	–	–	35	7.07 (d, 8.8)	130.2
18*	3.76 (dd, 13.6, 16.5)	42.7	36	6.68 (d, 8.5)	115.0
19	–	–	37	–	–

Table 2.2: *^{1}H and ^{13}C NMR data for γ-maleimidobutyric-Gly-Phe-Leu-Gly-OH (**30**). Recorded at 500 MHz in CD_3OD.*

[a] ^{1}H chemical shift values (δ ppm and referenced to $CD_2\mathbf{H}OD$, δ_H 3.31) followed by multiplicity and coupling constant (J/Hz). The amides were only partially observed in the ^{1}H spectrum but had exchanged before characterisation from other experiments could take place.

[b] ^{13}C chemical shift values (δ ppm) as determined from HSQC experiments.

** interchangeable*

2.6 Mass Spectrometry

ESI MS has been essential to this PhD project so a summary of the technique will follow. So as not to underplay the outstanding contribution of MALDI to protein analysis (but which was not available as a technique in this project), a brief description of this technique has also been included.

Since 1912 when Joseph Thomson first described the ability to separate atoms and molecules based on different size and charge,[177] mass spectrometry (MS) has been an indispensable tool in the analysis of small molecules. Few measurements are as fundamental as mass, but despite intense MS development, the goal of analysing large macromolecules, particularly proteins, remained elusive for over 70 years.

During the 1990's, changes in MS instrumentation and techniques revolutionalised protein chemistry and fundamentally changed the way protein analysis impacts biological research. These changes were catalysed by two technical breakthroughs in the late 1980s – specifically, the development of the two ionisation methods, electrospray ionisation (ESI) by John Fenn[178] and matrix-assisted laser desorption ionisation (MALDI) by Koichi Tanaka,[179] and Franz Hillenkamp.[180] The important application of these techniques to biological macromolecules was recognised with Fenn and Tanaka being awarded the 2002 Nobel Prize in Chemistry.

These methods solved the difficult problem of generating ions of large, non-volatile analytes, like proteins and peptides, for direct transfer into the gas phase and into the MS for mass analysis, and to achieve all that without analyte fragmentation.[178,181-186] The goal was to get the proteins to "fly", or as John Fenn said, to give "wings to molecular elephants".[184] Due to the lack or minimal extent of analyte fragmentation during the processes, ESI and MALDI are also referred to as "soft" ionisation methods.[183,186]

These techniques have been successfully applied to a wide range of compounds and biological systems, including proteins and peptides, nucleic acids, drugs and metabolite systems[180,181,183,185,187,188] as well as to some synthetic polymers.[185] ESI and MALDI are becoming the methods of choice for the detection and characterisation of post-

translational modifications of proteins,[180,187,188] for example glycosylations and phosphorylations. These ionisation methods are even allowing studies of molecular complexes that only have weak non-covalent interactions, such as protein-protein,[180,181] and enzyme-substrate complexes.[189]

2.6.1 Matrix Assisted Laser Desorption Ionisation

The principle of MALDI is based on a low melting point substrate (matrix) doped with analyte compound. Under pulsed laser irradiation, usually in the ultraviolet spectra region, the matrix material (typically a small organic molecule with absorbance at the wavelength of the laser employed, for example sinapinic acid) evaporates easily and transports the analyte molecules to the analysis region of the mass spectrometer with minimal fragmentation of the analyte. A charging of analyte molecules occurs during pulsed laser-induced desorption. MALDI has been demonstrated to have the advantage of spectral simplicity owing to the production of mainly singly charged ions.[179-181,183,185-187,190]

The MALDI technique is considered an off-line ionisation technique because the sample is purified, deposited, and dried on a sample plate before the analysis.[186]

2.6.2 Electrospray Ionisation

ESI MS is based on an elegant idea proposed originally by Dole in the 1960s.[191] Liquid containing the analyte is passed through a needle at high voltage to electrostatically disperse, or electrospray, a mist of small, highly charged droplets that rapidly evaporate and which impart their charge onto the analyte molecules. A countercurrent of hot nitrogen gas assists this. This process takes place at atmospheric pressure and is therefore very gentle (without fragmentation of analyte ions in the gas phase). The ions are then transferred into the vacuum of a mass spectrometer, where they are separated and detected based on their mass-to-charge (*m/z*) ratio.[178,180-182,184,186,187]

A wide range of compounds can be analysed by ESI MS; in principle the only requirement is that the molecule be sufficiently polar to allow attachment of a charge. Proteins and peptides are prominent examples of this category. They are thought to be protonated predominantly at the basically charged sites – the amino terminus, and at arginine, histidine and lysine residues.[181,182]

Fenn also discovered the process of multiple charging, which gives proteins, on average, one charge per kDa, and leads to the characteristic appearance of ESI spectra.[178,192] (Figure **2.19**) Multiple charging is the process by which molecules, particularly proteins and peptides, can pick up more than one charge and thereby generate a series of peaks at $(M_r + n \times m_H)/n$ where M_r is the relative molecular mass of the protein, m_H is the molecular mass of a proton and n is the number of charges. Since mass spectrometers normally measure mass-to-charge ratio, increasing the number of charges on the ion effectively multiplies the mass range of the instrument. It brings the ions into the range of *m/z* ratios measurable on typical mass spectrometers.[178,181,182,192]

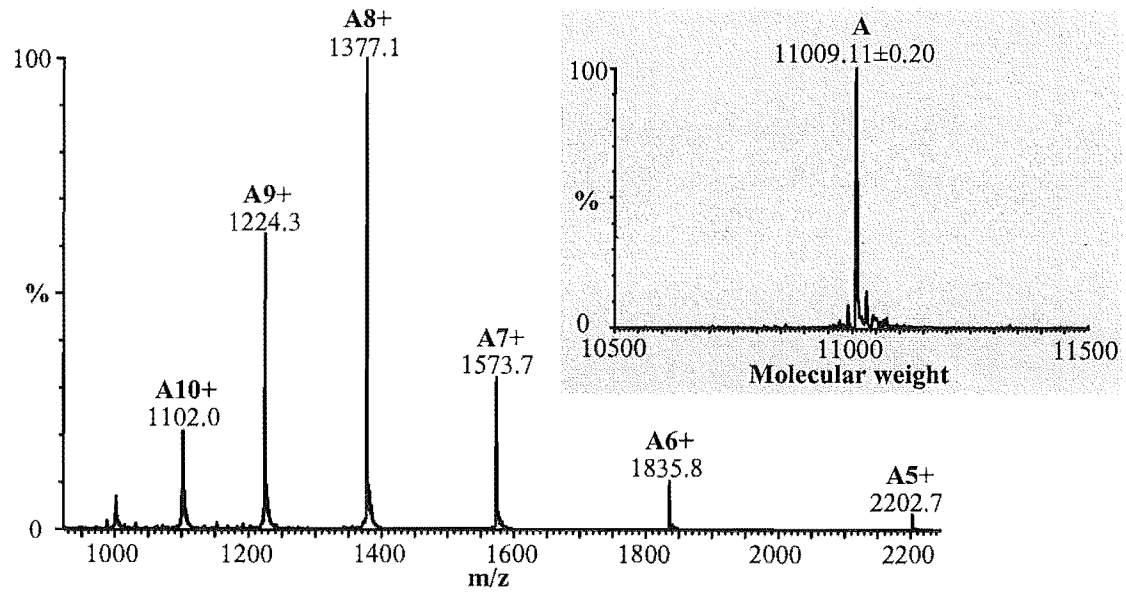

Figure 2.19: *Electrospray mass spectrum of a protein (cyanovirin-N). The attachment of many protons (from less than five to more than ten in this case) leads to a series of mass-to-charge ratio peaks for a single protein species. The insert shows a computer deconvolution of the series of peaks into a single peak at the correct protein mass.*

These spectra can be simplified by deconvolution, an algorithm that sums up the signal intensity into a single peak at the molecular weight of the analyte.[192] The maximum

entropy (MaxEnt) algorithm[193] has been used to process the spectra presented in this thesis (see Figure **2.19**, inset).

The ESI technique is an online ionisation technique because of the ease with which it can be interfaced with popular chromatographic and electrophoretic liquid phase separation techniques.[186] For example, when liquid chromatography and mass spectrometry are coupled (LC MS), MS analysis of the components of a sample takes place on-line as they elute from the chromatography column. In this scenario, sample cleanup, separation, and concentration are all achieved in a single step.

2.7 Conjugation Strategy: Model Systems

Due to the limited availability of CV-N (**28**) and the toxin derivatives, model systems were used to optimise the thiolation conjugation strategy.

It is well documented that 2-IT (**29**) is fully water-soluble and reacts with primary amine residues in the pH range 7 – 10 (Section **2.3**). The literature cites a number of different buffer systems that have been used successfully with 2-IT (**29**).[154] Obviously, they must be non-amine-containing. A sodium borate-based buffer (0.1 M sodium borate, 0.15 M NaCl, 0.001 M EDTA) was chosen to maintain the pH of the reaction system at 8.0. This buffer became referred to as the '**reaction buffer**'. Sulfhydryl groups are susceptible to oxidation and formation of disulfide cross-links. To prevent disulfide formation, oxygen was removed from all buffers by bubbling argon through all the solutions. In addition, ethylenediaminetetraacetic acid (EDTA) was added to the buffers to chelate metal ions, preventing metal-catalysed oxidation of sulfhydryl groups.

2.7.1 A Small-Molecule Model – β-alanine

N_{α}-Fmoc-lysine initially appeared as a good mimic of the lysine side chains in the protein, but difficulties were experienced due to insolubility in the reaction buffer. β-alanine (**39**) was an easier amine model to work with as it was more water-soluble. β-alanine (1 mg) was stirred with 1.3 equivalents of 2-IT (**29**) in reaction buffer. After one hour 1.3 equivalents of γ-maleimidobutyric acid (**40**) were added and stirred for a further ten minutes. ESI MS showed that the desired conjugate product **41** had been formed. Hydrolysed 2-IT (**29**), with subsequent reaction with the maleimide, was also a significant product present. This reaction side-product indicated that the intermediary thiolated protein product would have to be purified so as not to waste any of the precious maleimide-natural product combinations. The observations also implied that the 2-IT (**29**) reagent would need to be prepared freshly for each reaction, and used immediately.

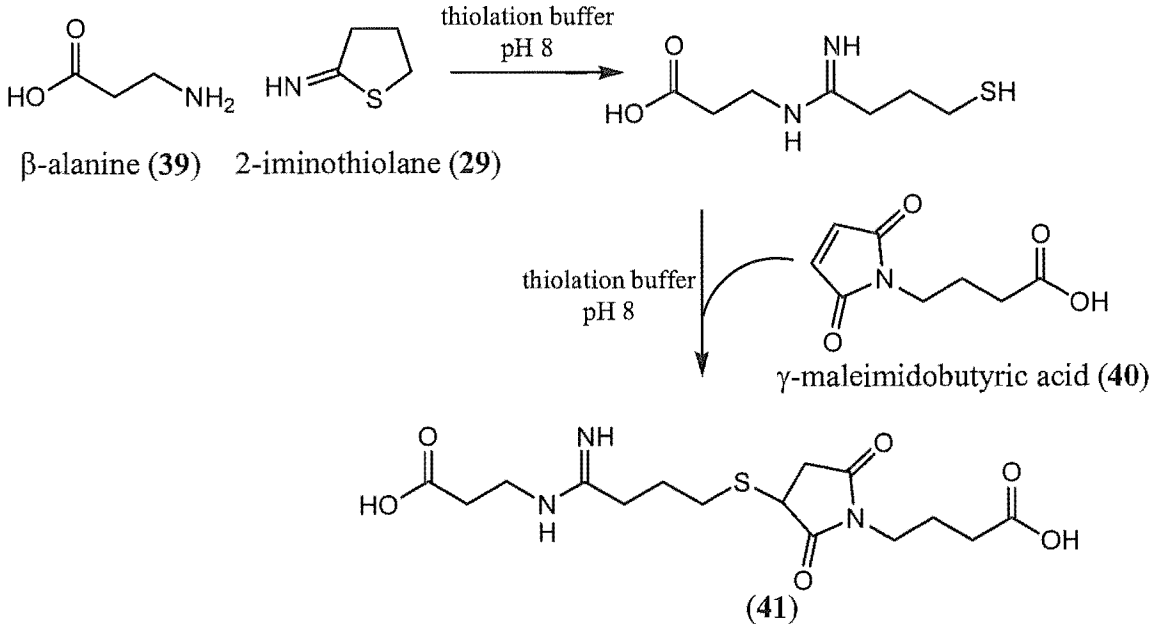

Figure 2.20: *A small-molecule model for the thiol-maleimide strategy.*

2.7.2 A Protein Model – Lysozyme

Chicken egg white lysozyme was selected as a model protein. With 129 amino acid residues, lysozyme has a molecular weight of approximately 14.3 kDa,[194] an ideal model molecular weight for the 11 kDa cyanovirin (**28**). Lysozyme is also readily commercially available. The protein has six lysine residues, and therefore seven possible sites for thiolation.

A method for purification of any protein derivatives needed to be established. It was important that thiolated protein was separated from the thiolation reagent so that an excess of the toxin component did not have to be added. As the protein molecular weight is significantly different from the thiolating reagent, initial separation/purification could be achieved by size exclusion gel filtration chromatography. Using a G-25 support, with an exclusion limit of a molecular weight of 5,000 Da, the conjugate/protein components elute before the thiolation reagent, 2-IT (**29**).

Lysozyme (200 μg) was loaded onto a G-25 column and eluted with a standard borate buffer (pH 7.2, 0.0025M sodium borate, 0.15 M NaCl). Mild elution conditions were required to minimise denaturation of the protein and to preserve the activity of the

conjugates. The column was monitored by a UV detector reading at λ 206 nm, and a peak eluting at the void volume (as determined by previous elution of the polysaccharide blue dextran) was collected.

The sample was initially analysed by direct infusion into the ESI MS. Although a protein component was obviously present, signal intensity was very low, and difficult to interpret. It is well reported that buffer-related cations, for example Na^+, produce additional features in an ESI-mass spectrum and usually manifest themselves as peaks near singly and multiply charged analyte ion signals.[187] These modifications inherently cause a reduction in analyte signal, because the signal is spread over multiple m/z peaks. For this reason, the proteins, and the resultant conjugates, would need to be visualised by reverse phase LC MS. A long gentle solvent gradient system was employed (Chapter **8**). The online coupling of the LC to the ESI MS served to eliminate these buffer-related issues, and separate the protein components. Traditionally, protein and peptide reverse phase HPLC separations are performed at low pH with a trifluoroacetic acid (TFA)-containing mobile phase where the TFA functions as an ion-pair reagent and complexes with the basic residues in proteins and peptides.[195] However, the formation of these complexes suppresses the ionisation of the protein, reducing sensitivity.[180] TFA was replaced in this project by either 0.5% formic acid (v/v) or 5% acetic acid (v/v) producing excellent chromatography and MS signal intensity.

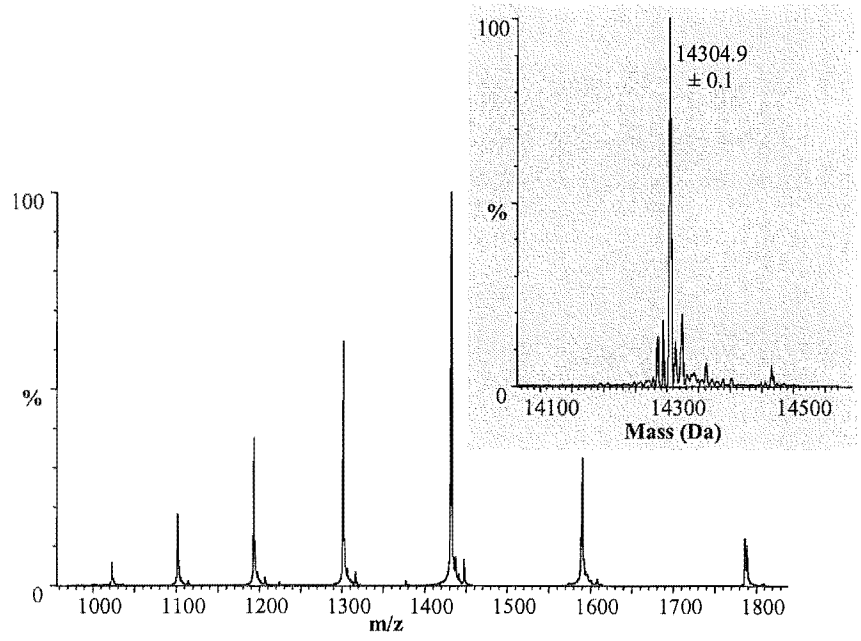

Figure 2.21: *The ESI-mass spectrum of chicken egg white lysozyme. The inset shows the deconvoluted, neutral-scale mass spectrum.*

The lysozyme sample was analysed, this time by LC MS. A broad peak eluted from the LC, visible in both the diode array (λ 254 nm) and total ion current spectra, at ~41-43 minutes. Figure **2.21** illustrates the ESI-mass spectrum that was represented by this peak. MaxEnt deconvolution of the mass spectrum collapses the charge state envelope to a single, principal peak (inset, Figure **2.21**) at 14,305 Da.

2.7.2.1 Thiolating Lysozyme

Section **2.3** discussed the use of 2-IT (**29**) to thiolate proteins, and the subsequent utilisation of the thiol(s) in a coupling strategy with a maleimide. This section outlines the development of this strategy with a model protein, lysozyme, in preparation for work with CV-N (**28**). Figure **2.22** illustrates this methodology.

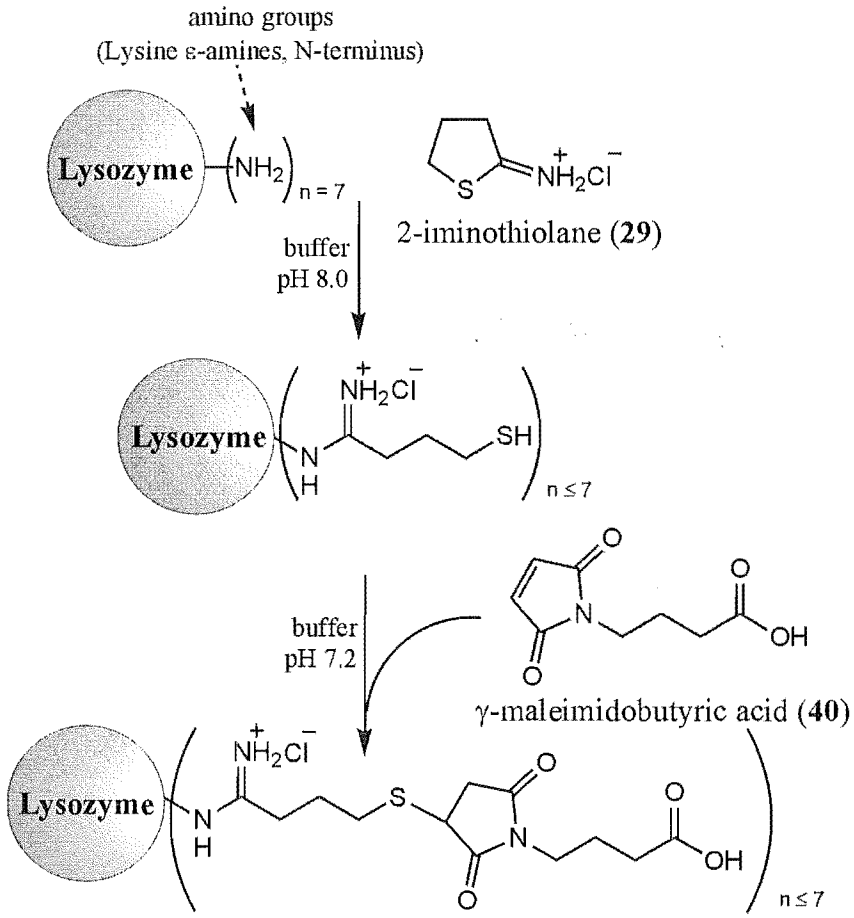

Figure 2.22: *Thiol/maleimide strategy for the modification of lysozyme.*

Lysozyme (200 μg) was dissolved in reaction buffer (200 μL). Five equivalents of 2-IT (**29**) in reaction buffer (10 μL) were added and the mixture was flushed with argon and capped for five hours at room temperature. The mixture was separated on a G-25 column as described previously and the protein fraction analysed by LC MS. Deconvolution of the ESI data produced the spectrum in Figure **2.23**. This spectrum illustrates that two main protein components were present, unreacted lysozyme (14,306 Da) and a singly-thiolated lysozyme (14,407 Da). 2-IT has an exact mass of 101.03 Da.

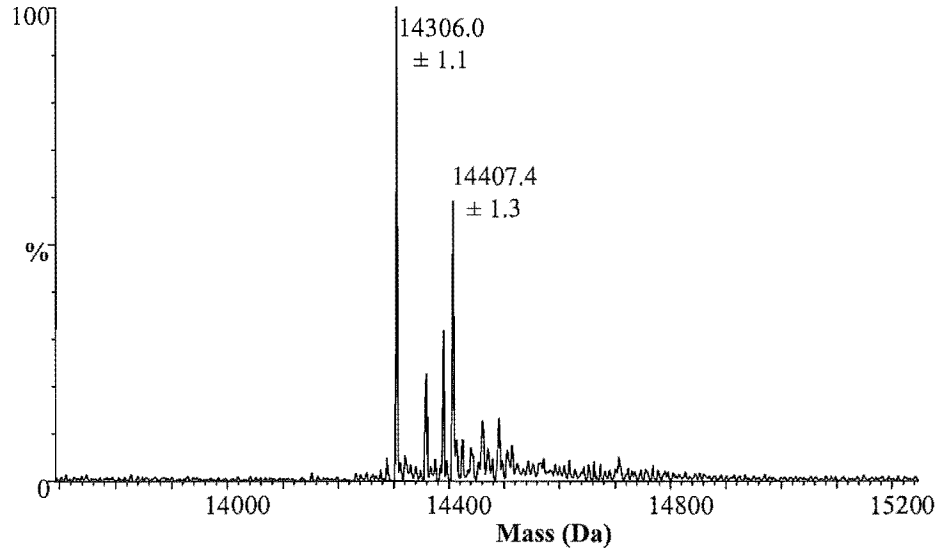

Figure 2.23: *The deconvoluted ESI-mass spectrum of the reaction between lysozyme and 2-IT (**29**).*

Importantly, the thiolated protein had survived chromatography on the G-25 column without cross-linking through the formation of disulfide bonds. The protein could therefore be purified from the thiolation reagent before reaction with the maleimide.

2.7.2.2 Thiolated Lysozyme and γ-Maleimidobutyric acid.

Immediately after the analysis above, the thiolated lysozyme solution was reacted with a model maleimide, γ-maleimidobutyric acid (**40**, MW 183.2, five equivalents, in minimal DMF). The reaction mixture was analysed by LC MS after two hours. Again, a single broad peak eluted at ~41 minutes, and analysis of this peak (Figure **2.24**) revealed that it encompassed unreacted lysozyme and the expected singly-modified conjugate product (14,589 Da).

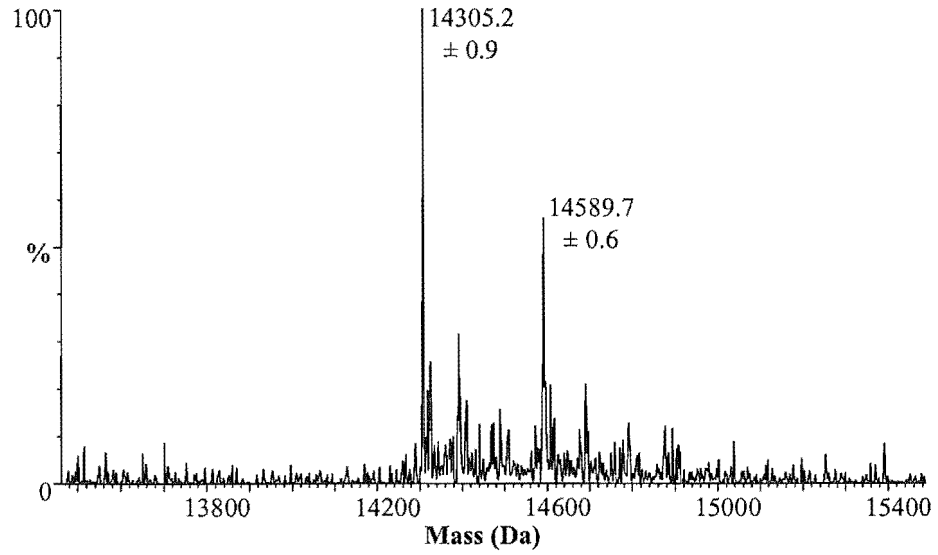

Figure 2.24: *The deconvoluted ESI-mass spectrum of the reaction between thiolated lysozyme and γ-maleimidobutyric acid (**40**).*

2.7.2.3 Thiolation Optimisation – Time and Temperature Dependence

To test the time dependence of the thiolation reaction, lysozyme was reacted with five equivalents of 2-IT (**29**) for 1, 5, 12, 24 and 48 hours at room temperature. At the conclusion of each of these time periods any free thiols were capped with the addition of five equivalents of γ-maleimidobutyric acid (**40**) *in situ*. Each of these samples were analysed by LC MS. A single broad peak eluted after ~42 minutes in each case. Analysis of the ESI MS data of these peaks (Figure **2.25**) revealed an interesting situation. After one hour of reaction a single addition of 2-IT/maleimide (14,590 Da) was visible. Substantial unreacted protein (14,305 Da) remained. Five hours of reaction afforded a second addition of the thiol/maleimide (14,873 Da). However, a peak 84 mass units higher than lysozyme (or 17 mass units lower than the thiolated protein, 14,390 Da) was also visible. Further, a peak with one addition of the thiol/maleimide and one 'plus 84' (14,673 Da) was also seen. After 12 hours, no maleimide addition was seen, but two (14,474 Da), three (14,557 Da) and four (14,641 Da) additions of 84 mass units were visible. This derivative appeared to be 'dead end' derivative, and did not react with the maleimide. No significant change was seen after 24 and 48 hours of reaction.

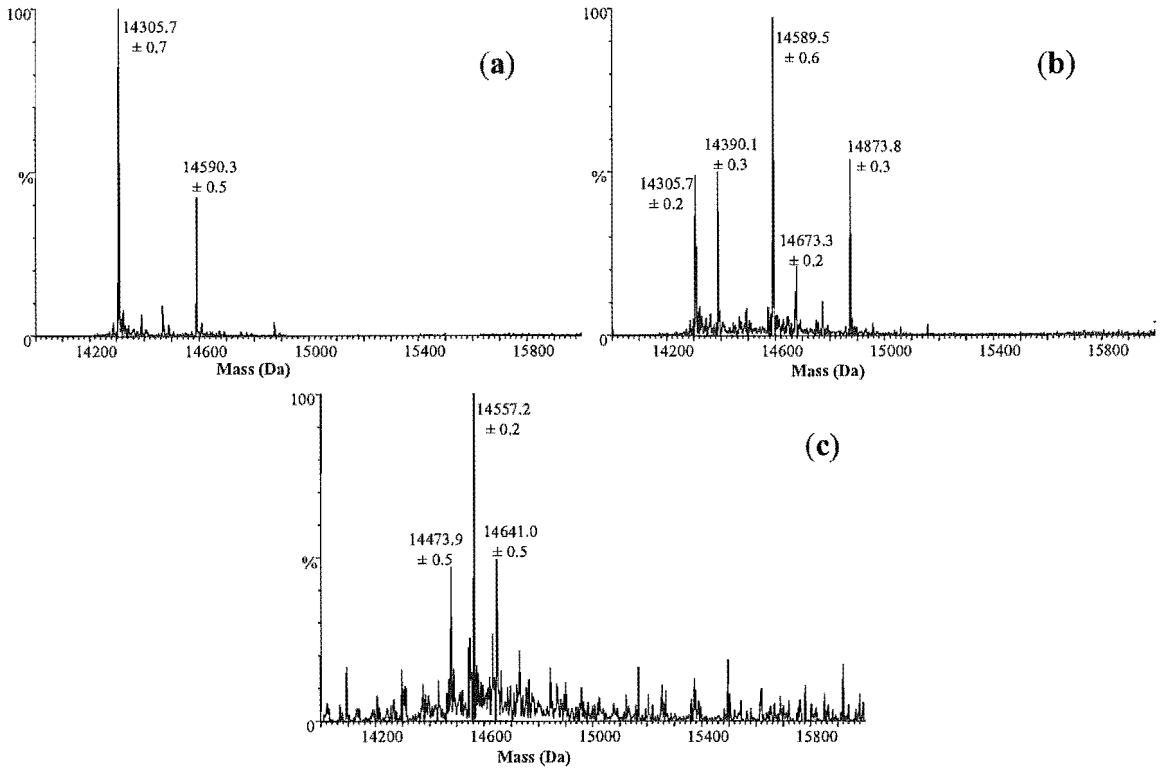

Figure 2.25: *Deconvoluted mass spectra of the addition 2-IT (**29**) to lysozyme, and then capped with the maleimide, **40**, at room temperature, after **(a)** one hour; **(b)** five hours; and (c) 12 hours*

The set of time dependent reactions was repeated at 0°C in an ice bath. The deconvoluted ESI MS data are represented in Figure **2.26**. This time, the addition process appeared to be considerably slower, but the presence of the by-product was significantly less. No addition was seen after one hour of reaction. After five hours of reaction however, a single addition of thiol/maleimide was present (14,590 Da). Twelve hours of reaction saw the appearance of two additions of the thiol/maleimide (14,874 Da). No by-product was present. Two (14,874 Da) and three (15,157 Da) additions of thiol/maleimide were seen after 24 hours. A small proportion of varying combinations of thiol/maleimide and the 'plus 84' product was now visible. A mass of 14,673 Da, for example, represents one thiol/maleimide and one 'plus 84'. No significant change was seen after 48 hours. The optimum reaction time was established to be 12 hours, with no non-thiol by-product produced at this time. Section **2.8.1.4** describes the characterisation of this thiolation by-product.

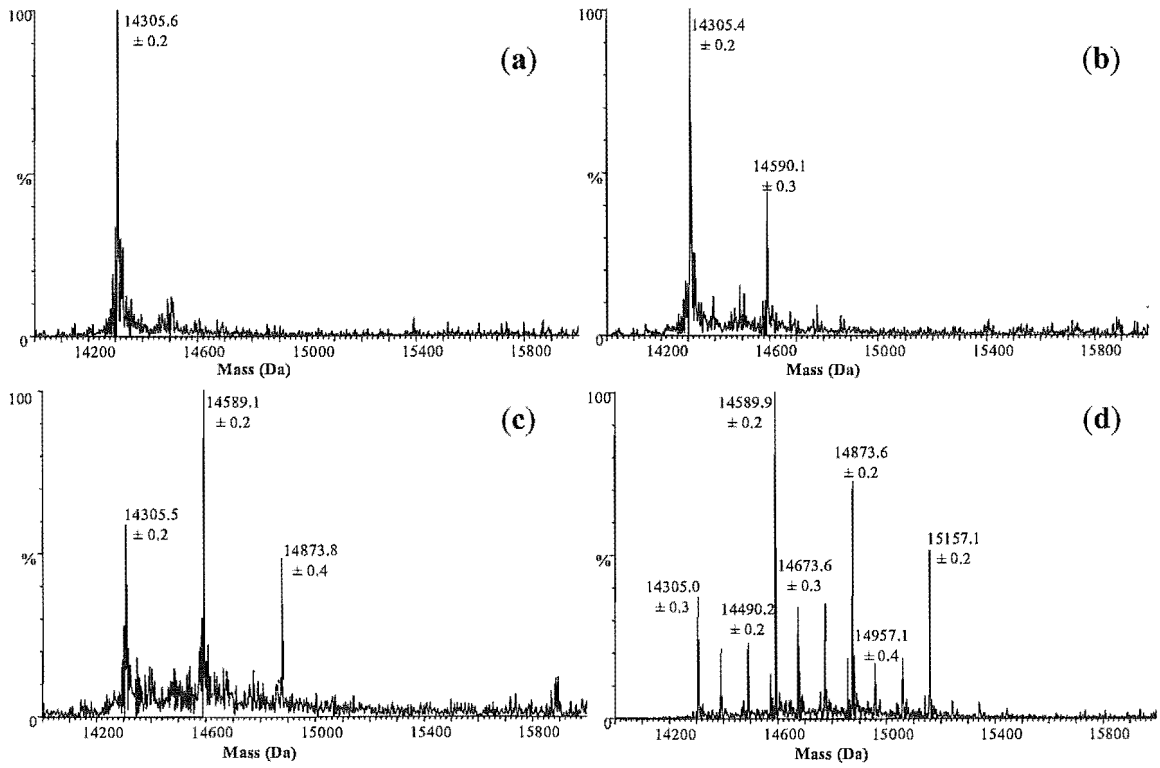

Figure 2.26: *Deconvoluted mass spectra of the addition 2-IT (**29**) to lysozyme, and then capped with the maleimide, **40**, at 0 °C, after (**a**) one hour; (**b**) five hours; (**c**) 12 hours; and (**d**) 24 hours.*

2.7.2.4 Characterisation of Thiolation By-product

Reaction products of protein and 2-IT (**29**) were shown to contain the expected derivatives together with a second product with mass 17 units lower. The characterisation of the thiolation by-product proved too difficult to achieve on the protein scale. Benzylamine (**42**) was chosen as a model amine with the advantages that it was soluble in the aqueous reaction conditions but was also soluble in organic solvents to aid in the purification procedures. Any products could also be characterised by NMR spectroscopy.

Benzylamine (**42**, 10 mg) was dissolved in degassed thiolation buffer and one equivalent of 2-IT (**29**) was added. The reaction was left for 24 hours at room temperature. At this time oily droplets were present in the mixture and these were extracted into ethyl acetate.

ESI MS revealed that this fraction contained only the 'plus 84' product (MH^+ 192) and not the thiolated product (**43**) (MH^+ 209).

As alluded to previously it was assumed that this by-product was not a thiol as it did not react with the maleimido compounds introduced. A ^1H NMR spectrum (500 MHz, $CDCl_3$) was obtained but it was not until HSQC and CIGAR 2D NMR experiments were recorded that this product, **44**, (Figure **2.27**) could be characterised. The arrows indicate the important correlations revealed in the 2D experiments. These correlations established that **44** contained a five-membered heterocycle. All protons of the heterocycle correlate to the imine carbon. This assignment would not be possible if it were an open chain structure.

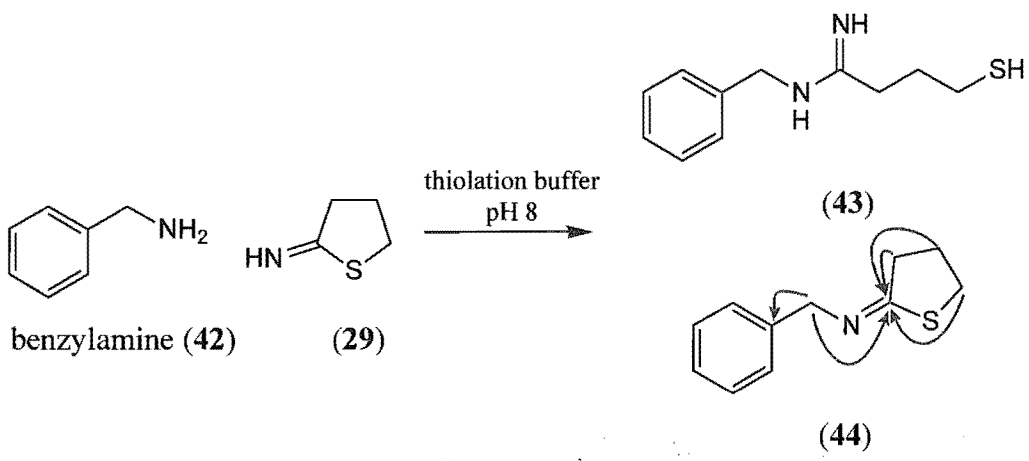

Figure 2.27: *Reaction of benzylamine (42) and 2-IT (29).*

The initially formed thiol product, **43**, decays to the non-thiol product, **44**. In this process the thiol adds to the imine carbon resulting ultimately in the formation of the cyclised product, **44**, by the loss of ammonia. Several publications have also recently cautioned in the use of 2-IT (**29**) due to the formation of this particular side product.[196,197]

2.7.2.1 Thiolation Optimisation – Ratio of 2-IT

To determine the optimum ratio of 2-IT (**29**) to lysozyme, a series of reactions were carried out using varying amounts of 2-IT (**29**).

Lysozyme (200 μg) was reacted with 5, 10, 25, 50 and 100 equivalents of 2-IT (**29**) in reaction buffer at 0°C. After 12 hours of reaction the available thiols were capped with equal equivalents of γ-maleimidobutyric acid *in situ*.

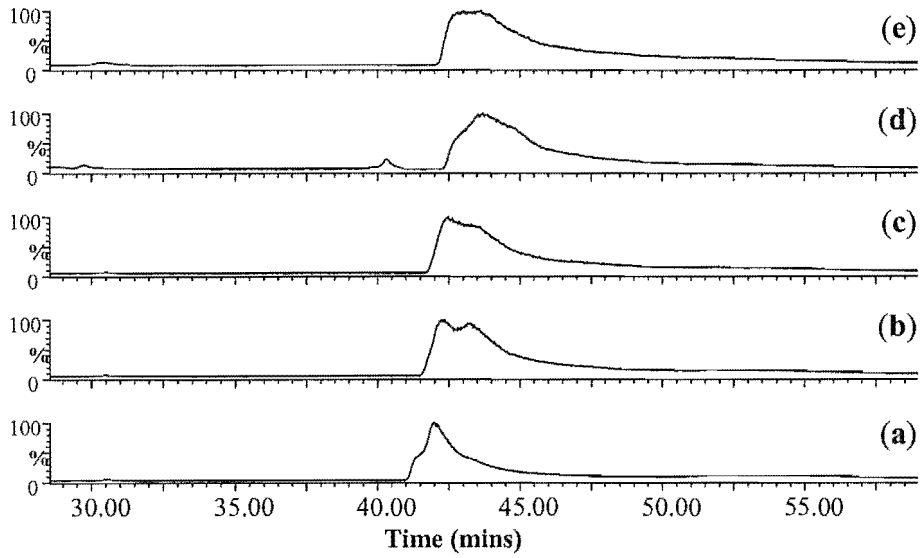

Figure 2.28: *Total Ion Current ESI+ chromatograms for the addition of varying concentrations of 2-IT (**29**) to lysozyme, and then capped with the maleimide, **40**. (a) 5 equivalents 2-IT; (b) 10 equivalents 2-IT; (c) 25 equivalents 2-IT; (d) 50 equivalents 2-IT; and (e) 100 equivalents 2-IT.*

Each sample was analysed by LC MS, and the resultant total ion current (TIC) chromatograms are shown in Figure **2.28**. With increasing concentration of 2-IT, the protein peak, eluting after ~42 minutes, broadens and shifts slightly to a longer retention time. A selection of the MaxEnt deconvoluted mass spectra, presented in Figure **2.29**, reveals that the shift in retention time is due to the addition of up to five of the thiol/maleimide combinations (in the case of the 100 equivalents of 2-IT (**29**)). An increase in the ratio of 2-IT (**29**) to lysozyme resulted in an increased number of thiolations, and subsequent reactions with the maleimide. A single addition (14,590 Da) of the 2-IT/maleimide was visible with five equivalents of 2-IT (**29**). Ten equivalents of 2-IT (**29**) resulted in a second addition (14,874 Da). Further additions were produced with 25, 50 and 100 equivalents of 2-IT (**29**). Six and seven thiolations were never seen. This may be due to the folding pattern of lysozyme, with some of the lysine residues being less accessible within the protein. Despite the cold reaction conditions, the thiolation by-product was still present, though somewhat reduced, and will need to be monitored in the reactions with CV-N (**28**).

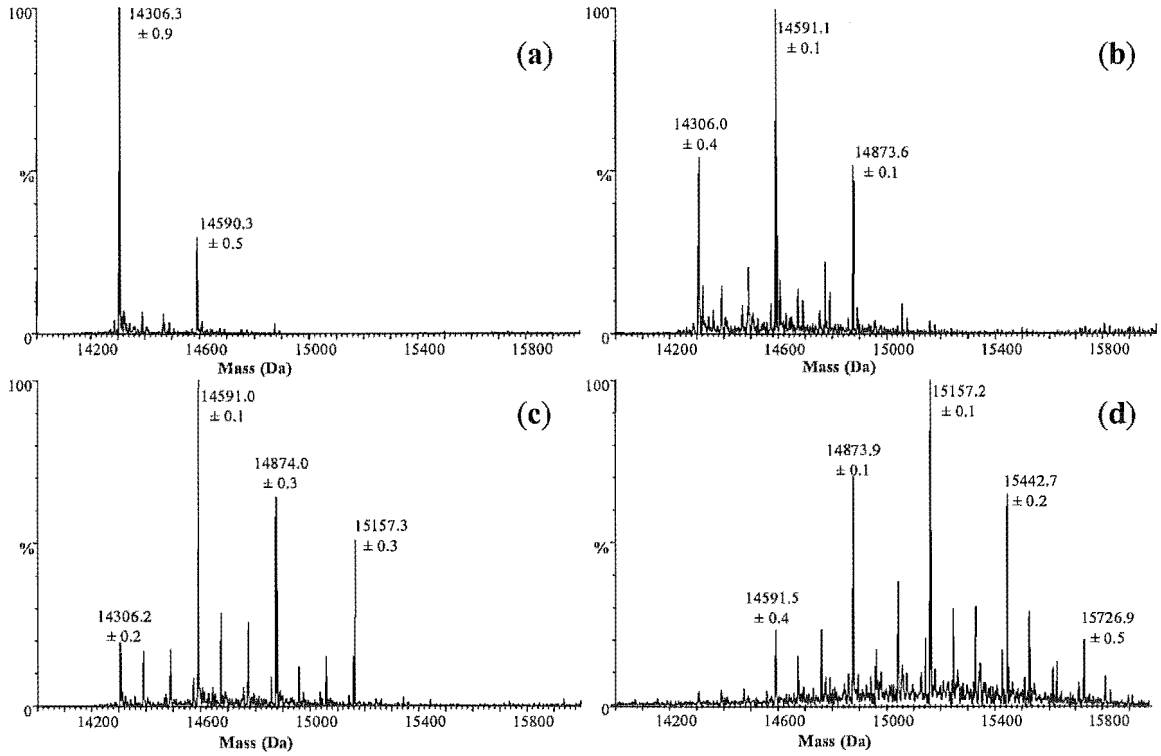

Figure 2.29: *Deconvoluted mass spectra of the addition of varying concentrations of 2-IT* ***(29)*** *to lysozyme, and then capped with the maleimide,* ***40****. (a) 5 equivalents 2-IT; (b) 10 equivalents 2-IT; (c) 25 equivalents 2-IT; and (d) 100 equivalents 2-IT.*

2.8 Conclusions

This chapter has outlined the development of a strategy to create CV-N (**28**)-toxin conjugates of the general design in Figure **2.1**.

A tetrapeptide, Gly-Phe-Leu-Gly, was selected as a biolinker, and as a substrate for the lysosomal cathepsin enzymes. This peptide has been designed to allow controlled release of the toxin – not too fast, not too slowly – within cells.[149]

A thioether bond was chosen to link the protein with the biolinker. This bond is stable in systemic circulation. The linkage could be achieved by thiolating the protein with an amine-specific reagent, 2-iminothiolane (**29**), and subsequent reaction with a maleimido-activated biolinker. Lysozyme was used as a model system to investigate the thiol/maleimide methodology. A number of thiol/maleimide additions were seen, and some degree of control could be achieved by varying reaction time, and the ratio of 2-IT (**29**) to the protein. Some caution needs to be taken in the use of 2-IT (**29**), due to the production of a non-thiol by-product that cannot be conjugated.

A maleimido-activated biolinker was synthesised on solid-phase and subsequently coupled to three toxins (homohalichondrin B (**22**), doxorubicin (**34**), and tyrosinamide (**36**)) *via* an amide bond. Homohalichondrin B (**22**) was hemi-synthetically modified so that it was functionalised with an amine (**31**) and could be coupled to the construct.

3 NATIVE CV-N CONJUGATES

NATIVE CV-N CONJUGATES

3.1 Introduction

In Chapter Two a strategic approach to developing CV-N-toxin conjugates, like that illustrated in Figure **2.1**, was introduced. This involved the selective conversion of exposed protein amino groups to sulfhydryl functionalities using 2-IT (**29**), and then the subsequent Michael addition of the sulfhydryl to a maleimido-activated biolinker-toxin construct. The viability of the thiol/maleimido approach was tested on a model system with the protein lysozyme, and a simple maleimide derivative. The conjugation methodology was ultimately successful with varying degrees of thiol/maleimide loading on the protein.

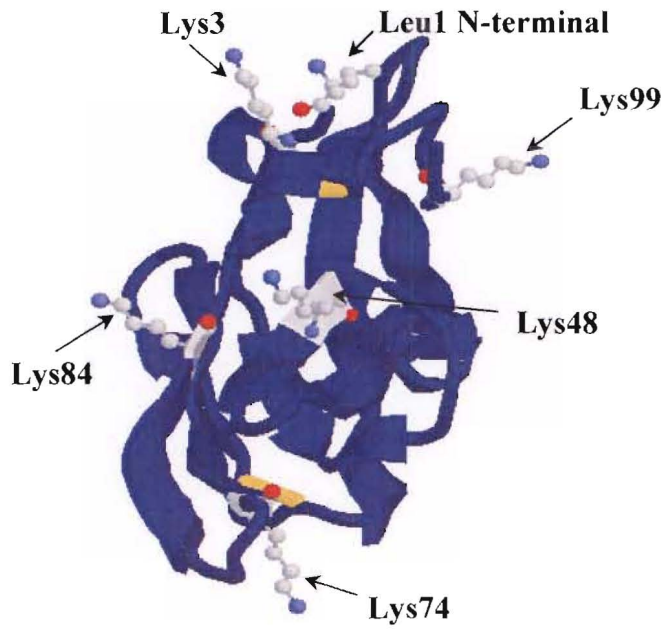

Figure 3.1: *Solution structure of CV-N (**28**) as determined by NMR spectroscopy. The protein is depicted as a ribbon with the Lysine (Lys) residues shown in ball and stick representation. The N-terminal, Leu1, is also highlighted. The diagram was produced with Protein Explorer from the RCSB PDB, entry 2ezm.*

This chapter describes the equivalent approach to the preparation of conjugates of native CV-N (**28**). With lysine residues at amino acid positions, 3, 48, 74, 84 and 99, CV-N (**28**)

has six possible sites for thiolation. The lysine residues, and the leucine N-terminal, are highlighted in the representation of the solution structure of CV-N (**28**) in Figure **3.1**. The amino groups all appear to be exposed on the surface of the protein, and therefore available for reaction with 2-IT (**29**).

Initially, CV-N was thiolated and derivatised with model maleimides in an effort to assess reactivity of the amino groups within CV-N (**28**), and the selectivity of the thiolation process.

Finally, the synthesis of a CV-N-tyrosinamide conjugate was undertaken.

The Molecular Targets Development Program, NCI-Frederick, Frederick, MD, USA, kindly supplied the CV-N (**28**) used in this project. The protein was recombinantly produced and is stored at 1 mg/mL in 0.9% saline solution.

3.2 LC MS of CV-N (28)

The analytical LC MS methodology, developed with lysozyme in Chapter **2**, was applied to a pure sample of CV-N (**28**). A single peak eluted from the reverse phase system with a retention time of approximately 46.5 minutes (Figure **3.2**). This peak was clearly visible in both the diode array and TIC chromatograms.

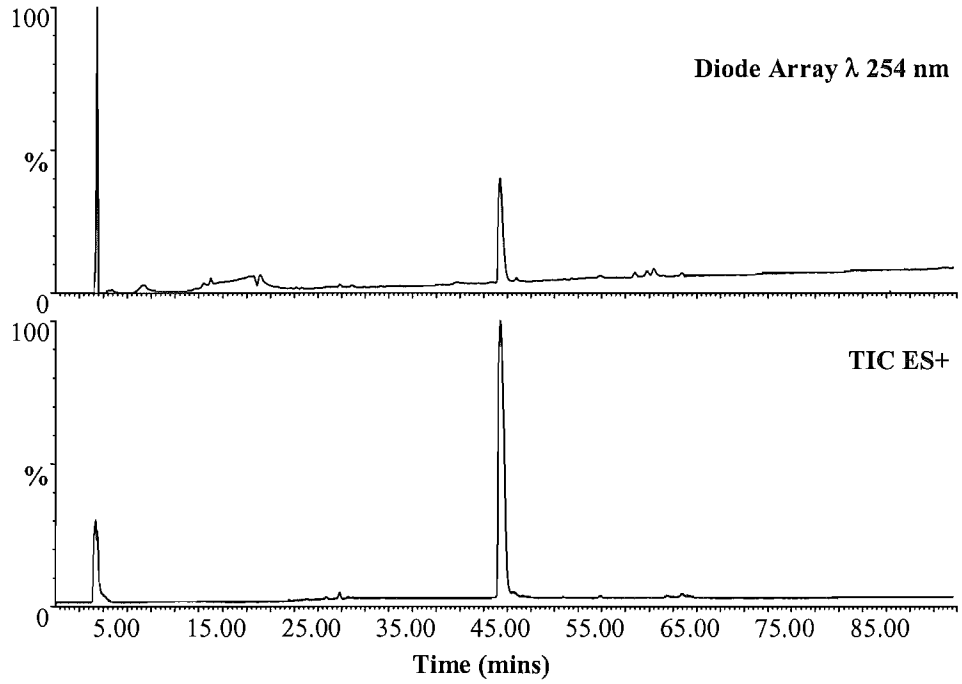

Figure 3.2: *Chromatogram of purified CV-N (28); Diode Array trace at λ 254 nm, and Total Ion Current (TIC) ES+ trace.*

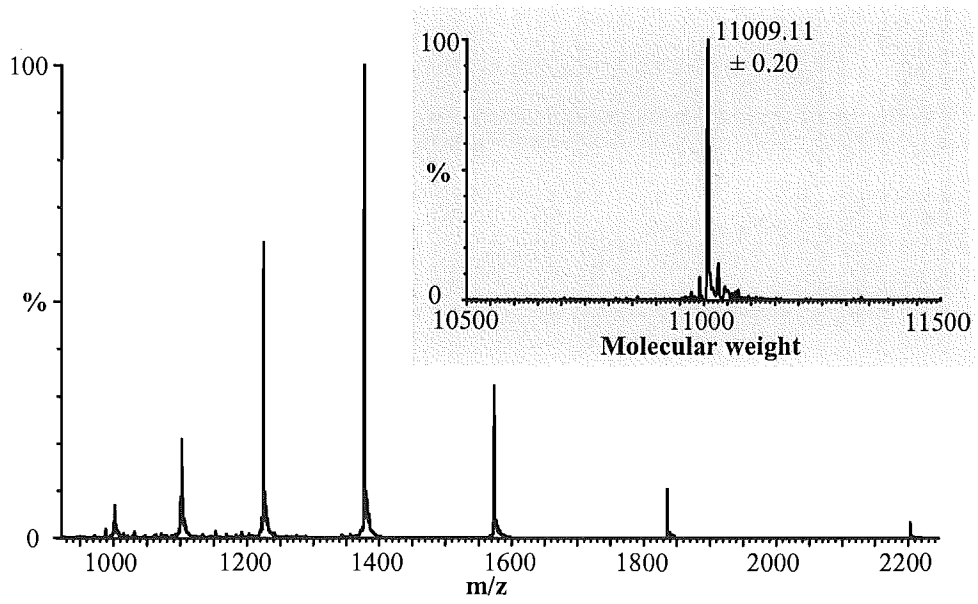

Figure 3.3: *The ESI-mass spectrum of CV-N (28). The inset shows the deconvoluted, neutral-scale mass spectrum.*

The ESI-mass spectrum of this peak is presented in Figure **3.3**. The spectrum of CV-N (**28**) consists of a simple and well-resolved series of charge state ions. This spectrum is easily deconvoluted to a single peak with the expected molecular weight of CV-N (28), 11,009 Da (inset, Figure **3.3**).

3.3 Modification of CV-N (28)

3.3.1 A Model System – 2-IT (29) and γ-maleimidobutyric acid (40)

The CV-N conjugate (**45**) illustrated in Figure **3.4** was chosen as a model target to test the viability of the thiolation approach with CV-N (**28**). The small molecule, model maleimide, γ-maleimidobutyric acid (**40**) had been ideal for the preliminary lysozyme investigations and was expected to provide a good starting point for modifying CV-N (**28**).

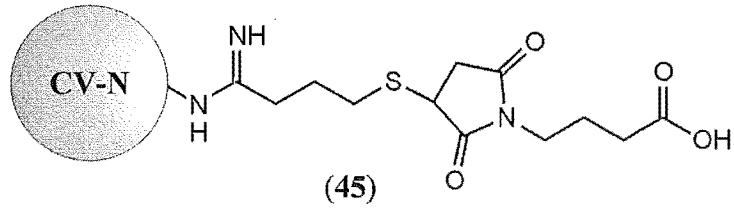

(45)

Figure 3.4: *CV-N-maleimidobutyric acid conjugate.*

CV-N (**28**, 100 μg) was reacted with 5, 10, 25, 50 and 100 equivalents of 2-IT (**29**) in reaction buffer at 0°C. After 12 hours of reaction the thiolated protein was capped with equal equivalents of γ-maleimidobutyric acid (in minimal DMF to aid with aqueous dissolution) *in situ*. Each sample was analysed by LC MS and the resultant diode array chromatograms (λ 254 nm) are presented in Figure **3.5**.

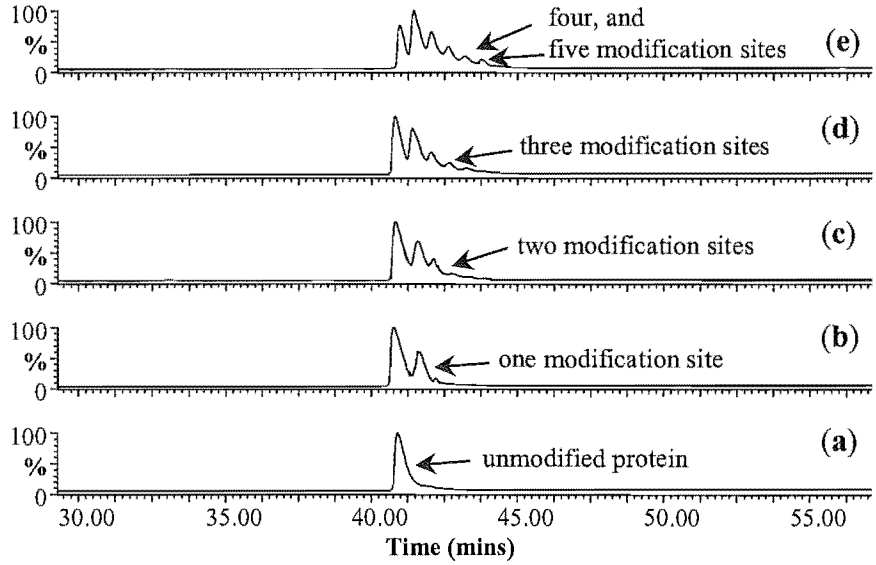

Figure 3.5: *Diode Array chromatograms (λ 254 nm) for the addition of varying concentrations of 2-IT (**29**) to CV-N (**28**), and then capped with the maleimide, **40**. (a) 5 equivalents 2-IT; (b) 10 equivalents 2-IT; (c) 25 equivalents 2-IT; (d) 50 equivalents 2-IT; and (e) 100 equivalents 2-IT.*

With increasing concentration of 2-IT (**29**), an increasing number of products were produced. Analysis of the ESI-data (Figure **3.6**) demonstrated that these peaks represented sequential addition of the thiol/maleimide combination. A maximum of five modifications was seen. Although base-line separation was not achieved between product peaks, each peak was quite clearly different from each other and ESI MS analysis was able to identify the primary product represented by each peak.

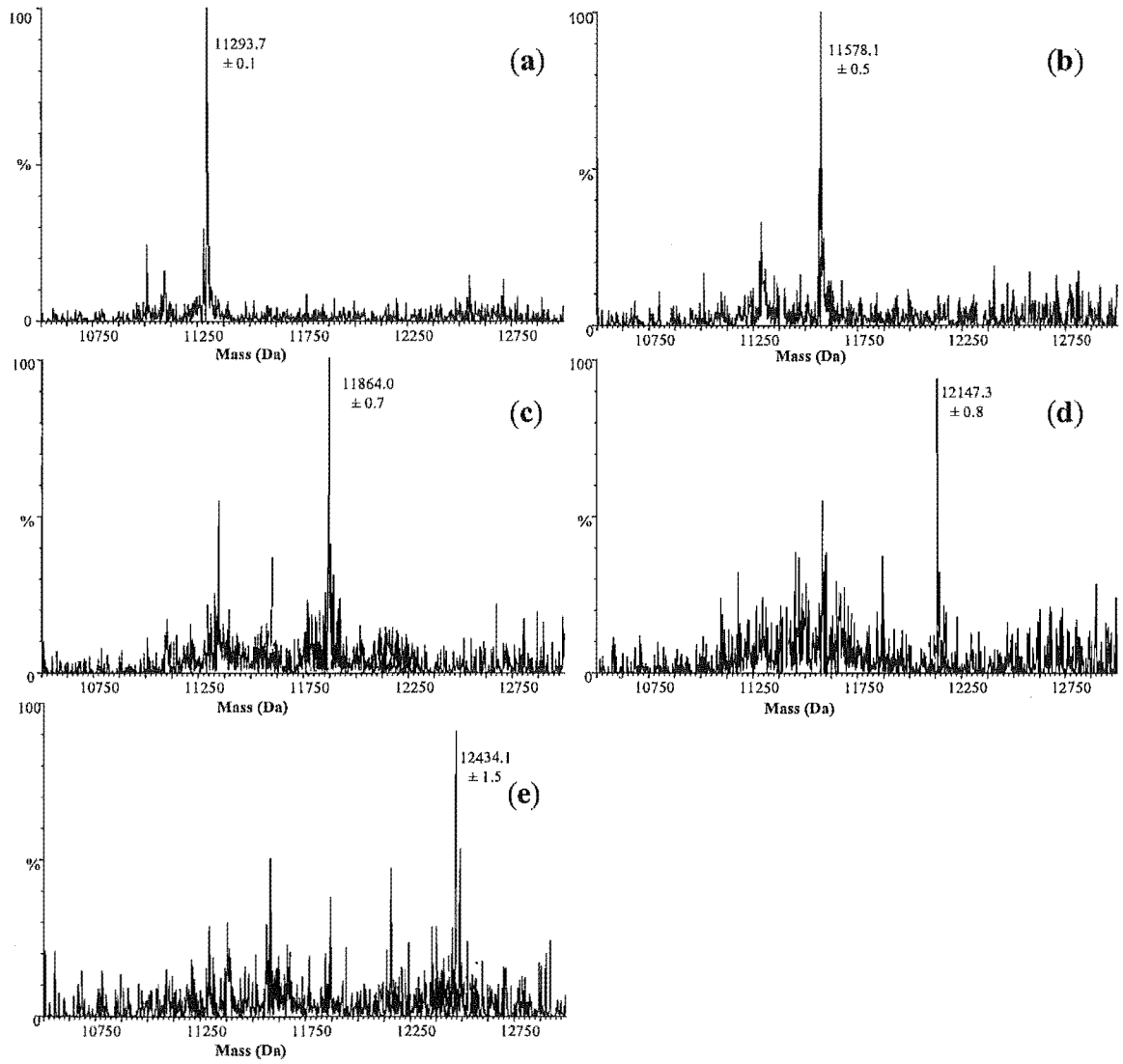

***Figure 3.6**: CV-N-maleimidobutyric acid conjugate (45): (a) one addition of thiol/maleimide; (b) two additions; (c) three additions; (d) four additions; and (e) five additions.*

CV-N (**28**, 100 μg) was thiolated with 2-IT (**29**, ten equivalents) at 0°C in reaction buffer for one hour. The sample was chromatographed on a G-25 column and eluted with the standard borate buffer. The column was monitored by a UV detector reading at λ 254 nm,

and a peak eluting at the void volume was collected and reacted directly with five equivalents of γ-maleimidobutyric acid (in minimal DMF). The reaction procedure was repeated a further four times, altering only the thiolation reaction time (5, 12, 24 or 48 hours). Each of the samples was analysed by LC MS in the same manner as above. Thiolation by-products (see Section **2.8.1.4**) became prominent after 24 hours (Figure **3.7**) with 'dead-end' peaks at 11,094 Da and 11,378 Da.

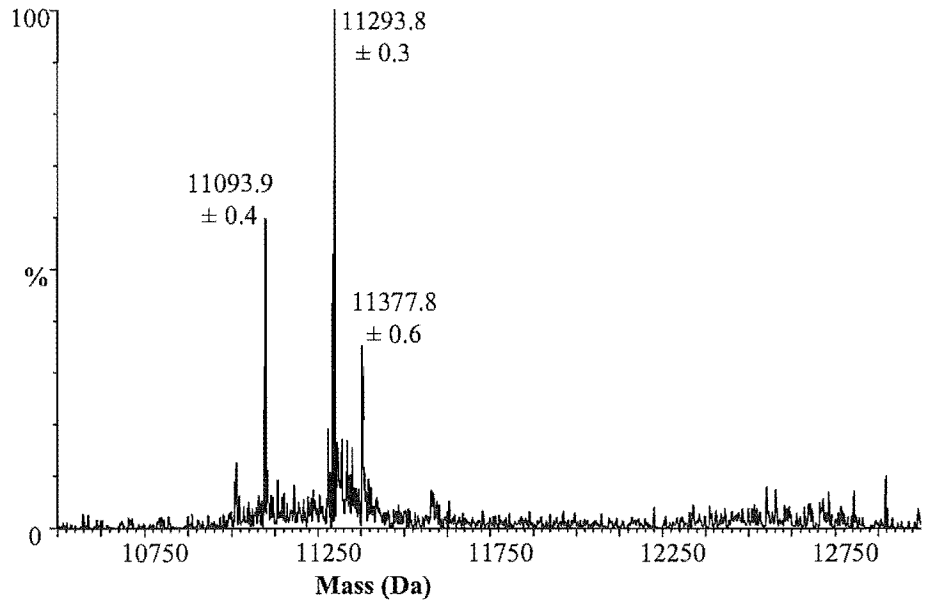

Figure 3.7: *Neutral-scale mass spectrum of reaction of CV-N (28) with 2-IT (29) and γ-maleimidobutyric acid (40) after 24 hours at 0 °C.*

A thiolating reaction time of twelve hours, with ten equivalents of 2-IT (**29**), provided the optimum conditions to produce a singly-derivatised conjugate product, with no interference from the thiolation by-product. To test these conditions further, a second model maleimide was chosen.

3.3.2 A Model System – 2-IT (**29**) and F-150 (**46**)

Fluorescein is perhaps the most popular of all fluorescent labeling agents.[154] The fluorescent properties are created by the multi-ring aromatic structure, and the planar nature of the upper, fused three-ring system (Figure **3.8**).

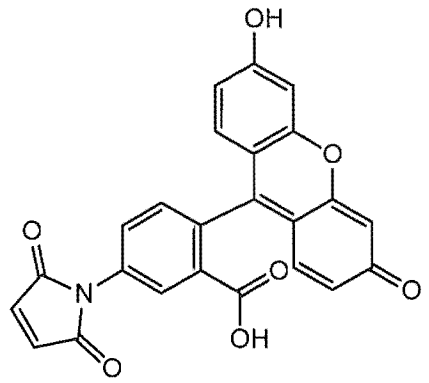

fluorescein-5-maleimide, F-150 (**46**)

Figure 3.8: *The fluorescent labeling agent: F-150.*

Fluorescein-5-maleimide, F-150, (**46**) is a commercially available (Molecular Probes Inc.) fluorescent probe containing a maleimide functionality attached to the lower ring structure. This fluorescein derivative possesses characteristic properties with an excitation wavelength at 490 nm and an emission wavelength of 515 nm, in the green spectral region.[154] F-150 (**46**) was chosen as a model maleimide to react with the thiolated CV-N. The fluorescent properties of F-150 (**46**) would allow for easy visualisation of CV-N conjugates, both by eye on a size exclusion column, or by diode array analysis.

The target fluorescent conjugate of CV-N (**47**) is illustrated in Figure **3.9**.

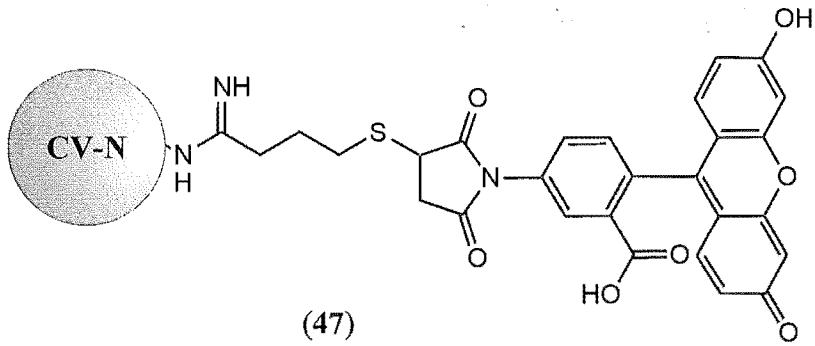

(**47**)

Figure 3.9: *CV-N-F-150 Conjugate.*

CV-N (**28**, 200 μg) was reacted with 2-IT (**29**, 10 equivalents) at 0°C in reaction buffer for 12 hours. The thiolation mixture was chromatographed on a size-exclusion (G-25) column eluted with standard borate buffer. The protein component eluted at V_0 and F-150 (**46**, five equivalents, in minimal DMF) was added immediately and the reaction left to stand for two hours. The protein solution was concentrated to ~500 μL under nitrogen gas

flow and purified on a G-25 column as described previously. Two fluorescent bands eluted from the column, one at the void volume (~20 mL), indicative of fluorescently tagged protein, and one 15 mL later, suggestive of free **46**. Both fluorescent bands were collected and analysed by LC MS (Agilent, Zorbax, C18) using the standard protein LC MS gradient. The second fraction was confirmed to be unreacted maleimide, **46**. The TIC chromatogram of the first fluorescent fraction is shown in Figure **3.10**.

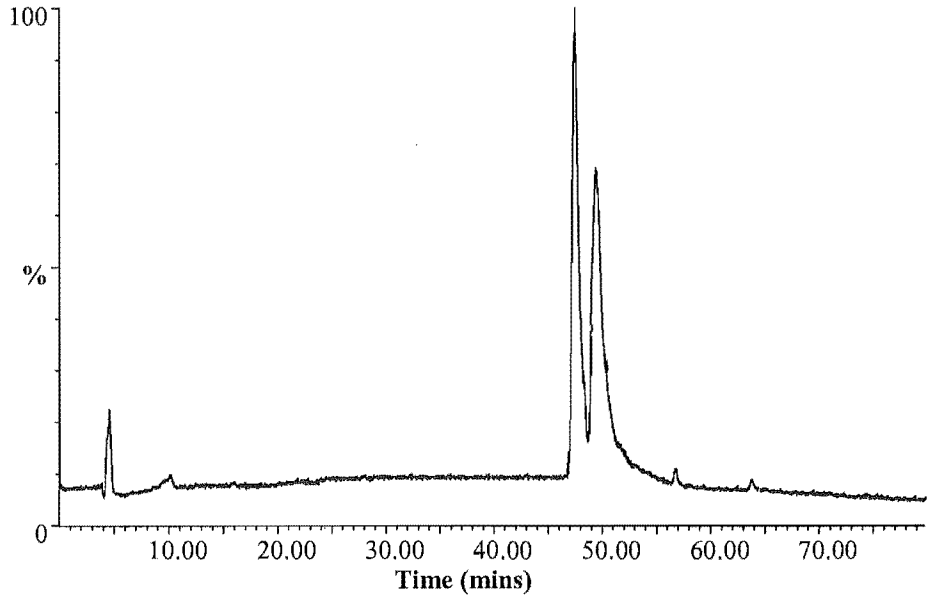

Figure 3.10: *Total Ion Current chromatogram of a preparation of a CV-N-F-150 conjugate (47).*

Two closely eluting broad peaks (~47 minutes and ~49 minutes) were present in the LC MS analysis. The ESI-data of the first peak was processed and was shown to be unreacted CV-N (**28**). The second peak demonstrated a strong absorbance at 450 nm in the diode array chromatogram, providing preliminary evidence that F-150 (**46**) was conjugated to CV-N (**28**). The MaxEnt deconvoluted ESI-mass spectral data for this peak is presented in Figure **3.11**. As illustrated by Figure **3.11 (a)**, the expected singly derivatised conjugate, **47**, (11,537 Da) had been formed. Interestingly though, a second product, 18 mass units higher (11,555 Da), was also present. The conjugate sample was reanalysed by LC MS four hours later. This analysis (Figure **3.11 (b)**) revealed that this secondary product was becoming more prominent. After 24 hours, a final LC MS analysis (Figure **3.11 (c)**) demonstrated that only the 'plus 18' product remained. Further analysis was required to determine the nature of this product (Section **3.4.3**).

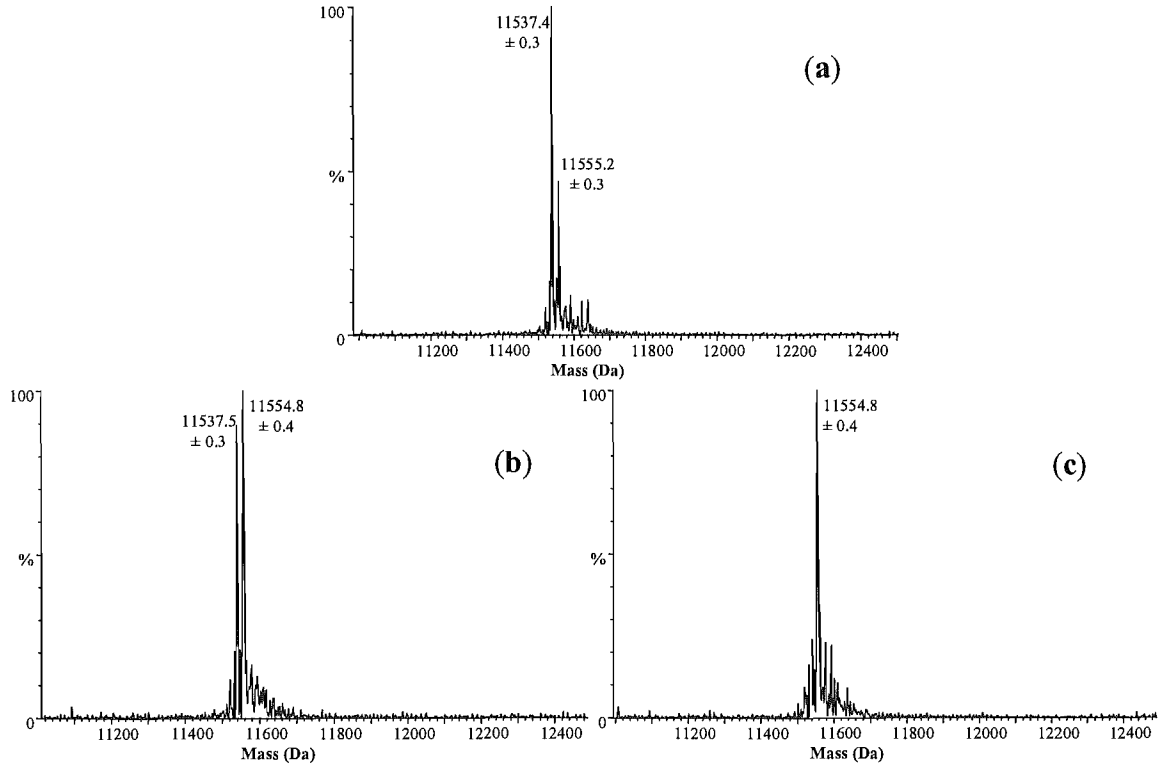

Figure 3.11: *Deconvoluted ESI-mass spectra of CV-N-F-150 conjugate (47): (a) two hours after preparation; (b) six hours after preparation; and (c) 24 hours after preparation.*

3.4 Tryptic Digestion

The results thus far have shown CV-N to be thiolated by 2-IT (**29**), but there has been no confirmation of the sites of modification. 2-IT (**29**) has, however, been shown to react preferentially with exposed lysine ε-amino groups but also at the N-terminal α-amino group of other proteins.[158] There are a number of complexities involved in achieving a successful conjugation strategy and the design of site-directed modification is just one example. A knowledge of the modification site(s) is important. This information allows rational design that should ensure good retention of activity. In order to fully characterise and determine the chemical nature of the conjugates, definition of the site of attachment is essential.

A solution to this problem was to produce fragments of the protein that are amenable to analysis by LC MS. The cleavage methods employed are usually enzymatic, but proteins can also be fragmented by chemical means, such as partial acid hydrolysis. Proteolytic enzymes offer an advantage in that they hydrolyse only specific peptide bonds, and this specificity immediately gives information about the peptide products if the protein amino acid sequence is known.

The proteolytic enzyme trypsin is one of the most commonly used reagents for specific protein digestion.[198] Trypsin specifically hydrolyses peptide bonds on the carboxyl side of lysine or arginine residues.[198] Therefore, in the case of CV-N (**28**), with five lysine and three arginine residues, nine peptide fragments would be expected if full digestion occurred. If a lysine residue has been modified then the residue is no longer recognisable as a substrate to trypsin and no cleavage occurs at that point.[198]

The initial commercial supply of trypsin was found to have chymotryptic activity. This complicated digests as fragments were produced with chymotryptic preferences. Hydrolysis of peptide bonds occurred on the carboxyl side of the aromatic amino acids, as well as leucine and histidine. To eliminate this problem, as much as possible, L-1-tosylamido-2-phenylethylchloromethyl ketone (TPCK) treated trypsin was utilised. TPCK inactivates chymotryptic activity.[199]

3.4.1 Tryptic Digestion of Native CV-N (**28**)

A tryptic digest was first performed on a sample of pure native CV-N (**28**). This would allow for development of methodology without the complicating factor of derivatisation. CV-N (**28**, 100 μg, 100 μL of 1 mg/mL in 0.9% saline solution) was diluted in ammonium bicarbonate buffer (100 μL). TPCK treated trypsin (10% by weight to the analyte protein) was added in 1% acetic acid. This trypsin enzyme-to-substrate ratio was used to avoid having to consider trypsin autolysis in the sample digests. The trypsin enzyme has been observed to cleave itself to a limited extent.[187] The digest was left at 37°C for 24 hours and analysed by reverse phase LC MS running a slow and gentle acetonitrile/water (0.5% formic acid) gradient (Section **2.8.1**). The TIC chromatogram of the digestion mixture is presented in Figure **3.12**.

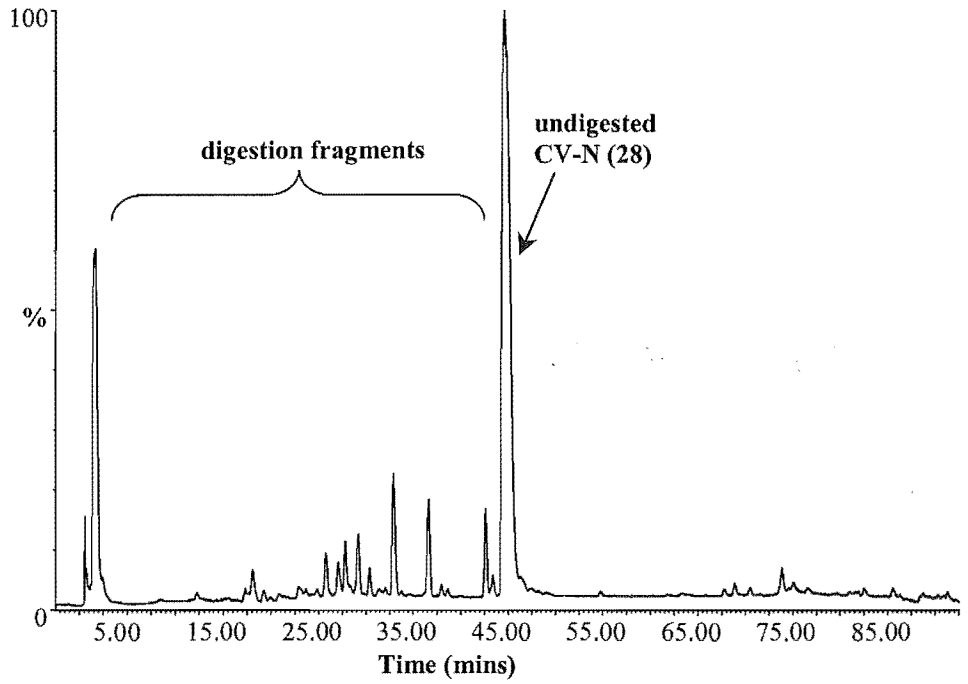

Figure 3.12: *Total Ion Current (TIC) chromatogram of a tryptic digest of CV-N (28).*

The LC MS data from the chromatogram in Figure **3.12** was processed and the fragment molecular weights were calculated by considering the m/z values found, and the charge state ions observed (for example, $(M + 2H)^{2+}$, $(M + 3H)^{3+}$). The experimentally determined masses were searched for within the peptide structure using protein software developed by Lewis Pannell.[200] This program provides a list of all possible peptide fragments of a given amino acid sequence based on the proteolytic selectivity of a

selected digestion enzyme. A match was made if the experimental MW was within 0.05% of the predicted MW. Table **3.1** details the data collected from the LC MS of the CV-N (**28**) tryptic digest, and the peptide fragment assignments that were made.

Retention Time (mins)	Experimental MW (Da)	Tryptic/Chymotryptic Cleavage Sites and Fragments
20.60	907.8	907.5 Da, peptide from 77 to 84. (R)A....K(I)
30.30	1182.2	1182.5 Da, peptide from 88 to 98. (L)D....(L)K
31.68	2292.6	2292.0 Da, peptide from 4 to 24. (K)F....R(T), intact disulfide
35.04	1650.2	1650.8 Da, peptide from 85 to 99. (K)I....K(Y)
39.13	2898.2	2898.3 Da, peptide from 49 to 59 and 60 to 74. (K)W....R(N) and (R)N....K(T), intact disulfide
45.27	2496.8	2496.2 Da, peptide from 25 to 48. (R)T....K(W)

Table 3.1: *Data from LC MS of tryptic digest of native CV-N (28). MW = molecular weight.*

Figure **3.16** (see three pages over) maps out the assigned peptide fragments against the template of the amino acid sequence of CV-N (**28**). 93% of the protein is identified.

3.4.2 Tryptic Digestion of CV-N-maleimidobutyric acid conjugate (45)

A sample of the singly derivatised CV-N-maleimidobutyric acid conjugate (**45**) was digested with TPCK treated trypsin in the same manner as for the native CV-N (Section **3.4.1**). The singly derivatised conjugate was chosen for digestion so an understanding of the distribution of modifications on the protein would result. The digested conjugate was analysed by LC MS, and experimental peptide fragment masses were determined (Table **3.2**) by processing the ESI data of the prominent peaks in the TIC chromatogram. If the fragment masses identified did not match a predicted fragment from the digest database,[200] the mass was converted to a calculated molecular weight without 2-IT/γ-maleimidobutyric acid attached. This generated series of calculated peptide molecular weights was then compared to the database. Table **3.2** shows the data collected for this digest, and the fragment assignments that were made as a result. A match was made if the experimentally determined MW was within ±0.05% of the predicted MW. Two fragments were found (retention time of 21.20 minutes and 38.39 minutes) that had been derivatised, and matched an amino sequence that included both the *N*-terminus and the lysine residue at position 3. The assumption was made that derivatisation had occurred at the lysine

residue, as digestion had not occurred at this point, suggesting that it was no longer a recognisable substrate for the trypsin enzyme. If derivatisation had occurred at the *N*-terminus an enzymatic cut would have been seen at the lysine residue.

Retention Time (mins)	Experimental MW (Da)	Calculated MW (Da) Without IT/Malei	Tryptic/Chymotryptic Cleavage Sites and Fragments
4.37	275.2		275.1 Da, peptide from 75 to 76. (K)T....(A)
10.07	310.1		310.1 Da, peptide from 100 to 101. (K)Y....E
20.40	907.4		907.5 Da, peptide from 77 to 84. (R)A....K(I)
21.20	748.0	463.1	463.3 Da, peptide from 1 to 4. L...F(S) **derivatised at Lys3**
31.60	2292.4		2292.0 Da, peptide from 4 to 24. (K)F....R(T)
34.93	1650.9		1650.8 Da, peptide from 85 to 99. (K)I....K(Y)
38.89	2873.6	2588.7	2588.6 Da, peptide from 1 to 24. L....R(T), **derivatised at Lys3**
38.90	2898.0		2898.3 Da, peptide from 49 to 59 and 60 to 74. (K)W....R(N) and (R)N....K(T), intact disulfide
39.22	3438.6	3153.7	3153.9 Da, peptide from 49 to 59 and 60 to 76. (K)W....R(N) and (R)N....R(A), intact disulfide, **derivatised at Lys74**
40.60	2823.6	2538.7	2538.3 Da, peptide from 77 to 99. (R)A....K(Y), **derivatised at Lys84**
40.60	2226.6	1941.7	1941.4 Da, peptide from 85 to 101 (K)I....E, **derivatised at Lys99**
45.17	2496.0		2496.2 Da, peptide from 25 to 48. (R)T....K(W)
46.21	5663.7	5378.8	5378.5 Da, peptide from 25 to 59 and 60 to 74. (R)T....R(N) and (R)N....K(T), intact disulfide, **derivatised at Lys48**

Table 3.2: *Selected data from LC MS of tryptic digest of the CV-N-maleimidobutyric acid conjugate (**45**). IT/Malei = 2-iminothiolane (**29**) and γ-maleimidobutyric acid (**40**), MW = molecular weight.*

The assigned peptide fragments for the digest of **45** are mapped out against the template of the amino acid sequence of CV-N (**28**) in Figure **3.16** (see two pages over).

3.4.3 Tryptic Digestion of CV-N-F150 (47)

The same enzymatic digestion procedure, as discussed above, was used for a tryptic digest of the CV-N-F150 conjugate (**47**). It was hoped that the digestion might shed some light on the nature of the 'plus 18' product. Like the previous digests, the sample was analysed by LC MS (Figure **3.13**). This time however, the derivatised fragments were very easily visualised with a strong absorbance at 450 nm in the diode array chromatogram (Figure **3.13**).

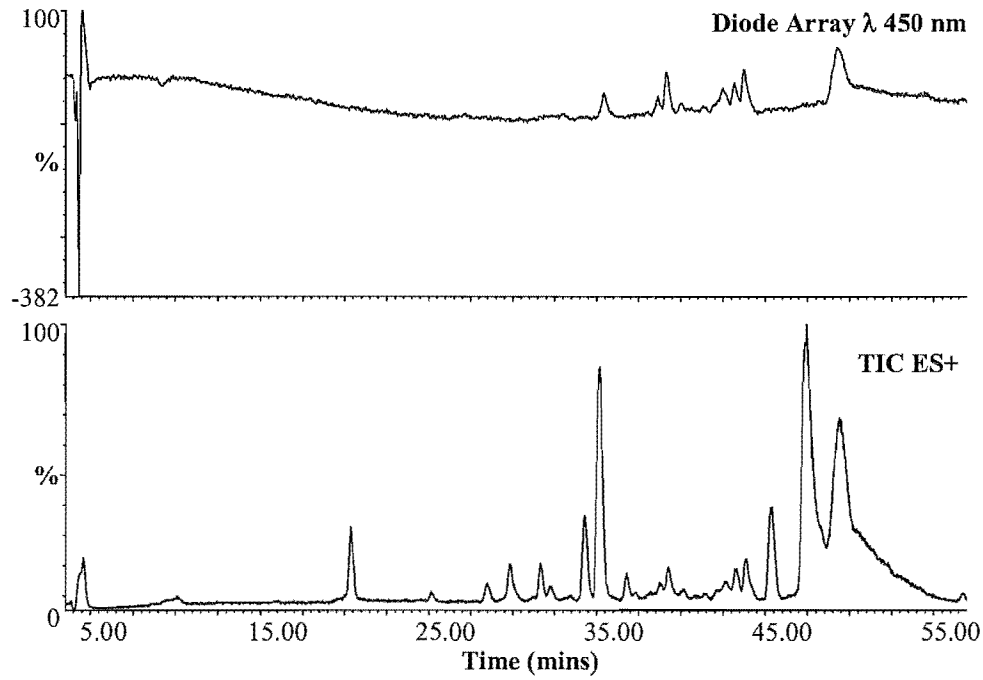

Figure 3.13: *Tryptic digest of CV-N-F-150 conjugate (47); Diode Array trace at λ 450 nm and Total Ion Current (TIC) ES+ trace.*

The ESI-data was analysed as described in Section **3.4.2**, taking into account addition of 2-IT/F-150. This time however, a second series of calculated molecular weights were also generated. These calculated masses allowed for the possibility that the 18 mass units had been incorporated in the 2-IT/F-150 section of the conjugate. Table **3.3** itemises the fragments that were identified, and their points of derivatisation. Figure **3.16** (one page over) displays the assigned peptide fragments against the amino acid sequence of CV-N (**28**).

Retention Time (mins)	Experimental MW (Da)	Calculated MW (Da) Without IT/Malei	Without + 18	Tryptic/Chymotryptic Cleavage Sites and Fragments
4.43	275.3			275.1 Da, peptide from 75 to 76. (K)T....(A)
10.16	310.2			310.1 Da, peptide from 100 to 101. (K)Y....E
20.38	907.6			907.5 Da, peptide from 77 to 84. (R)A....K(I)
31.71	2292.3			2292.0 Da, peptide from 4 to 24. (K)F....R(T)
35.02	1651.0			1650.8 Da, peptide from 85 to 99. (K)I....K(Y)
40.16	3134.8	2606.7	2588.7	2588.6 Da, peptide from 1 to 24. L....R(T), **derivatised at Lys3**
39.05	2892.0			2898.3 Da, peptide from 49 to 59 and 60 to 74. (K)W....R(N) and (R)N....K(T), intact disulfide
35.20	3699.2	3171.1	3153.1	3153.9 Da, peptide from 49 to 59 and 60 to 76. (K)W....R(N) and (R)N....R(A), intact disulfide, **derivatised at Lys74**
42.50	3085.0	2556.9	2538.9	2538.3 Da, peptide from 77 to 99. (R)A....K(Y), **derivatised at Lys84**
39.28	2487.6	1959.5	1941.5	1941.4 Da, peptide from 85 to 101 (K)I....E, **derivatised at Lys99**
45.24	2496.6			2496.2 Da, peptide from 25 to 48. (R)T....K(W)
43.86	5924.4	5396.3	5378.3	5378.5 Da, peptide from 25 to 59 and 60 to 74. (R)T....R(N) and (R)N....K(T), intact disulfide, **derivatised at Lys48**

Table 3.3: *Selected data from LC MS of tryptic digest of CV-N-F-150 conjugate (47). IT/Malei = 2-iminothiolane (**29**) and F-150 (**46**), MW = molecular weight.*

As demonstrated by the analysis of the ESI data of the tryptic digest, the extra 18 mass units were carried though to the derivatised peptide fragments and so were most likely associated with addition to the maleimide.

A well-documented problem in the synthesis of aspartic acid-containing peptides is aspartamide, cyclic imide (Figure **3.14**) formation.[201-204] This imide ring formed is susceptible to opening by the nucleophilic attack of water on either of the carbonyl carbons, resulting in two aspartate regioisomers, but with the isomer containing the β-amide bond being the main by-product (Figure **3.14**).[203,204]

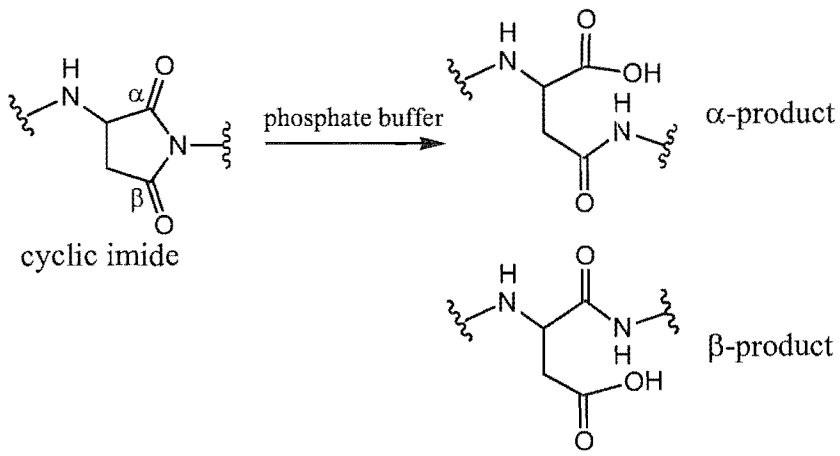

Figure 3.14: *Ring-opening hydrolysis of a cyclic imide.*[204]

It is proposed that the thioether/succinimidyl entity in the CV-N-F-150 conjugate is being hydrolysed in a similar manner (Figure **3.15**), despite the mild buffer conditions.

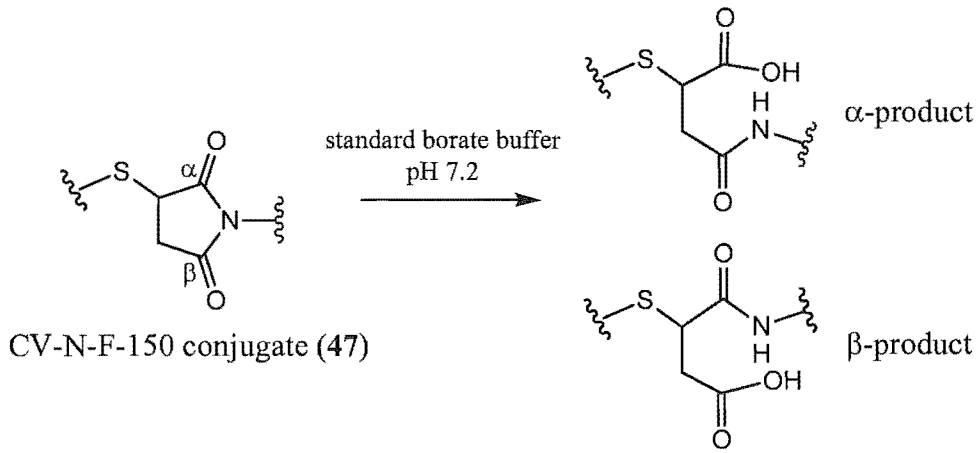

Figure 3.15: *Proposed hydrolysis of the CV-N-F-150 conjugate, 47.*

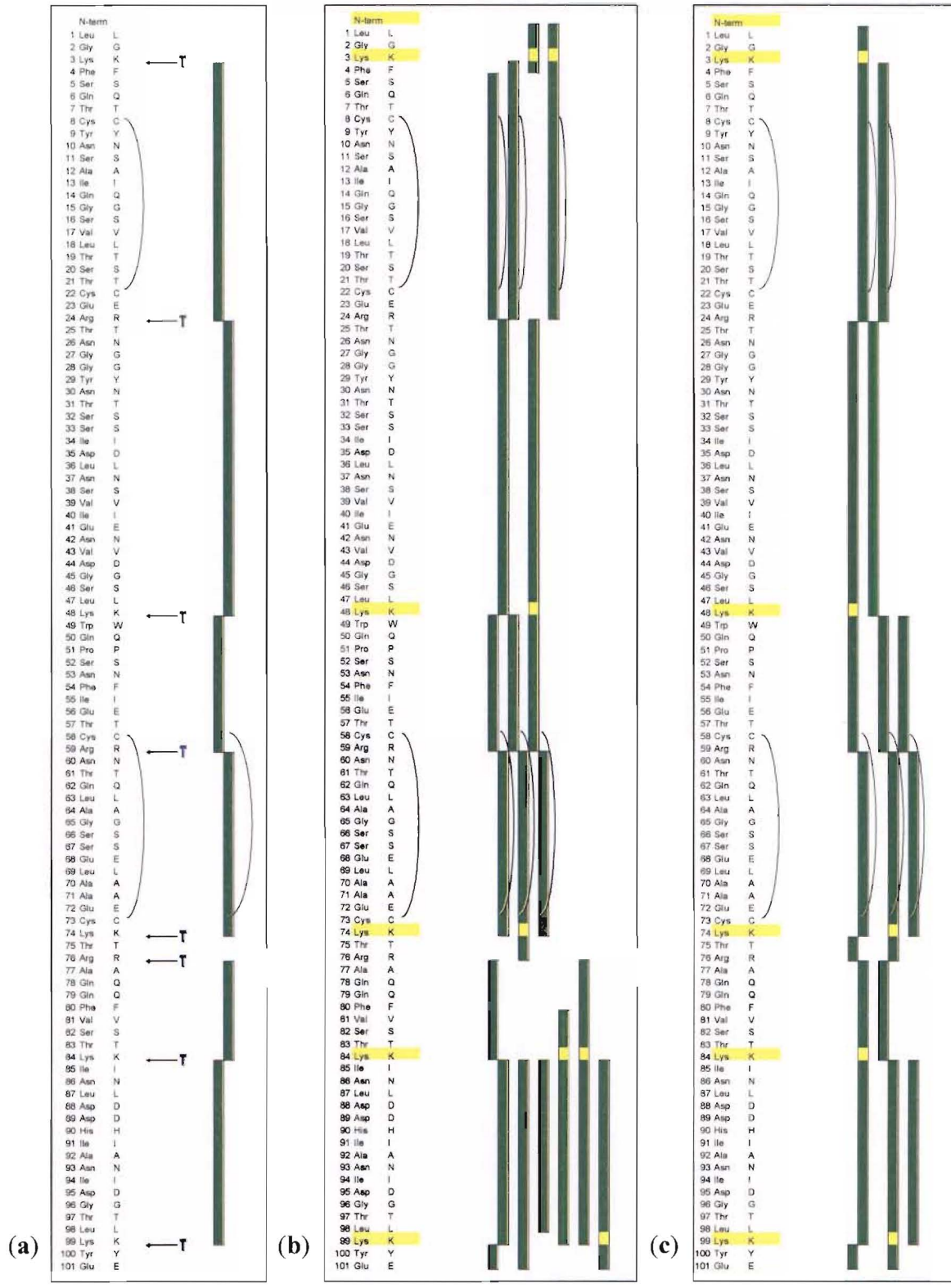

Figure 3.16: *Digest fragments identified, disulfides intact, points of derivatisation in yellow.* **T** *=cleavage points for trypsin* ***(a)*** *CV-N* ***(28)****;* ***(b)*** *CV-N 2-iminothiolane/maleimidobutyric acid conjugates* ***(45)****;* ***(c)*** *CV-N 2-iminothiolane/F-150 conjugates* ***(47)****.*

Although singly derivatised CV-N conjugates had been produced, Figure **3.16** illustrates that there was evidence for reaction at all five lysine residues, with no initial apparent selectivity for any particular residue. No attempt has been made at this point however, to closer investigate the relative reactivity of the lysine residues. There was no evidence for thiolation at the N-terminus.

The selectivity for the ε-amino groups cannot be described based on theoretical pKa values. Each type of ionisable group in the protein will have a unique pKa based upon the theoretical value for the amino acid and modulated from that value by its own surrounding microenvironment. The fact that no reaction was observed at the N-terminus suggests that it is completely protected from reaction by spatially close neighbours and the folding design of the protein.

3.5 CV-N-tyrosinamide Conjugate (48)

Reaction conditions had been optimised with model maleimides for the production of singly derivatised CV-N conjugates. However, the synthesis of the toxin conjugates needed to be addressed. The CV-N-tyrosinamide conjugate, **48**, was selected to test the addition of the maleimido-tetrapeptide-toxin construct prepared in Chapter **2**.

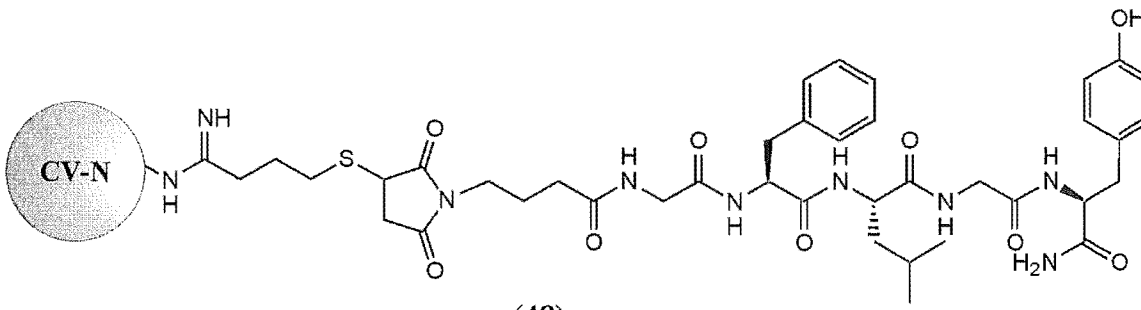

(48)

Figure 3.17: *CV-N-tyrosinamide Conjugate.*

CV-N (**28**, 400 μg, 400 μL of 1 mg/mL in 0.9% saline solution) was diluted with reaction buffer (150 μL) and placed in a 0°C water bath. Ten equivalents of 2-IT (**29**, 50 μL of a freshly made 1 mg/mL solution in reaction buffer) were added and the reaction vial was capped and left at 0°C for 12 hours. The protein was purified from the thiolating reagent on a G-25 column, eluting with the standard borate buffer (as discussed previously). The fraction eluting at V_0 was collected (fraction volume ~5 mL) and reacted immediately with two equivalents of γ-maleimidobutyric-Gly-Phe-Leu-Gly-tyrosinamide (**37**, Section **2.4.3**, in minimal DMF) at 0°C. After two hours the sample was concentrated to ~600 μL by evaporation under nitrogen gas flow. This sample was reloaded onto the G-25 size exclusion column (once again eluting with the standard borate buffer) to separate unreacted maleimide from the protein components. The proteinaceous fraction was analysed by the reverse phase standard protein LC MS methodology (Agilent, Zorbax, C3). Figure **3.18** shows the TIC ESI chromatogram of this analysis. Two closely eluting, but base-line separated, peaks (~41 minutes and ~43 minutes) were seen. Deconvolution of the mass spectral data revealed that the first peak was unreacted protein and the second peak was the desired singly-derivatised tryosinamide conjugate (**48**, 11,829 Da) of CV-N.

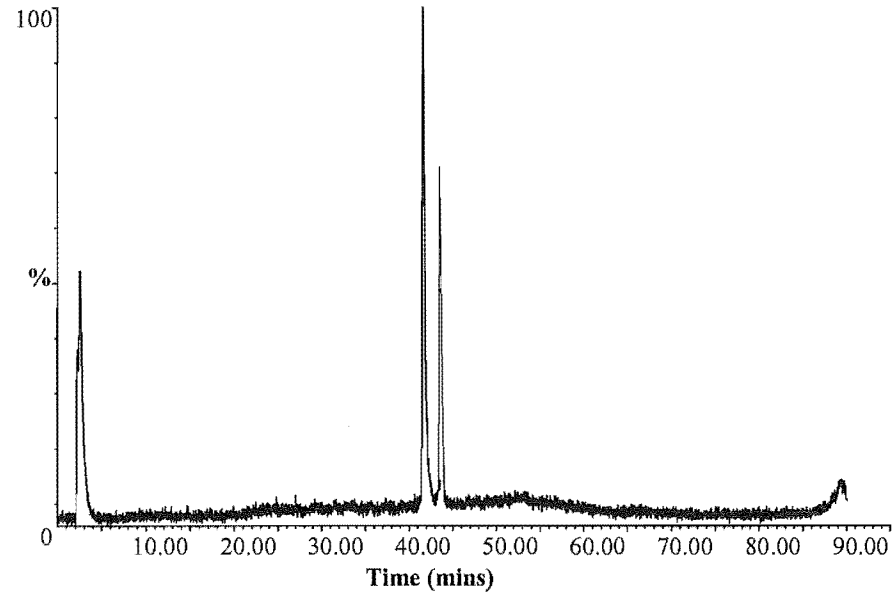

Figure 3.18: *Total Ion Current (TIC) ES+ chromatogram of the preparation of a CV-N-tyrosinamide conjugate (**48**).*

With chromatographic base-line separation (Figure **3.18**), the conjugate product (**48**) could be purified from any underivatised CV-N (**28**) using the standard protein LC MS gradient. The protein sample was concentrated from to ~500 μL under nitrogen gas flow. Aliquots (40 μL) of this mixture were purified using the LC MS method with manual collection of the required peak. The purification was guided by MS analysis, with ~10% of the sample directed to the mass spectrometer, and 90% of the sample collected.

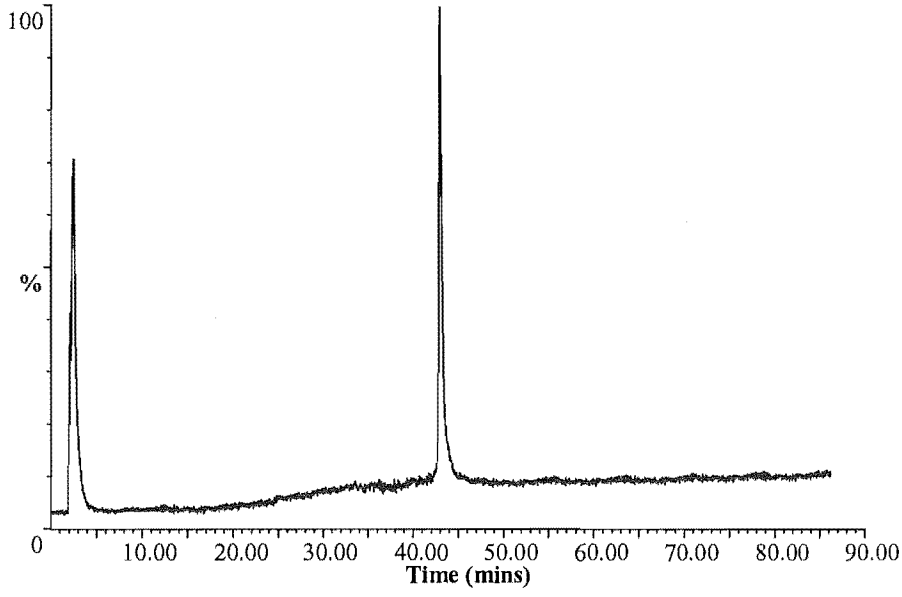

Figure 3.19: *Total Ion Current (TIC) ES+ chromatogram of the purified CV-N-tyrosinamide conjugate (**48**).*

Figure **3.19** demonstrates the effectiveness of this purification method, with a single peak eluting at the retention time of the conjugate, **48**. Analysis of the mass spectral data however, revealed that the conjugate now had a molecular weight of 11,848 Da (Figure **3.20**), 18 mass units higher than expected. It is believed that this is due to the hydrolysis of the succinimide functionality, as discussed in Figure **3.4.3**.

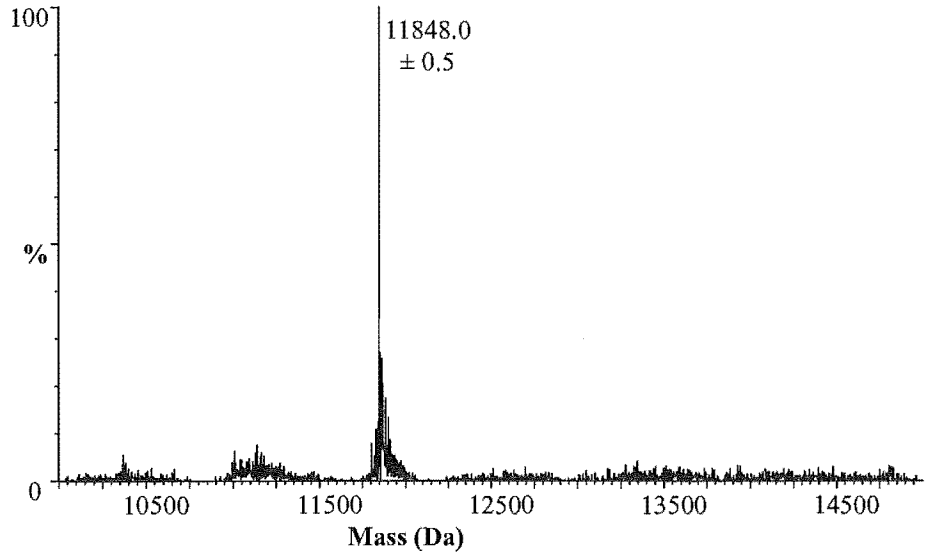

***Figure 3.20**: Deconvoluted, neutral-scale mass spectrum of the CV-N-tyrosinamide conjugate (**48**).*

3.6 Conclusions

For the CV-N-toxin conjugates to be viable as therapeutic agents, homogeneity of product is of primary importance. Limited homogeneity was achieved with CV-N conjugates prepared using the thiol/maleimide methodology. A distribution of derivatisation over all the lysine residues, but not at the *N*-terminus, was observed. While exact points of interaction between CV-N (**28**) and gp120 are still not known, the *N*-terminus is believed to be involved.[96,106] By avoiding derivatisation at the *N*-terminal amino group, the chance of producing conjugates that do not interfere with the binding of CV-N to gp120 is increased.

Ideally, a more selective and defined modification of the protein is needed.

With reactivity at all lysine residues it is possible, nonetheless, to have some control over the loading of toxin derivatives onto CV-N (**28**). By creating a range of conjugate products, the optimum pharmacokinetic properties can be determined.

A tyrosinamide-based conjugate has been produced. This conjugate can be radio-labelled, and will be useful in cellular and body distribution studies of the CV-N conjugates.

4 MUTANT CV-N CONJUGATES

MUTANT CV-N CONJUGATES

4.1 Introduction

The heterogeneity of a therapeutic conjugate presents a regulatory challenge for the pharmaceutical industry. By comparison with synthetic polymers, working with CV-N (**28**), as a defined entity, is helpful in this context. However, there still exists, within CV-N (**28**) the potential for heterogeneity. Chapter **3** described a number of native CV-N (**28**) conjugates prepared by covalent linkages with lysine amino groups. Invariably, this gave a broad distribution of products. Five products are possible, even with mono-derivatised CV-N (**28**), and each of these are inseparable from each other. The heterogeneity of the product mixture can be significantly reduced by using a very high excess of the modifying reagent, resulting in complete modification of all available amino groups. However, in this case, the problem of site-selective attachment of toxin remains unsolved.

The goal of the following chapter of work was to produce conjugates of CV-N; selectively, controllably, and uniformly modified with the biolinker-toxin constructs prepared in Chapter **2**. In rare cases, selective protein modification and formation of a homogeneous bioconjugate can be achieved if the protein happens to have only a single reactive amino acid residue targeted by the modifying agent. In general, however, strategies relying on a single attachment point on the protein molecule can hardly be considered a general method of preparation of homogeneous conjugates because proteins typically bear multiple reactive groups on their surface.

A solution to the problem of the site-specific preparation of homogeneous bioconjugates of CV-N (**28**) was provided by a four recombinantly-produced mutant CV-N proteins. These proteins were supplied by Nektar™ Therapeutics. Through site-directed mutagenesis, each of these new proteins had varying numbers of the lysine residues in CV-N (**28**) replaced by arginine residues. Arginine does not have the ε-amino functional group, and is therefore not reactive to the thiolating reagent, 2-IT (**29**). The mutant

proteins provided were: CV-N: K3R (**49**); CV-N: K3R, K48R (**50**); CV-N: K3R, K48R, K74R (**51**); and CV-N: K3R, K48R, K74R, K84R (**52**). Protein **52**, for example, has only one lysine residue at position 99. This is advantageous as it allows for only a single attachment point on the protein.

This chapter describes the synthesis of homogeneous samples of singly- and doubly-substituted toxin conjugates of CV-N, through modification of CV-N: K3R, K48R, K74R, K84R (**52**), and CV-N: K3R, K48R, K74R (**51**), respectively.

4.2 Recombinant Mutant CV-N Proteins

4.2.1 Purification

The four mutant proteins (**49**, **50**, **51**, **52**) were supplied as partially purified samples and each needed further purification before conjugate preparation could continue. Each protein was purified using a semi-preparative polymeric reverse phase (PRP-3) HPLC system. A PRP column was chosen as this type of column had previously been shown to have good recovery of protein samples.[205] A 45-minute method (Section **8.4**), with monitoring at λ 210 nm, was utilised. The major component eluted at 28 minutes in each case and was collected using a fraction collector. LC MS (Agilent 1100, see Section **8.4** for method) confirmed the exact mass and purity of each sample, and a representative TIC ES+ chromatogram of a purified protein is presented in Figure **4.1**. A single component eluted at ~21.5 minutes in each case. The purified proteins were all taken to dryness under nitrogen gas flow, and reconstituted in distilled water (1 mg/mL) for storage.

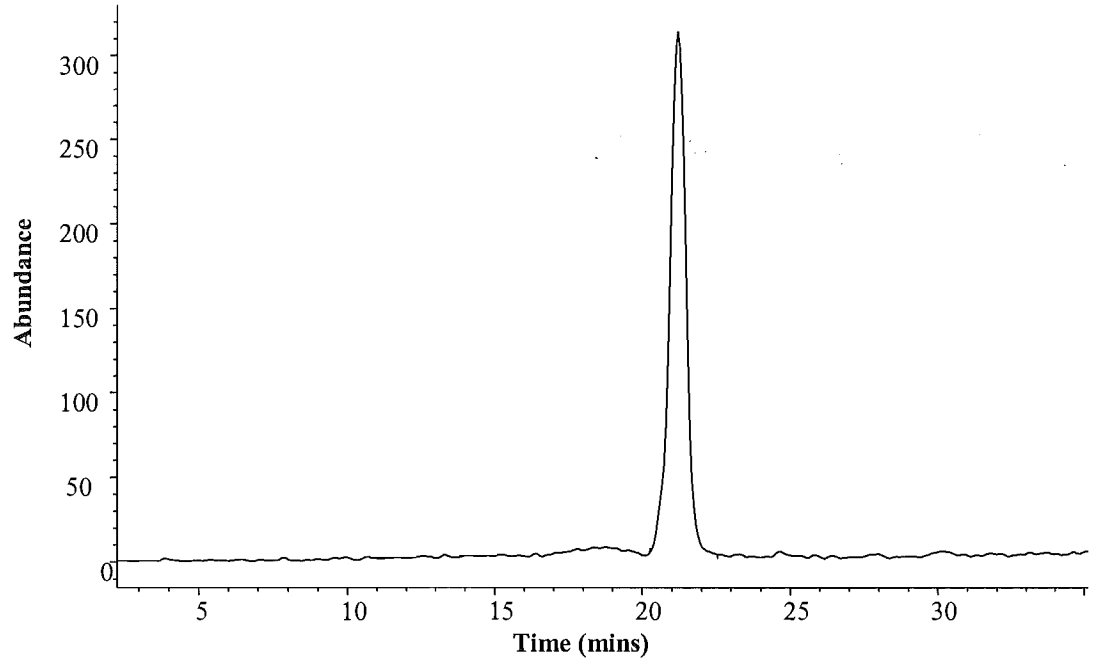

Figure 4.1: *TIC ES+ Chromatogram of purified CV-N: K3R, K48R, K74R, K84R (**52**).*

A deconvoluted mass spectrum (prepared using HP ChemStation) of each of the mutant proteins is shown in Figure **4.2**. The expected molecular weight was obtained in each case.

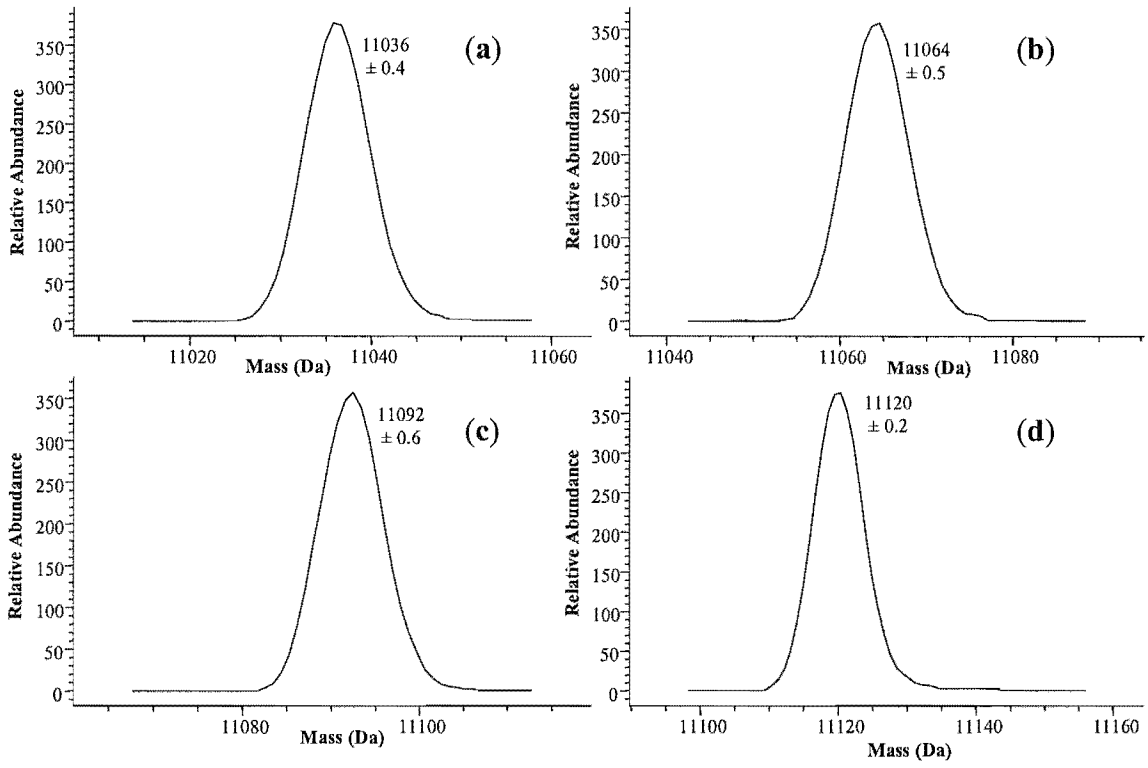

Figure 4.2: *Deconvoluted mass spectra of mutant CV-N proteins: (a) CV-N: K3R (**49**); (b) CV-N: K3R,K48R (**50**); (c) CV-N: K3R, K48R, K74R (**51**); and (d) CV-N: K3R, K48R, K74R, K84R (**52**).*

Two of the mutant proteins were chosen for further conjugate development. CV-N: K3R, K48R, K74R, K84R (**52**) was a particularly attractive protein. With just a single lysine residue remaining, at postion 99, this protein presented an ideal opportunity to selectively modify CV-N as discussed in Chapters **2** and **3**. A single, defined product would be produced. CV-N: K3R, K48R, K74R (**51**) was chosen as it presented two available lysine residues (at positions 84 and 99), and offered the prospect of producing doubly-substituted protein-toxin conjugates that were also well defined and characterised. The production of a doubly-substituted protein would allow investigations to determine the optimum pharmacokinetics of the CV-N conjugates to begin.

The two remaining mutant proteins may be of use in future experimental design.

4.2.2 Tryptic Digestion

A tryptic digest was performed on both CV-N: K3R, K48R, K74R, K84R (**52**) and CV-N: K3R, K48R, K74R (**51**) to confirm the respective amino acid sequences, and the replacement of the appropriate lysine residues by arginine. The digestions followed the same procedure discussed in Section **3.4** and were analysed by LC MS (standard protein LC MS gradient). A list of predicted peptide fragments was created using the digest software[200] and these fragments were compared to the experimentally determined masses after processing the ESI MS data. The relevant ESI MS digest data, and the resultant fragment assignments, for CV-N: K3R, K48R, K74R, K84R (**52**) and CV-N: K3R, K48R, K74R (**51**) is presented in Table **4.1** and **4.2** respectively.

Retention Time (mins)	Experimental MW (Da)	Tryptic/Chymotryptic Cleavage Sites and Fragments
11.9	935.6	936.0 Da, peptide from 77 to 84. (R)A . . . . R(I)
14.4	1019.8	1019.1 Da, peptide from 60 to 69. (R)N . . . . L(A)
15.9	747.5	747.8 Da, peptide from 4 to 9. (R)F . . . . Y(N)
21.3	1187.8	1188.2 Da, peptide from 19 to 29. (L)T . . . . Y(N)
21.9	1549.0	1549.7 Da, peptide from 60 to 74. (R)N . . . . R(T)
	1565.2	1565.7 Da, peptide from 10 to 24. (Y)N . . . . R(T)
	548.3	548.6 Da, peptide from 70 to 74. (L)A . . . . R(T)
27.3	1651.2	1651.8 Da, peptide from 85 to 99. (R)I . . . . K(Y)
29.2	1379.8	1380.5 Da, peptide from 49 to 59. (R)W . . . . R(N)
	2294.4	2295.5 Da, peptide from 4 to 24. (R)F . . . . R(T)
37.8	2524.8	2525.7 Da, peptide from 25 to 48. (R)T . . . . R(W)
41.4	11119.4	undigested protein

Table 4.1: *Selected ESI-MS data from LC MS of tryptic digest of CV-N: K3R, K48R, K74R, K84R (52). MW = molecular weight.*

Retention Time (mins)	Experimental MW (Da)	Tryptic/Chymotryptic Cleavage Sites and Fragments
13.2	907.6	908.0 Da, peptide from 77 to 84. (R)A....K(I)
15.8	747.4	747.8 Da, peptide from 4 to 9. (R)F . . . . Y(N)
22.6	1549.0	1549.7 Da, peptide from 60 to 74. (R)N . . . . R(T)
	1565.0	1565.7 Da, peptide from 10 to 24. (Y)N . . . . R(T)
	548.3	548.6 Da, peptide from 70 to 74. (L)A . . . . R(T)
28.0	1651.2	1651.8 Da, peptide from 85 to 99. (K)I . . . . K(Y)
	1310.8	1311.4 Da, peptide from 88 to 99. (L)D . . . . K(Y)
29.8	1379.8	1380.5 Da, peptide from 49 to 59. (R)W . . . . R(N)
38.7	1505.0	1505.7 Da, peptide from 75 to 87. (R)T . . . . L(D)
	2524.5	2525.7 Da, peptide from 25 to 48. (R)T . . . . R(W)
40.5	2508.6	2508.8 Da, peptide from 2 to 24. (L)G . . . . R(T)

Table 4.2: *Selected ESI-MS data from LC MS of tryptic digest of CV-N:K3R, K48R, K74R (51). MW = molecular weight.*

All peaks in the TIC chromatograms of the digests were matched with a predicted fragment (or fragments). Some chymotryptic activity was also seen, with cleavage after leucine and tyrosine residues in some instances. A map of both proteins was created, providing confirmation of the amino acid sequence in each case.

4.3 CV-N: K3R, K48R, K74R, K84R (52)

4.3.1 CV-N: K3R, K48R, K74R, K84R-F-150 Conjugate (53)

The model maleimide, F-150 (**46**), was employed again for initial reactivity and method development studies. The target (**53**); a singly-derivatised, conjugate of CV-N: K3R, K48R, K74R, K84R (**52**) is illustrated in Figure **4.3**.

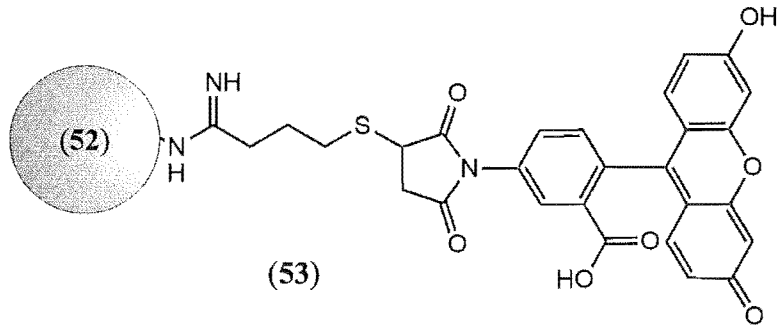

Figure 4.3: *CV-N: K3R, K48R, K74R, K84R-F-150 Conjugate.*

CV-N: K3R, K48R, K74R, K84R (**52**, 200 μg) was thiolated with 2-IT (**29**, 25 equivalents) in reaction buffer at 0°C in an ice bath for 12 hours. The protein was separated from 2-IT (**29**) on a G-25 column eluting with standard borate buffer, while monitoring at λ 206 nm. The peak that eluted at ~20 minutes was collected and reacted directly with F-150 (**46**, two equivalents in minimal DMF) for five hours at 0°C. The reaction mixture was concentrated (~200 μL) and purified on a further G-25 column, this time eluting with distilled water. A fluorescent yellow band eluted at the void volume (V_0). This fraction was collected and analysed by LC MS (Waters/Micromass, Zorbax-C3, standard protein LC MS gradient). Two primary peaks eluted in the TIC chromatogram (Figure **4.4**). The second peak is visible at 450 nm, suggesting that it has been tagged by F-150 (**46**). Analysis of the ESI MS data demonstrated that unreacted protein (11,119 Da) was eluting at 42.6 minutes and that the conjugate **53** (11,648 Da) was eluting at 44.5 minutes (Figure **4.5**). A doubly-substituted product was not observed.

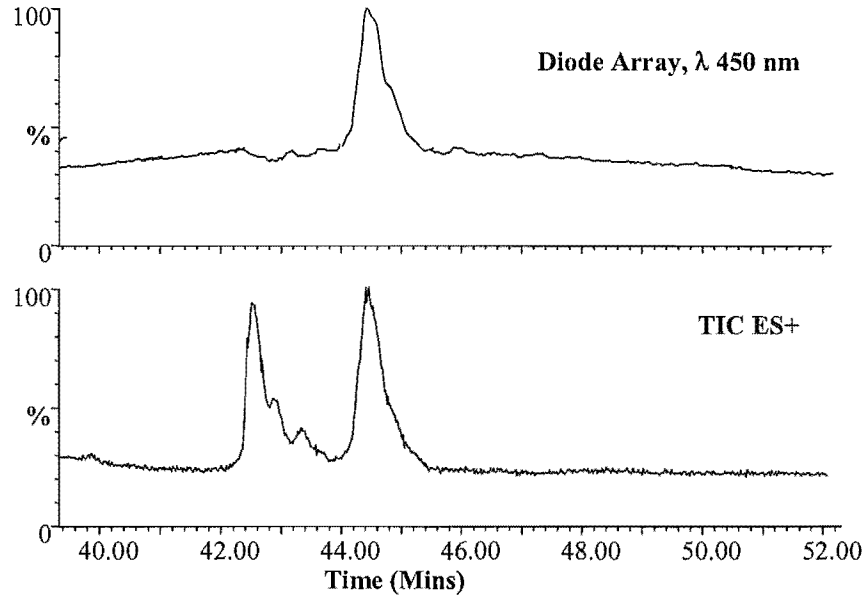

Figure 4.4: *Expansion of a section of the chromatogram of the preparation of CV-N: K3R, K48R, K74R, K84R-F-150 Conjugate (**53**). Diode Array trace at λ 450 nm and Total Ion Current (TIC) ES+ trace.*

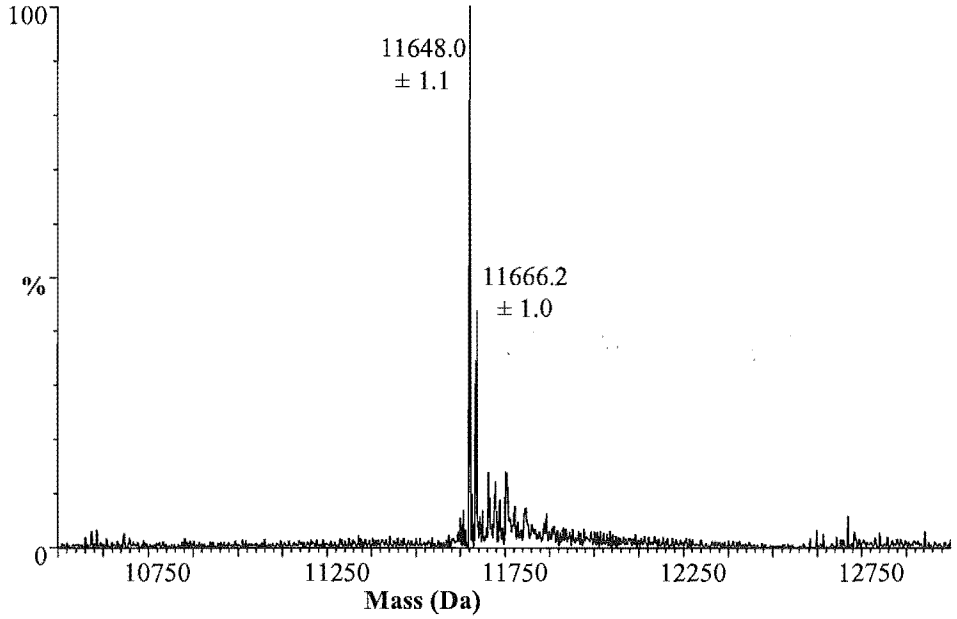

Figure 4.5: *ESI deconvoluted mass spectrum of CV-N: K3R, K48R, K74R, K84R-F-150 Conjugate (**53**).*

The succinimide ring-opened component (11,666 Da), as discussed in Section **3.4.3**, was also present and increased in proportion over time until it became the sole product.

Increasing the amount of 2-IT (**29**), or an increase in thiolation reaction time, served only to introduce the thiolation by-product. A 100% yield of the conjugate product was never obtained. However, with base-line chromatographic separation of the unreacted protein (**52**) and the conjugate (**53**), the conjugate could be readily purified.

4.3.2 CV-N: K3R, K48R, K74R, K84R-norhomohalichondrin B Conjugate

The ultimate goal of this project was to combine the potent toxicity of homohalichondrin B (**22**) with the anti-HIV targeting ability of CV-N (**28**). This section of work set out to prepare the mono-derivatised CV-N: K3R, K48R, K74R, K84R-norhomohalichondrin conjugate (**54**) illustrated in Figure **4.6**.

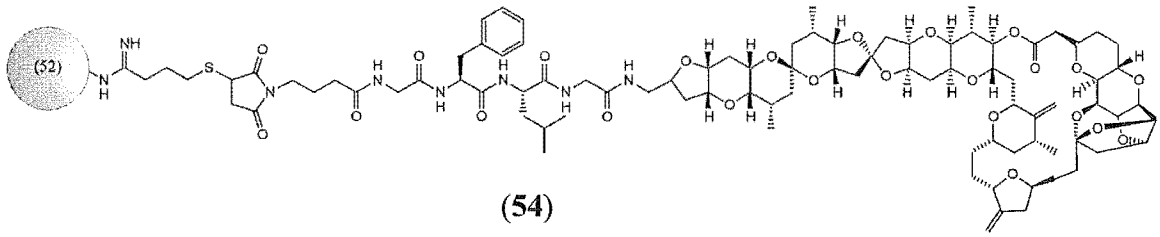

(54)

Figure 4.6: *CV-N: K3R, K48R, K74R, K84R-norhomohalichondrin B Conjugate.*

Protein **52** (4.5 mg) was dissolved in degassed reaction buffer (4.5 mL) and thiolated with 2-IT (**29**, 25 equivalents) at 0°C for 12 hours. The reaction mixture was chromatographed on a G-25 column (2.5 cm x 40 cm) with standard borate buffer at a flow rate of 3 mL/min, and visualised with a diode array detector set at 280 nm. The protein fraction was collected after 19 minutes. This fraction was concentrated to ~4 mL by centrifugation in a centriprep concentrator (YM-3 regenerated cellulose 3000MW). γ-Maleimidobutyric-Gly-Phe-Leu-Gly-norhomohalichondrin B (**32**, Section **2.4.1**, one equivalent, in miminal DMF) was added, and the reaction left to stand at 0°C overnight. LC MS analysis confirmed that the reaction was complete at this point and that a single, mono-derivatised product (**54**) had been produced (Figure **4.7**). Disappointingly, it appeared only ~10% of the mutant protein had been derivatised (Figure **4.7**). However, with unreacted protein eluting at 15.7 minutes, and a small proportion of thiolation by-product eluting at 17.1 minutes, conjugate **54** (21.2 minutes) could be purified using analytical reverse phase HPLC. A solvent gradient comprising the following steps was used: a linear gradient from 20-45% CH_3CN/H_2O (0.5% acetic acid) over 25 minutes; a linear gradient to 100% CH_3CN over five minutes; isocratic at 100% CH_3CN for five minutes; and then a return to 20% CH_3CN/H_2O over five minutes. Despite concerns of the stability of the halichondrin component of the sample, the acid modifier was essential for chromatography; no conjugate was observed without it. Conjugate **54** eluted at 21.2

minutes, and was collected manually and dried down under nitrogen immediately to avoid any possible degradation of the halichondrin by acetic acid.

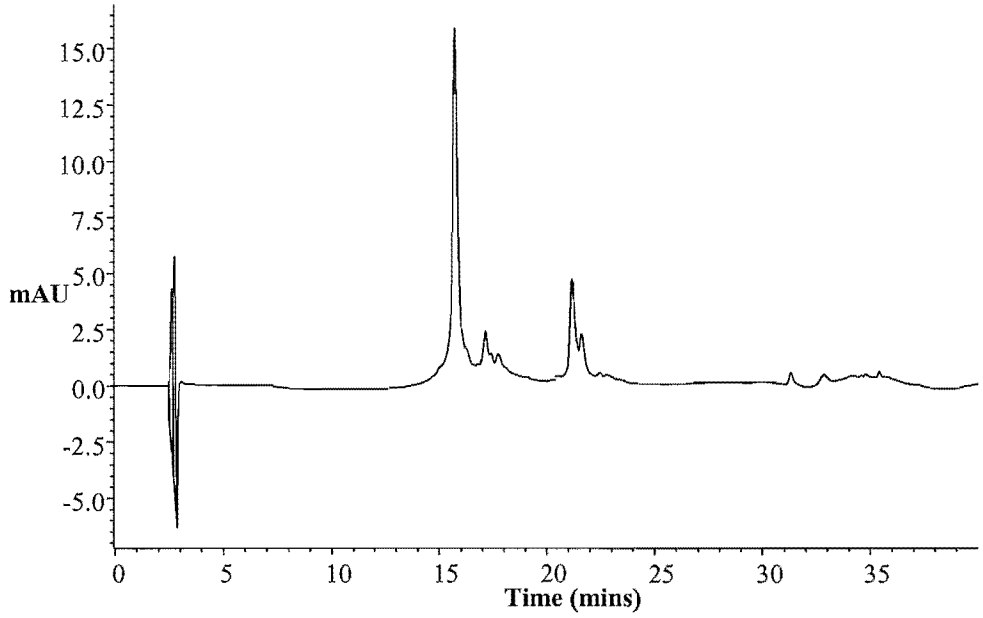

Figure 4.7: *Diode Array chromatogram (λ 280 nm) for the preparation of CV-N: K3R, K48R, K74R, K84R-norhomohalichondrin B Conjugate (**54**).*

After collection, **54** was reanalysed by LC MS to assess the final purity of the sample. The sample was essentially a single component. This component had a mass 18 Da higher (12,870 Da) than that expected for **54**. (Figure **4.8**) This mass difference had been observed previously with model systems (Section **3.4.3**).

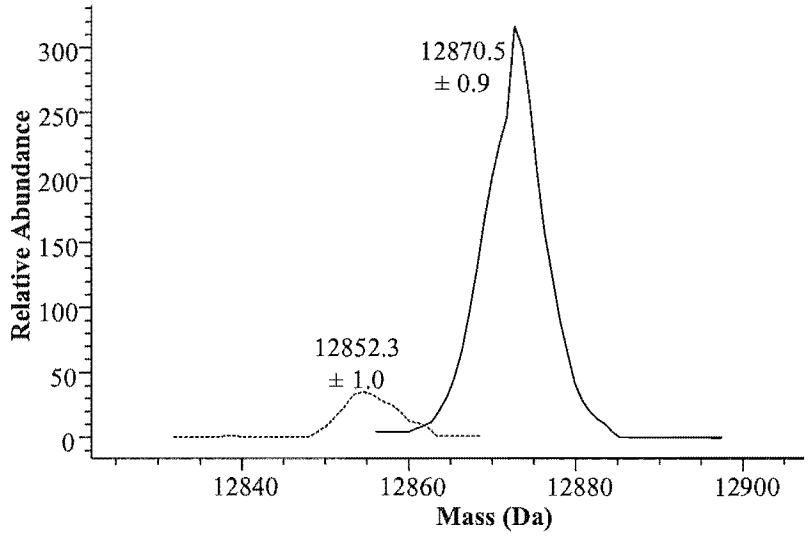

Figure 4.8: *Neutral-scale deconvoluted mass spectrum for purified CV-N: K3R, K48R, K74R, K84R-norhomohalichondrin B conjugate (**54**).*

A number of analytical experiments were undertaken to quantify **54**, and to confirm the exact site of derivatisation.

4.3.2.1 Amino Acid Analysis

Conjugate **54** was submitted for amino acid analysis. This gave a protein quantitation of 50.8 μg. This quantity of conjugate, though small, would be enough for preliminary investigations. Amino acid analysis also confirmed a ratio of one Gly-Phe-Leu-Gly biolinker to each protein molecule.

4.3.2.2 Amino Acid Sequencing

Conjugate **54** (0.846 μg) was submitted for amino acid sequencing by an Applied Biosystems Procise Sequencer. The sequencer chemically cleaves amino acids one by one from the N-terminus of the protein and identifies them chromatographically. The first nine amino acids from the N-terminus were sequenced correctly. This suggests that the primary product being sequenced had not been derivatised at the N-terminal amine. The sequencer would not have recognised the N-terminus otherwise. This consolidates previous results.

4.3.2.3 Tryptic Digest

Conjugate **54** (4.2 μg) was digested with TPCK-treated sequencing grade trypsin in the same manner as discussed in Section **3.4** and analysed by LC MS after 12 hours. A reverse phase (Zorbax-C3) system was used for the analysis. The solvent elution gradient consisted of the following timetable; a very long linear gradient from 100% H_2O (5% acetic acid) to 40% CH_3CN/H_2O over 135 minutes, and then an increase in CH_3CN concentration to 100% over 15 minutes. A small amount of dithiothreitol (DTT) was added to the LC MS sample just before analysis to break any disulfide bonds that might be binding two fragments together. All peaks in the resultant LC MS trace (Figure **4.9**) were accounted for with a peak eluting at 123 minutes being particularly notable. This peak represented the amino acid residues, 85 to the C-terminus of **52**, derivatised by 2-IT (**29**) and γ-maleimidobutyric-Gly-Phe-Leu-Gly-norhomohalichondrin B (**32**). Since trypsin cleaves on the carboxyl side of lysine, the lack of cleavage of this fragment at residue 99 is also indicative of derivatisation of lysine at this point. Other fragment assignments can be seen in Table **4.3**.

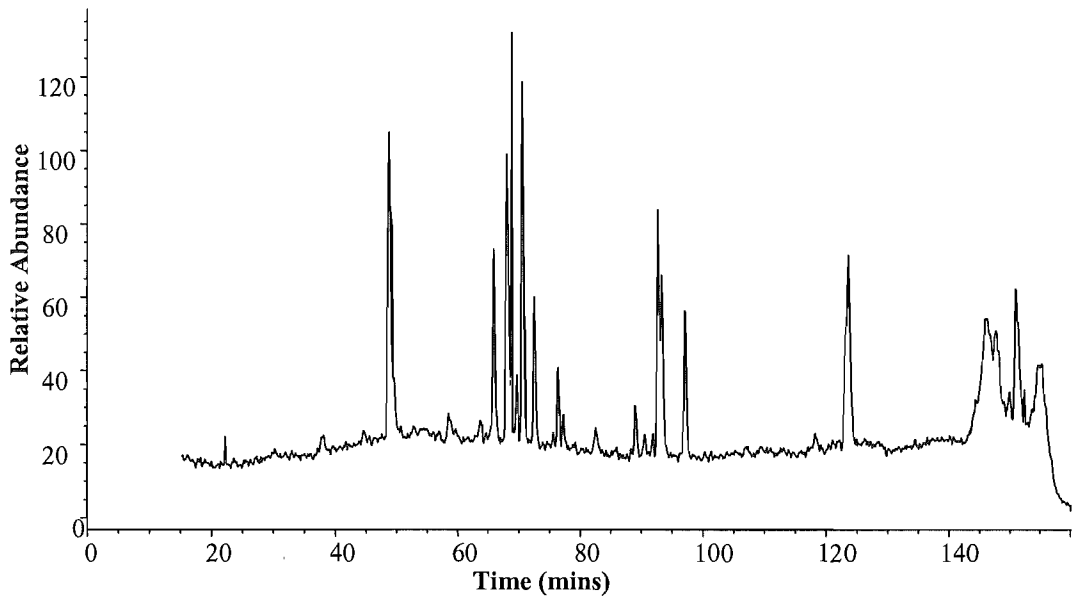

Figure 4.9: *Total ion current chromatogram of the tryptic digest of CV-N:K3R, K48R, K74R, K84R-norhomohalichondrin B Conjugate (**54**).*

Retention Time (mins)	Experimental MW (Da)	Calculated MW (Da) Without IT/Malei	Without H_2O	Tryptic/Chymotryptic Cleavage Sites and Fragments
48.75	1549.0			1549.7 Da, peptide from 60 to 74. (R)N . . . . R(T)
65.89	1380.0			1380.5 Da, peptide from 49 to 59. (R)W . . . . R(N)
68.00	935.7			936.0 Da, peptide from 77 to 84. (R)A . . . . R(I)
68.79	1018.8			1019.1 Da, peptide from 60 to 69. (R)N . . . . L(A)
70.51	2294.9			2295.5 Da, peptide from 4 to 24. (R)F . . . . R(T)
97.05	2525.5			2525.7 Da, peptide from 25 to 48. (R)T....K(W)
123.61	3676.3	1944.3		1944.1 Da, peptide from 85 to 101 (K)I....E,
				derivatised at Lys99
	3694.2		1944.2	1944.1 Da, peptide from 85 to 101 (K)I....E,
				derivatised at Lys99

Table 4.3: *Selected ESI MS data from the LC MS of the tryptic digest of CV-N:K3R, K48R, K74R, K84R-norhomohalichondrin B conjugate (**54**). MW = molecular weight. IT/Malei = 2-IT (**29**)/ γ-maleimidobutyric-Gly-Phe-Leu-Gly-norhomohalichondrin B (**32**).*

The biological testing of this conjugate is discussed in Chapter **6**.

4.3.3 CV-N: K3R, K48R, K74R, K84R-Doxorubicin Conjugate (**55**)

Over the past 33 years, doxorubicin (**34**) unquestionably has proven to be of considerable medical value because of its outstanding anti-cancer activity. The importance of doxorubicin (**34**) is well documented in a huge number of publications.[135,171,175,206-209]

Spurred on by the positive results reported by Kratz *et al.* with transferrin[135] and albumin[144,210] protein conjugates of doxorubicin (**34**), and the traverse of the polymer therapeutics of doxorubicin (**34**) (PK1[142,171] and PK2[143,211]) through clinical trials, the goal of this section of work was to combine doxorubicin (**34**) and CV-N (**28**) in a unique therapeutic (**55**, Figure **4.10**) for HIV.

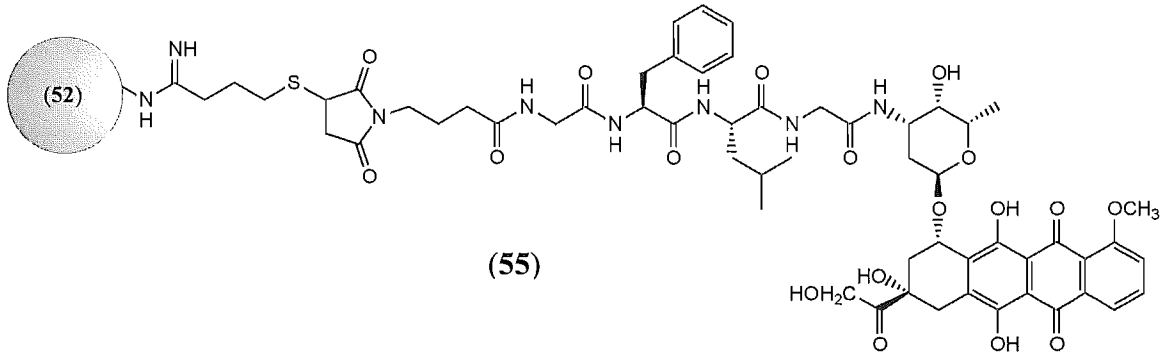

Figure 4.10: *CV-N: K3R, K48R, K74R, K84R-Doxorubicin Conjugate.*

CV-N: K3R, K48R, K74R, K84R (200 μg) was reacted with 2-IT (**29**) in reaction buffer at 0°C for 12 hours. A size-exclusion column (G-25), eluted with standard borate buffer, was utilised to separate the protein from excess thiolating reagent. This column was monitored at 206 nm with a diode array detector. A peak eluting at 20 minutes was collected and reacted directly with γ-maleimidobutyric-Gly-Phe-Leu-Gly-doxorubicin (**35**, two equivalents in minimal DMF) for two hours. The reaction mixture was concentrated (~200 μL) and purified on a further G-25 column, this time eluting with distilled water. A pale pink band eluted at 20 minutes. This fraction was collected and analysed by LC MS (Micromass/Waters, Zorbax-C3, standard protein LC MS gradient) (Figure **4.11**).

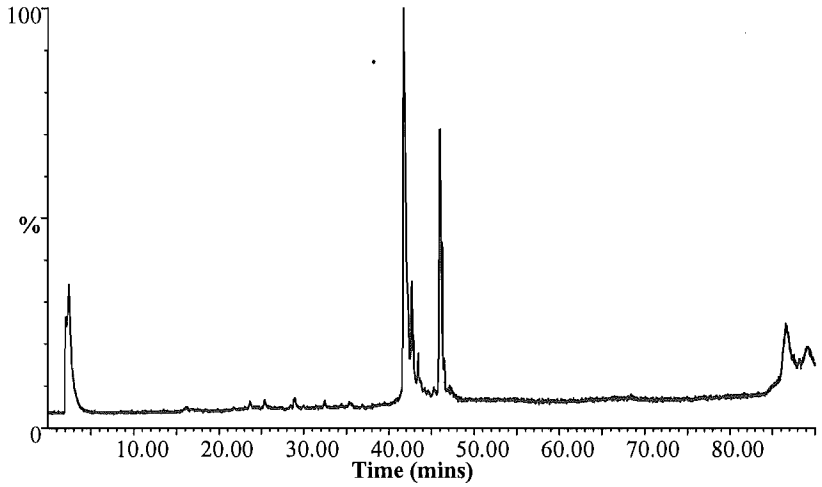

Figure 4.11: *Total Ion Current chromatogram of the preparation of CV-N: K3R, K48R, K74R, K84R-doxorubicin conjugate (55).*

Two peaks were predominant in the LC MS analysis. The second peak demonstrated a strong absorbance at 480 nm in the diode array, indicative of a doxorubicin derivative. Analysis of the TIC data showed that unreacted protein (11,120 Da) was eluting at 42.05 minutes and that **55** (12,304 Da) was eluting at 46.20 minutes (Figure **4.12**).

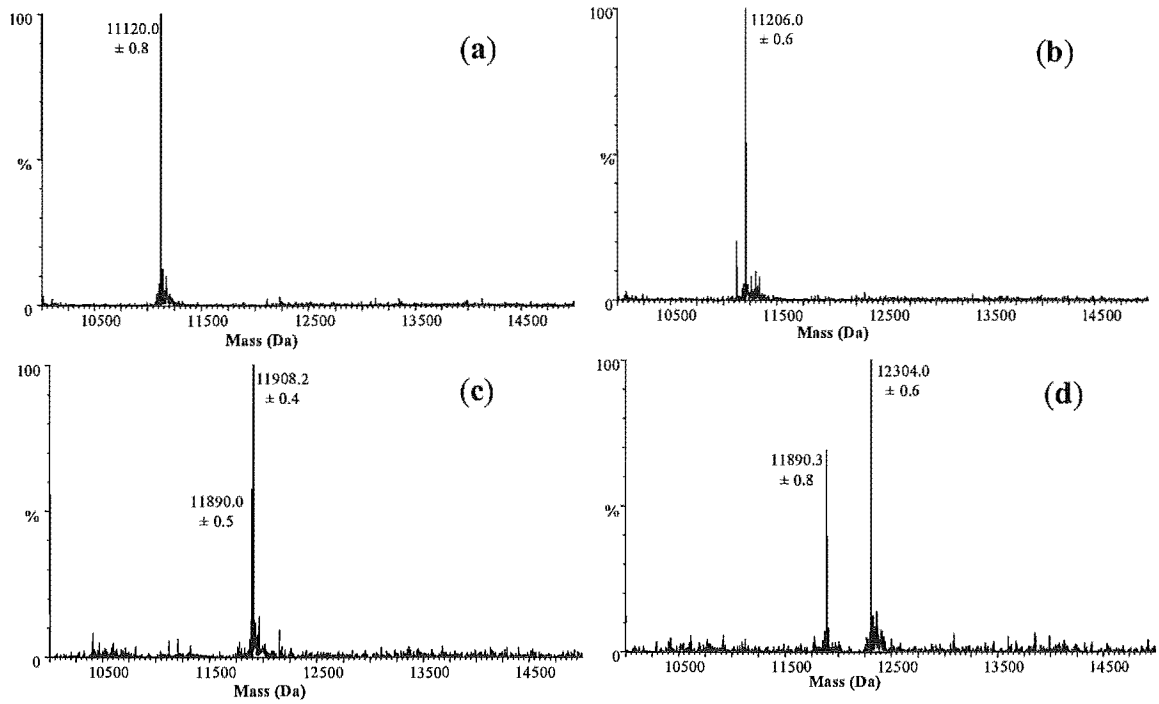

***Figure** 4.12: ESI MS deconvoluted data from the preparation of CV-N: K3R, K48R, K74R, K8R-doxorubicin conjugate (55). (a) retention time 42.05 minutes; (b) retention time 42.75 minutes; (c) retention time 43.42 minutes; and (d) retention time 46.20 minutes.*

A small peak elutes closely to the unreacted protein (42.75 minutes) and this was confirmed to be the thiolation by-product (Figure **4.12**) as previously discussed. With good separation from the product conjugate, the formation of this by-product does not present purification issues. There were two significant elements of concern however. Deconvolution of the product peak (46.20 minutes, Figure **4.12**) presents two products: the expected conjugate (12,304 Da) and a peak with a mass of 11,890 Da. This appears to be loss of the anthracyline, and water, from the conjugate, perhaps in the mass spectrometer. Significantly more alerting was the presence of small peak (Figure **4.12**) eluting at 43.42 minutes. Deconvolution of the ESI MS data showed that this compound had a mass of 11,908 Da. This compound does not absorb at 480 nm in the diode array indicating a loss of the anthracycline functionality. Based on the mass, this peak appears

to be loss of the anthracycline from the conjugate. Interestingly, a peak of 11,890 Da is also present in this spectrum, and is possibly loss of water from the degraded conjugate in the mass spectrometer. The sample was analysed with further LC MS runs, and an overlay of the resultant chromatograms is presented in Figure **4.13**. The conjugate (**55**, 46.20 minutes) degrades over time, and the peak at 43.42 minutes grows. Within 24 hours the conjugate (**55**) was no longer present.

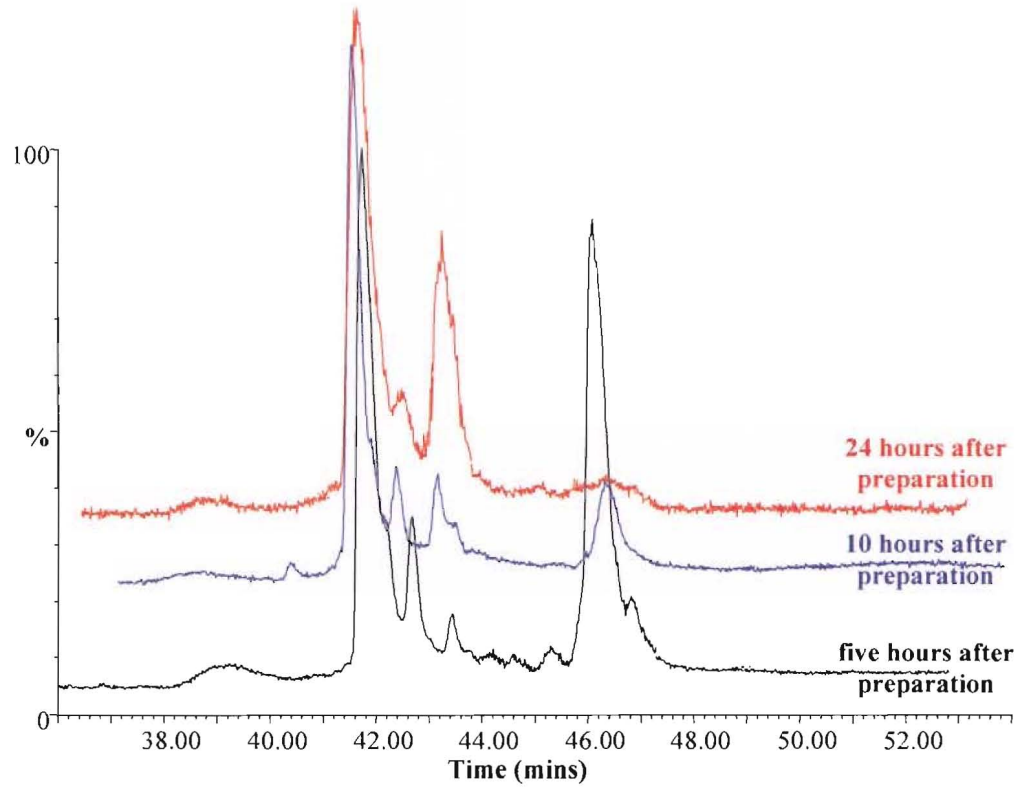

Figure 4.13: *TIC chromatogram overlay of the degradation of conjugate* ***55****.*

A literature search reveals that doxorubicin (**34**) is far from an ideal drug. It interacts with all kinds of ions, chelates strongly with divalent and trivalent metal ions, adsorbs onto various materials, particularly glass surfaces, tends to self-associate in concentrated solutions, and is liable to photolytic degradation, and to oxidation.[212-214] A number of systematic studies into the chemical degradation processes have been completed. The studies have focused on the kinetics of doxorubicin degradation, primarily in aqueous solution, as a factor of pH, buffers, temperature, ionic strength and drug concentration.[212-214] There are a number of degradation conditions that are particularly important in relation to this project. Firstly, the degradation rate of doxorubicin is strongly influenced by the pH of the medium, decomposing under both acidic and basic

conditions. The compound shows maximum stability at pH 4.[213] Secondly, in the region of up to pH 9.5, catalysis by acetate, phosphate and carbonate buffer components have been demonstrated.[213,214] And finally, it has also been shown that in the presence of light; even room light, or light from photodiode array detectors, degradation of doxorubicin (**34**) occurs.[212]

In acidic solution (pH < 4) the initial degradation step of doxorubicin (**34**) is conversion into the 7-hydroxyaglycone, doxorubicinone (**56**, Figure **4.14**) and the amino sugar, daunosamine (**57**, Figure **4.14**). At pH > 4 the degradation pattern of doxorubicin (**34**) has not been elucidated completely, but compound **58** appears as the main degradation product.[213]

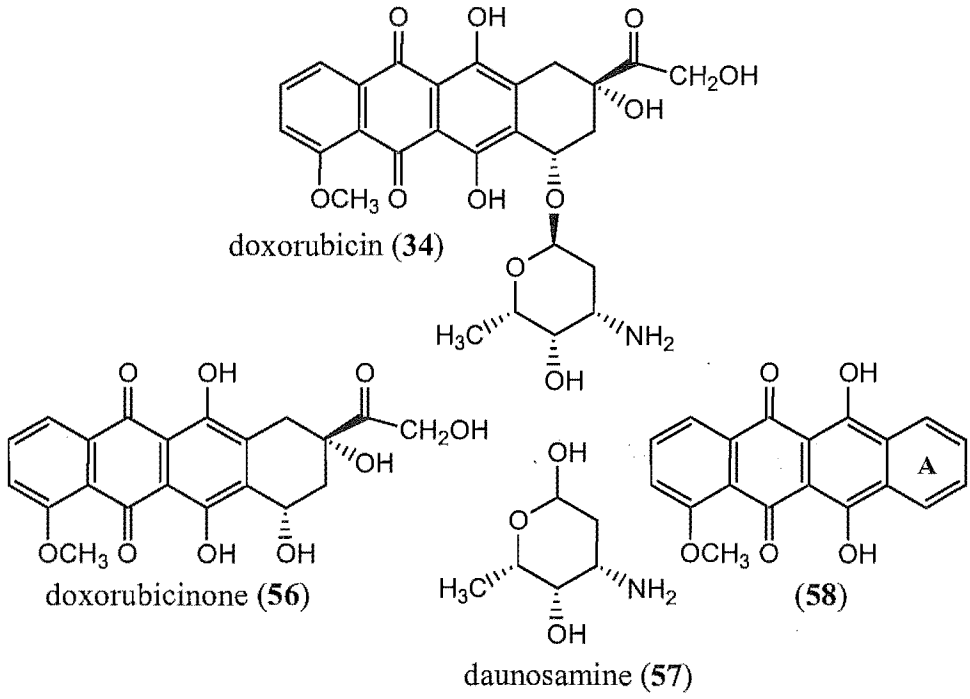

Figure 4.14: *Doxorubicin, and structures of the doxorubicin degradation products.*

Beijnen *et al.*[213] proposed a degradation mechanism. Enolisation of the α-ketol side chain is assumed to be the first step in the degradation reaction of doxorubicin (**34**). Abstraction of a benzylic proton, and cleavage of the side chain and the amino sugar (**57**) yields doxorubicinone (**56**). The high stability of the resulting degradation product is the driving force of the full aromatisation of the A ring (**58**) after cleavage of the side chain.

We assume that the degradation product observed in our case is the conjugate (**59**) illustrated in Figure **4.15**. The sugar remains attached to the biolinker, while the anthraquinone functionality is expelled.

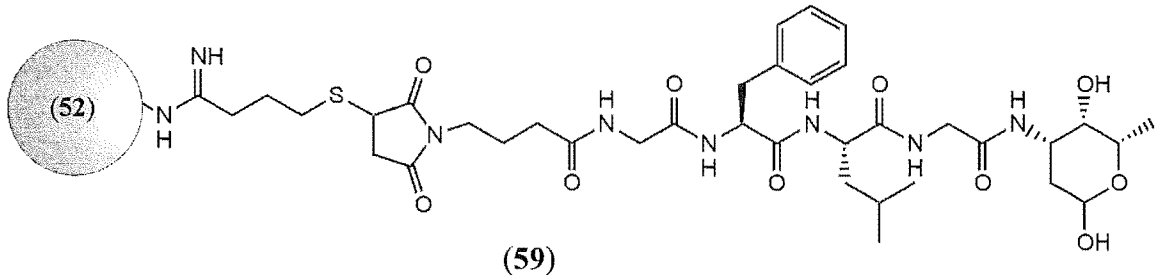

(59)

Figure 4.15: *Degradation product of the CV-N: K3R, K48R, K74R, K84R-Doxorubicin conjugate (55).*

This degradation probably occurs as a function of interrelated factors, particularly of pH, buffers, and light conditions. The degradation product (**59**) was seen at the same retention time as the conjugate product (**55**) in the LC MS analysis, perhaps due to fragmentation in the mass spectrometer, but was also seen at an earlier retention time, suggesting degradation in the sample vial.

This raises a complex issue. The authors of publications reporting the preparation of polymeric[142,143,171,172,215] and protein[135,144,210] constructs of doxorubicin (**34**) claim that the conjugate systems increase the therapeutic index of the drug: that cardiotoxicity decreases, while the cytostatic action is preserved. The publications make no mention of degradation products, or in fact complete degradation (as in our case). Interestingly, the preparation of the albumin[144,210] and transferrin[135] conjugates of doxorubicin (**34**) utilise very similar reaction conditions to those used in this project, and stock solutions of the conjugates were kept in a standard borate buffer (0.0025 M sodium borate, 0.15 M NaCl, pH 7.5). The lack of reported degradation of these conjugates raises questions about the cytotoxic action of the parent compound and the degradation products. More research will need to be done to evaluate this further.

4.4 CV-N: K3R, K48R, K74R (51)

Potency of the therapeutic agent, and the clinical dose required must be considered in the development of a drug. One of the most important limiting factors when designing a drug delivery system is its drug carrying capacity, not only in terms of the theoretical possibilities for chemical conjugation, but also practical issues such as water solubility of the product and the influence of high drug substitution on the pattern of biodistribution of the conjugate. This latter issue is of primary importance with the binding specificity of CV-N to gp120. Research has shown a maximum drug loading does not always yield a product with maximum efficacy.[121] The issue of increased toxin loading on CV-N was addressed with modification of the mutant protein CV-N: K3R, K48R, K74R (**51**).

4.4.1 CV-N: K3R, K48R, K74R-F-150 Conjugate (**60**)

The doubly-substituted fluorescent conjugate (**60**, Figure **4.16**) was selected as the initial target.

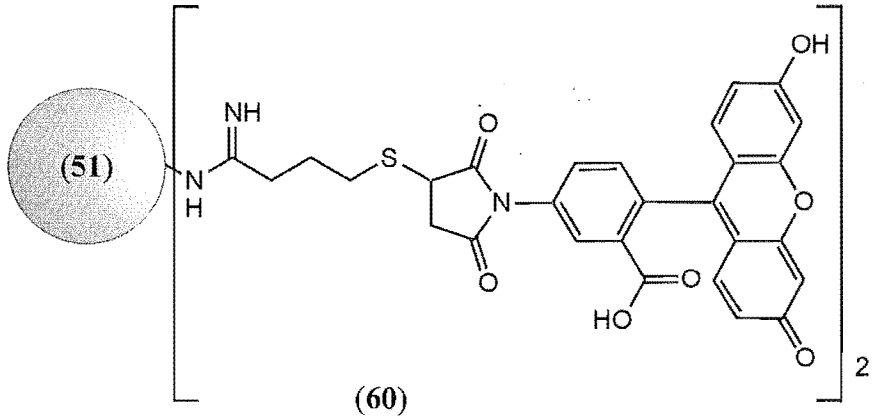

(**60**)

Figure 4.16: *CV-N: K3R, K48R, K74R-F-150 Conjugate.*

CV-N: K3R, K84R, K74R (200 μg) was thiolated with 2-IT (**28**, 35 equivalents) in reaction buffer for 12 hours at 0°C. Like after most previous thiolation reactions, the reaction mixture was chromatographed on a G-25 column. The protein component eluted at 20 minutes and this solution was reacted directly with F-150 (**46**, four equivalents in minimal DMF) for five hours. The sample was concentrated and purified on a further

size-exclusion column, this time eluting with distilled water. The fluorescent yellow band that eluted at ~20 minutes was collected and analysed by LC MS (Micromass/Waters, Zorbax-C3, standard protein LC MS gradient).

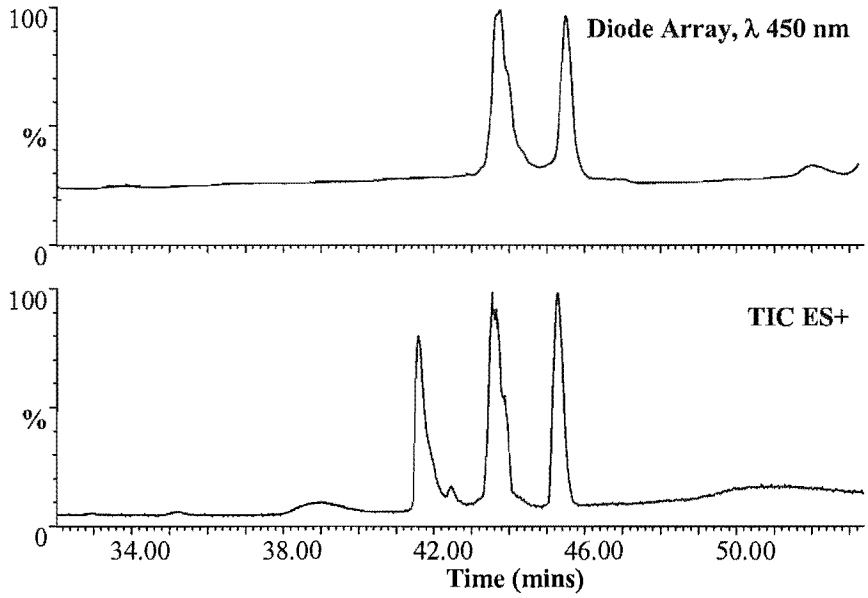

Figure 4.17: *Expansion of a section of the chromatogram of the preparation of CV-N:K3R, K48R, K74R-F-150 conjugate (**60**). Diode Array trace at λ 450 nm, and Total Ion Current (TIC) ES+ trace.*

The spectrum max diode array, and the TIC chromatogram (Figure **4.17**) showed three peaks, eluting at 41.7 minutes, 43.4 minutes and 45.4 minutes. The second and third peaks appeared to be tagged with F-150 as they absorbed at 450 nm in the diode array. Analysis of the TIC data showed that unreacted protein (11,119 Da) was eluting at 41.7 minutes and that **60** (12,149 Da) was eluting at 45.4 minutes (Figure **4.18**). The compound eluting at 43.4 minutes was a singly-derivatised CV-N: K3R, K84R, K74R.

Better product ratios were never achieved. However, purification of the doubly-substituted conjugate (**60**) was possible with collection of the desired peak after HPLC separation using the standard protein LC MS gradient. The mass spectrometer was used as a guide of retention time, with a 1:9 split of sample to the mass spectrometer and the collection vial.

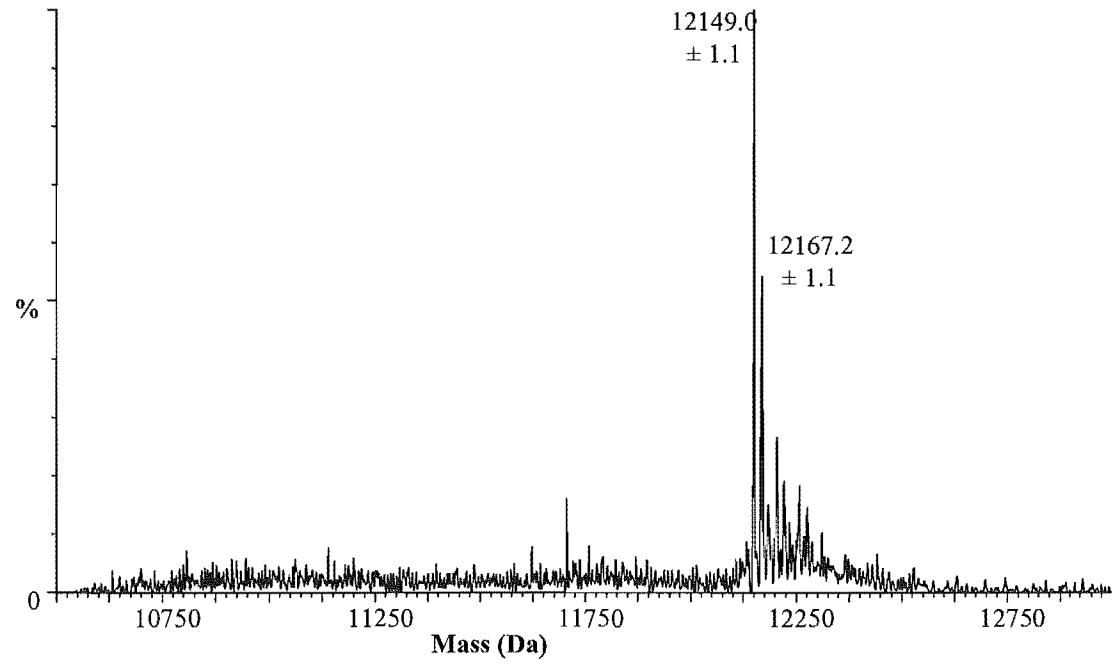

Figure 4.18: *ESI deconvoluted spectrum of CV-N: K3R, K48R, K74R-F-150 conjugate (**60**).*

4.4.2 CV-N: K3R, K48R, K74R-norhomohalichondrin B (**61**)

The final goal of this section of work was to create the doubly-substituted norhomohalichondrin B conjugate of CV-N (**61**), illustrated in Figure **4.19**.

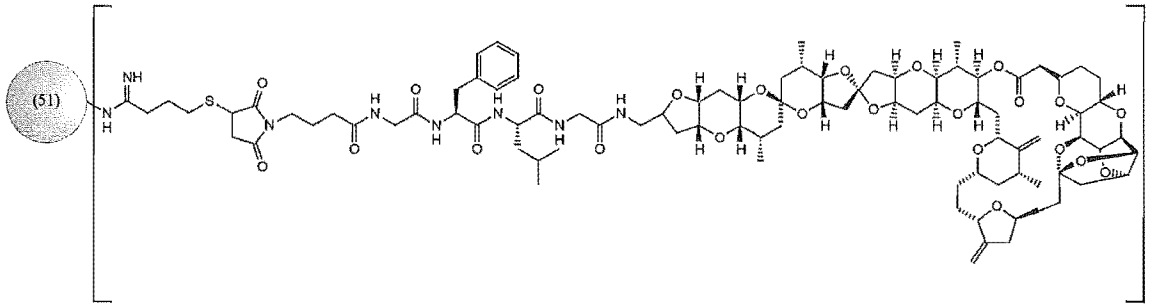

(61)

Figure 4.19: *CV-N: K3R, K48R, K74R-norhomohalichondrin B Conjugate.*

CV-N: K3R, K84R, K74R (200 μg) was thiolated with 2-IT (**28**, 35 equivalents) in reaction buffer, for 12 hours at 0°C. The reaction mixture was purified on a G-25 column. The protein component eluted from the column at 20 minutes and this solution was reacted directly with γ-maleimidobutyric-Gly-Phe-Leu-Gly-norhomohalichondrin B (**32**, four equivalents in minimal DMF) for ten hours. The sample was concentrated, and then

purified on a further size-exclusion column with distilled water as the eluant. A peak absorbing at λ 206 nm was detected at ~20 minutes and this was collected and analysed by LC MS (Micromass/Waters, Zorbax-C3). Figure **4.20** presents the TIC chromatogram of the protein fraction. The halichondrin family of compounds are unstable in acid conditions, so for this reason LC MS analysis was attempted without an acid additive. It was found, however, that formic acid (0.1%), was required to achieve good chromatography.

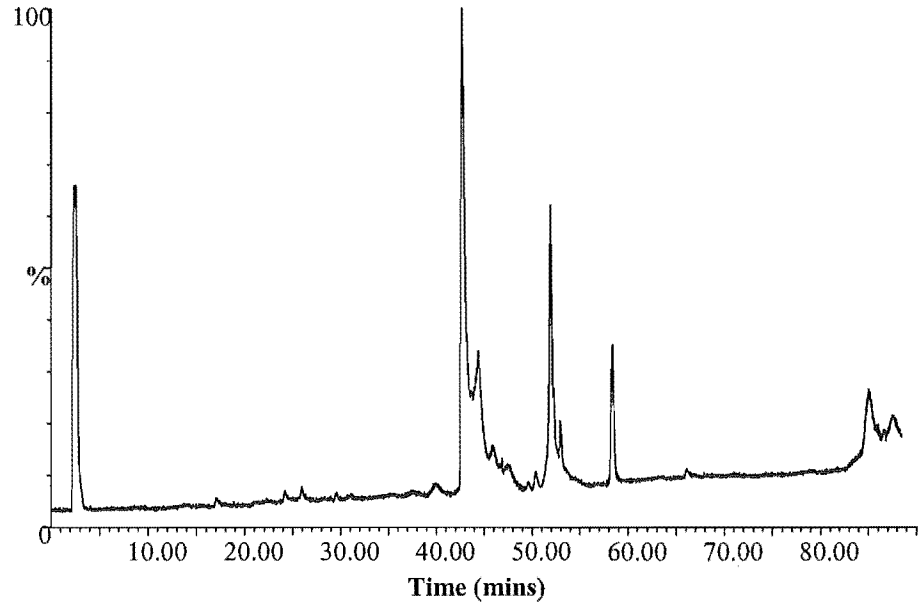

Figure 4.20: *Total Ion Current chromatogram of the preparation of CV-N: K3R, K48R, K74R-norhomohalichondrin B Conjugate* ***(61)****.*

Figure **4.20** shows the TIC chromatogram of the LC MS analysis. MaxEnt deconvolution of the ESI MS data of each peak revealed that the desired conjugate, (**61**, 14,557 Da) was eluting at 58.5 minutes (Figure **4.21**). This product was accompanied by two further products, 14,574 Da, and 14,593 Da, which demonstrate one and two, hydrolysed succinimides, respectively.

A singly-derivatised norhomohalichondrin B conjugate of CV-N: K3R, K48R, K74R (12 723 Da) was seen to be eluting ~52 minutes. It was followed by a closely eluting derivative (12,807 Da) that showed a second addition of 2-IT (**29**) that had cyclised into the unreactive 'dead end' by-product. Unreacted protein (11,092 Da) and protein showing addition of the thiolation by-product (11,176 Da and 11,260 Da) were present at 43.1 minutes and 44.2 minutes respectively.

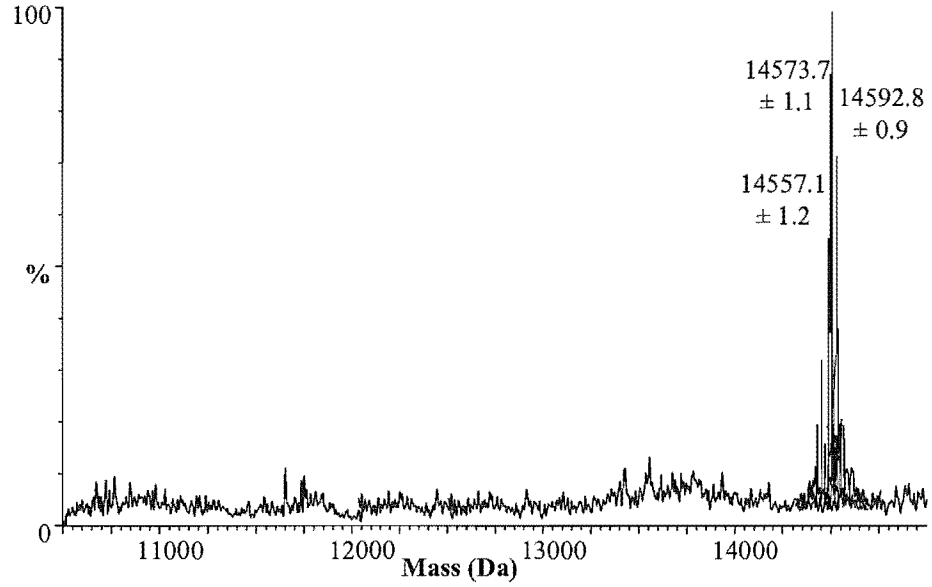

Figure 4.21: *Neutral-scale deconvoluted mass spectrum of the purified CV-N: K3R, K48R, K74R-norhomohalichondrin B conjugate (**61**).*

The conjugate, **61**, was purified from the other protein components using the standard protein LC MS gradient in the same manner as described in Section **4.4.1**. As Figure **4.20** illustrates, good chromatographic separation is achieved between the various components with this method. The collected fraction was taken to dryness immediately and reanalysis by LC MS confirmed that the halichondrin component had not degraded in the purification steps. The conjugate sample has not been quantified.

The purified CV-N: K3R, K48R, K74R-norhomohalichondrin B conjugate (**61**) has been submitted for biological testing to assess its cytotoxicity, and its binding affinity to gp120.

4.5 Conclusions

Two recombinantly produced mutant CV-N proteins, CV-N: K3R, K48R, K74R (**51**) and CV-N: K3R, K48R, K74R, K84R (**52**), allowed for the production of two selectively modified double- and single-norhomohalichondrin B conjugates of CV-N. Somewhat disappointingly, the production was not high yielding, but both conjugates could be readily purified. The toxin-conjugate preparations presented in this thesis were one off experiments. With a greater availability of the toxin construct, conjugate yield may be optimised in the future. However, the preparation of these conjugates had addressed the problem of being able to produce highly defined and characterised protein products that could be utilised in a therapeutic application.

Doxorubicin proved to be a troublesome drug, with the conjugate degrading rapidly. The instability of this compound raises questions as to the nature of other published drug preparations.

5 HSA CONJUGATES

HSA CONJUGATES

5.1 Introduction

Human serum albumin (HSA) is the most prevalent circulating protein in the bloodstream.[216] Albumin plays numerous important biological roles, including involvement in regulating osmotic blood pressure and transporting fatty acids from the liver to tissues.[216] Serum albumin possesses a unique capability to bind, covalently and reversibly, a great number of endogenous and exogenous compounds (for example, bilirubin, the breakdown product of heme, therapeutic drugs such as aspirin, penicillins and sulfonamides, and the metal ions, copper(II), nickel(II) and calcium(II)).[119,217] This blood serum protein also serves as an important source of amino acids for cells.[119,216]

HSA is a single-chain protein synthesised and secreted from liver cells. The protein is produced at a rate of approximately 10-12 g daily and exhibits an average half-life of 19 days.[217] HSA has 585 amino acids and has a molecular weight of 66,500 Da.[217] Albumin lacks prosthetic groups and covalently bound carbohydrate and lipid. According to X-ray crystallographic analyses (Figure **5.1**) of HSA, the polypeptide chain forms a heart-shaped protein with approximately 67% α-helix but no β-sheet.[217] All but one (Cys-34) of the 35 cysteine residues are involved in the formation of stabilising disulfide bonds.[144,217,218]

In the middle of last century the first reports appeared in the literature that tumours might be able to trap plasma proteins.[219] In the following 30 years only a small number of investigations addressed the role of albumin in tumour growth.[119] The reason for neglecting the significance of albumin for tumour proliferation and metabolism may be due to a reluctance to believe that such an abundant protein should show a selective uptake in tumour tissue. Matsumura and Maeda coined the expression "EPR" (Section **1.5**) in 1989 after they studied the uptake of macromolecules, including serum albumin, by mouse tumours.[220] Since that time, an increasing number of distribution studies concerning the uptake of labeled albumin in animal tumours have appeared in the

literature.[119,130] These studies showed that between 3-25% of the applied dose was found in the tumour.[119] In contrast to the EPR effect as an explanation for the accumulation of HSA in tumours, Stehle *et al.* have also proposed that plasma proteins such as albumin are major energy and nutrition sources for tumour growth. With the increased metabolism and proliferation of cancer cells, this could explain the high rate of serum albumin turnover in tumours.[119,216]

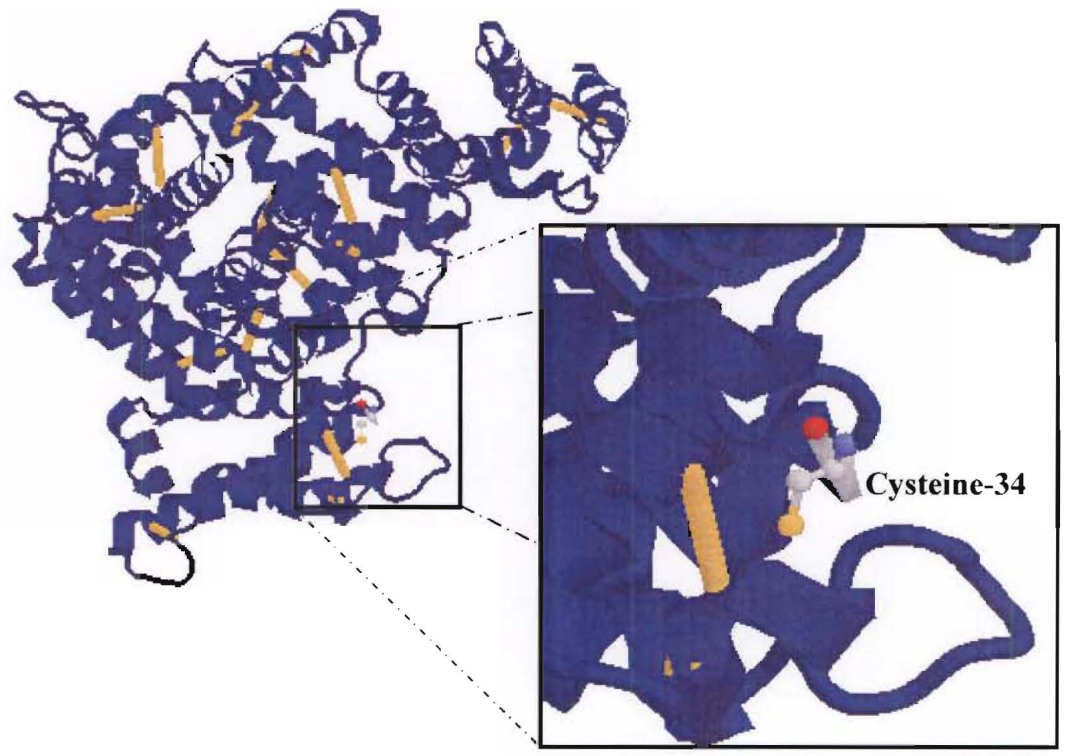

Figure 5.1: *Crystal structure of human serum albumin. Cysteine-34 is shown in ball and stick representation (inset). The disulfide bonds are highlighted in yellow. The diagram was produced with Protein Explorer from the RCSB PDB, entry 1AO6.*

The preferential uptake of HSA in tumour tissue, the good biological stability of the protein, and its non-toxic, non-immunogenic nature, has provoked the development of a number of HSA conjugates. The anthracyclines, doxorubicin[210,221] and daunorubicin,[222] the folate antagonist methotrexate,[223] and further anti-cancer agents such as camptothecin[224] and chlorambucil[134] have been conjugated to HSA *via* a number of methods. Many of these conjugates have shown high anti-tumour activity in *in vitro* and *in vivo* models. These conjugates also demonstrated a prolonged half-life of the drug in the plasma, and increased water solubility of the cytotoxin.[134]

Of particular relevance to this project was the development of albumin conjugates of the anti-cancer drug chlorambucil.[134] Maleimido derivatives of chlorambucil were bound to HSA that had been thiolated with 2-iminothiolane. The average number of introduced thiol groups was 3.0.[134] *In vitro* and preliminary *in vivo* studies demonstrated positive anti-tumour efficacy. The conjugates also exhibited an increased serum stability compared to the free chlorambucil.[134]

As discussed and demonstrated in Chapter **2, 3** and **4,** 2-iminothiolane reacts with primary amines. HSA has 59 lysine residues (and therefore 59 ε-amino groups), and allows very little control over the number and distribution of thiol derivatives. This presents difficulties in characterising the resultant conjugates.

Approximately 70% of circulating albumin in the blood stream is mercaptalbumin that contains an accessible free thiol at cysteine-34 (Figure **5.1**) that is not blocked by endogenous sulfhydryl molecules such as cysteine or glutathione.[144,218] Commercially available albumins are a mixture of mercaptalbumin and non-mercaptalbumin, containing approximately 20-60% of the free sulfhydryl compound.[221] The X-ray structure of the protein (PDB entry 1AO6, Figure **5.1**) reveals that cysteine-34 is located in a hydrophobic crevice on the surface of the protein.[144]

Kratz *et al.* have paid considerable attention to developing anti-cancer albumin conjugates that exploit the availability of cysteine-34.[218,221,224] The advantage of these conjugates is that only one product can be formed, and the thiolating step is avoided. Maleimido derivatives of doxorubicin have been synthesised and coupled to exogenous serum albumin through cysteine-34.[221] Several of these conjugates demonstrate anti-proliferative activity in *in vitro* studies.

To avoid the *ex vivo* synthesis and characterisation of drug albumin conjugates, Kratz *et al.* have also proposed the use of *in situ* binding of a maleimido-derivatised drug to the cysteine-34 position of circulating albumin after intravenous administration.[144,218,224] An acid-sensitive (maleimidophenylacetyl)hydrazone derivative of doxorubicin bound preferentially and rapidly to cysteine-34 of endogenous albumin and demonstrated superior anti-tumour efficacy in murine renal cell carcinoma compared to doxorubicin.[218]

Similar albumin-binding derivatives of camptothecin have also been produced. These constructs were well tolerated and showed enhanced anti-tumour efficacy when compared to camptothecin.[224]

This chapter describes the synthesis and characterisation of protein conjugates designed to act as anti-cancer therapeutics, by attaching low-molecular-weight cytotoxic compounds to HSA. The target structure is shown schematically in Figure **5.2**. The rationale was that HSA would deliver the drug to cancerous cells. Selective cleavage of the biolinker, within diseased cells, would release the drug and the inherent cytoxicity.

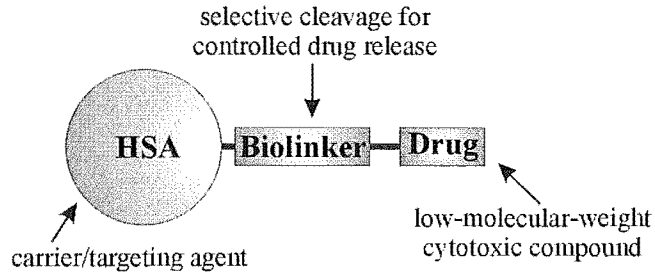

Figure 5.2: *Schematic of a human serum albumin conjugate.*

The positive results demonstrated by Kratz *et al.* encouraged the exploitation of the free thiol at cysteine-34 to create these conjugates. The goal was to take advantage of the maleimido-tetrapeptide derivatives of homohalichondrin B (**32**), doxorubicin (**35**), and tyrosinamide (**37**), prepared in Chapter **2**, to selectively bind to the cysteine-34 position of exogenous human serum albumin (Figure **5.3**)

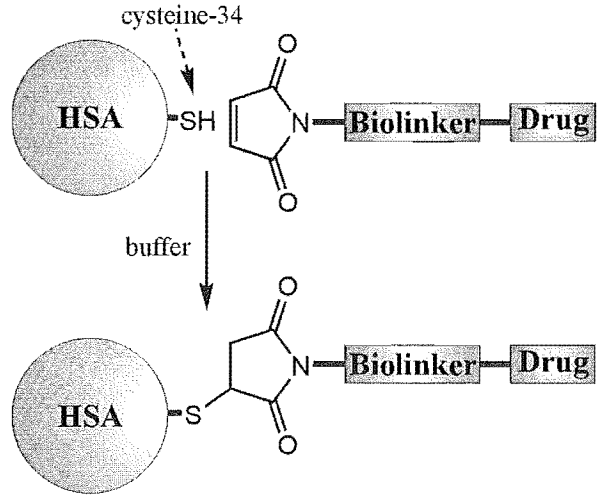

Figure 5.3: *Preparation of a human serum albumin conjugate – utilising HSA-cysteine-34 and a maleimido activated drug derivative.*

5.2 LC MS of HSA

The characterisation of the HSA conjugates generated in this project depended solely on LC MS analysis. Human serum albumin, at 66,500 Da, is a considerably larger protein than lysozyme or cyanovirin-N (**28**). Because of the greater molecular weight, the ESI-mass spectrum of HSA is more complex. A larger series of peaks are observed representing a greater number of charge states.

Initial analyses of HSA proved difficult to decipher. Direct injection of analyte, or the coupling of a LC system employing a short solvent gradient method (Zorbax 300SB-C3, 20-50% CH_3CN/H_2O (0.5% formic acid) over 15 minutes) to the mass spectrometer, generated a low-intensity, poorly resolved series of peaks such as the spectrum presented in Figure **5.4**.

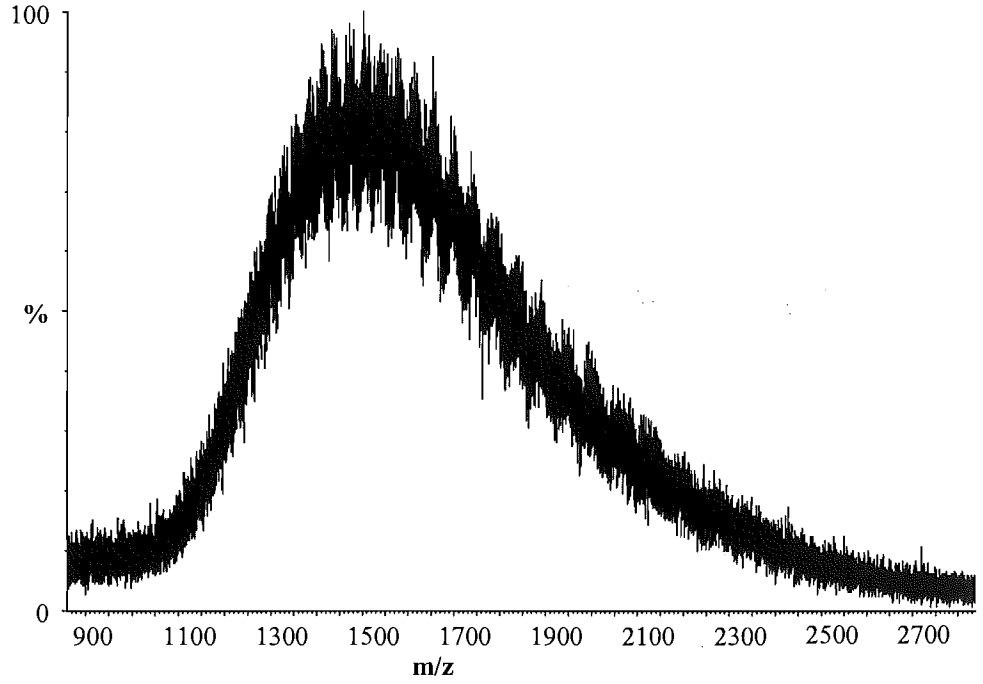

Figure 5.4: *A low intensity, poorly resolved ESI-mass spectrum of HSA.*

As discussed in Chapter **2.8.1**, impurities and buffer-related cations inherently cause a reduction in the mass spectral response of a protein. With the large number of charge states possible for HSA, the cation effect was such that the resultant spectra were impossible to interpret. For this reason it was essential to desalt the protein from any storage or reaction buffers before ESI analysis. Online coupling of the mass spectrometer

to an HPLC, running a long gentle solvent gradient system, served to both desalt/purify and separate the analytes. The gradient comprised of a 105 minute run with a flow rate of 200 μL/min, and consisted of the following solvent gradient timetable: a slow gradient from 0% - 60% CH_3CN/H_2O (0.5% formic acid) over 80 minutes to free the protein of any salts, followed by ramp in concentration to 100% CH_3CN over five minutes, an isocratic hold on 100% CH_3CN for five minutes and then a restoration to 0% CH_3CN over five minutes. The method was finished with an isocratic hold on 0% CH_3CN over five minutes (Zorbax 300SB-C3). A broad peak eluted at ~47-51 minutes. This peak represented a well-resolved, decipherable mass spectrum of HSA, presented in Figure **5.5**. An organic modifier, formic acid (0.5%), or acetic acid (5%), in the solvent system was essential for good spectral results. This method became known as the **standard protein LC MS gradient**.

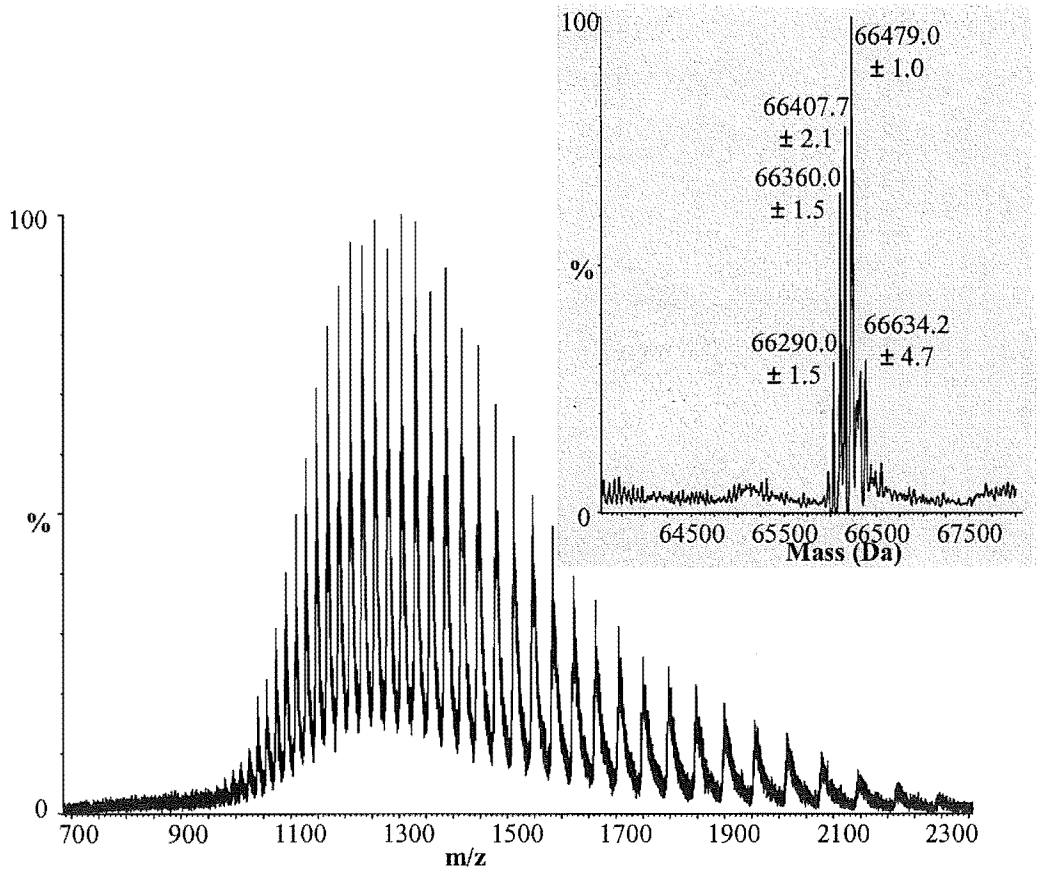

Figure 5.5: *The ESI-mass spectrum of human serum albumin (supplied by Sigma®). The inset shows the deconvoluted, neutral-scale mass spectrum.*

Initial analyses of human serum albumin employed a lyophilised and crystallised form supplied by Sigma®, quoted at being 97-99% pure. Deconvolution of the ESI-mass

spectrum for this supply of HSA (inset, Figure **5.5**) revealed the presence of approximately five protein forms with similar masses to HSA. The principal peak was at 66,479 Da. Some of the components may represent non-mercaptalbumin, with cysteine-34 bound to various thiol-containing compounds, such as cysteine or homocysteine. It was decided not to attempt to eliminate these components by reducing this bond, for fear of reducing some of the 17 stabilising disulfide bonds. This would destroy the advantage of just one free thiol available for reaction. Since approximately 30% of circulating albumin is non-mercaptalbumin, and considering the non-immunogenic, biodegradable, non-toxic nature of HSA,[119] it was believed that the presence of these components would not be a problem in the development of HSA as a drug carrier.

The maleimido fluorescein dye, F150 (**46**), was chosen as a model maleimide. It would test the feasibility of reaction at HSA-cysteine-34 before commitment of the toxin derivatives. Fluorescently-labelled HSA would have the added advantage of being chromatographically distinct by UV profile (and by eye). HSA (Sigma®, 400 μg) was dissolved in a borate buffer (pH 7.2). F-150 (**46**, 5 equivalents, in minimal DMF to aid water solubility) was added and the reaction was left at RT for 24 hours. The reaction mixture was then separated on a size-exclusion (G-25) column with distilled water. Two fluorescent yellow bands eluted off the column, one at the void volume (V_0), suggestive of labelled protein, and the other 15 mL later, suggestive of 'small molecule' unreacted F-150 (**46**). Both fluorescent bands were collected and analysed by LC MS (Agilent, Zorbax, C3) using the standard protein LC MS gradient. The first fraction showed a single broad peak at ~50 minutes with an absorbance at λ 440 nm. HSA is not visible at this wavelength normally. The ESI-mass spectrum of this peak was unable to be deconvoluted with MaxEnt. It appeared that several of the protein components had reacted with F-150, creating a large number of overlapping charge states. An alternative, purer, more homogeneous, supply of HSA needed to be sought. The second fraction off the G-25 column was confirmed to be excess, unreacted F-150.

After consultation with Felix Kratz on the most suitable commercially available form of HSA, a sample, "Dessau", was obtained from Pharma Dessau, FRG. This was a 20% solution of HSA prepared in 16 mM sodium octanoate. This new sample of HSA was analysed by LC MS using the standard protein LC MS gradient. Deconvolution of the

ESI data collected produced the spectrum in Figure **5.6**. This spectrum demonstrated that there were just two main protein components. The principal peak had a mass of 66,445 Da.

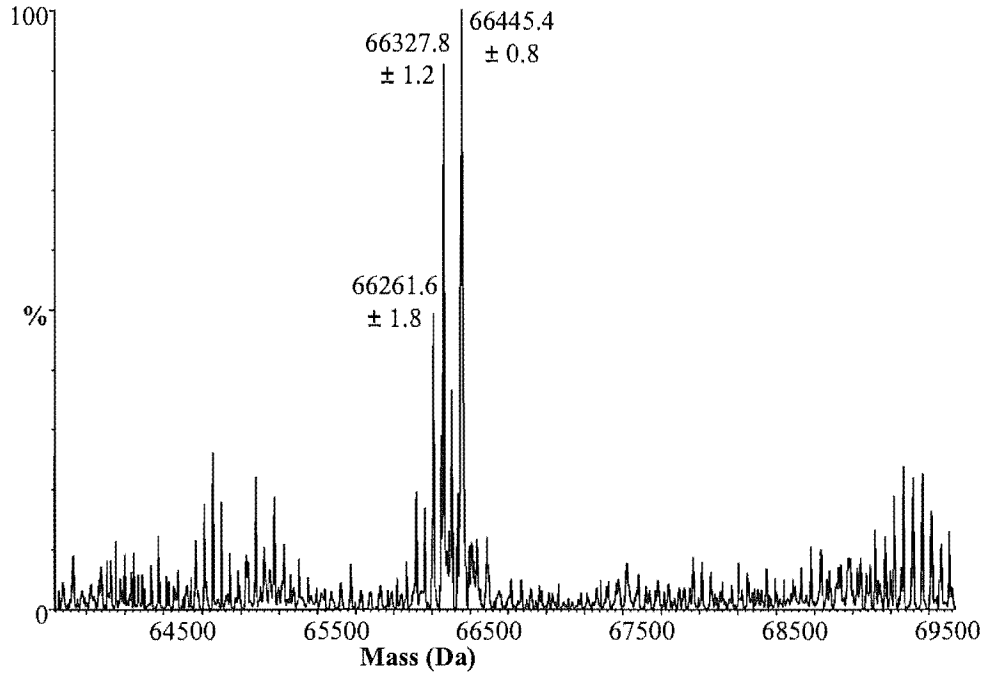

Figure 5.6: *The deconvoluted ESI-mass spectrum of human serum albumin (supplied by Pharma Dessau).*

The HSA supplied by Pharma Dessau was a considerably purer sample than the protein obtained from Sigma®. For this reason "Dessau" was employed for the continuation of the construction of the HSA conjugates. No step was taken to eliminate any non-mercaptalbumin.

5.3 A Model System – HSA-F150 Conjugate (62)

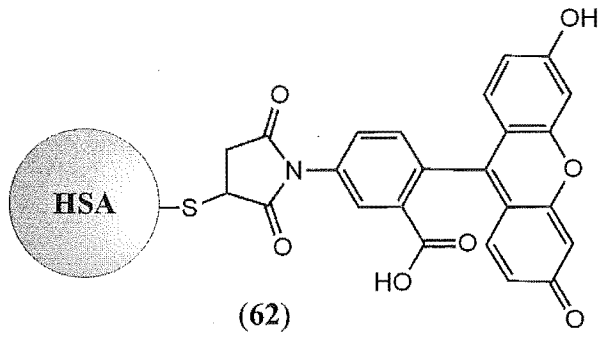

(62)

Figure 5.7: *HSA-F150 conjugate.*

F-150 (**46**) was again chosen as a model maleimide because of its fluorescent properties and the ease of which derivatised protein could be traced. HSA (Pharma Dessau, 400 μg, 60 μL of the commercially prepared solution) was diluted in a borate buffer (pH 7.2). F-150 (**46**, 2 equivalents, in minimal DMF) was added and the reaction was left at RT for 12 hours. At this time the sample was analysed by LC MS using the standard protein LC MS gradient (Figure **5.8**).

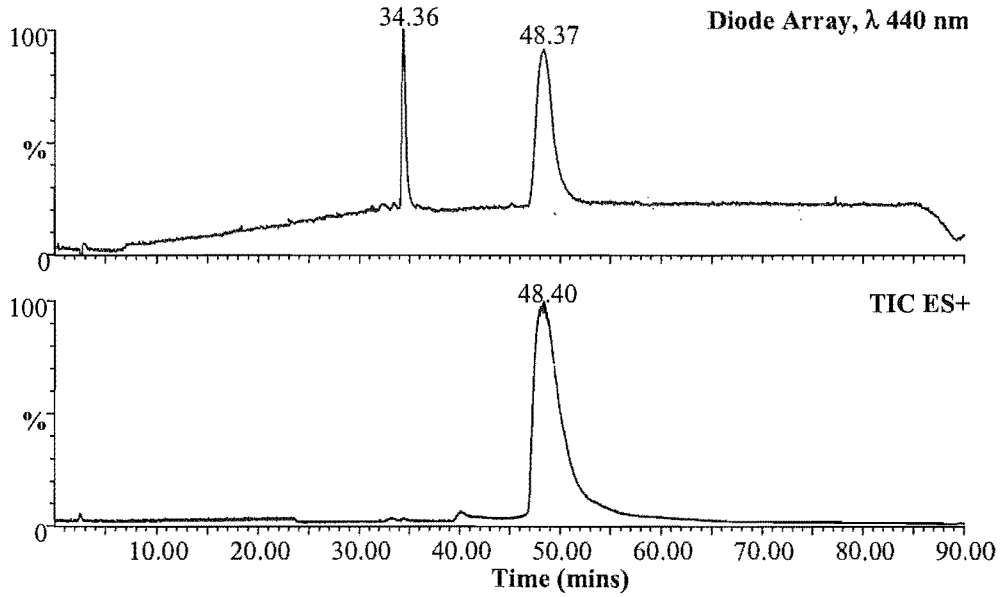

Figure 5.8: *Chromatogram of the preparation of an HSA-F150 conjugate (**62**); Diode Array trace at λ 440 nm and Total Ion Current (TIC) ES+ trace.*

As Figure **5.8** demonstrates, one large broad peak, with a retention time of 47 to 52 minutes, is visible in the TIC spectrum. This peak represents protein, and as evidenced by the analysis at λ 440 nm in the diode array spectrum, has been tagged by F-150 (**46**). The sharp peak at 34.4 minutes, visible at a wavelength of 440 nm, was unreacted F-150 (**46**).

The protein was purified from the excess F-150 (**46**) by passing the sample through a size-exclusion (G-25) column, eluting with distilled water. The fluorescent yellow band eluting at the void volume was collected and reanalysed by reversed phase LC MS to confirm the purity of the sample. This analysis showed one broad peak, with a retention time of 47 to 52 minutes, in both the diode array at λ 440 nm and the TIC spectra. Analysis of the mass spectral data showed that the broad peak encompassed both unreacted albumin (67,572 Da) and the conjugate product **62** (67,008 Da, approximately 50% yield). (Figure **5.9**) Clearly, a mass of approximately 427 (F-150, **46**) had been added onto HSA, but further analysis of the sample was required to confirm the nature of the product.

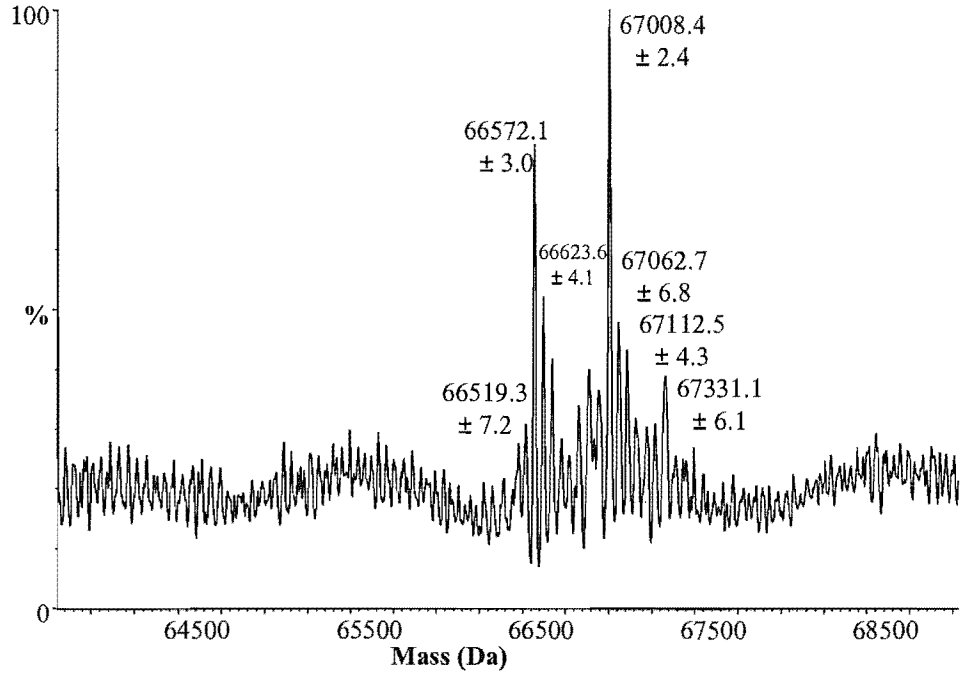

Figure 5.9: *Deconvoluted, neutral-scale mass spectrum of the HSA-F150 Conjugate (**62**).*

HSA presents problems for analysis by mass spectrometry because of the high molecular weight (~66500 Da) and hence the large number of possible charge states. Derivatisation of the protein results in products that are inseparable from unreacted protein. The conjugation of F-150 (**46**) to HSA for example, does not change the polarity of the protein significantly, so the components are unable to be separated by chromatography. The problem is compounded when there are several protein forms already present in the sample. The charge state peaks in the m/z spectra become very broad and overlap, creating difficulties in resolving the charge distributions of the compounds present. Further, a small shift in the calibration of the m/z data, results in a significant shift of the

absolute molecular weight determined in the deconvoluted spectrum. For example, a shift of 0.5 on the m/z scale at the 53rd charge state will result in a mass difference in the deconvoluted spectra of approximately 25 Da.

A tryptic digest was performed on the sample containing **62** to confirm that F-150 (**46**) had tagged HSA and to confirm the expected site of derivatisation. Conjugate **62** (100 μg) was taken up in ammonium bicarbonate buffer (10 mM, pH 8). TPCK treated trypsin (10% by weight to analyte protein) was added in 1% acetic acid. The digest was left at 37°C for 24 hours and assessed by a reverse phase LC MS system running the standard protein LC MS gradient (Figure **5.10**). A small amount of dithiothreitol (DTT) was added to the sample, just before analysis, to break any disulfides that might be binding two fragments together.

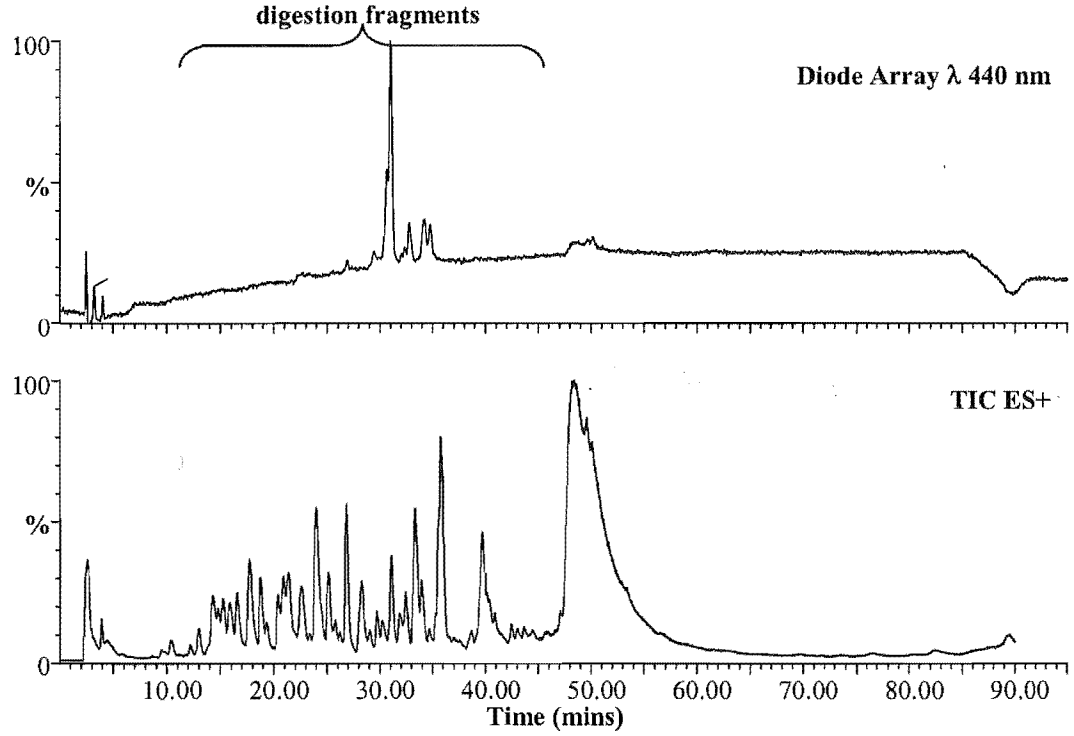

Figure 5.10: *Tryptic digest of HSA-F-150 Conjugate (62); Diode Array trace at λ 440 nm and Total Ion Current (TIC) ES+ trace.*

Analysis of a tryptic digest of HSA is not trivial. According to the peptide and protein software set up by Lewis Pannell,[200] there are 3,569 possible tryptic fragments, and over 20,000 possible enzymatic cuts if one takes chymotryptic activity into account. To simplify the analysis of the tryptic digest of **62**, only those peaks representing fragments that were visible at 440 nm (and hence likely to have been derivatised by F-150 (**46**))

were processed (Figure **5.10**). Table **5.1** shows the data collected for this selection of peaks. In each case the fragment masses identified at each retention time (experimental MW) were converted to a calculated MW without F-150 (**46**) attached. A further 18 mass units were subtracted from these fragments to generate a second series of possible fragments. An increase of 18 mass units had been seen in the case of the CV-N conjugates. This was attributed to hydrolysis of the succinimide ring of the biolinker, and the assumption was made that this could also be occurring in the case of these HSA conjugates. The two generated series of calculated molecular weights were compared against the predicted digest fragments. Of the possible digest fragments (as determined by the peptide and protein software[200] and with the assumption that the amino acid sequence of the employed Pharma Dessau HSA sample matched the sequence in the database), only those containing cysteine-34 were searched for mass matches. Therefore, this does not discount derivatisation at another site in the protein.

Retention Time (mins)	Experimental MW (Da)	Calculated MW (Da) Without F-150	Calculated MW (Da) Without H_2O	Tryptic/Chymotryptic Cleavage Sites and Fragments
26.84	1640.0	1212.6	1194.6	
	1174.6	747.2	729.2	
	1080.7	653.3	635.3	
	1051.4	624.1	606.1	
29.72	2163.1	1735.8	1717.8	
	801.5	374.1	356.1	
31.09	1854.0	1426.6	1408.6	1428.7 Da, peptide from 25 to 36. (L)I . . . . F(E)
	1609.8	1182.5	1164.5	
31.85	1600.4	1173.0	1155.0	
	1536.9	1109.5	1091.5	
32.42	2609.9	2182.5	2164.5	2162.4 Da, peptide from 32 to 49. (L)Q . . . . F(A)
	2273.9	1846.5	1828.5	1825.2 Da, peptide from 21 to 36. (K)A . . . . F(E)
33.34	1874.4	1447.0	1429.0	1428.7 Da, peptide from 25 to 36. (L)I . . . . F(E)
	1341.4	914.0	896.0	
	851.5	424.1	406.1	
33.94	2722.1	2294.8	2276.8	
	3405.1	2977.8	2959.8	
34.74	2151.6	1724.3	1706.3	
	1472.2	1044.8	1026.8	
	742.4	315.0	297.0	

Table 5.1: *Selected ESI-MS data from LC MS of tryptic digest of HSA-F-150 (**62**). MW = molecular weight*

A match was made if the calculated MW was within ±0.2% of the predicted MW. There are four possible peptide matches, which contain the cysteine-34 residue, for the fragments seen.

5.4 HSA-norhomohalichondrin B Conjugate (63)

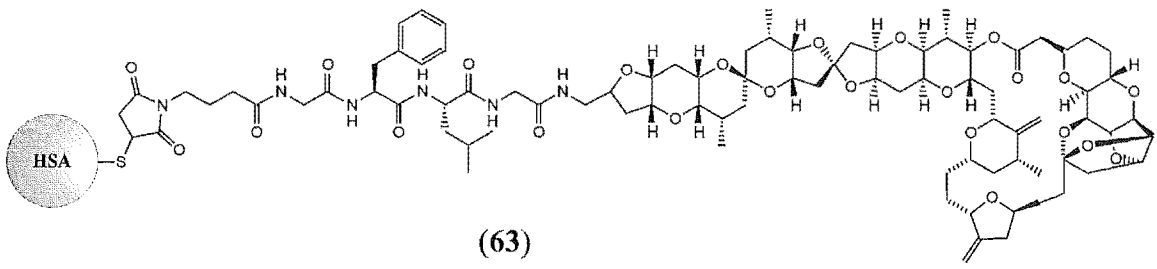

(63)

Figure 5.11: *HSA-norhomohalichondrin B Conjugate.*

HSA (Pharma Dessau, 200 μg) was dissolved in borate buffer (pH 7.2) and reacted with two equivalents of γ-maleimidobutyric-Gly-Phe-Leu-Gly-norhomohalichondrin B (**32**, Section **2.4.1**, in a minimal volume of DMF) for three days. The protein component was separated from excess **32** by passing the sample through a G-25 size exclusion column. Unlike in the case of F-150, the derivatised protein could not be tracked by fluorescence, so a single beam UV detector set at λ 206 nm was used to monitor the column. The peak that eluted at the void volume was collected and analysed by LC MS. This analysis showed a single broad peak, at a retention time of 47-51 minutes, in both the spectrum max diode array and TIC traces. Figure **5.12** shows the ESI-mass spectrum of this peak. On an initial glance at the spectrum it does not appear that any conjugation has taken place. This is because the addition of 1,631 Da (**32**) to HSA shifts the charge envelope up so that the product charge states almost overlap completely with those of unreacted albumin. However, at the 47^{th} charge state, for example, the product is separated from unreacted HSA by approximately 4 Da on the m/z scale. An expansion of several charge state peaks shows this fine detail (inset, Figure **5.12**). The 46^{th} and 47^{th} charge states of component A (unreacted HSA) are shown to almost overlap the 47^{th} and 48^{th} charge states of component B (conjugate product, **63**).

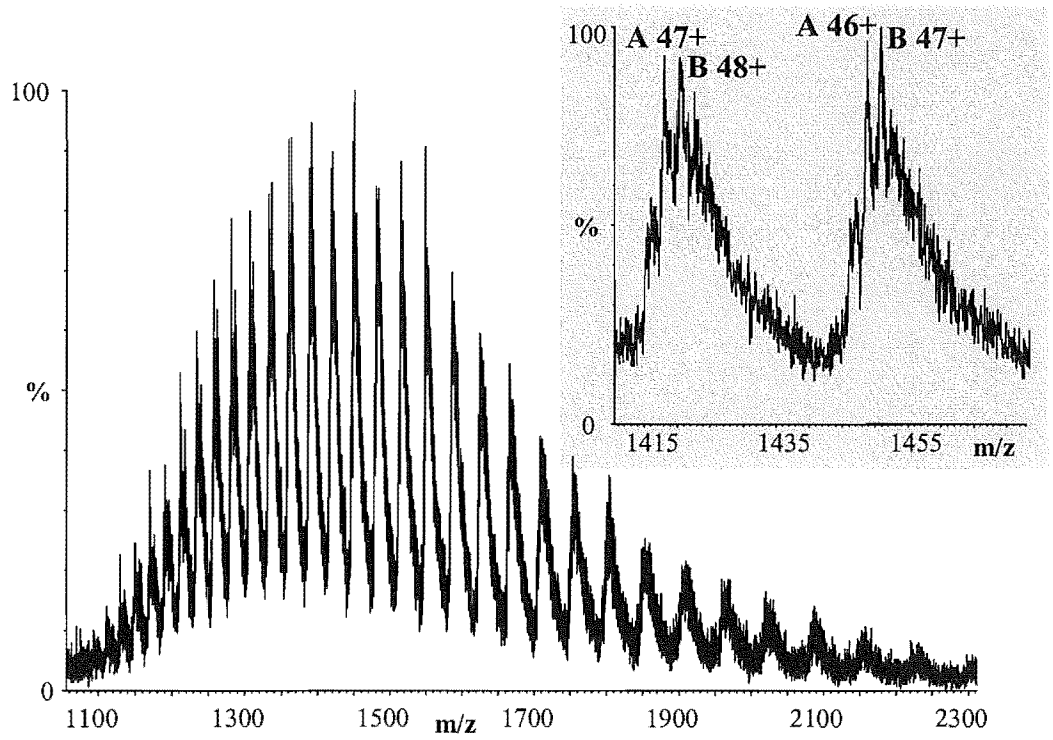

Figure 5.12: *The ESI-mass spectrum of the HSA-norhomohalichondrin B conjugate* ***(63)****. The inset shows an expansion of the 46th and 47th charge states of component A (unreacted HSA), and the 47th and 48th charge states of component B (conjugate product,* ***63****).*

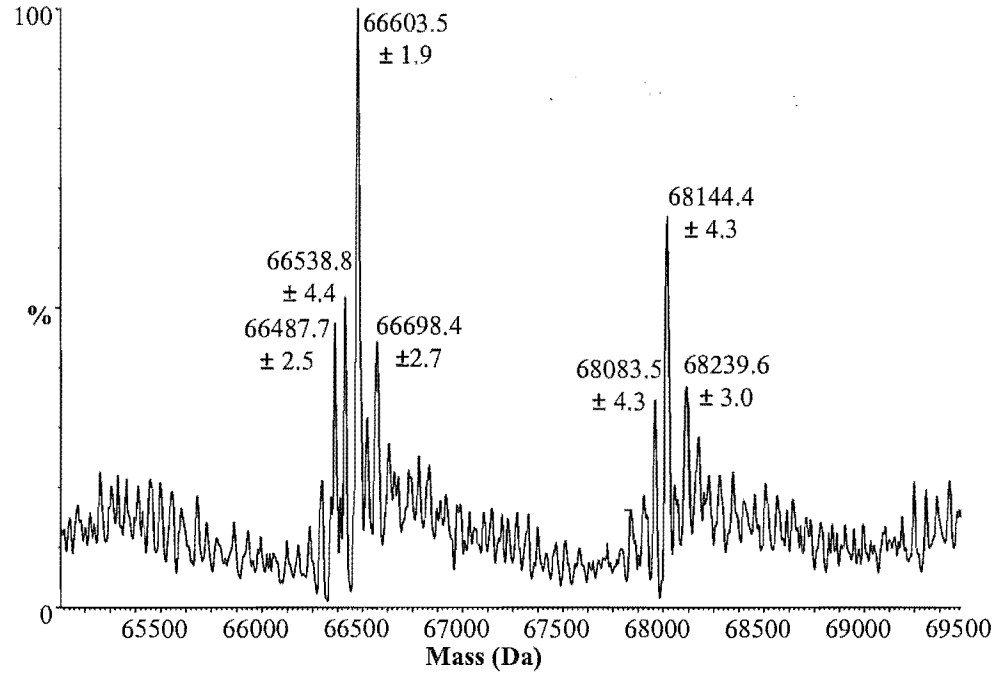

Figure 5.13: *Deconvoluted, neutral-scale mass spectrum of the HSA-norhomohalichondrin B conjugate* ***(63)****.*

Deconvolution of the mass spectral data with MaxEnt confirms that the broad peak in the LC MS trace encompassed both unreacted albumin and the conjugate product (**63**, 68,144 Da, approximately 33% yield). (Figure **5.13**) It is believed that the unreacted albumin is nor-mercaptalbumin, with the cysteine-34 blocked by thiol containing compounds. This sample was not purified further; LC MS demonstrated only protein was present, and that these components could not be chromatographically separated.

This conjugate (**63**) was not digested by trypsin because of the limited supply of homohalichondrin B, and the requirement to submit the conjugate for biological assay. For anti-cancer biological assay results of **63**, see Chapter **6**.

5.5 HSA-doxorubicin Conjugate (64)

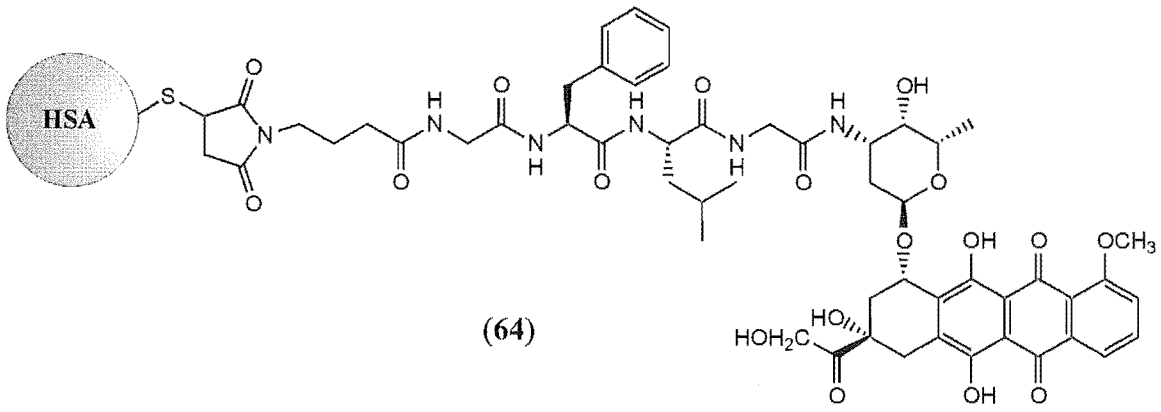

Figure 5.14: *HSA-doxorubicin conjugate.*

HSA (Pharma Dessau, 200 μg) was dissolved in borate buffer (pH 7.2) and reacted with two equivalents of γ-maleimidobutyric-Gly-Phe-Leu-Gly-doxorubicin (**35**, Section **2.4.2**, in minimal DMF) for 24 hours. The protein component was then separated from excess **35** by passing the reaction mixture down a G-25 size-exclusion column with distilled water. The pink fraction that eluted at the void volume was collected and analysed by LC MS.

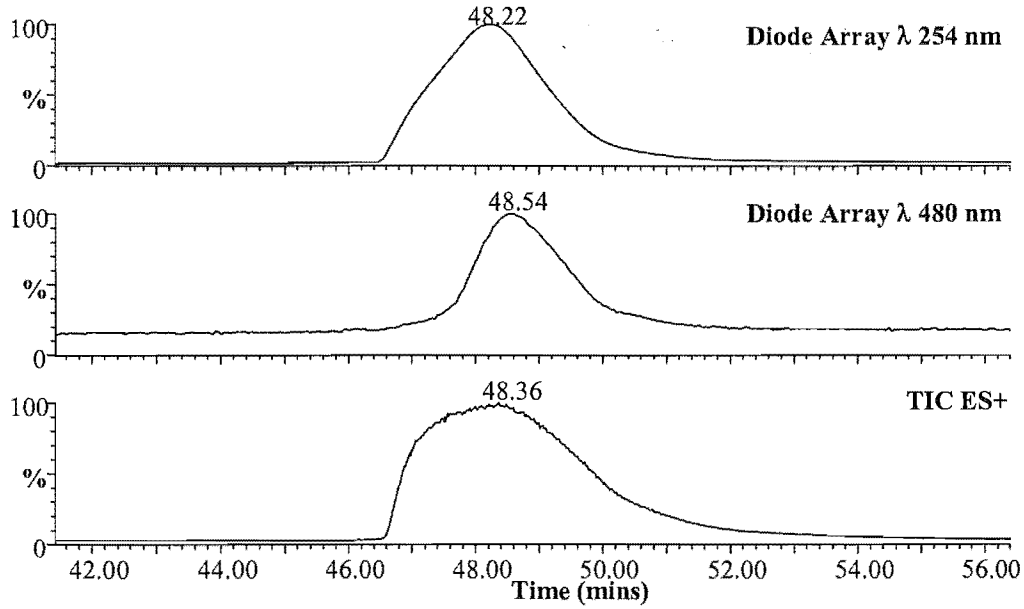

Figure 5.15: *Expansion of a section of the chromatogram of the preparation of an HSA-doxorubicin conjugate (**64**); Diode Array trace at λ 254 nm, Diode Array trace at λ 480 nm and Total Ion Current (TIC) ES+ trace.*

This analysis (Figure **5.15**) showed one broad peak, with a retention time of 47 to 52 minutes, in both the diode array at λ 254 nm and TIC spectra. Analysis at λ 480 nm also presents a peak at this retention time, evidence that **35** had tagged HSA. HSA is not visible at this wavelength normally. Closer examination of this peak at λ 480 nm demonstrated that the conjugate product was concentrated in the latter half of the total protein peak.

Unlike with the HSA-norhomohalichondrin B conjugate (**64**), the ESI-mass spectrum of the protein fraction of the doxorubicin conjugation quite clearly showed two series of charge state peaks. These two series of peaks have been highlighted in Figure **5.16**.

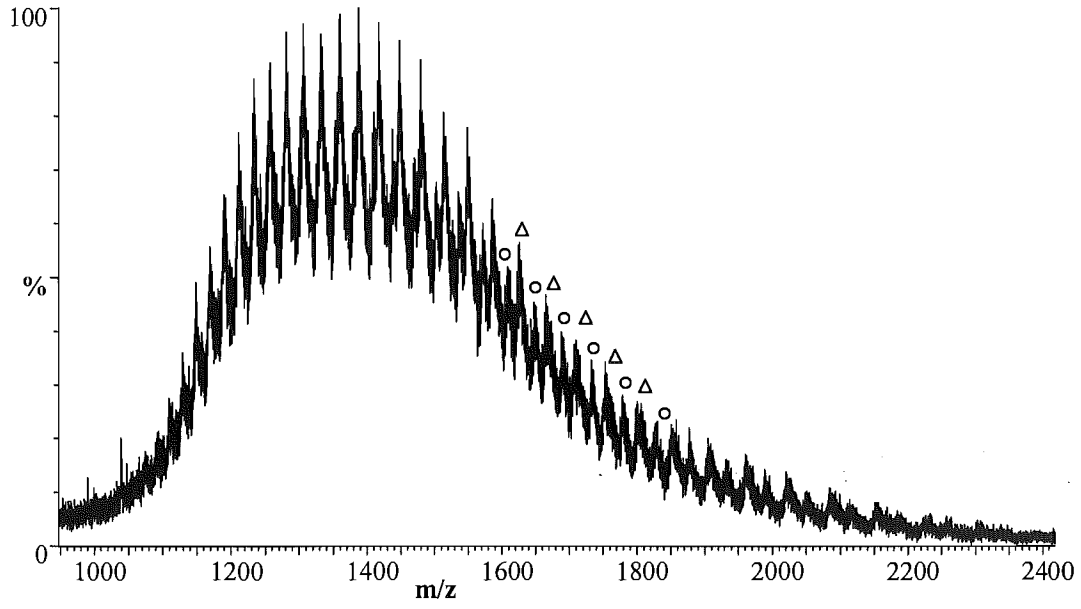

Figure 5.16: *The ESI-mass spectrum of the HSA-doxorubicin conjugate (64). A section of charge states is highlighted, series 1: circles, and series 2: triangles.*

Analysis of the mass spectral data showed that the broad peak encompassed both unreacted albumin and the conjugate product (**64**) (67,531 Da, approximately 25% yield). (Figure **5.17**) Disappointingly, however, the peak also encompassed a degradation product (67,115 Da). This product represented the loss of the anthracycline portion (**56**) of doxorubicin from the conjugate (as discussed in Chapter **4**). A small sample of this protein mixture was left at room temperature in distilled water for 48 hours. Within this period the conjugate had completely degraded to the product mentioned above.

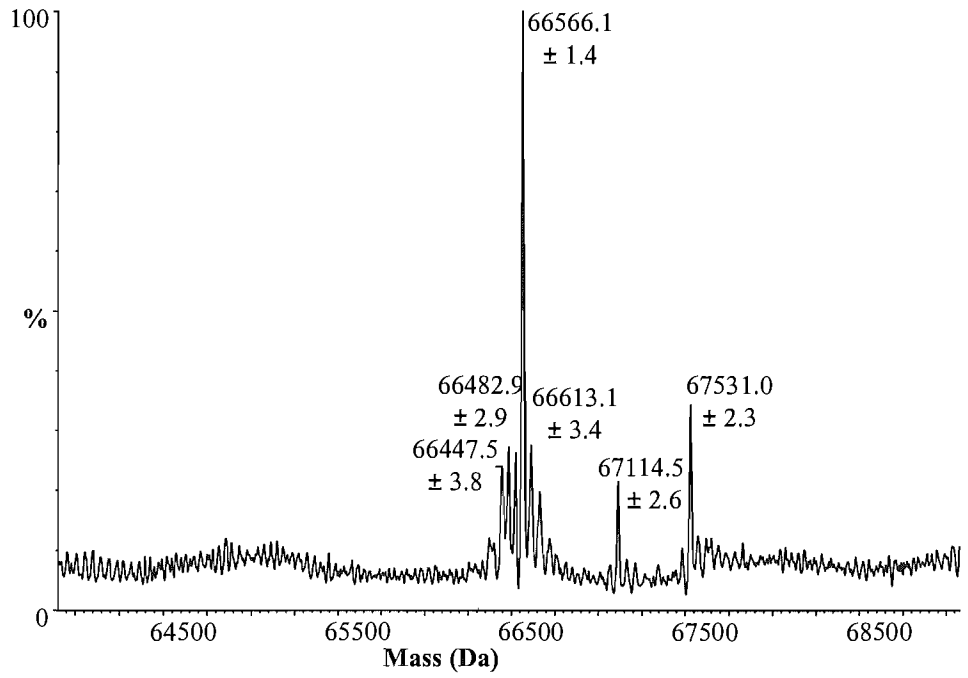

Figure 5.17: *Deconvoluted, neutral-scale mass spectrum of the HSA-doxorubicin conjugate (**64**)*

Due to the problems of degradation, conjugate **64** was kept dry, and in the dark, until further analysis and biological assays could be completed. No further purification steps were taken, for unlike the CV-N conjugate (**55**), this HSA conjugate could not be separated from unreacted protein. This minimised handling, and would hopefully extend the half-life of the protein conjugate.

A tryptic digest was performed on the sample containing **64** to confirm that γ-maleimidobutyric-Gly-Phe-Leu-Gly-doxorubicin (**35**) had indeed tagged HSA, and that derivatisation had occurred at cysteine-34. The enzymatic digest was performed in a similar fashion to the previous digests, but in this case analysis took place after just 12 hours of reaction time. It was hoped, optimistically, that a fraction of the doxorubicin in the sample remained intact, and that peptide fragments could be found bound to **35**.

Figure **5.18** shows the analysis of the digest by LC MS using the standard protein LC MS gradient. To simplify the analysis of the tryptic digest of **64**, only those peaks representing fragments that were visible at λ 480 nm (and hence likely to be derivatised by **35**) were processed.

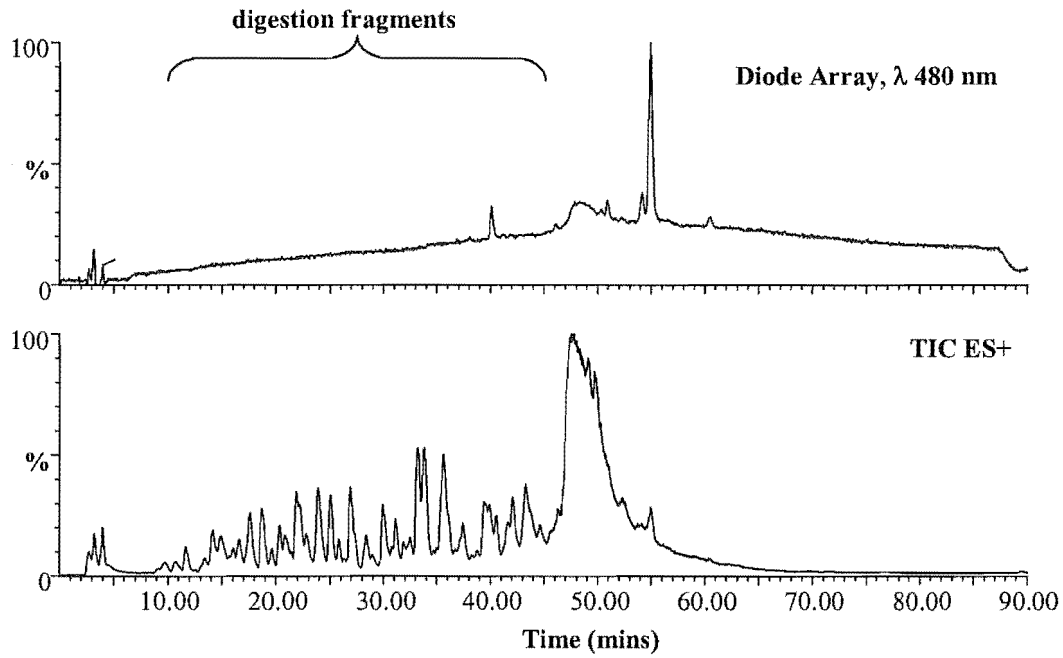

Figure 5.18: *Tryptic digest of the HSA-doxorubicin conjugate (**64**); Diode Array trace at λ 480 nm and Total Ion Current (TIC) ES+ trace.*

Table **5.2** shows the data collected from this selection of peaks. In each case the fragment masses identified at each retention time (experimental MW) were converted to a calculated MW without **35** (Dox) attached. A further 18 mass units were subtracted from these fragments to generate a second series of possible fragments, for the reasons discussed in Section **5.3**. The two generated series of calculated molecular weights were compared to the predicted digest fragments.[200] Of the possible digest fragments, only those containing cysteine-34 were searched for mass matches. As before, this does not discount derivatisation at another site in the protein.

A match was made if the calculated MW was within ±0.2% of the predicted MW. There are three possible peptide matches, which contain the cysteine-34 residue, for the fragments seen.

Retention Time (mins)	Experimental MW (Da)	Calculated MW (Da) Without Dox	Calculated MW (Da) Without H_2O	Tryptic/Chymotryptic Cleavage Sites and Fragments
39.42	2917.6	1835.2	1817.2	1819.1 Da, peptide from 28 to 42. (F)A . . . . L(V)
	3363.1	2280.7	2262.7	
39.93	2508.4	1426.0	1408.0	1428.7 Da, peptide from 25 to 36. (L)I . . . . F(E)
	2542.5	1460.1	1442.1	
	3893.5	2811.1	2793.1	
40.56	4047.7	2965.3	2947.3	
44.64	3543.6	2461.2	2443.2	
46.26	6622.0	5539.6	5521.6	
	6992.0	5909.6	5891.6	
47.76	2433.2	1350.8	1332.8	
	2559.2	1476.8	1458.8	1456.7 Da, peptide from 31 to 42. (Y)L . . . . L(V)
49.11	2403.8	1321.4	1303.4	
49.71	9125.9	8043.5	8025.5	
50.56	9126.0	8043.6	8025.6	
54.12	11389.0	10306.6	10288.6	
54.95	3102.9	2020.5	2002.5	

Table 5.2: *Selected ESI-MS data from LC MS of the tryptic digest of the HSA-doxorubicin conjugate* ***(64)****, Dox = γ-maleimidobutyric-Gly-Phe-Leu-Gly-doxorubicin* ***(35)****, MW = molecular weight.*

The biological assay results for **64** are discussed in Chapter **6**.

5.6 HSA-tyrosinamide Conjugate (65)

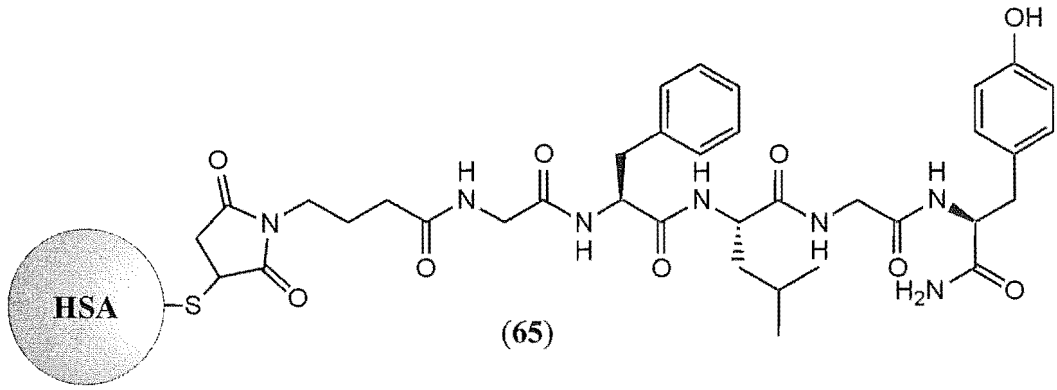

Figure 5.19: *HSA-tyrosinamide Conjugate.*

HSA (200 μg, Pharma Dessau) was combined with two equivalents of γ-maleimidobutyric-Gly-Phe-Leu-Gly-tyrosinamide (**37**, Section **2.4.3**, in minimal DMF to aid solubility) in a borate buffer (pH 7.2). After 24 hours at room temperature, the reaction mixture was placed on a G-25 column. This column was eluted with distilled water and detection was with a diode array detector set at 206 nm. This wavelength was selected as the tyrosinamide construct lacked a distinctive UV absorbance, like that in the case of F-150 (**46**) and doxorubicin (**34**). The peak that eluted at V_0 was collected, and analysed by LC MS using the same method that had been utilised for the other HSA derivatives. This analysis showed one broad peak, with a retention time of 47 to 53 minutes, in both the spectrum max diode array and TIC spectra.

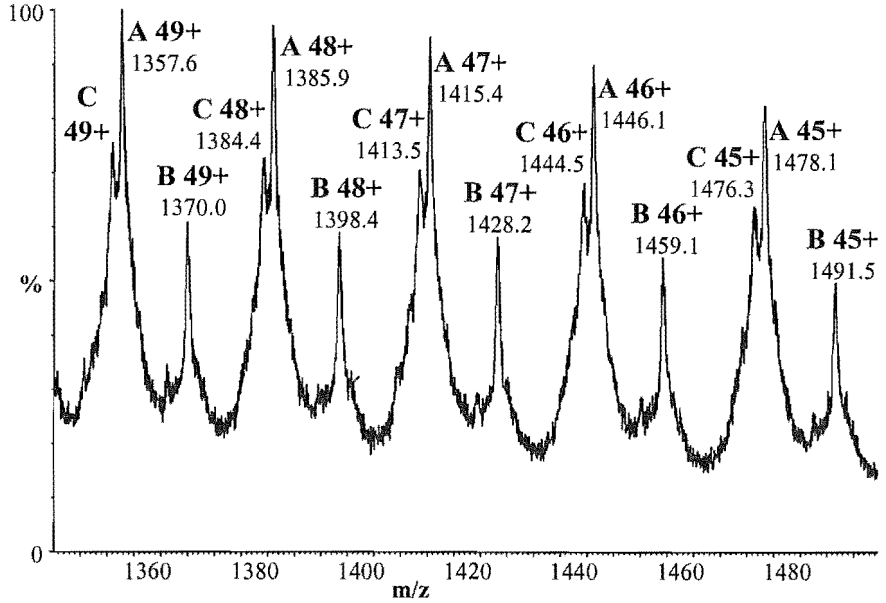

Figure 5.20: *Expanded region of the ESI-mass spectrum of the HSA-tyrosinamide conjugate (**65**). Three series of peaks can be seen, A, B and C.*

Three series of charge states (A, B and C), very clearly resolved, were visible in the ESI-mass spectrum. Figure **5.20** provides an expansion of a small region of the ESI-mass spectrum to demonstrate this. Deconvolution of the mass spectral data collapses the charge state series' to A: 66,480 Da, B: 67,079 Da and C: 66,390 Da (Figure **5.21**). Unreacted albumin and the conjugate product **65** (67,079 Da) were both present in the sample.

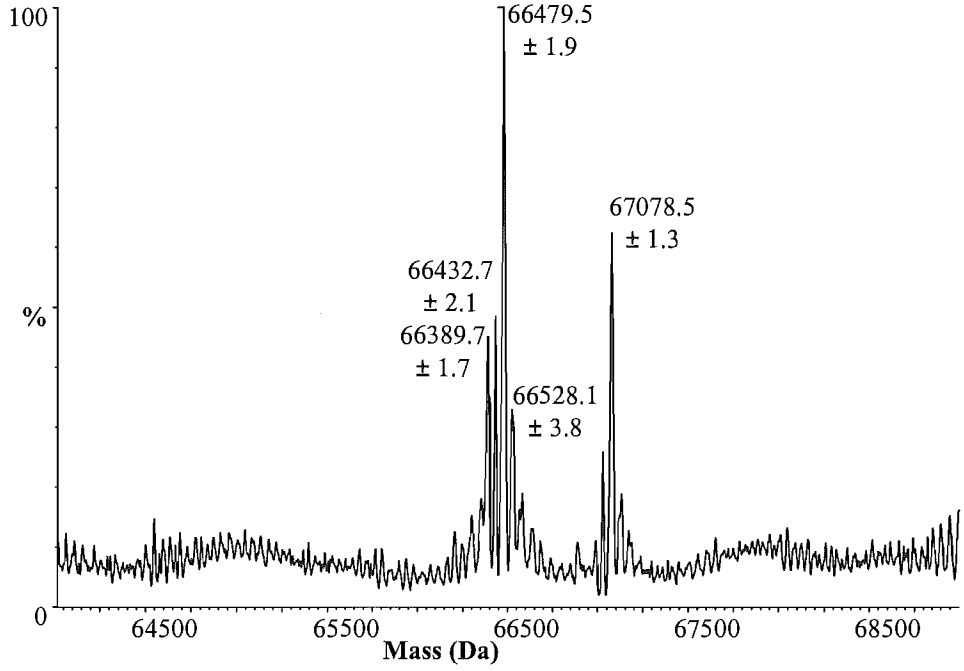

Figure 5.21: *Deconvoluted, neutral-scale mass spectrum of the HSA-tyrosinamide conjugate (**65**).*

The sample containing **65** was enzymatically digested with trypsin, in a similar manner to the previous digests. This would identify if γ-maleimidobutyric-Gly-Phe-Leu-Gly-tyrosinamide (**37**) had been conjugated to HSA at cysteine-34. The analysis of this digest was somewhat more time consuming than the previous tryptic digests. For the F-150 and doxorubicin conjugates, distinctive UV absorbances had been relied on to highlight significant derivatised fragments. Tyrosinamide (**36**) lacks this useful property, so each peak in the LC MS of the digest had to be analysed.

Table **5.3** shows the data collected from the LC MS of the tryptic digest of the sample containing **37**. Fragments smaller than **37** in molecular weight were ignored, as these peptides had obviously not been modified. In each case the fragment masses identified at each retention time (experimental MW) were converted to a calculated MW without **37** (Tyro) attached. A further 18 mass units were subtracted from these fragments to generate

a second series of possible fragments (see Section **5.3**). The two generated series of calculated molecular weights were compared to the predicted digest fragments.[200] Of the possible digest fragments, only those containing cysteine-34 were searched for mass matches. Again, this does not discount derivatisation at another site in the protein.

Retention Time (mins)	Experimental MW (Da)	Calculated MW (Da) Without Tyro	Calculated MW (Da) Without H_2O	Tryptic/Chymotryptic Cleavage Sites and Fragments
21.0	1148.6	429.3	411.3	
	959.6	240.3	222.3	
22.3	999.7	280.4	262.4	
	981.6	262.3	244.3	
23.0	1056.6	337.3	319.3	
	907.6	188.3	170.3	
24.0	1621.2	901.9	883.9	
	1639.2	919.9	901.9	
24.6	1260.8	541.5	523.5	
	1038.6	319.3	301.3	
	1141.6	422.3	404.3	
	1159.2	439.9	421.9	
	1242.6	523.3	505.3	
	1491.8	772.5	754.5	
25.5	1019.6	300.3	282.3	
	1511.0	791.7	773.7	
26.0	1012.7	293.4	275.4	
26.7	993.6	274.3	256.3	
27.6	2163.2	1443.9	1425.9	1428.7, peptide from 25 to 36. (L)I . . . . F(E)
	2383.2	1663.9	1645.9	
	1480.8	761.5	743.5	
	1357.8	638.5	620.5	
	1294.8	575.5	557.5	
28.0	1467.0	747.7	729.7	
	2737.5	2018.2	2000.2	
	1496.8	777.5	759.5	
28.5	1853.0	1133.7	1115.7	
	1609.8	890.5	872.5	
29.8	1599.8	880.5	862.5	
31.1	1341.5	622.2	604.2	
31.6	2721.5	2002.2	1984.2	
	1390.8	671.5	653.5	
	2488.2	1768.9	1750.9	
32.8	1471.8	752.5	734.5	
	1478.8	759.5	741.5	
33.1	2045.1	1325.8	1307.8	
34.0	3241.3	2522.0	2504.0	
34.9	2935.4	2216.1	2198.1	
37.5	2917.6	2198.3	2180.3	
38.9	1639.0	919.7	901.7	
	2933.4	2214.1	2196.1	
40.1	1344.8	625.5	607.5	
	1742.0	1022.7	1004.7	
42.4	1660.8	941.5	923.5	
	1677.0	957.7	939.7	
	1408.8	689.5	671.5	
	1622.8	903.5	885.5	
	3750.5	3031.2	3013.2	
43.1	1625.0	905.7	887.7	
	1851.0	1131.7	1113.7	
	3701.0	2981.7	2963.7	2969.4, peptide from 25 to 49. (L)I . . . . F(A)
	4063.0	3343.7	3325.7	

Table continued on next page....

Retention Time (mins)	Experimental MW (Da)	Calculated MW (Da) Without Tyro	Calculated MW (Da) Without H_2O	Tryptic/Chymotryptic Cleavage Sites and Fragments
43.7	2072.1	1352.8	1334.8	
	2447.4	1728.1	1710.1	
	2465.4	1746.1	1728.1	
	2480.7	1761.4	1743.4	
	2465.4	1746.1	1728.1	
44.4	3072.8	2353.5	2335.5	
45.3	1695.0	975.7	957.7	
	3389.0	2669.7	2651.7	
	5475.0	4755.7	4737.7	
45.9	2434.0	1714.7	1696.7	
	5029.0	4309.7	4291.7	
46.4	1456.0	736.7	718.7	
	4368.0	3648.7	3630.7	
47.5	1451.0	731.7	713.7	
	1603.0	883.7	865.7	
	4352.0	3632.7	3614.7	
49.5	1683.0	963.7	945.7	
	3367.0	2647.7	2629.7	

Table 5.3: *ESI-MS data from LC MS of tryptic digest of the HSA-tyrosinamide conjugate (**65**), Tyro = γ-maleimidobutyric-Gly-Phe-Leu-Gly-tyrosinamide (**37**), MW = molecular weight.*

A match was made if the calculated MW was within ±0.2% of the predicted MW. There are two possible peptide matches, which contain the cysteine-34 residue, for the fragments seen. It was noted that a peptide fragment of approximately 1428 Da (amino acid residues 25-36) was produced in both this digest and in the previous digests of the HSA conjugates (Sections **5.3** and **5.5**). This was taken as evidence that derivatisation has occurred at the same place, at cysteine-34, in each case.

5.7 Conclusions

Among naturally occurring proteins, albumin is a potential carrier of anti-cancer drugs because it demonstrates significant uptake by tumour cells and due to its biocompatibility.

This chapter outlined the synthesis and characterisation of four human serum albumin-based conjugates. The syntheses exploited the availability of a free thiol moiety at cysteine-34 of HSA, and the specific and selective reaction of this thiol with a maleimide functional group. The generation of these conjugates took advantage of the maleimido-tetrapeptide derivatives of homohalichondrin B (**32**), doxorubicin (**35**), and tyrosinamide (**37**) synthesised in chapter **2**. The fluorescent maleimide, F-150 (**46**), was also conjugated to HSA to establish the feasibility of this preparation method, and to develop analytical methodologies for characterising the resultant conjugates. The HSA conjugate syntheses were simple and required very little protein manipulation. Much like its CV-N counterpart, the HSA-doxorubicin degraded under gentle conditions.

LC MS was essential to the analysis of the conjugates. A long, gentle, LC solvent gradient system was critical to achieving good mass spectral results as it served to both purify and desalt the protein derivatives. Tryptic digestion of the HSA-based conjugates demonstrated that conjugation of the maleimido-tetrapeptide-drug constructs with HSA had indeed occurred at cysteine-34 of HSA.

Complete reaction of HSA was not seen in the production of the HSA conjugates. This was ascribed to the cysteine-34 residue being unavailable for reaction in some cases, as a proportion of the sample of HSA has this residue blocked by disulfide bond formation with other thiol containing molecules, such as glutathione. The high molecular weight of HSA presented difficulties when it came to purifying the conjugate product away from unreacted protein. As HSA is biodegradeable, non-immunogenic and non-toxic,[119,144] the inseparable mixture of unreacted protein and toxin conjugate will not be a problem in the development of HSA as a drug carrier.

Chapter **6** describes the anti-cancer biological assay results for the HSA conjugates.

6 BIOLOGICAL TESTING

BIOLOGICAL TESTING

6.1 Introduction

The goal of this study was to establish the feasibility of the use of protein-toxin conjugates to target, deliver, and release cytotoxins for the elimination of HIV-infected or cancerous cells. Although the synthesis of various CV-N- and HSA-toxin conjugates was successful, the determining factor in deciding their therapeutic potential can only be evaluated with extensive biological testing. This chapter explores preliminary biological analyses of several of the conjugates.

The tetrapeptide, Gly-Phe-Leu-Gly, was designed as a substrate for the cathepsin enzymes (see Section **2.2**).[128,146,147] The linker was tailored to allow drug/toxin liberation at an appropriate rate intracellularly. The following work sought to provide proof that the toxin could be released from the conjugate, an essential principle of the conjugate design.

CV-N (**28**) is a novel anti-HIV protein due to its ability to bind with high affinity to the viral envelope glycoprotein gp120. To utilise CV-N (**28**) as a gp120-targeting, and therefore HIV-targeting, moiety, the covalent linkage of cytotoxic agents to CV-N (**28**) must not diminish the protein's gp120 binding affinity. An Enzyme Linked Immunosorbent Assay (ELISA) was employed to assess the ability of the conjugates to bind gp120.

The ultimate test, for both the CV-N conjugates and the HSA conjugates, is to determine if the cell-killing ability of the toxin moiety can be selectively applied to diseased cells. Preliminary *in vitro* cytotoxicity assays have been completed and are presented in this chapter.

6.2 Biological Testing of CV-N Conjugates

6.2.1 Cathepsin B Digest

Attachment of a drug to a macromolecule restricts its mode of uptake by cells to the process of pinocytosis and thus provides an opportunity to direct an otherwise freely permeating drug specifically to the cell type where the cytotoxic action is required.[149,150] Such a delivery system can only be effective if the drug is firmly bound to its carrier during transport to cells and if controlled release of drug occurs after its arrival within the cell. To fulfil this role, a tetrapeptide, Gly-Phe-Leu-Gly, was selected to link the proteins to the toxins. This oligopeptide had previously been shown to be susceptible to specific hydrolysis by the intralysosomal cathepsin enzymes (as discussed in section **2.2**).[149,150]

In vitro release of norhomohalichondrin B amine (**31**) and degradation of the tetrapeptide, Gly-Phe-Leu-Gly, from the CV-N: K3R, K48R, K74R, K84R-norhomohalichondrin B conjugate (**54**), by cathepsin B has been demonstrated using a method adapted from that developed by Pechar *et al.*[146,147] CV-N: K3R, K48R, K74R, K84R-norhomohalichondrin B (**54**, 1 μg) was incubated with cathepsin B (3 μg, 4 x 10^{-7} M) in a phosphate buffer (0.05 M KH_2PO_4, 0.001 M EDTA, 0.005 M glutathione, pH 6.0) at 37°C.

The degradation of the conjugate (**54**) was monitored by reverse phase (C18) LC MS after 5, 24 and 48 hours of incubation with cathepsin B. A solvent gradient (200 μL/min) comprising the following steps was used: a slow linear gradient from 0-60% CH_3CN/H_2O (5% acetic acid) over 60 minutes; a linear gradient to 100% CH_3CN over two minutes; isocratic at 100% CH_3CN for five minutes; a return to 100% H_2O over five minutes; and finally an isocratic hold on 100% H_2O for 2 minutes. The progress of the digestion can be seen in the LC MS traces pictured in Figure **6.1**. Conjugate **54** elutes at 42 minutes.

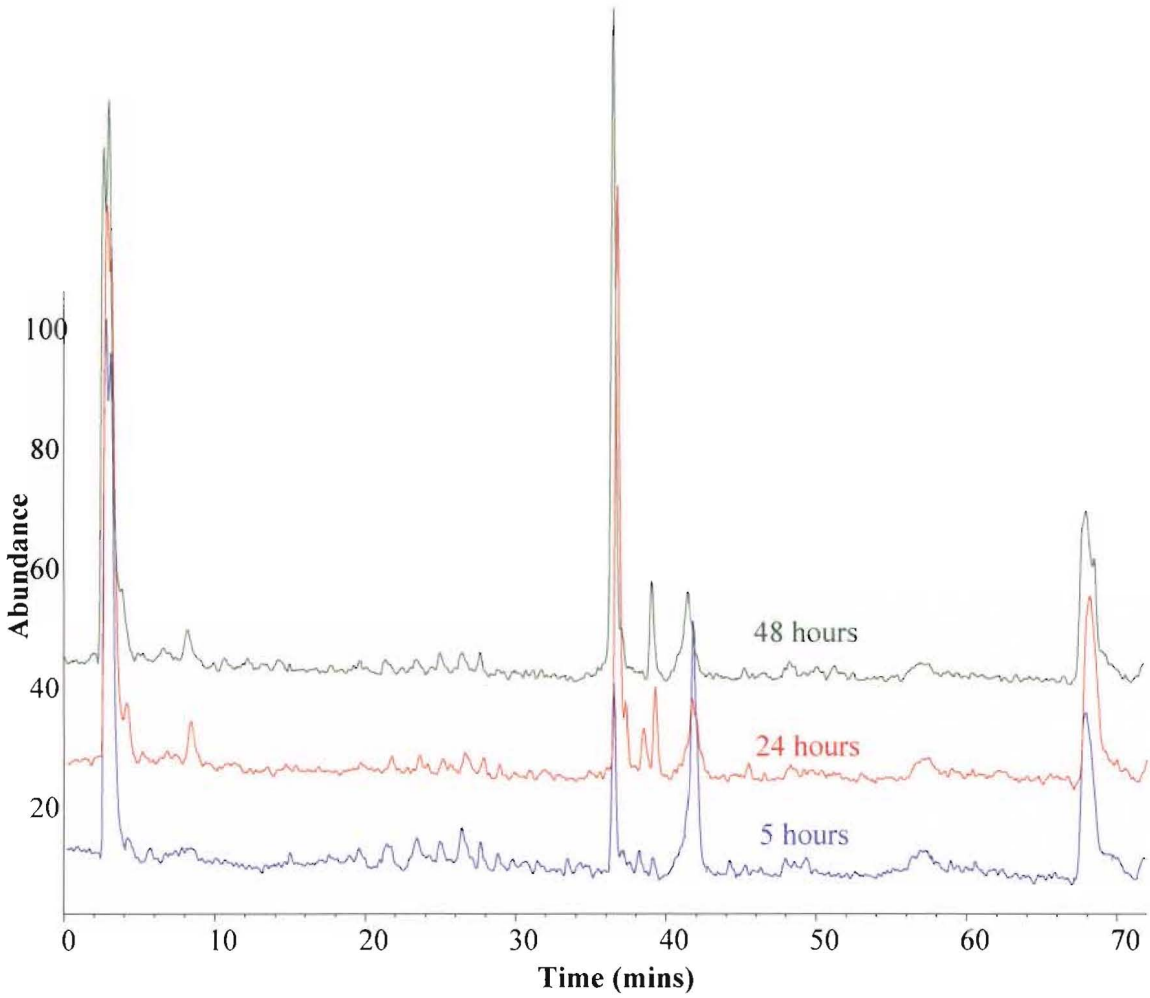

Figure 6.1: *Overlay of the total ion current traces of the Cathepsin B digest of CV-N: K3R, K48R, K74R, K84R-norhomohalichondrin B Conjugate (**54**).*

After five hours, a digestion product could be seen eluting at 37 minutes. This had a mass of 12,871 Da and is equivalent to the thioether glycine derivative of CV-N: K3R, K48R, K74R, K84R (**66**), as illustrated in Figure **6.2**. Cleavage of the oligopeptide linker had occurred between the glycine and the phenylalanine residues. After 24 hours, further digestion of the conjugate could be seen. Significantly, norhomohalichondrin B amine (**31**) with a mass of 1,092 Da, and a glycine derivative (**67**) with a mass of 1,149 Da, were visible, both eluting at 39 minutes. No intact conjugate could be resolved after 48 hours.

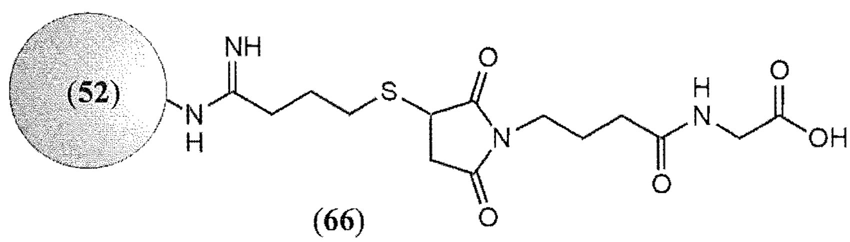

(66)

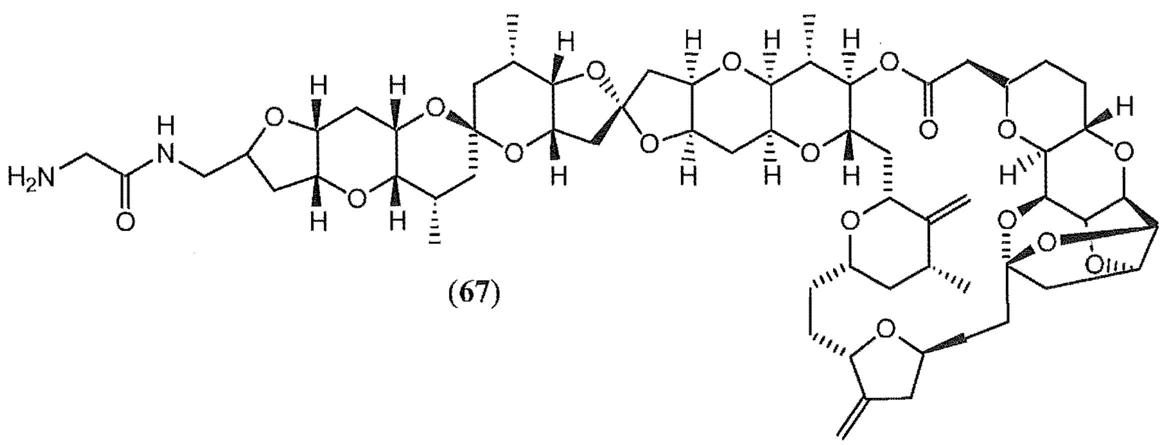

(67)

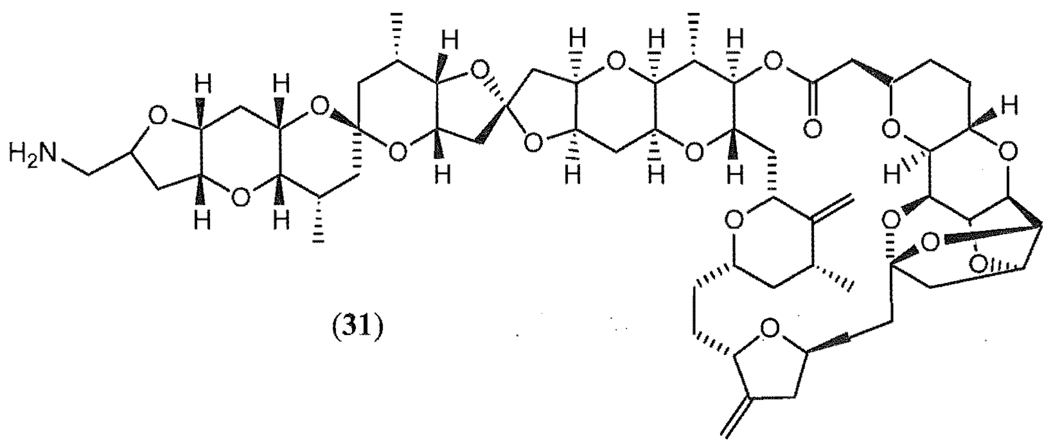

(31)

Figure 6.2: *Degradation products of a cathepsin B digest of the CV-N: K3R, K48R, K74R, K84R-norhomohalichondrin B Conjugate (54).*

These results support the hypothesis of using Gly-Phe-Leu-Gly as a biodegradable linker and as a substrate for cathepsin B. This confirms the results of Pechar *et al.* on their development of a conjugate of doxorubicin.[146] These researchers found that during the incubation of their conjugate with cathepsin B, a glycine derivative of doxorubicin was released together with the free drug. The glycine derivative was further degraded to free doxorubicin when tritosomes (mixture of rat-liver lysosomal enzymes) were used instead of cathepsin B.

6.2.2 Enzyme Linked Immunosorbent Assay

Low nanomolar concentrations of CV-N (**28**) irreversibly inactivate isolates of HIV-1. Furthermore, CV-N (**28**) prevents *in vitro* fusion and transmission between cells.[95] The anti-HIV activity of CV-N (**28**) is mediated, at least in part, through high-affinity interactions with the viral envelope protein gp120. Therefore, conjugate development must not interfere with the essential, and unique, binding of the protein to gp120. With the attachment of large molecules, such as the toxin constructs prepared in Chapter **2**, there is the potential to block CV-N binding to gp120. This was presumed to be the case for the CV-N-PE38 conjugate previously constructed and tested by Mori *et al.*[95] where the gp120 binding affinity of the conjugate was significantly reduced. The same method of testing, and using, an ELISA system developed by the LDDRD, was used to determine the relative affinity of the conjugates prepared in this project for gp120. This assay was critical in determining if the modification of the lysine ε-amino groups had resulted in loss of binding affinity.

The Enzyme Linked Immunosorbent Assay (ELISA) is a sensitive and precise method used to detect the presence of antigens or antibodies of interest in a wide variety of biological samples.[225] Many variations in the methodology of the ELISA have evolved since its development in the 1960s.[225] An ELISA has been applied for the detection and quantification of the binding of CV-N to gp120.

This assay is based on the Sandwich ELISA design with indirect detection of binding.[225] A schematic of this methodology is shown in Figure **6.3**. The assay is performed in a 96-well plate. Gp120 is initially bound to the plate itself. After two hours of incubation, the plate is thoroughly washed. Any sites unfilled by gp120 are capped by incubating overnight with bovine serum albumin (BSA). Once again, the plate is thoroughly washed. CV-N and its derivatives are introduced and incubated for one hour so that they can selectively bind to the gp120. Those molecules not bound are washed away and CV-N antibodies (Rabbit-anti-CV-N Ab) are added to the plate. These are in turn bound by a second antibody (anti-Rabbit-IgG-Ab-AP) which has a terminal alkaline phosphatase (AP) enzyme. Finally the substrate buffer (10% diethanolamine, 10 mM $MgCl_2$, 4 mg/mL *p*-nitrophenylphosphate (*p*NPP), pH 9.8) is loaded on the plate. This buffer develops a

yellow colour on reaction with the AP enzyme. The plate can be read at 405 nm in a plate reader. The intensity of the colour is proportional to the degree of binding. Hence, any change in the binding affinity of the CV-N derivatives to gp120 results in fewer antibodies binding at each step, and therefore was a less intense yellow colour.

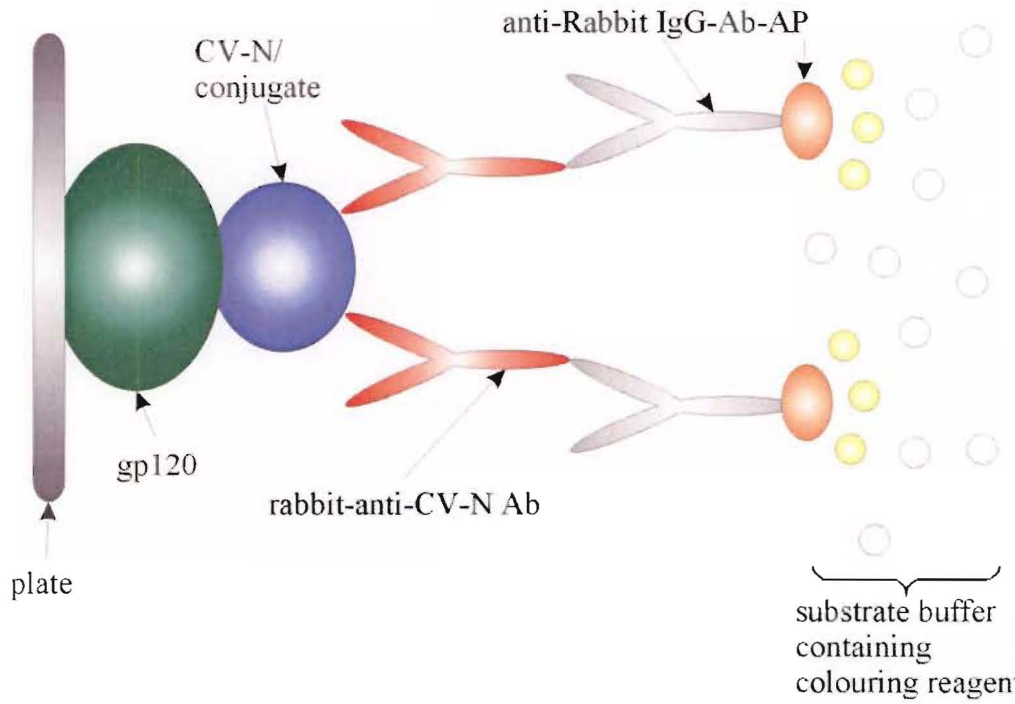

Figure 6.3: *Schematic of the ELISA methodology for testing the binding of CV-N.*

Figure **6.4** shows the typical layout of a 96-well plate. The outer wells of the plate are not loaded with gp120. This provides a background reading for the assay and ensures that the assay is working correctly. Rows B, C and D are used as a standard reference for each plate, and are loaded with native CV-N, or with a mutant CV-N. In turn, the CV-N conjugates are placed in rows E, F and G. The concentration of CV-N placed in each cell increases from column two to 11 in a logarithmic fashion. Each concentration is measured in triplicate to ensure uniformity of readings. The large range of concentrations results in a precise and quantitative measurement of the binding affinity of the CV-N to gp120. This data can be graphically represented as a sigmoidal curve. A comparison of the data for the standard reference *versus* the CV-N conjugates at the point where half the gp120 are bound gives an indication of their relative binding affinities.

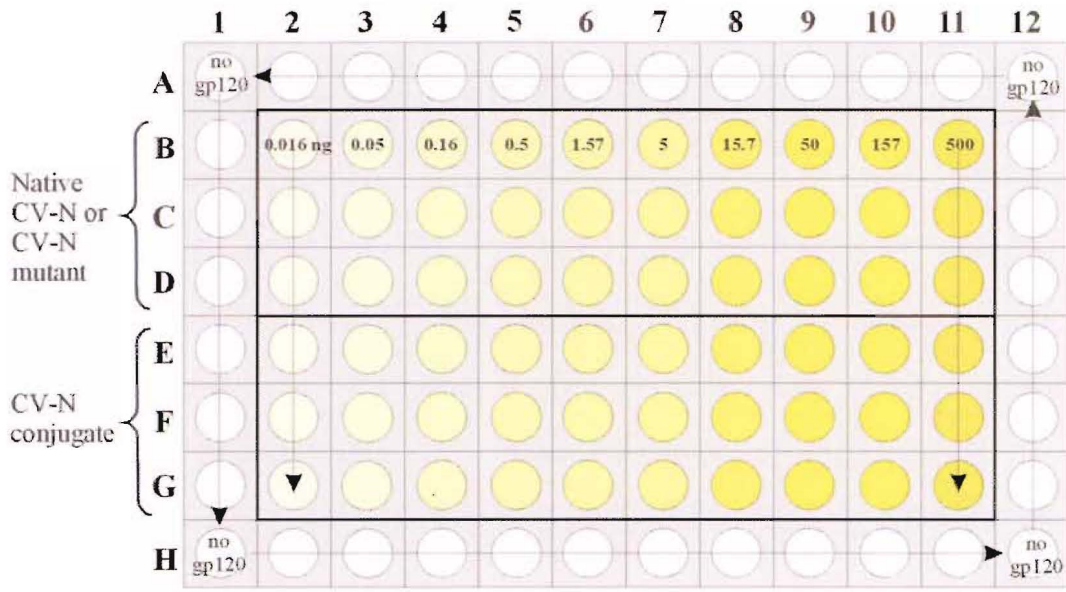

Figure 6.4: *Layout of the 96-well plate in the CV-N ELISA assay.*

The CV-N: K3R, K48R, K74R, K84R-norhomohalichondrin B conjugate (**54**) and the parent mutant protein, CV-N: K3R, K48R, K74R, K84R (**52**), were both assayed using the process described above. Figure **6.5** shows a graphical representation of the results obtained.

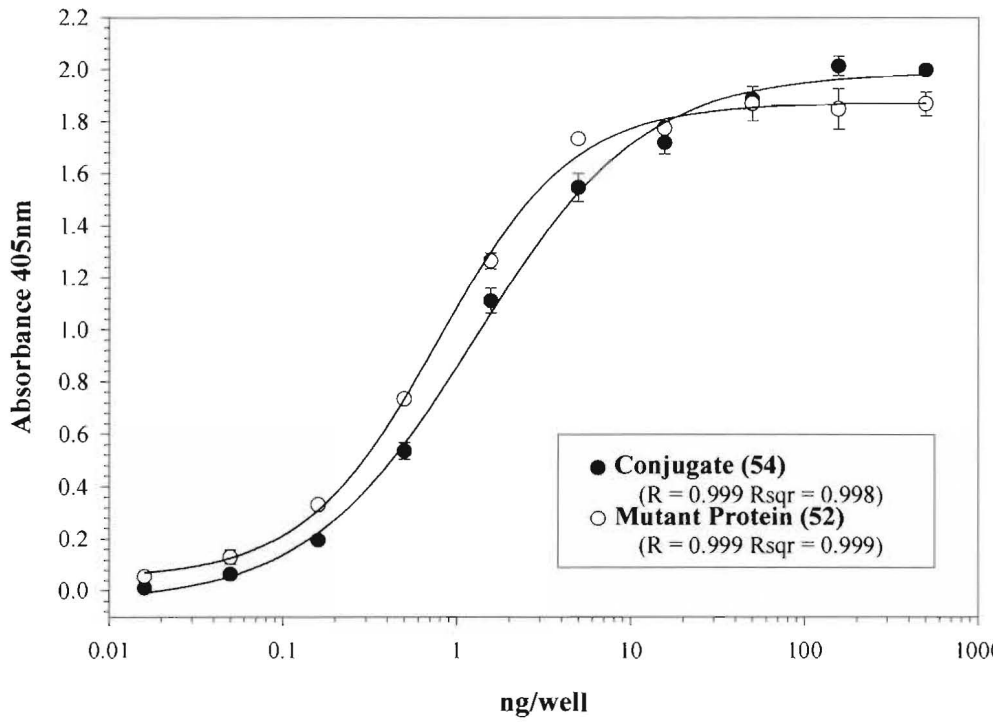

Figure 6.5: *Plot of the ELISA assay results for the mutant protein (**52**), and norhomohalichondrin B conjugate (**54**).*

1.42 ng of **54** was required for half the gp120 to be bound. In comparison, 0.71 ng of **52** was required. This shows the unmodified protein (**52**) has a two-fold better binding affinity for gp120 over the conjugate (**54**). This may be due to steric hindrance of the CV-N-gp120 interactions and/or to changes in the tertiary structure of the CV-N moiety. This small reduction in binding affinity is not thought to be particularly significant, however.[205]

The mutant protein (**52**) and wild-type CV-N (**28**) had been shown previously to have comparable binding affinities for gp120 in a similar ELISA assay procedure.[205]

6.2.3 Cytotoxicity Assays

The anti-HIV assay is a relatively simple method to determine the ability of a drug to protect cells against the cytopathic effects of HIV. T-lymphocyte-derived CEM-SS cells are added to 96-well microtitre plates along with cell-free HIV (RF strain) and the test agent at ½-log dilutions over a multi-dose range. Six days after infection, a tetrazolium reagent, XTT, is added to the wells. In the presence of viable cells, XTT is metabolized to an orange coloured formazan, such that the quantity of viable cells, and thus the protective ability of the test agent, is proportional to the depth of the colour. Uninfected cells are also treated with the drug in order to determine the cytotoxicity of the drug, if any, to the CEM-SS cells.

The CV-N: K3R, K48R, K74R, K84R-norhomohalichondrin B conjugate (**54**) and free norhomohalichondrin B amine (**31**) were submitted for the above HIV cytotoxicity assay at the NCI-Frederick. A graphical illustration of the cytotoxicity results is presented in Figure **6.6**. The IC_{50} values obtained from this data were expressed in units of pg/mL. These values were converted to pmol/mL so that a more accurate comparison between the toxicities of the conjugate and the free drug could take place (Table **6.1**).

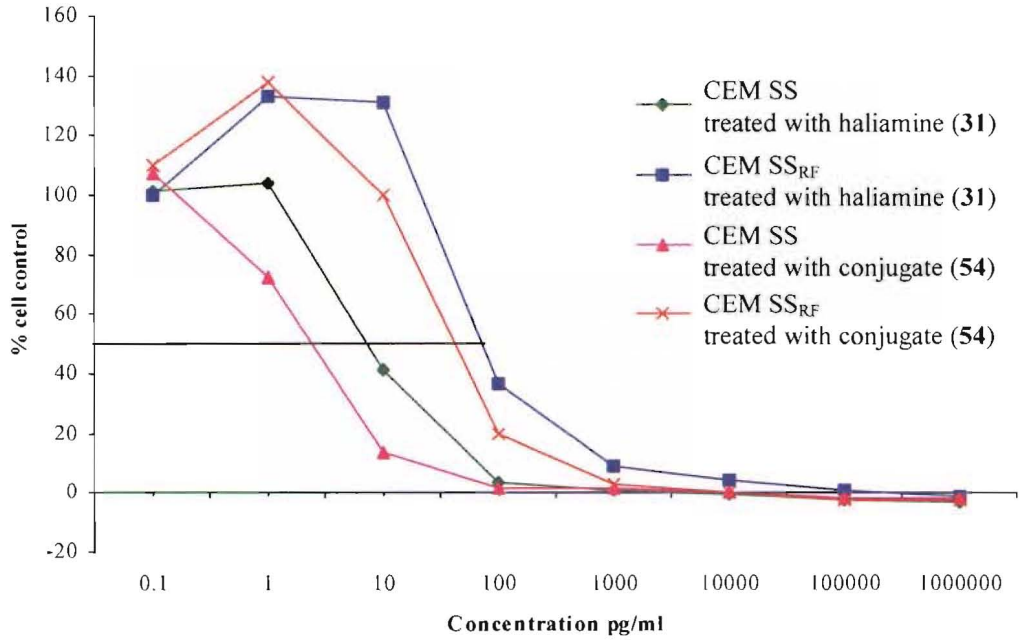

Figure 6.6: *XTT assay for the detection of cell killing of HIV-infected cells (CEM SS_{RF}) and uninfected (CEM SS) cells (expressed in pg/mL), by norhomohalichrondrin B amine (**31**, halimamine) and CV-N: K3R, K48R, K74R, K84R-norhomohalichondrin B Conjugate (**54**).*

Compound	CEM SS		CEM SS_{RF}	
	IC_{50}[a] (pg/mL)	IC_{50}[a] (pmol/mL)	IC_{50}[a] (pg/mL)	IC_{50}[a] (pmol/mL)
haliamine (**31**)	7.2	0.0066	71.1	0.0651
malei-tet-hali (**32**)	13.5	0.0083	116.1	0.0712
Conjugate (**54**)	2.4	0.0002	43.2	0.0036

[a] Inhibition Concentration

Table 6.1: *Cytotoxicity of norhomohalichondrin B amine (**31**, haliamine), γ-maleimido-Gly-Phe-Leu-Gly-norhomohalichondrin B (**32**, malei-tet-hali) and CV-N: K3R, K48R, K74R, K84R-norhomohalichondrin B Conjugate (**54**, conjugate) against HIV infected (CEM SS_{RF}) and uninfected (CEM SS) cells. IC_{50} expressed in both pg/mL and pmol/mL.*

Surprisingly, the conjugate shows quite the opposite cytotoxicity results to that predicted from the previous studies by Mori *et al.*[95] The conjugate does not show selective toxicity for the HIV-infected cells. It is interesting to note that both the free drug (**31**) and the

conjugate (**54**) demonstrate higher toxicity to the non-infected cell line (CEM-SS) over the HIV-infected cells (CEM-SS_{RF}). This may be due to the HIV infection interfering the cellular mechanisms of uptake in this cell-line. The conjugate (**54**) was significantly more toxic to both cell lines (33 fold for uninfected cells and 18 fold for infected cells) over the free drug. It is not known why this is the case, and further investigations are required, however there are a number of hypotheses that may offer an explanation. Norhomohalichondrin B amine (**31**) has limited aqueous solubility. Attachment of the toxin to the hydrophilic protein may have resulted in improved solubility of the conjugate over the free halichondrin. Further, conjugation to the protein may allow for improved membrane permeability and uptake into the cell. Active transport of the CV-N carrying norhomohalichondrin B (in both infected and uninfected cells) may also be occurring.

Mori *et al.*[95] evaluated the CV-N-PE38 conjugate against HIV infected H9/HIV-1_{IIIb} cells and uninfected H9 cells using the XTT-tetrazolium cell viability assay. The human T-cell line H9 chronically infected with HIV-1_{IIIb} (H9/HIV-1_{IIIb}) is known to express viral envelope glycoprotein gp120 on the cell surface.[95] No steps have been taken to quantify the amount of gp120 being expressed on the surface of the HIV infected CEM SS cell-line at this stage. The CV-N conjugates prepared in this thesis will be also be tested against H9/HIV-1_{IIIb} cells to establish whether selective toxicity is cell-line dependent.

Further developments on the assay, the cell line, and quantitation of gp120 on the cells in question, are in progress at the NCI.

Once assay procedures are established, the doubly-derivatised CV-N norhomohalichondrin B conjugate (**61**) will also be tested. This will evaluate the effect of toxin loading on the pharmacokinetics of the conjugates.

6.3 Biological Testing of HSA Conjugates

6.3.1 Cytotoxicity Assays

The HSA-based conjugates, and the various individual components of the constructs, were screened in the Marine Chemistry Group's in-house anti-tumour assay. This *in vitro* 'anti-tumour' assay uses the P388 cell line (murine leukaemia cells). A two-fold dilution series of the sample of interest is incubated with P388 cells. Sample, media, cell and solvent controls are also run. After 72 hours of incubation, MTT, a yellow tetrazolium salt is added. After a further two hours the concentration of the sample required to reduce the number of viable cells by fifty percent relative to a control is calculated. The mitochondria of viable leukaemia cells reduce the yellow MTT dye to a purple formazan derivative.[226] By measuring the light absorbance at 540 nm in each well, a direct quantification of formazan formation, and therefore the number of viable cells, is able to be determined. The absorbance is expressed as a percentage cell viability relative to the control, and is plotted against sample concentration in the well to generate a sample concentration *vs* cell viability curve. The concentration producing a fifty percent reduction in the number of viable cells gives the IC_{50} result, which is usually expressed in units of ng/mL.

The cytotoxicity results of the HSA-norhomohalichondrin B conjugate (**63**) and the HSA-doxorubicin conjugate (**64**) are presented in Table **6.2**. The maleimido-tetrapeptide (**30**), norhomohalichondrin B amine (**31**), doxorubicin (**34**), and the maleimidobutyric-tetrapeptide-toxin constructs (**32** and **35**) were also tested (Table **6.2**). The IC_{50} values obtained were expressed in units of ng/mL. These values were converted to nmol/mL so that a more accurate comparison could take place. Several assumptions were made in the analysis of this data. From mass spectrometric analysis of the protein conjugates, it appeared that there was approximately one-third conjugate to two-thirds unreacted HSA in each of the samples. This factor of three was taken into account in the assay data. Instability issues had been experienced with doxorubicin and the doxorubicin conjugates (see Section **4.3.3**). The samples tested here were stored dry, in the dark, and in the freezer until just before analysis. The assumption was made that doxorubicin had not degraded at this point.

	P388	
Compound	**IC_{50}[a] (ng/mL)**	**IC_{50}[a] (nmol/mL)**
malei-tet (**30**)	NA	NA
haliamine (**31**)	9.5	0.009
malei-tet-hali (**32**)	16.3	0.01
HSA-hali (**63**)	183	0.0027
doxorubicin (**34**)	707.3	1.3
malei-tet-dox (**35**)	5315	4.9
HSA-dox (**64**)	4429	0.067

[a] Inhibition Concentration

NA = not active at highest concentration

Table 6.2: *Cytotoxicity of γ-maleimidobutyric-Gly-Phe-Leu-Gly-OH (**30**, malei-tet), norhomohalichondrin B amine (**31**, haliamine), γ-maleimidobutyric-Gly-Phe-Leu-Gly-norhomohalichondrin B (**32**, malei-tet-hali), HSA-norhomohalichondrin B conjugate (**63**, HSA-hali), doxorubicin (**34**), γ-maleimidobutyric-Gly-Phe-Leu-Gly-doxorubicin (**35**, malei-tet-dox) and HSA-doxorubicin conjugate (**64**, HSA-dox) against the P388 murine leukaemia cell line.*

The maleimido-tetrapeptide (**30**) showed no toxicity at the highest concentration tested. As expected, both the free toxins demonstrated good toxicity, with norhomohalichondrin B amine (**31**) proving to be especially potent. Derivatisation of norhomohalichondrin B amine (**31**) with the maleimido-tetrapeptide (**30**) to form γ-maleimidobutyric-Gly-Phe-Leu-Gly-norhomohalichondrin B (**32**) did not result in any significant loss of toxicity. γ-Maleimido-Gly-Phe-Leu-Gly-doxorubicin (**35**) demonstrated a 3.8 fold loss of cytoxicity over free doxorubicin (**34**).

What is especially interesting about these results is that both conjugates show an increased cytotoxicity, in the P388 anti-tumour assay, over the free toxin. Factors such as increased membrane permeability, active transport of the HSA conjugates into the cells, and increased solubility of the conjugate compared to the free toxin, may also come into play here. Further biological testing is required to test these hypotheses.

6.4 Conclusions

In vitro release of norhomohalichondrin B amine (**31**) and degradation of the tetrapeptide, Gly-Phe-Leu-Gly, from the CV-N: K3R, K48R, K74R, K84R-norhomohalichondrin B conjugate (**54**) by cathepsin B has been demonstrated. These results support the hypothesis of using Gly-Phe-Leu-Gly as a biodegradable linker that would allow controlled release of a drug within diseased cells.

The ability of the conjugate, CV-N: K3R, K48R, K74R, K84R-norhomohalichondrin B (**54**), to bind gp120 was assessed in an ELISA assay. Both the conjugate (**54**) and the mutant protein (**52**) showed comparable binding affinities to gp120. These results demonstrate the feasibility for further pursuit of the concept of CV-N-based conjugates, through modification of the lysine ε-amino groups with low-molecular-weight compounds.

The concept behind drug targeting, and controlled drug release formulations, is to design a conjugate which will reduce the peak plasma concentration of the drug and in theory prolong exposure to an effective drug concentration, leading to both a reduction in toxicity and also increased efficacy.[121] It was encouraging to see that the HSA and CV-N-based conjugates demonstrated potent cytotoxicity. However, disappointingly, these conjugates exhibited an increased cytotoxicity over the free toxins, and no selectivity has been demonstrated at this point. This increased cytotoxicity may be beneficial provided selectivity for diseased cells can be achieved. Selectivity may not be demonstratable in a cell-based assay and a move to *in vivo* studies may be appropriate. Further investigations to clarify the mechanisms behind these results, and the implementation of alternative assay systems, are underway.

7 CONCLUSIONS

CONCLUSIONS

The aim of this project was to create protein-based drug delivery systems – delivery systems that would package, target, and deliver cytotoxins to diseased cells. Primarily, this project explored the use of the protein CV-N (**28**) to actively target and deliver cytotoxic natural products to HIV-infected cells. This project also investigated the use of human serum albumin as a protein carrier to passively target and deliver cytotoxic natural products to cancerous cells.

Chapter **2** outlined a strategic approach to the development of these therapeutics. Of primary importance was the judicious selection of the protein-toxin linker, a tetrapeptide Gly-Phe-Leu-Gly, which would allow for the site and rate of drug liberation *in vivo* to be controlled by enzymatic means. Maleimido-activated tetrapeptide toxin constructs were prepared in readiness for selective reaction with proteins carrying thiol functionalities.

Native CV-N conjugates were prepared by thiolation of the lysine amino groups, and the subsequent reaction with maleimido-activated compounds. A distribution of products, with reaction across all lysine residues, introduced the issue of heterogeneity and the difficulties this presents in defining a therapeutic. A singly substituted, but randomly distributed, tyrosinamide conjugate of CV-N was prepared. This conjugate can be radio-labelled and could then be used as a tracer in cellular and body distribution studies.

Two recombinantly produced mutant CV-N proteins, CV-N: K3R, K48R, K74R (**51**) and CV-N: K3R, K48R, K74R, K84R (**52**), allowed for the preparation of two selectively modified double- and single-norhomohalichondrin B conjugates of CV-N. This section of work addressed the issue of preparing homogeneous bioconjugates that could be utilised in a therapeutic application.

Digestion of the CV-N: K3R, K48R, K74R, K84R-norhomohalichondrin B conjugate (**54**) with the enzyme cathepsin B, and subsequent release of norhomohalichondrin B

amine (**31**), provided proof-of-principle that the toxin would be released from the conjugate once it was internalised within affected cells.

Homohalichondrin B, doxorubicin, and tyrosinamide conjugates of HSA were prepared. The syntheses exploited the availability of a free thiol moiety at cysteine-34 of HSA, and the specific and selective reaction of this thiol with the maleimido-activated tetrapeptide derivatives of the toxins. Although unreacted protein and the conjugate products could not be separated, the biodegradable and non-immunogenic nature of HSA suggests that this will not present a significant problem.

No matter what modifications are made to CV-N, the critical issue is whether those alterations interfere with the unique binding affinity of the protein to gp120. The results for the CV-N: K3R, K48R, K74R, K84R-norhomohalichondrin B conjugate (**54**), in the gp120-based ELISA assay, clearly indicate that no discernable inhibition of gp120 binding was taking place. However, the ultimate goal is to show targeted delivery of the conjugate to HIV-infected cells. Although the conjugate demonstrated potent toxicity, there is doubt over whether it is demonstrating selective toxicity. This could be a factor of the whole cell-based assay system, and a move to animal models may be appropriate. However, homohalichondrin B (**22**) may simply be too toxic. With chemical attachment to the construct at a point distant from the biologically active portion of the molecule, homohalichondrin B (**22**) is possibly not acting as a prodrug. The entire construct may be a toxic entity, even before drug release.

Similarly, the HSA-based conjugates exhibited excellent toxicity in the P388 murine leukaemia biological screen. Whether this is targeted toxicity however, remains a point of further investigation.

The three basic components of a protein-drug conjugate (protein, linker and toxin) must be optimally matched to maximise therapeutic potential. Potency of the agent to be delivered (and therefore the clinical dose) is one factor that must be taken into consideration. Realising that a relatively small proportion of the dose administered may reach the infected site, high doses (500 mg/kg) of polymer carriers of methotrexate (of mild potency) are routinely administered.[121] This concept seems fraught with possible

problems, with issues such as additional toxicological burden, immunogenic responses, and problems with metabolism/excretion from the body. For this reason, in this initial study, we chose to combine the particularly potent toxins, homohalichondrin B (**22**) and doxorubicin (**34**), with CV-N (**28**) and HSA. Homohalichondrin B (**22**) was available in-house and showed potent *in vitro* and *in vivo* cytotoxicity. Doxorubicin (**34**) was available commercially. By operating on a proof-of-concept approach, these compounds have provided an excellent starting point for the preparation of the anti-HIV and anti-cancer therapeutics discussed in this thesis. The CV-N- and HSA-norhomohalichondrin B conjugates that were prepared have yet to be fully evaluated *in vitro* and *in vivo*, but there is the distinct possibility that their extreme potency and chemical sensitivity might limit their further development. Somewhat suprisingly, doxorubicin (**34**) too, proved to be a difficult drug due to instability problems.

From the experience gained in this project I would conclude that for these innovative CV-N (**28**) and HSA therapeutics to be viable, a more suitable toxin needs to be incorporated into the construct. The toxin should be more suitable in terms of:

1) Reduced toxicity.
2) Behaving as a prodrug until the conjugate was internalised and the "active" drug was released within the affected cell.
3) Chemical stability. The toxin should be amenable to easy synthetic modification and incorporation into the conjugate, and be stable within systemic circulation.
4) Supply, with a requirement to be readily available on a commercial scale.

Of course it will be very difficult to identify a toxin, be it natural or synthetic, which is ideal in every respect, but a literature search for an alternative revealed large numbers of possible candidates. Five interesting cytotoxic compounds that show potential for further development have been selected for discussion below.

Although homohalichondrin B (**22**) might never progress further as a potential drug, in part due to supply problems, and in part due to toxicity problems, the synthesis of structurally simplified synthetic halichondrin analogues may result in a commercially viable exploitation of the extraordinary cytotoxicity of the polyether macrolide. The

synthetic ketone analogue (**27**)[88] retains the exceptional *in vitro* and *in vivo* activity of the parent halichondrins, but with substantially lower toxicity in *in vivo* trials. The amine functionality could be readily attached to the maleimido-tetrapeptide construct (**40**, prepared in Section **2.4**) *via* an amide bond. However, with the knowledge that the cytotoxic activity resides in the macrocycle, the problem of harnessing the cytotoxicity might remain a problem under a prodrug rationale.

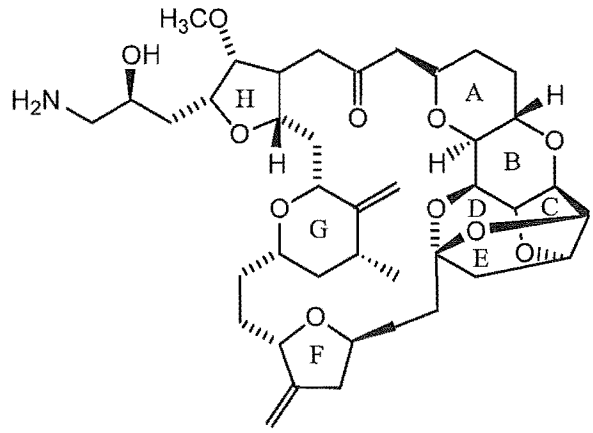

ER-086526 (**27**)

Figure 7.1: *Ketone analogue of halichondrin B, ER-086526.*

Maintaining a New Zealand focus in conjugate development, pateamine A (**66**), a novel sulfur-containing heteroaromatic macrolide with potent *in vitro* cytotoxic activity, is another possibility. This compound was isolated originally from the marine sponge, *Mycale* sp., off the South-West coast of the South Island of New Zealand.[227] Several groups have published synthetic routes towards pateamine A (**66**) and a number of simplified derivatives.[228,229] Interestingly, C3-amino acylated derivatives display a reduced activity from the parent. This suggests that pateamine A (**66**) may well be efficacious as a prodrug in the acylation strategy employed in this project.

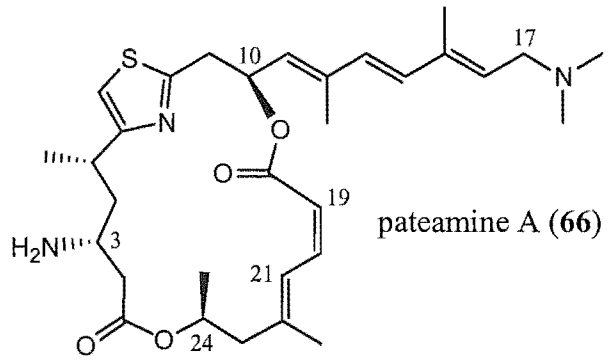

pateamine A (**66**)

Figure 7.2: *The thiazole-containing macrolide, pateamine A.*

At the other end of the spectrum, in terms of structural complexity, 5-fluorouracil (5-fluoro-pyrimidine-2,4-dione) (**67**) is an antimetabolite with a broad spectrum of activity against solid tumours.

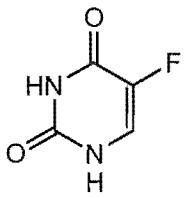

5-fluorouracil (**67**)

Figure 7.3: *5-Fluorouracil.*

Various conjugates of 5-fluorouracil (**67**) and poly(ethylene glycol),[230] dextran[230] or *N*-(2-hydroxypropyl)methacrylamide-based copolymers,[231] have been reported. In these conjugates, 5-fluorouracil (**67**) is linked to the polymer carriers at the α-position of a C-terminal glycine residue of peptide spacers of different amino acid sequences. These conjugates are reported to act as prodrugs and are able to cause a site-specific release of free 5-fluorouracil (**67**) under the action of enzymes occurring in the vicinity of, or inside tumour cells. The release mechanism of 5-fluorouracil (**67**) from the glycine α-carbon stems from the inherent instability of α-substituted glycines.[231] 5-Fluorouracil might be attached to the tetrapeptide construct (**40**, prepared in Section **2.4**) in a similar manner.

Squalamine (**68**) was the first aminosterol isolated from tissues of dogfish shark *Squalus acanthias*.[232] Squalamine (**68**) inhibits angiogenesis and tumour growth in several animal models and is currently in Phase II clinical trial for treatment of non-small cell lung cancer.[233]

Several syntheses of squalamine (**68**) and simplified squalamine analogues have been published. The stereoselective syntheses of squalamine dessulfate analogues that use 7α-aminocholesterol as an intermediate were reported very recently.[233] Compound **69**, for example, exhibits comparable cytotoxicity to the parent compound. The simplicity of the synthetic strategy, and the simplicity of the molecule itself, lends squalamine (**68**), and **69**, to being very attractive options for incorporation into constructs, like those prepared in this project.

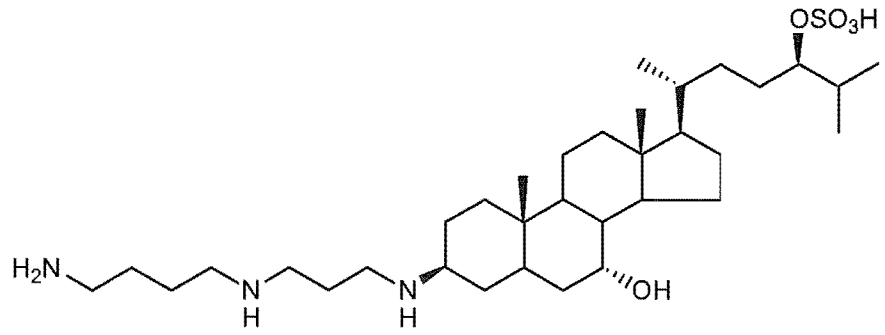

squalamine (**68**)

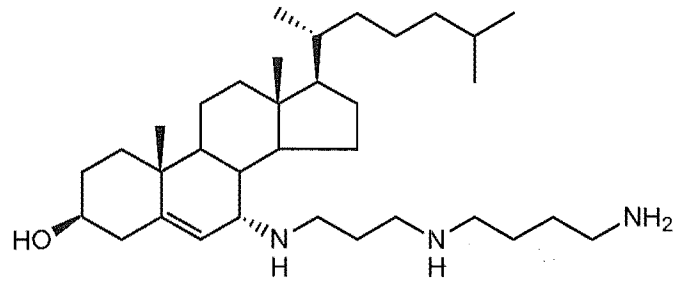

7α-*N*-[3*N*-(4-aminobutyl)aminopropyl]aminocholesterol (**69**)

Figure 7.4: *Structures of squalamine (68) and a dessulfate analogue, 69.*

Targeted delivery of drugs is one of the most actively pursued goals in anti-HIV and anti-cancer chemotherapy. It is evident from the preliminary studies presented in this thesis that both CV-N (**28**) and HSA show enormous potential as macromolecular carriers of toxins, for the targeted treatment of HIV-infected and cancerous cells, respectively. Their further success will hinge upon the selection of a suitable toxin, and a focused effort to understand the details of the biological fate of the conjugates.

8 EXPERIMENTAL

EXPERIMENTAL

8.1 General Methods

8.1.1 Nuclear Magnetic Resonance

NMR spectra were recorded at 23°C on a Varian Unity INOVA-500 spectrometer, operating at 500 MHz and 125 MHz for ^{1}H and ^{13}C, respectively. Other NMR experiments described in this thesis *viz* COSY, and the reverse detected HSQC and CIGAR experiments were recorded on the INOVA 500 spectrometer, at 500 MHz. The spectrometer was fitted with a pulsed field MLD driver with a 5 mm Indirect Detection Probe.

Chemical shifts in this thesis are described in parts per million (ppm), on the δ scale, and were referenced to the appropriate solvent peaks: Chloroform (with 0.1% pyridine for halichondrin-based compounds); $CDCl_3$ (d_1) referenced to $\mathbf{C}HCl_3$ at δ_H 7.26 ppm (^{1}H) and $\mathbf{C}HCl_3$ at δ_C 77.0 ppm (^{13}C); Methanol; CD_3OD (d_4) referenced to $\mathbf{C}HD_2OD$ at δ_H 3.31 ppm (^{1}H) and $\mathbf{C}D_3OD$ at δ_C 49.3 ppm (^{13}C); Dimethylsulphoxide; $(CD_3)_2SO$ (d_6) referenced to $(\mathbf{C}H_3)_2SO$ at δ_H 2.60 ppm (^{1}H) and $(\mathbf{C}H_3)_2SO$ at δ_C 39.6 ppm (^{13}C). Tetramethylsilane (TMS) was used as an internal reference.

^{1}H NMR spectra were recorded using an acquisition time (AT) of 1.892 s; ^{13}C NMR spectra were recorded using an AT of 1.3 s. COSY experiments were recorded using an AT of typically 0.215 s and a relaxation delay (D1) of 1.0 s. HSQC experiments were run with an AT of typically 0.14 s, a D1 of 1.0 s and $^{1}J_{CH}$ of 140 Hz. CIGAR experiments were recorded with an AT of typically 0.250 s, D1 of 1.0 s and $^{n}J_{CH}$ of 8.3 Hz.

8.1.2 Mass Spectrometry

Electrospray ionisation mass spectra (ESI MS) were recorded from a Micromass LCT TOF mass spectrometer, with a probe voltage of 3,200 V at 150°C, a source temperature of 80°C, nebuliser gas flow of 160 L/hr and desolvation gas flow of 520 L/hr. Direct injection used 10 μL of a 10 μg/mL solution. The carrier solvent was 50% CH_3CN/H_2O at a flow rate of 20 μL/min. The cone voltage was typically 25 V unless otherwise stated. This system was controlled by MASSLYNX (Version 4.0) software.

The majority of LC MS samples were analysed with a Waters 2790 HPLC system and a Waters 996 photodiode array (PDA) detector coupled in parallel to a Micromass LCT mass spectrometer equipped with an electrospray ionisation (ESI) probe. Samples were analysed at the same operating conditions as above. Protein samples were analysed with a cone voltage of typically 45 V unless otherwise stated. Non-protein samples were analysed with a cone voltage of 25 V unless otherwise stated. This system was controlled by MASSLYNX (Version 4.0) software. LC MS analysis used one of the following two columns (as stated): Agilent, Zorbax 300SB-C3, 5μ, 2.1 x 150 mm; or Agilent, Zorbax SB-C18, 5μ, 2.1 x 250 mm. A flow rate of 200 μL/min and varying solvent profiles of acetonitrile (Scharlau, Acetonitrile, Multisolvent®, HPLC grade) with water (purified using a MilliQ deionising system), or water with 0.5% formic acid was ultilised. A 9:1 solvent split was employed to deliver 20 μL/min solvent to the mass spectrometer and 180 μL/min solvent to the diode array detector.

A standard HPLC solvent gradient was developed to analyse protein samples on the Zorbax 300SB-C3 column. This was known as the **standard protein LC MS gradient.** The gradient comprised of a 105 minute run with a flow rate of 200 μL/min, and consisted of the following solvent gradient timetable: a slow gradient from 0% - 60% CH_3CN/H_2O (0.5% formic acid) over 80 minutes, followed by ramp in concentration to 100% CH_3CN over five minutes, an isocratic hold on 100% CH_3CN for five minutes and then a restoration to 0% CH_3CN over five minutes. The method was finished with an isocratic hold on 0% CH_3CN over five minutes.

LC MS analysis also took place while a guest at the MTDDP, NCI, Frederick, Maryland, USA (as stated in text). This analysis used an Agilent 1100 series LC MS with an electrospray interface. This system was set with a capillary voltage of 4,000 V, a gas temperature of 350°C, and a drying gas flow of 10 L/min. A fragmentor of 50 V was typically used unless otherwise stated. One of two columns was utilised (as stated), a Zorbax 300SB-C3 (5μ, 2.1 x 150 mm), or a Zorbax SB-C18 (5μ, 2.1 x 150 mm). A flow rate of 200 μL/min and varying solvent profiles of acetonitrile (Scharlau, Acetonitrile, Multisolvent®, HPLC grade) with water (purified using a MilliQ deionising system), or water with acetic acid (varying concentrations, stated) was ultilised.

8.1.3 High Performance Liquid Chromatography

Semi-preparative reverse phase HPLC work described in this thesis was performed on one of two machines (stated). A Shimadzu LC-4A instrument equipped with a Shimadzu UV Spectrotometric Detector SPD-2AS and Hewlett Packard 3390A integrator was used at the Chemistry Department, University of Canterbury, Christchurch, New Zealand. A Phenomenex, Luna column (C18, 100Å, 5μ, 10 x 250 mm) with a flow rate of 5 mL/min and varying solvent profiles consisting of acetonitrile (Scharlau, Acetonitrile, Multisolvent®, HPLC grade) with water (purified using a MilliQ deionising system), or water with 0.5% formic acid was ultilised. Solvents were degassed using a flow of helium.

HPLC purification of CV-N mutant proteins took place while a guest at the MTDP, NCI-Frederick, Frederick, MD, USA and used a BioCAD® Sprint Chromatography System (Applied Biosystems, Inc.) with a reversed phase PRP-3 column (Hamilton, 7 x 305 mm). A flow rate of 2 mL/min and a solvent gradient consisting of acetonitrile (Scharlau, Acetonitrile, Multisolvent®, HPLC grade) (0.1% TFA) with water (purified using a MilliQ deionising system) (0.1% TFA), was used.

Analytical and small-scale preparative work was performed on one of two HPLC systems (stated). The first system was a Shimadzu VP. The complete setup involved a Shimadzu LC-10AC VP liquid chromatograph coupled to a SIL-10A VP auto-injector, a CTO-10A

VP column oven set to 40°C, and a SPD-M10A VP diode array detector. A Shimadzu degasser was utilised for the degassing of all solvents used in this machine. This system was controlled by Shimadzu CLASS-VP (Version 5.023) software.

A Dionex HPLC system was also used. (P680 HPLC pump, ASI 100 automated sample injector, TCC 100 column oven operating at 40°C, UVD 340U diode array detector and an ELSD 800 light scattering mass detector.) A Dionex degasser was utilised for the degassing of all solvents used in this machine. This system was controlled by Chromeleon (Version 6.50 SP3 Build 980) software.

A Phenomenex Prodigy reverse phase column (C18, 5μ, 4.6 x 250 mm) with a flow rate of 1 mL/min and variable concentration gradients of acetonitrile (Scharlau, Acetonitrile, Multisolvent®, HPLC grade) with water (purified using a MilliQ deionising system), or water with 0.05% TFA was ultilised for both analytical HPLC systems.

A standard HPLC gradient was used to analyse samples on these columns. This was known as the **standard HPLC gradient**. The gradient consisted of a 40 minute run with a flow rate of 1ml/min, following a solvent gradient comprised of the following steps: two minutes at 10% CH_3CN/H_2O followed by a linear gradient to 75% CH_3CN/H_2O over a period of 12 minutes, an isocratic hold at 75% CH_3CN/H_2O for ten minutes then a linear gradient to 100% CH_3CN/H_2O over two minutes. 100% CH_3CN/H_2O was maintained for four minutes before the solvent ratio was returned to 10% CH_3CN/H_2O in two minutes. The 10% CH_3CN/H_2O was held for eight minutes to allow the column to re-equilibrate. Depending on the sample (stated) the water was modified with 0.05% TFA.

8.1.4 Other Chromatography

Reverse phase C18 chromatography of doxorubicin and halichondrin containing compounds used Bakerbond spe™ Octadecyl (C18) disposable extraction cartridges. (Reversed phase octadecylsilane bonded to silica gel (40 μm APD, 60Å), 3 mL solid phase extraction column, 500 mg per column.)

Chromatography of proteins used Sephadex® G-25 in glass columns with the dimensions and appropriate solvents stated. The chromatography was visualised by a single beam UV monitor LKB 2238 Uvicord S II (λ 206 nm, time constant = 1, absorbance range = 0.1).

Analytical reverse phase thin layer chromatography (TLC) was carried out on Merck RP-18 R_{254} TLC plates (0.2 mm thickness). Normal phase TLC was performed using Merck silica gel 60 F_{254} aluminium backed sheets (0.2 mm thickness) and Merck DIOL F_{254} glass backed plated (0.2 mm thickness). Some TLC plates were initially visualised under a short-wave UV lamp (λ 254 nm) and then further developed with iodine (I_2), potassium permanganate dip (3 g $KMnO_4$, 20 g K_2CO_3 and 5 mL 5% NaOH in 300 mL H_2O), phosphomolybdic acid (PMA) spray (10% PMA in EtOH, *w/v*) or ninhydrin spray (5% ninhydrin in EtOH, *w/v*).

8.1.5 Solvents

All technical grade solvents were distilled prior to use. Methanol (MeOH) was distilled twice. Dry solvents were obtained using the following standard methods. MeOH was distilled from magnesium metal and iodine and stored over activated molecular sieves (4 Å). Pyridine was refluxed over CaH_2 before distillation. Tetrahydrofuran (THF) was refluxed over sodium metal and benzophenone before distillation directly prior to use. Dichloromethane (DCM) was refluxed over calcium hydride before distillation. DMF was dried by treating twice overnight with 4 Å molecular sieves, followed by storage over 4 Å sieves. Isopropyl alcohol (IPA) was refluxed over calcium hydride for 3 hours before distillation and stored over 4 Å sieves.

The pH 8.0 thiolation **'reaction buffer'** was prepared in distilled water, and consisted of 0.1 M sodium borate, 0.15 M NaCl, and 0.001 M EDTA. Size exclusion columns and maleimide-based reactions were carried out in a **'standard borate buffer'** (pH 7.2, 0.0025 M sodium borate, 0.15 M NaCl). Both the above buffers were degassed thoroughly for 1 hour before use by bubbling argon through the solutions.

8.1.6 Kaiser Test[164]

For SPPS of peptides the Kaiser test was used to determine the presence (or not) of free amines. Several beads from the resin synthesis were removed and washed with 3 x 1 mL EtOH in a small glass vial. The following three stock solutions were made and 3 drops from each were added to the resin ensuring all beads were completely covered in solution.

1) 2.5 g of ninhydrin in 50 mL of EtOH
2) 40 g phenol in 10 mL of EtOH
3) 0.001 M KCN (6.5 g in 100 mL water) and 12 mL of pyridine

The vial was capped and placed in an oven (100°C) for approximately 5 min. A positive result – that is, the presence of a free amine – was indicated by the beads turning blue, while a negative result – no free amine – was shown by no change in colour (beads remain yellow).

8.2 Work Described in Chapter 2

8.2.1 Fmoc-Gly-Resin

All amino acids used in the following preparations were of L-configuration. Wang resin (4-Benzyloxybenzyl alcohol polystyrene, 100-200 mesh, 2 g, 1.5 meq/g, 3 mmol hydroxymethyl groups) and Fmoc-Gly-OH (0.98 g, 3.3 mmol) were dissolved/suspended in dry DMF (20 mL) at RT for 15 minutes. Pyridine (1.67 mL, 20.70 mmol) and 2,6-dichlorobenzoyl chloride (2,6-DCBC, 1.48 mL, 10.35 mmol) were added successively and the suspension was shaken for 15 hours at RT. Fmoc-Gly-Resin was filtered and washed with DMF (3 x 10 mL), IPA (3 x 10 mL) and DCM (3 x 10 mL) before being dried *in vacuo* for 12 hours.

8.2.2 Capping Resin

Fmoc-Gly-Resin was benzoylated with benzoyl chloride (1.35 mL, 12 mmol) and pyridine (1.46 mL, 18 mmol) by shaking in dichloroethane (DCE, 20 mL) for three hours at RT. The resin was filtered and washed with DCE (3 x 10 mL) and DCM (3 x 10 mL), and dried under high vacuum for 12 hours.

8.2.3 Determination of Amino Acid Loading of Fmoc-Gly-Resin

Dry Fmoc-Gly-Resin (0.46 mg) and 20% piperidine in DMF (3 mL) were mixed for two minutes. The absorbance at 290 nm was read in a UV-visible spectrophotometer (Varian Cary 50 Probe). Absorbance = 0.6468. This was repeated with a second sample of Fmoc-Gly-Resin (0.97 mg). Absorbance = 1.4307. 20% piperidine in DMF was used as a solvent blank. The degree of resin loading was determined on basis of a linear relationship between absorbance at 290 nm and the quantity of Fmoc-amino acid present, with one mmol of Fmoc-amino acid giving an absorbance of 1.650. Average loading = 0.873 mmol Fmoc/g resin.

8.2.4 Synthesis of γ-Maleimidobutyric-Gly-Phe-Leu-Gly-OH, (**30**)

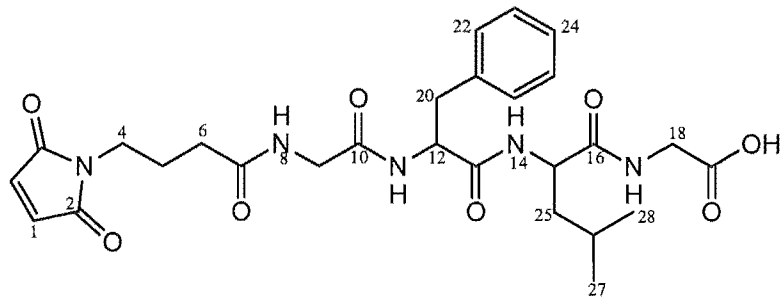

γ-maleimidobutyric-Gly-Phe-Leu-Gly-OH (**30**)

The SPPS of **30** was performed in a glass apparatus fitted with a frit (porosity 3) that allowed bubbling of the resin with N_2 gas from below, and subsequent removal of the solvent by vacuum after each reaction step.

Fmoc-Gly-Resin (2 g, 1.746 mmol) was bubbled with dry DMF (20 mL) for 30 minutes, drained, and bubbled with 20% piperidine/DMF solution (20 mL) for 10 minutes. The resin was filtered by suction for 15 minutes, and then washed with DMF (3 x 20 mL) and IPA (3 x 20 mL). Several beads were removed and analysed using the Kaiser Test (see General Methods, section **7.1.6**). A positive result was recorded, so the resin was washed with further DMF (3 x 20 mL) and the collection flask was replaced to remove filtrate. Fmoc-Leu-OH (1.234 g, 3.492 mmol), HBTU (1.324 g 3.492 mmol), HOBt (0.472 g, 3.492 mmol) and DIPEA (1.22 mL, 6.984 mmol) were combined in DMF (10 mL) for two minutes. This solution was then bubbled with the resin for 60 minutes. The resin was filtered and washed with DMF (3 x 20 mL) and IPA (3 x 20 mL). Several beads were removed and analysed using the Kaiser Test, and a negative result was recorded. The resin was washed again with DMF (3 x 20 mL). The above procedure of coupling and deprotection was repeated for the sequential addition of Fmoc-Phe-OH (1.352 g, 3.492 mmol), Fmoc-Gly-OH (1.038g, 3.492 mmol) and γ-maleimidobutyric acid (0.640 g, 3.492 mmol), with all other reagents remaining the same. The sample was left to dry overnight *in vacuo* inside the glass apparatus, in the presence of P_2O_5. The resin was then bubbled for 20 minutes with 40 mL 95% TFA, 2.5% TES, and 2.5% water, drained and rinsed with TFA (2 x 15 mL). The acidic fractions were combined and alternately concentrated under vacuum and precipitated with water to remove TFA from the solution.

Semi-preparative reverse phase HPLC (Shimadzu LC-4A) was used to purify **30** from the sample. A solvent gradient comprising the following steps was used: an isocratic hold on 15% CH_3CN/H_2O (0.05% TFA) for two minutes; a linear gradient to 50% CH_3CN/H_2O over 20 minutes; a return to 15% CH_3CN/H_2O over one minute; and finally an isocratic hold on 15% CH_3CN/H_2O for two minutes. The system was monitored at 213 nm and a peak eluting at 15.6 minutes was collected manually and the solvent removed under nitrogen gas flow to give **30**. Yield 535 mg (55%) HRESIMS MH^+ 558.2563 ($C_{27}H_{36}N_5O_8$ requires 558.2564) ^1H NMR (500 MHz, CD_3OD) δ 0.89 (d, J_{HH} = 6.5 Hz, 3H, H28), δ 0.93 (d, J_{HH} = 6.5 Hz, 3H, H27), δ 1.62 (m, 3H, H25, H26), δ 1.84 (m, 2H, H5), δ 2.21 (t, J_{HH} = 7.5 Hz, 2H, H6), δ 2.96 (dd, J_{HH} = 8.5, 13.5 Hz, 2H, H20α), δ 3.15 (dd, J_{HH} = 8.5, 13.5 Hz, 2H, H20β), δ 3.50 (m, 2H, H4), δ 3.72 (d, J_{HH} = 16.5 Hz, 2H, H9α), δ 3.80 (d, J_{HH} = 16.5 Hz, 2H, H9β), δ 3.86 (s, 2H, H18), δ 4.41 (m, 1H, H15), δ 4.62 (m, 1H, H12), δ 6.80 (s, 1H, H1), δ 7.23 (m, 3H, H22, H23, H24) amide protons not observed. ^{13}C NMR (CD_3OD) as determined by 2D ^1H NMR experiments: δ 174.4 (C7), δ 173.6 (C19), δ 172.4 (C13), δ 171.5 (C2, C16), δ 171.0 (C10), δ 137.2 (C21), δ 134.3 (C1), δ 129.1 (C22), δ 128.3 (C23), δ 126.7 (C24), δ 55.0 (C12), δ 51.9 (C15), δ 42.5 (C9), δ 40.6 (C18), δ 40.4 (C25), δ 37.0 (C20), δ 36.8 (C24), δ 36.6 (C4), δ 32.2 (C6), δ 24.5 (C26), δ 24.1 (C5), δ 22.3 (C27), δ 20.5 (C28).

8.2.5 Norhomohalichondrin B aldehyde, (**33**)

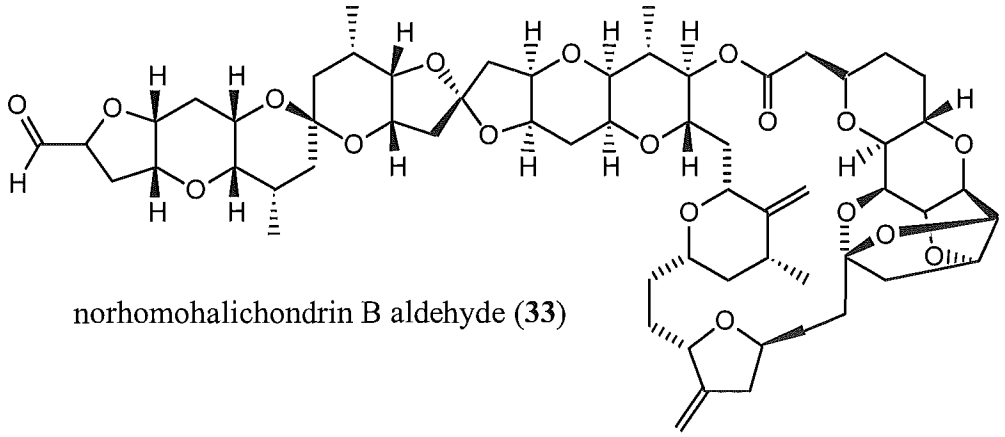

norhomohalichondrin B aldehyde (**33**)

Homohalichondrin B (**22**, 2 mg, 1.8 μmol) was dissolved in MeOH (3 drops) and stirred with aqueous sodium periodate ($NaIO_4$, 1 mL, 30mM) at RT. TLC (DIOL, 5% MeOH/DCM, PMA) was used to monitor the reaction and indicated the reaction was complete after 24 hours by the disappearance of **22** (R_f 0.1) and the appearance of a new

spot (R_f 0.6). The aqueous reaction mixture was extracted with ethyl acetate (3 x 1 mL). The organic fractions were combined and evaporated under nitrogen to give norhomohalichondrin B aldehyde (**33**) in quantitative yield. ^{1}H NMR (500 MHz, $CDCl_3$) was identical to that previously reported (Figure **2.9**).[89] HRESIMS MH^+ 1091.5607 ($C_{60}H_{83}O_{18}$ requires 1091.5579)

8.2.6 Norhomohalichondrin B amine, (**31**)

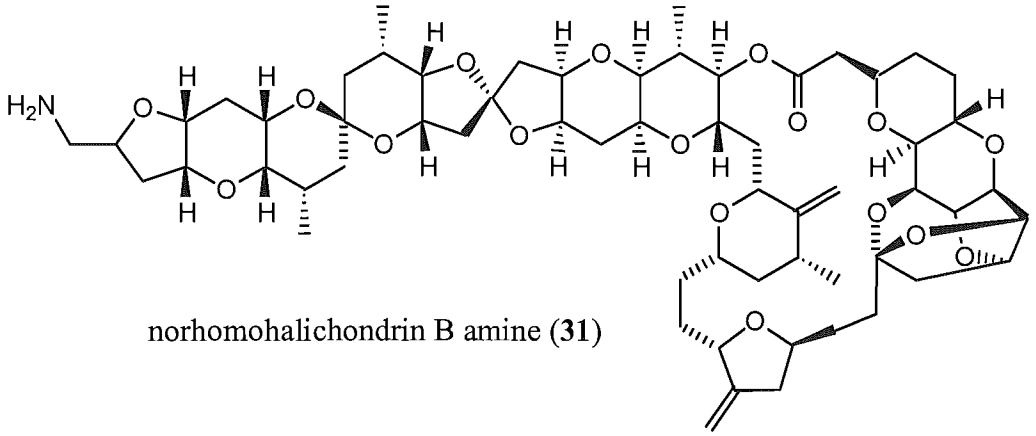

norhomohalichondrin B amine (**31**)

Norhomohalichondrin B aldehyde (**33**, 1.7 mg, 1.6 μmol) and NH_4CH_3COO (12 mg, 160 μmol) were stirred with crushed activated 3 Å molecular sieves in dry MeOH (1 mL, saturated with $(NH_4)_2CO_3$) for 30 minutes. $NaCNBH_3$ (489 μg, 8 μmol) in dry MeOH (100 μL, saturated with $(NH_4)_2CO_3$) was added. A TLC (SiO_2, 10% MeOH/DCM, PMA and ninhydrin) taken after 12 hours of reaction showed the disappearance of the aldehyde (**33**, R_f 0.8, PMA) and the appearance of a spot closer to the baseline (R_f 0.2) that was positive to both ninhydrin and PMA. The reaction solution was diluted with water (10 mL) and passed through a C18 cartridge (see Section **8.1.4**) pre-equilibrated with water, washed with further water (10 mL) and eluted with MeOH (5 mL). The methanol fraction was dried down to provide crude **31** as confirmed by HRESIMS $(MNa)^{2+}$ 557.7884 ($C_{60}H_{85}NO_{17}$ requires 557.7897). Yield 1.5 mg (88%). **31** was acylated (see below) without further purification.

8.2.7 γ-Maleimidobutyric-Gly-Phe-Leu-Gly-norhomohalichondrin B, (**32**)

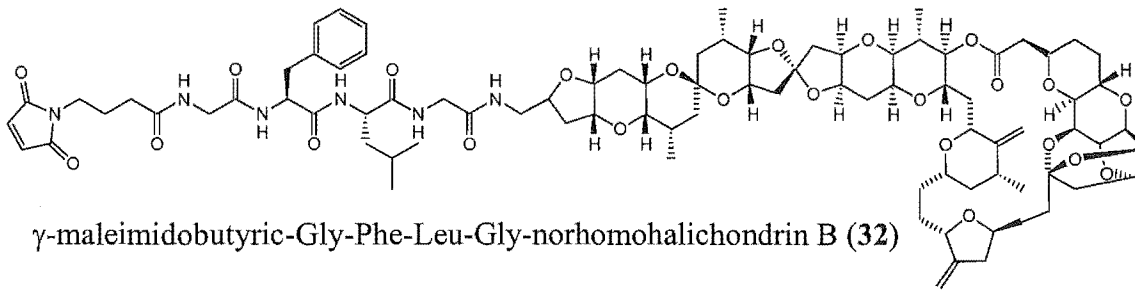

γ-maleimidobutyric-Gly-Phe-Leu-Gly-norhomohalichondrin B (**32**)

30 (858 μg, 1.54 μmol) was activated by stirring, under nitrogen atmosphere, for two minutes with *N*-hydroxysuccinimide (NHS, 322 μg, 2.8 μmol) and dicyclohexylcarbodiimide (DCC, 578 μg, 2.8 μmol) in 1 mL dry THF. (Refluxed over sodium wire and benzophenone.) Norhomohalichondrin B amine (**31**, 1.5 mg, 1.4 μmol) was added to the reaction in dry THF (1 mL). The reaction was left to stir under nitrogen atmosphere for 60 hours at which time analytical HPLC established the reaction was complete. Compound **32** was purified using an analytical reverse phase HPLC system (Agilent 1100) on a Zorbax SB-C18 column (5μ, 2.1 x 150 mm) at a flow rate of 200 μL/min. A solvent gradient comprising the following steps was used (note: no acid used): an isocratic hold on 20% CH_3CN/H_2O for two minutes; a linear gradient to 60% CH_3CN/H_2O over 40 minutes; a linear gradient to 100% CH_3CN/H_2O over two minutes followed by a return to 20% CH_3CN/H_2O over three minutes; and finally an isocratic hold on 20% CH_3CN/H_2O for five minutes. A peak eluting at 33.7 minutes was collected manually and the solvent removed under nitrogen gas flow to give **32**. Insufficient sample (0.4 mg) was obtained for NMR analysis but ESI MS analysis confirmed the preparation of **32**. HRESIMS $(MH)^{2+}$ 816.4157 ($C_{87}H_{119}N_6O_{24}$ requires 816.4177).

8.2.8 Doxorubicin, (**34**)

A reversed phase C18 cartridge (Reversed phase octadecylsilane bonded to silica gel (40 μm APD, 60Å) 3 mL solid phase extraction column, 500 mg per column.) was pre-equilibrated with 0.05% NH_4OH/H_2O (6 mL). 0.05% NH_4OH/H_2O (1.5 mL) was added to doxorubicin hydrochloride (3 mg), resulting in a dark purple solution that was immediately loaded onto the cartridge. The cartridge was washed with 0.05%

NH_4OH/H_2O (5 mL). Washing with acetone (5 mL) eluted **34** in quantitative yield after drying under nitrogen gas flow. ^1H NMR (500 MHz, $(CD_3)_2SO$) was identical to that previously reported.[234] Confirmation was obtained by HRESIMS MH^+ 544.1836 ($C_{27}H_{29}NO_{11}$ requires 544.1819)

8.2.9 γ-Maleimidobutyric-Gly-Phe-Leu-Gly-doxorubicin, (**35**)

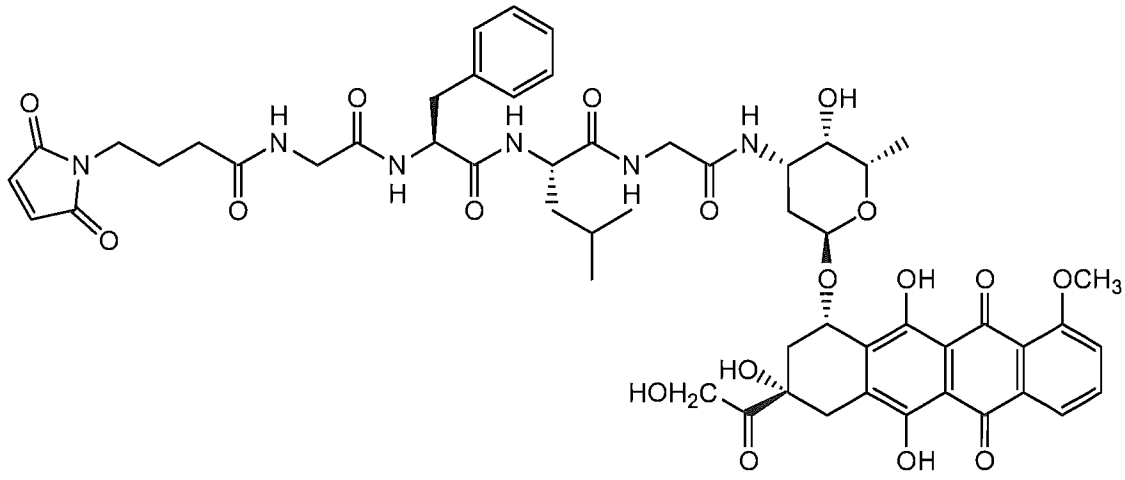

γ-maleimidobutyric-Gly-Phe-Leu-Gly-doxorubicin (**35**)

30 (2.26 mg, 4.1 μmol) was activated by stirring, under nitrogen atmosphere, for two minutes with *N*-hydroxysuccinimide (NHS, 0.82 mg, 7.2 μmol) and dicyclohexylcarbodiimide (DCC, 1.49 mg, 7.2 μmol) in 1 mL dry THF. Doxorubicin (**34**, 2 mg, 3.6 μmol) was added to the reaction in dry THF (1 mL). The reaction was left to stir under nitrogen atmosphere for 24 hours at which time analytical HPLC established the reaction was complete. Compound **35** was purified using an analytical reverse phase HPLC system (Shimadzu VP) at a flow rate of 1 mL/min. A solvent gradient comprising the following steps was used: an isocratic hold on 55% CH_3CN/H_2O (0.05% TFA) for two minutes; a linear gradient to 69% CH_3CN/H_2O over eight minutes; a return to 55% CH_3CN/H_2O over one minute; and finally an isocratic hold on 55% CH_3CN/H_2O for two minutes. A peak eluting at 4.3 minutes was collected manually and the solvent removed under nitrogen gas flow to give **35** as a red solid. HRESIMS MNa^+ 1105.4034 ($C_{54}H_{62}N_6O_{18}Na$ requires 1105.4018) The ^1H NMR spectrum in CD_3OD was assigned as far as possible through comparison with the spectra of **30** and **34** (Figure **2.14**).

8.2.10 γ-Maleimidobutyric-Gly-Phe-Leu-Gly-tyrosinamide, (**37**)

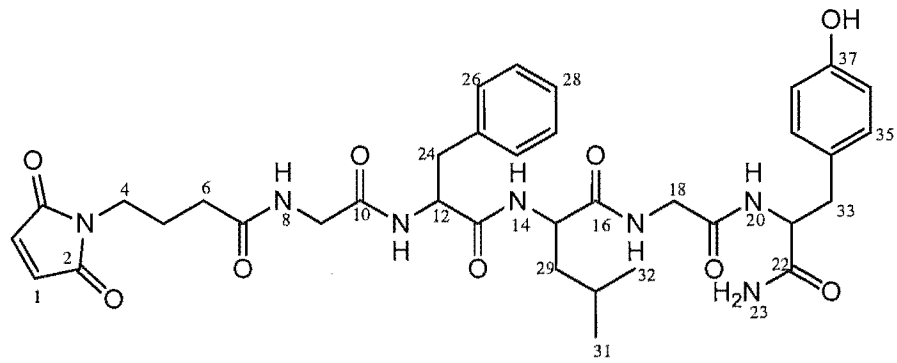

γ-maleimidobutyric-Gly-Phe-Leu-Gly-tyrosinamide (**37**)

30 (3 mg, 0.0054 mmol) was activated by stirring under argon atmosphere for two minutes with *N*-hydroxysuccinimide (NHS, 1.12 mg, 0.0098 mmol) and dicyclohexylcarbodiimide (DCC, 2.02 mg, 0.0098 mmol) in 2 mL dry THF. Tyrosinamide (**36**, 0.88 mg, 0.0049 mmol) was added to the reaction in dry THF (1 mL). The reaction was left to stir under argon atmosphere for 24 hours at which time analytical HPLC established the reaction was complete. Compound **37** was purified from the reaction mixture using a semi-preparative reverse phase HPLC system (Shimadzu LC-4A) at a flow rate of 5 mL/min. A solvent gradient comprising the following steps was used: an isocratic hold on 15% CH_3CN/H_2O (0.05% TFA) for two minutes; a linear gradient to 50% CH_3CN/H_2O over 20 minutes; a return to 15% CH_3CN/H_2O over one minute; and finally an isocratic hold on 15% CH_3CN/H_2O for two minutes. The system was monitored at 213 nm and a peak eluting at 13.8 minutes was collected manually and the solvent removed under nitrogen gas flow to give **37**. HRESIMS MNa^+ 742.3152 ($C_{36}H_{45}N_7O_9Na$ requires 742.3176) ^1H NMR (CD_3OD) δ 0.88 (d, J_{HH} = 6.2 Hz, 3H, H32), δ 0.92 (d, J_{HH} = 6.2 Hz, 3H, H31), δ 1.28 (m, 2H, H29), δ 1.61 (m, 1H, H30), δ 1.83 (m, 2H, H5), δ 2.20 (t, J_{HH} = 7.2 Hz, 2H, H6), δ 2.85 (dd, J_{HH} = 9.0, 14.0 Hz, 2H, H33α), δ 2.98 (dd, J_{HH} = 9.0, 14.3 Hz, 2H, H33β), δ 3.08 (dd, J_{HH} = 5.1, 13.8 Hz, 2H, H24α), δ 3.16 (dd, J_{HH} = 5.4, 14.2 Hz, 2H, H24β), δ 3.49 (m, 2H, H4), δ 3.65 (d, J_{HH} = 16.5 Hz, 2H, H9α*), δ 3.76 (dd, J_{HH} = 13.6, 16.5 Hz, 2H, H18*), δ 3.86 (d, J_{HH} = 16.5 Hz, 2H, H9β*), δ 4.22 (dd, J_{HH} = 4.8, 10.2 Hz, 1H, H15), δ 4.50 (dd, J_{HH} = 5.0, 9.3 Hz, 1H, H21), δ 4.60 (dd, J_{HH} = 5.6, 9.1 Hz, 1H, H12), δ 6.68 (d, J_{HH} = 8.5 Hz, 1H, H36), δ 6.79 (s, 1H, H1), δ 7.07 (d, J_{HH} = 8.8 Hz, 1H, 3H, H35), δ 7.23 (m, H26, H27, H28) amide protons

not observed, *interchangeable. ^{13}C NMR (CD_3OD) as determined by 2D ^{1}H NMR experiments. δ 134.5 (C1), δ 130.2 (C35), δ 129.1 (C26), δ 128.4 (C27), δ 126.8 (C28), δ 115.0 (C36), δ 55.2 (C12), δ 55.2 (C21), δ 52.8 (C15), δ 42.7 (C18*), δ 42.5 (C9*), δ 36.8 (C24), δ 36.7 (C33), δ 36.6 (C4), δ 32.1 (C6), δ 29.4 (C29), δ 27.3 (C30), δ 25.0 (C5), δ 22.3 (C31), δ 20.5 (C32).

8.2.11 Reaction of β-alanine (**39**) with 2-IT (**29**) and γ-Maleimidobutyric acid (**40**)

β-alanine (**39**, 1 mg, 0.01 mmol) was dissolved in reaction buffer (1 mL). 2-IT (**29**, 2.0 mg, 0.015 mmol) was added, the reaction was flushed with argon, capped and left for one hour. γ-maleimidobutyric acid (**40**, 2.7 mg, 0.015 mmol) was added in minimal DMF and the reaction was left for 10 minutes. The reaction mixture was analysed by direct infusion ESI MS.

8.2.12 Size-exclusion Purification of Lysozyme

Lysozyme (200 μg) was dissolved in reaction buffer (200 μL) and chromatographed on a G-25 column (1 x 40 cm) with standard borate buffer. The column was monitored by UV detector set at λ 206 nm, and a peak eluting at V_0 (20 mL, as determined by calibration with blue dextran) was collected (total volume ~4 mL). The sample was concentrated (~1 mL) by evaporation under nitrogen gas flow.

8.2.13 MS Analysis of Lysozyme

Lysozyme solution (10 μL), as prepared in Section **8.2.12**, was directly infused in to the mass spectrometer. No useful MS result was obtained.

Lysozyme solution (40 μL), as prepared in Section **8.2.12**, was analysed by a reversed phase (Agilent, Zorbax 300SB-C3, 5 μ, 2.1 x 150 mm) LC MS system (Waters/Micromass). The solvent gradient comprised of a 105 minute run with a flow rate of 200 μL/min, and consisted of the following solvent gradient timetable: a slow gradient from 0% - 60% CH_3CN/H_2O (0.5% formic acid) over 80 minutes, followed by ramp in concentration to 100% CH_3CN over five minutes, an isocratic hold on 100% CH_3CN for five minutes and then restoration to 0% CH_3CN over five minutes. The method was finished with an isocratic hold on 0% CH_3CN over five minutes. A broad peak eluted at a retention time of ~41-43 minutes. The ESI-mass spectrum and the MaxEnt deconvoluted, neutral-scale mass spectrum of lysozyme, can be seen in Figure **2.20**.

8.2.14 Thiolation of Lysozyme

Lysozyme (200 μg, 0.014 μmol) was dissolved in reaction buffer (200 μL). 2-IT (**29**, 0.07 μmol, 10 μL of 1 mg/mL solution in reaction buffer, freshly made) was added and the mixture was flushed with argon, capped and left for five hours at room temperature. The sample was chromatographed on a G-25 column (1 x 40 cm) and eluted with standard borate buffer (1 mL/min). The column progress was monitored by a single beam UV detector set at λ 206 nm. A peak eluting at V_0 (20 mL) was collected and analysed by LC MS following the method established in Section **8.2.13**. A broad peak eluted after 42 minutes (visible in both TIC and diode array chromatograms). The deconvoluted mass-spectrum of the thiolated protein is presented in Figure **2.22**.

8.2.15 Thiolated Lysozyme and γ-maleimidobutyric acid.

Immediately after LC MS analysis, the sample prepared in Section **8.2.14** was reacted with γ-maleimidobutyric acid (**40**, 12.8 μg, 0.07 μmol, 12.8 μL of 1 mg/mL in DMF). After two hours the sample was concentrated (~1 mL) and analysed by LC MS following the method in Section **8.2.13**. A broad peak eluted at a retention time of ~41 minutes. Analysis of this peak can be seen in Figure **2.23**.

8.2.16 Thiolation Optimisation – Time and Temperature Dependence

Lysozyme (200 μg, 0.014 μmol) was dissolved in reaction buffer (200 μL). 2-IT (**29**, 0.07 μmol, 10 μL of 1 mg/mL solution in reaction buffer, freshly made) was added and the mixture was flushed with argon, capped and left for one hour at room temperature. γ-maleimidobutyric acid (**40**, 12.8 μg, 0.07 μmol, 12.8 μL of 1 mg/mL in DMF) was added *in situ* and the reaction was left for a further two hours. This reaction was repeated a further four times, with the thiolation step left for 5, 12, 24 and 48 hours respectively, before the malemide was added. Each of the samples were analysed by LC MS following the method in Section **8.2.13**. A broad peak eluted at a retention time of ~41 minutes in each case. Mass spectral results are depicted in Figure **2.24**.

The group of time dependent reactions above were repeated at 0°C and analysed in the same manner by LC MS. Deconvoluted mass spectra of these samples are presented in Figure **2.25**.

8.2.17 Characterisation of Thiolation By-product

Benzylamine (**42**, 10 mg, 0.09 mmol) was dissolved in degassed thiolation reaction buffer (1 mL). 2-IT (**29**, 0.09 mmol) was added and the reaction was left to proceed for 24 hours at room temperature. Oily droplets were seen in the reaction mixture. The oily droplets were extracted into ethyl acetate (3 x 2 mL). TLC (silica, 30% MeOH/EtOAc) showed a single UV active spot with R_f 0.83. Benzylamine standard, R_f 0.40. The ethylacetate fraction was evaporated *in vacuo*. HRESIMS, and a number of NMR experiments ($CDCl_3$, ^1H, ^{13}C, HSQC, CIGAR) led to the assignment of the product **44**.

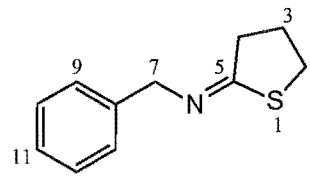

(44)

HRESIMS MH^+ 192.0846 ($C_{11}H_{14}NS$ requires 192.0847) ^1H NMR ($CDCl_3$, 500 MHz) δ 2.14 (p, J_{HH} = 5.0, 10.0 Hz, 2H, H3), δ 2.73 (t, J_{HH} = 5.0 Hz, 2H, H2), δ 3.27 (t, J_{HH} = 6.5

Hz, 2H, H4), δ 4.40 (s, 2H, H7), δ 7.34 (m, 5H, H9-11). ^{13}C NMR ($CDCl_3$, 75 MHz) δ 139.5 (C8), δ 128.4 (C9), δ 128.0 (C10), δ 126.8 (C11), δ 61.5 (C7), δ 39.0 (C2), δ 33.9 (C4), δ 26.9 (C3).

8.2.18 Thiolation Optimisation – Ratio of 2-IT (**29**)

Lysozyme (200 μg, 0.014 μmol) was dissolved in reaction buffer (200 μL). 2-IT (**29**, 0.07 μmol, 10 μL of 1 mg/mL solution in reaction buffer, freshly made) was added and the mixture was flushed with argon, capped and left for 12 hours at 0°C. γ-Maleimidobutyric acid (**40**, 12.8 μg, 0.07 μmol, 12.8 μL of 1 mg/mL in DMF) was added *in situ* and the reaction was left for a further two hours. This reaction was repeated a further four times with 2-IT (**29**, 0.14 μmol, 0.35 μmol, 0.7 μmol and 1.4 μmol). Equal equivalents of γ-maleimidobutyric acid (**40**) were added after 12 hours. Each of the samples were analysed by LC MS following the method in Section **8.2.13**. A broad peak eluted at a retention time of ~41 minutes in each case (Figure **2.27**). Mass spectral results are depicted in Figure **2.28**.

8.3 Work Described in Chapter 3

8.3.1 LC MS of CV-N (**28**)

CV-N solution (10 μL of 1 mg/mL in 0.9% saline solution) was analysed by a reversed phase (Agilent, Zorbax SB-C18, 5 μ, 2.1 x 250 mm) LC MS system (Waters/Micromass) employing the standard protein LC MS gradient. The resultant diode array and TIC chromatograms are presented in Figure **3.2**. Analysis of the ESI-mass spectral data of the single peak (~46.5 minutes) is shown in Figure **3.3**.

8.3.2 Modification of CV-N (**28**)

8.3.2.1 A Model System – 2-IT (**29**) and γ-Maleimidobutyric acid (**40**)

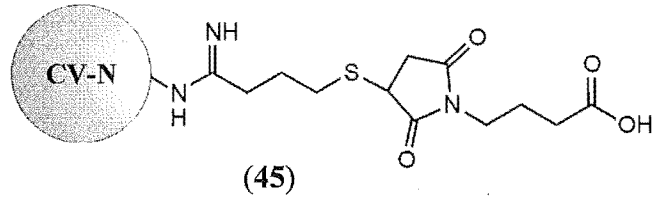

(**45**)

CV-N (**28**, 100 μg, 100 μL of 1 mg/mL in 0.9% saline solution, 9.1 nmol) was diluted with reaction buffer (50 μL) and kept at 0°C. 2-IT (**29**, 6 μL of 1 mg/mL in reaction buffer, 45.5 nmol) was added to the protein solution. The reaction vial was flushed with argon, capped, and held at 0°C. γ-Maleimidobutyric acid (**40**, 8.3 μL of 1 mg/mL in DMF, 45.5 nmol) was added *in situ* after 12 hours. This reaction procedure was repeated a further four times with varying amounts of 2-IT (**29**, 12.5 μL of 1 mg/mL in reaction buffer, 91 nmol; 31.5 μL of 1mg/mL in reaction buffer, 0.23 μmol; 63 μL of 1 mg/mL in reaction buffer, 0.46 μmol; and 125 μL of 1 mg/mL in reaction buffer, 0.91 μmol). Equal equivalents of γ-maleimidobutyric acid (**40**, 16.7 μL of 1 mg/mL in DMF, 91 nmol; 21 μL of 2 mg/mL in DMF, 0.23 μmol; 42 μL of 2 mg/mL in DMF, 0.46 μmol; and 42 μL of 4 mg/mL in DMF, 0.91 μmol) were added after 12 hours. Each of the samples were analysed by LC MS following the method in Section **8.2.13**. The diode array chromatograms of the LC MS analyses are presented in Figure **3.5**, with selected MaxEnt deconvoluted mass spectral data shown in Figure **3.6**.

CV-N (**28**, 100 μg, 100 μL of 1 mg/mL in 0.9% saline, 9.1 nmol) was diluted with reaction buffer (87.5 μL) and the sample was kept at 0°C. 2-IT (**29**, 12.5 μL of 1 mg/mL in reaction buffer, 91 nmol) was added and the mixture was flushed with argon, capped, and left for one hour at 0°C. The sample was chromatographed on a G-25 column (1 x 40 cm) and eluted with standard borate buffer (1 mL/min). The column progress was monitored by a single beam UV detector (λ 206 nm). A peak eluting at V_0 (20 mL) was collected and reacted directly with γ-maleimidobutyric acid (**40**, 16.7 μL of 1 mg/mL in DMF, 91 nmol) for two hours. This reaction was repeated a further four times, with the thiolation step left for 5, 12, 24 and 48 hours respectively, before the maleimide was added. Each of the samples were analysed by LC MS following the method in Section **8.2.13**. An example mass spectral result is presented in Figure **3.7**.

8.3.2.2 A Model System – 2-IT (**29**) and F-150 (**46**)

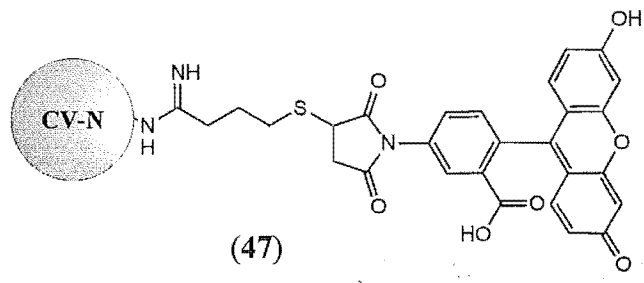

(**47**)

CV-N (**28**, 200 μg, 200 μL of 1 mg/mL in 0.9% saline, 18.2 nmol) was diluted with reaction buffer (187.5 μL) and the sample was kept at 0°C. 2-IT (**29**, 25 μL of 1 mg/mL in reaction buffer, 182 nmol) was added and the mixture was flushed with argon, capped, and left for one hour at 0°C. The sample was chromatographed on a G-25 column (1 x 40 cm) and eluted with standard borate buffer (1 mL/min). The column progress was monitored by a single beam UV detector (λ 206 nm). A peak eluting at V_0 (20 mL) was collected and reacted directly with F-150 (**46**, 39 μL of 2 mg/mL in DMF, 182 nmol) and for two hours. The reaction mixture was concentrated under nitrogen gas flow (~500 μL) and purified on a G-25 column as described above. The two fluorescent bands eluting from the column (~20 minutes and ~35 minutes) were collected and analysed by reverse phase LC MS (Agilent, Zorbax, C18) using the standard protein LC MS gradient. The TIC chromatogram is presented in Figure **3.10**, and mass spectra of the conjugate are shown in Figure **3.11**.

8.3.3 Tryptic Digestion of Native CV-N (**28**)

CV-N (**28**, 100 μg, 100 μL of 1 mg/mL in 0.9% saline solution) was diluted with ammonium bicarbonate buffer (8mM, pH 8, 100 μL). TPCK treated trypsin (10% by weight to analyte protein, 10 μg, 10 μL of 1 mg/mL in 1% acetic acid) was added and the digest was left at 37°C for 24 hours. The digest was analysed by LC MS (Waters/Micromass, Zorbax, SB-C18, standard protein LC MS gradient). See Figure **3.12** for the TIC ES+ chromatogram. The ESI MS data was processed as discussed in Section **3.4.1**. The relevant ESI MS data from this digest, and the assignment of peptide fragments can be seen in Table **3.1**. The assigned peptide fragments are mapped against the amino acid sequence of CV-N (**28**) in Figure **3.16**.

8.3.4 Tryptic Digestion of CV-N-Maleimidobutyric acid Conjugate (**45**)

The singly-derivatised CV-N-maleimidobutyric acid conjugate (**45**) prepared in Section **8.3.2.1** was concentrated to ~100 μL by evaporation under nitrogen gas flow. TPCK treated trypsin (10% by weight to analyte protein, 10 μg, 10 μL of 1 mg/mL in 1% acetic acid) was added and the digest was left at 37°C for 24 hours. The digest was analysed by LC MS (Waters/Micromass, Zorbax, SB-C18, standard protein LC MS gradient). The ESI MS data was processed as discussed in Section **3.4.2**. The relevant ESI MS data from this digest, and the assignment of peptide fragments can be seen in Table **3.2**. The assigned peptide fragments are mapped against the amino acid sequence of CV-N (**28**) in Figure **3.16**.

8.3.5 Tryptic Digestion of CV-N-F150 Conjugate (**47**)

The CV-N-F-150 conjugate (**47**) prepared in Section **8.3.2.2** was concentrated to ~100 μL by evaporation under nitrogen gas flow. TPCK treated trypsin (10% by weight to analyte protein, 10 μg, 10 μL of 1 mg/mL in 1% acetic acid) was added and the digest was left at 37°C for 24 hours. The digest was analysed by LC MS (Waters/Micromass, Zorbax, SB-C18, standard protein LC MS gradient). The ESI MS data was processed as discussed in

Section **3.4.3**. The relevant ESI MS data from this digest, and the assignment of peptide fragments can be seen in Table **3.3**. The assigned peptide fragments are mapped against the amino acid sequence of CV-N (**28**) in Figure **3.16**.

8.3.6 Preparation of CV-N-Tyrosinamide Conjugate (**48**)

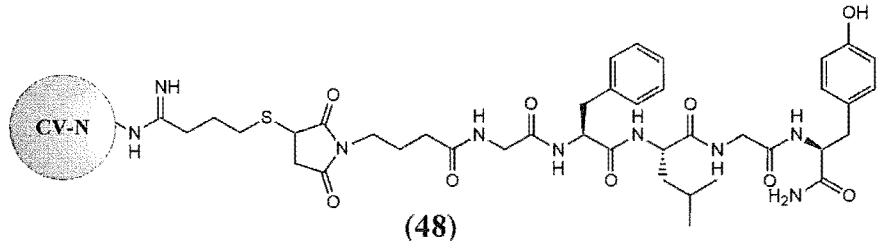

(48)

CV-N (**28**, 400 μg, 400 μL of 1 mg/mL in 0.9% saline solution, 36 nmol) was diluted with reaction buffer (150 μL) and held at 0°C. 2-IT (**29**, 50 μL of 1 mg/mL in reaction buffer, 360 nmol) was added. The reaction was flushed with argon, capped and left at 0°C for 12 hours. The sample was chromatographed on a G-25 column (1 x 40 cm), eluting with standard borate buffer (1 mL/min), and monitored by a diode array detector (λ 206 nm). The protein component eluting at the void volume (~20 mL) was collected and reacted directly with γ-maleimidobutyric-Gly-Phe-Leu-Gly-tyrosinamide (**37**, 52 μL of 1 mg/mL in DMF, 72 nmol) at 0°C. After two hours the sample was concentrated (~600 μL) by evaporation under nitrogen gas flow, and chromatographed on G-25 as above. The protein component, eluting at V_0 (~20 mL) was collected and analysed by LC MS (Waters/Micromass, Zorbax, SB300-C3, standard protein LC MS gradient). The TIC chromatogram of this analysis is shown in Figure **3.18**. The protein sample was once again concentrated (~500 μL) under nitrogen gas flow. Aliquots (40 μL) of this mixture were purified using the LC MS method above, with manual collection of the required peak. The purification was guided by MS analysis, with ~10% of the sample directed to the mass spectrometer, and ~90% collected. The TIC ES+ chromatogram and the deconvoluted mass spectrum of the purified CV-N-tyrosinamide conjugate (**48**), are shown in Figure **3.19** and **3.20** respectively.

8.4 Work Described in Chapter 4

8.4.1 Purification of Mutant CV-N Proteins

Four recombinantly produced mutant CV-N proteins were supplied by Nektar™ Therapeutics. These were CV-N: K3R (**49**, 6.5 mg/mL); CV-N: K3R, K48R (**50**, 3.63 mg/mL); CV-N: K3R, K48R, K74R (**51**, 4.55 mg/mL); and CV-N: K3R, K48R, K74R, K84R (**52**, 10.58 mg/mL).

The four proteins samples (**49**, **50**, **51**, **52**) were each diluted with double distilled H_2O (0.1% TFA, 1 mg/mL). These samples were purified using semi-preparative reverse phase (PRP-3, 305 x 7mm) HPLC. This was completed at a flow rate of 2 mL/min using a solvent gradient comprised of the following steps: a five minute wash with 100% H_2O (0.1% trifluoroacetic acid (TFA)), followed by a slow linear gradient to 60% CH_3CN/H_2O (0.1% TFA) over 28 minutes, then a linear gradient to 100% CH_3CN (0.1% TFA) over 5 minutes, with a final hold on 100% CH_3CN (0.1% TFA) 7 minutes; and monitored at λ 210 nm and λ 280 nm. The sample was purified over multiple injections (1 mL aliquots). The major component eluted at 27 minutes in each case and was collected using a fraction collector (1/minute). The fractions containing the major component were combined and taken to dryness under a flow of nitrogen gas. Purified mass: **49**, ~26.3 mg; **50**, ~3.7 mg; **51**, ~7.4 mg; **52**, 9.9 mg. Each protein was reconstituted in distilled water (1 mg/mL) for storage.

LC MS (Agilent 1100, Zorbax-C3, 2.1 x 150 mm) confirmed the exact mass and purity of each sample (See Section **4.2.1**, Figure **4.1** and Figure **4.2**). The method comprised of a 40 minute run with a flow rate of 200 µL/min, and consisted of the following solvent gradient timetable: a linear gradient from 0% - 60% CH_3CN/H_2O (5% acetic acid) over 30 minutes, followed by ramp in concentration to 100% CH_3CN over two minutes and an isocratic hold on 100% CH_3CN for three minutes, followed by a restoration to 0% CH_3CN over five minutes.

8.4.2 Tryptic Digestion of CV-N: K3R, K48R, K74R (**51**)

CV-N: K3R, K48R, K74R (**51**, 100 μg, 100 μL of 1 mg/mL in distilled H_2O), purified in Section **8.4.1**, was diluted with ammonium bicarbonate buffer (8 mM, pH 8, 100 μL). TPCK treated trypsin (10% by weight to analyte protein, 10 μg, 10 μL of 1 mg/mL in 1% acetic acid) was added and the digest was left at 37°C for 24 hours. The digest was analysed by LC MS (Waters/Micromass, Zorbax, SB-C18, standard protein LC MS gradient). The ESI MS data was processed as discussed in Section **3.4**. The relevant ESI MS data from this digest, and the assignment of peptide fragments can be seen in Table **4.2**.

8.4.3 Tryptic Digestion of CV-N: K3R, K48R, K74R, K84R (**52**)

CV-N: K3R, K48R, K74R, K84R (**52**, 100 μg, 100 μL of 1 mg/mL in distilled H_2O), purified in Section **8.4.1**, was diluted with ammonium bicarbonate buffer (8 mM, pH 8, 100 μL). TPCK treated trypsin (10% by weight to analyte protein, 10 μg, 10 μL of 1 mg/mL in 1% acetic acid) was added and the digest was left at 37°C for 24 hours. The digest was analysed by LC MS (Waters/Micromass, Zorbax, SB-C18, standard protein LC MS gradient). The ESI MS data was processed as discussed in Section **3.4**. The relevant ESI MS data from this digest, and the assignment of peptide fragments can be seen in Table **4.1**.

8.4.4 CV-N: K3R, K48R, K74R, K84R (**52**) and F-150 (**46**)

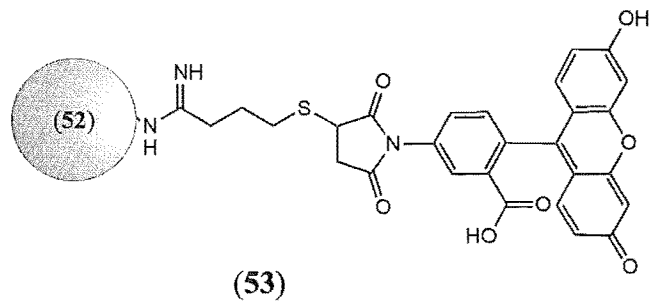

(**53**)

CV-N: K3R, K48R, K74R, K84R (**52**, 200 μg, 200 μL of 1 mg/mL in distilled H_2O, 18.0 nmol) was diluted with reaction buffer (138 μL) and the sample was kept at 0°C. 2-IT

(**29**, 62 µL of 1 mg/mL in reaction buffer, 450 nmol) was added and the mixture was flushed with argon, capped, and left for 12 hours at 0°C. The sample was chromatographed on a G-25 column (1 x 40 cm) and eluted with standard borate buffer (1 mL/min). The column progress was monitored by a single beam UV detector (λ 206 nm). A peak eluting at V_0 (20 mL) was collected and reacted directly with F-150 (**46**, 15 µL of 1 mg/mL in DMF, 36.0 nmol) for two hours. The reaction mixture was concentrated under nitrogen gas flow (~200 µL) and purified on a G-25 column as described above. The two fluorescent bands eluting from the column (~20 minutes and ~35 minutes) were collected and analysed by reverse phase LC MS (Agilent, Zorbax, C18) using the standard protein LC MS gradient. An expanded region of the TIC chromatogram, and the diode array at λ 450 nm, is presented in Figure **4.4**, and mass spectrum of the conjugate is shown in Figure **4.5**. The protein sample was once again concentrated (~200 µL) under nitrogen gas flow. Aliquots (40 µL) of this mixture were purified using the LC MS method above, with manual collection of the peak at 44.5 minutes. The purification was guided by MS analysis, with ~10% of the sample directed to the mass spectrometer, and ~90% collected.

8.4.5 CV-N: K3R, K48R, K74R, K84R (**52**) and γ-Maleimidobutyric-Gly-Phe-Leu-Gly-norhomohalichondrin B (**32**)

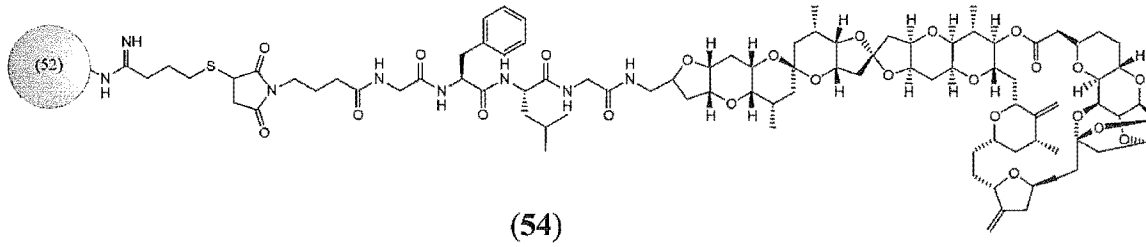

(**54**)

CV-N: K3R, K48R, K74R, K84R (**52**, 4.5 mg, 450 µL of 1 mg/mL in distilled H_2O, 0.4 µmol) was taken to dryness by evaporation and then reconstituted in reaction buffer (4.5 mL) and kept at 0°C. 2-IT (**29**, 1.4 mg, 10 µmol) was added, the mixture was flushed with argon, capped, and left for 12 hours at 0°C. The sample was chromatographed on a G-25 column (2.5 x 40 cm) and eluted with standard borate buffer (3 mL/min), and visualised with a diode array detector (λ 280 nm). The protein fraction was collected after 19 minutes. This fraction was concentrated (~4 mL) by centrifugation in a centriprep

concentrator (YM-3 regenerated cellulose 3000 MW). γ-Maleimidobutyric-Gly-Phe-Leu-Gly-norhomohalichondrin B (**32**, Section **2.4.1**, 0.4 μmol, 65 μL of 10 mg/mL in DMF) was added, and left at 0°C overnight. LC MS analysis (Agilent 1100, Zorbax C3, 2.1 x 150 mm) confirmed that the reaction was complete at this point. A solvent gradient comprising the following steps was used: a linear gradient from 20-45% CH_3CN/H_2O (0.5% acetic acid) over 25 minutes; a linear gradient to 100% CH_3CN over five minutes; isocratic at 100% CH_3CN for five minutes; and then a return to 20% CH_3CN/H_2O over five minutes. The TIC chromatogram is presented in Figure **4.7**. Unreacted protein eluted at 15.7 minutes, and the conjugate, **54**, eluted at 21.2 minutes (Figure **4.8**). The sample was concentrated by evaporation under nitrogen flow (~1 mL). Conjugate **54** was purified by disconnecting the mass spectrometer, and following the diode array chromatogram (280 nm), collecting the peak at 21.2 minutes. Multiple injections (50 μL) were made. The collected fraction was dried down under nitrogen immediately (~300 μg), and reconstituted in double distilled H_2O (750 μL). Reanalysis of the purified sample (LC MS method above) demonstrated a single component was present.

8.4.6 Amino Acid Analysis of **54**

Amino acid analysis and protein quantitation was performed by staff in the Protein Chemistry Laboratory at the NCI-Frederick, MD, USA.

Conjugate **54** (50 μL of 750 μL solution prepared in Section **8.4.5**) was submitted for analysis. Using the amino acid concentrations, the conjugate was quantitated at 50.8 μg in the 750 μL solution. This analysis also confirmed the ratio of one biolinker (Gly-Phe-Leu-Gly) to one protein molecule.

8.4.7 Amino Acid Sequencing of **54**

Amino Acid sequencing was performed by an Applied Biosystems Procise Sequencer at the MTDP, NCI-Frederick, Frederick, MD, USA. Conjugate **54** (12.5 μL of 750 μL

solution prepared in Section **8.4.5**, 65.7 pmol as determined above) was submitted for analysis. The first nine amino acids were sequenced as LGRFNQXAYN.

8.4.8 Tryptic Digest of **54**

CV-N: K3R, K48R, K74R, K84R-norhomohalichondrin B (**54**, 4.2 μg, 62.5 μL of 750 μL solution from Section **8.4.5**) was diluted with ammonium bicarbonate buffer (8 mM, pH 8, 100 μL). TPCK treated trypsin (2.5 μg, 2.5 μL of 1 mg/mL in 1% acetic acid) was added and the digest was left at 37°C for 24 hours. DTT (20 μg) was added to the digest. The digest was analysed by LC MS (Agilent, Zorbax, SB-C18 2.1 x 150 mm, 200 μL/min) using the following solvent gradient: 100% H_2O (0.5% acetic acid) for 15 minutes; a linear gradient to 40% CH_3CN (0.5% acetic acid) over 135 minutes followed by a gradient to 100% CH_3CN (0.5% acetic acid) over 15 minutes. The ESI MS data was processed as discussed in Section **3.4**. The relevant ESI MS data from this digest, and the assignment of peptide fragments can be seen in Figure **4.9** and Table **4.3**.

8.4.9 CV-N: K3R, K48R, K74R, K84R (**52**) and γ-maleimidobutyric-Gly-Phe-Leu-Gly-doxorubicin (**35**)

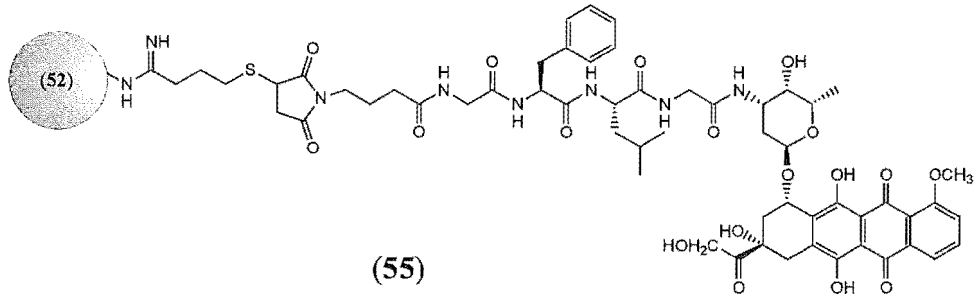

(**55**)

CV-N: K3R, K48R, K74R, K84R (**52**, 200 μg, 200 μL of 1 mg/mL in distilled H_2O, 18.0 nmol) was diluted with reaction buffer (138 μL) and the sample was kept at 0°C. 2-IT (**29**, 62 μL of 1 mg/mL in reaction buffer, 450 nmol) was added and the mixture was flushed with argon, capped, and left for 12 hours at 0°C. The sample was chromatographed on a G-25 column (1 x 40 cm) and eluted with standard borate buffer (1 mL/min). The column progress was monitored by a single beam UV detector (λ 206 nm).

A peak eluting at V_0 (20 mL) was collected and reacted directly with γ-maleimidobutyric-Gly-Phe-Leu-Gly-doxorubicin (**35**, 39 μL of 1 mg/mL in DMF, 36.0 nmol) for two hours. The reaction mixture was concentrated under nitrogen gas flow (~200 μL) and purified on a G-25 column as described above. A pale pink band (~20 minutes) was collected and analysed by LC MS (Micromass/Waters, Zorbax-C3, standard protein LC MS gradient). The TIC chromatogram is illustrated in Figure **4.11**. The sample was analysed by LC MS in the same manner, 10 and 24 hours after preparation. An overlay of the TIC chromatograms from these analyses is shown in Figure **4.13**. Selected MaxEnt deconvoluted ESI MS data is presented in Figure **4.12**.

8.4.10 CV-N: K3R, K48R, K74R (**51**) and F-150 (**46**)

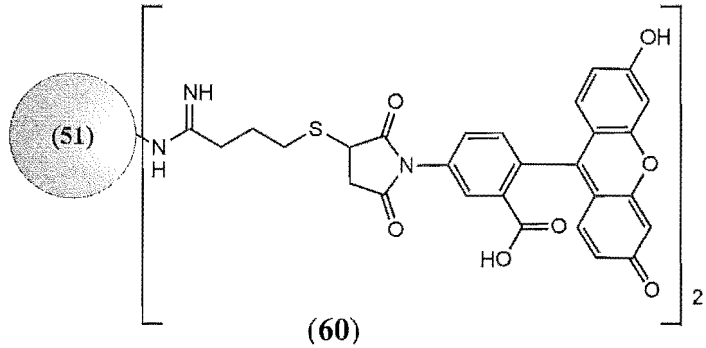

(60)

CV-N: K3R, K48R, K74R (**51**, 200 μg, 200 μL of 1 mg/mL in distilled H_2O, 18.0 nmol) was diluted with reaction buffer (114 μL) and the sample was kept at 0°C. 2-IT (**29**, 86 μL of 1 mg/mL in reaction buffer, 630 nmol) was added and the mixture was flushed with argon, capped, and left for 12 hours at 0°C. The sample was chromatographed on a G-25 column (1 x 40 cm) and eluted with standard borate buffer (1 mL/min). The column progress was monitored by a single beam UV detector (λ 206 nm). A peak eluting at V_0 (20 mL) was collected and reacted directly with F-150 (**46**, 15 μL of 2 mg/mL in DMF, 72.0 nmol) for two hours. The reaction mixture was concentrated under nitrogen gas flow (~200 μL) and purified on a G-25 column as described above. The two fluorescent bands eluting from the column (~20 minutes and ~35 minutes) were collected and analysed by reverse phase LC MS (Agilent, Zorbax, C18) using the standard protein LC MS gradient. An expanded region of the TIC chromatogram, and the diode array at λ 450 nm, is presented in Figure **4.17**, and the mass spectrum of the conjugate is shown in Figure **4.18**. The protein sample was once again concentrated (~200 μL) under nitrogen gas flow.

Aliquots (40 μL) of this mixture were purified using the LC MS method above, with manual collection of the peak at 45.4 minutes. The purification was guided by MS analysis, with ~10% of the sample directed to the mass spectrometer, and ~90% collected. The mass of purified conjugate was not determined.

8.4.11 CV-N: K3R, K48R, K74R (**51**) and γ-Maleimidobutyric-Gly-Phe Leu-Gly-norhomohalichondrin B (**32**)

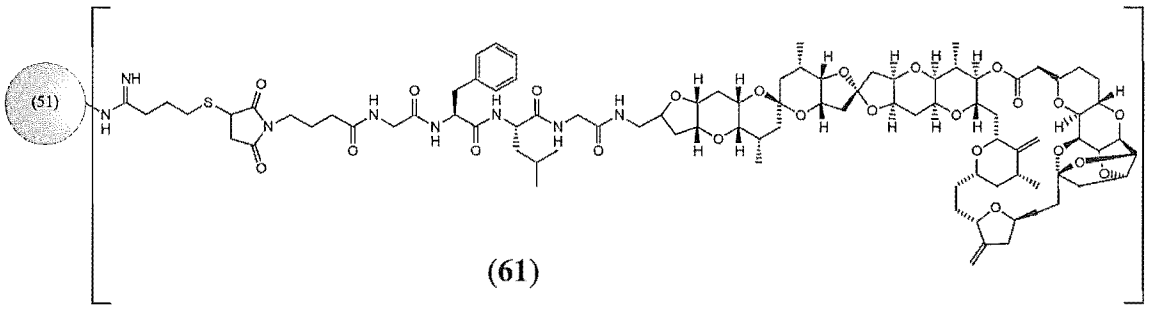

(61)

CV-N: K3R, K48R, K74R (**51**, 200 μg, 200 μL of 1 mg/mL in distilled H_2O, 18.0 nmol) was diluted with reaction buffer (114 μL) and the sample was kept at 0°C. 2-IT (**29**, 86 μL of 1 mg/mL in reaction buffer, 630 nmol) was added and the mixture was flushed with argon, capped, and left for 12 hours at 0°C. The sample was chromatographed on a G-25 column (1 x 40 cm) and eluted with standard borate buffer (1 mL/min). The column progress was monitored by a single beam UV detector (λ 206 nm). A peak eluting at V_0 (20 mL) was collected and reacted directly with γ-Maleimidobutyric-Gly-Phe-Leu-Gly-norhomohalichondrin B (**32**, Section **2.4.1**, 72 nmol, 59 μL of 2 mg/mL in DMF) for 10 hours. The sample was concentrated (~ 200 μL) under nitrogen gas flow and purified on a G-25 column in the same manner as above, using distilled H_2O as the eluant. A peak (~20 minutes) was collected, concentrated (~200 μL), and analysed by LC MS (standard protein LC MS gradient, 0.1% formic acid). The TIC chromatogram is presented in Figure **4.20**. Aliquots (40 μL) of this mixture were purified using the LC MS method above, with manual collection of the peak at 58.5 minutes. The purification was guided by MS analysis, with ~10% of the sample directed to the mass spectrometer, and ~90% collected. The mass of purified conjugate was not determined. The mass spectrum of the purified conjugate (**61**) is shown in Figure **4.21**.

8.5 Work Described in Chapter 5

8.5.1 MS analysis of HSA (Sigma®)

HSA was initially sourced from Sigma® (97-99%, Lyophilized powder, purified by 1x crystallisation).

HSA (Sigma®, 2 nmol, 10 μL of a 13.3 mg/mL solution in borate buffer (0.0025 M sodium borate, 0.15 M NaCl, pH 7.2)) was directly infused into the mass spectrometer. No useful MS result was obtained.

HSA (Sigma®, 0.6 nmol, 40 μL of a 1 mg/mL solution in borate buffer (0.0025 M sodium borate, 0.15 M NaCl, pH 7.2)) was analysed by a reversed phase (Agilent, Zorbax 300SB-C3, 5 μ, 2.1 x 150 mm) LC MS system (Waters/Micromass) employing a short solvent gradient method (20-50% CH_3CN/H_2O (0.5% formic acid)) over 15 minutes. A broad peak eluted at a retention time of ~10-13 minutes. No useful MS result was obtained.

HSA (Sigma®, 0.6 nmol, 40 μL of a 1 mg/mL solution in borate buffer (0.0025 M sodium borate, 0.15 M NaCl, pH 7.2)) was analysed by a reversed phase (Agilent, Zorbax 300SB-C3, 5 μ, 2.1 x 150 mm) LC MS system (Waters/Micromass). The standard protein LC MS gradient (Section **8.1.2**) was employed. A broad peak eluted at a retention time of ~47-51 minutes. The ESI-mass spectrum and the MaxEnt deconvoluted, neutral-scale mass spectrum, of HSA (Sigma®), can be seen in Figure **5.5**.

8.5.2 HSA (Sigma®) and F-150 (**46**)

HSA (Sigma®, 400 μg, 6 nmol) was dissolved in borate buffer (400 μL, 0.0025 M sodium borate, 0.15 M NaCl, pH 7.2). F-150 (**46**, 12.8 μL of 1 mg/mL in DMF, 30 nmol) was added and the reaction was left at RT for 24 hours. The reaction mixture was then chromatographed on a G-25 column (Sephadex®, 1 x 40 cm) with distilled water (1 mL/min) and visualised with a diode array detector set at 206 nm. Two fluorescent yellow

bands eluted down the column, one at the void volume (V_0, approximately 20 mL), and the other 15 mL later. Both fluorescent bands were collected, and analysed by LC MS (Agilent, Zorbax, C3) using the standard protein LC MS gradient. The first fraction showed a single broad peak at a retention time of ~50 minutes with an absorbance at λ 440 nm. No useful MS result was obtained. The second fluorescent fraction presented a peak at a retention time of 34 minutes and was determined to be unreacted F-150 (**46**).

8.5.3 LC MS analysis of HSA (Pharma Dessau, FRG)

An alternative source of HSA came from Pharma Dessau, FRG.

HSA (Pharma Dessau, 0.6 nmol, 40 μL of a 1 mg/mL solution (60 μL of commercially prepared 20% solution in 16 mM sodium octanoate diluted with borate buffer (340 μL, 0.0025 M sodium borate, 0.15 M NaCl, pH 7.2))) was analysed by a reverse phase (Agilent, Zorbax 300SB-C3, 5 μ, 2.1 x 150 mm) LC MS system (Waters/Micromass). The standard protein LC MS gradient was utilised and a single broad peak eluted at a retention time of 47-52 minutes. The raw ESI data was deconvoluted with MaxEnt to give the deconvoluted ESI-mass spectrum presented in Figure **5.6**.

8.5.4 HSA (Pharma Dessau, FRG) and F-150 (**46**), (**62**)

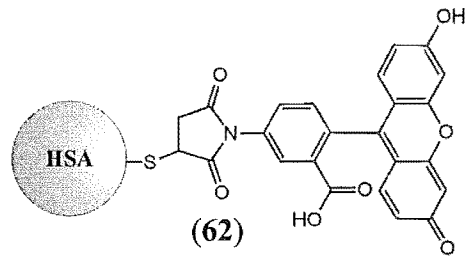

(62)

HSA (Pharma Dessau, 400 μg, 60μL of a commercially prepared 20% solution in 16 mM sodium octanoate, 6 nmol) was diluted with borate buffer (340 μL, 0.0025 M sodium borate, 0.15 M NaCl, pH 7.2). F-150 (**46**, 5.1 μL of 1 mg/mL in DMF, 12 nmol) was added and the reaction was left at RT for 12 hours. At this time the sample was analysed by LC MS (Waters/Micromass, Zorbax 300SB-C3) using the standard protein LC MS

gradient (Figure **5.8**). As Figure **5.8** demonstrated, one large broad peak, with a retention time of 47 to 52 minutes, was visible in the TIC spectrum. This peak represented protein, and was also visible at λ 440 nm in the diode array spectrum. A sharp peak at 34.4 minutes, visible at a wavelength of 440 nm, was unreacted F-150. The protein was purified from the excess F-150 by passing the sample through a size-exclusion column (Sephadex® G-25, 1 x 40 cm), eluting with distilled water (1 mL/min) and visualised with a diode array detector set at 206 nm. The fluorescent yellow band eluting at the void volume (~20 minutes) was collected and taken to dryness by evaporation with N_2. The sample was then reconstituted in distilled water (400 μL) and reanalysed by reversed phase LC MS (standard protein LC MS gradient) to confirm the purity of the sample. This analysis showed one broad peak, with a retention time of 47-52 minutes, in both the diode array at λ 440 nm and the TIC spectra. Analysis of the mass spectral data showed that the broad peak encompassed both unreacted albumin and the conjugate product **62** (67,008 Da, approximately 50% yield) (Figure **5.9**). Unreacted protein and the conjugate product could not be separated. The sample containing **62** was again taken to dryness by evaporation under nitrogen gas flow and stored at 3°C until further analyses took place.

8.5.5 Tryptic Digest of HSA-F-150 (**62**)

Conjugate **62** (100 μg, 1.5 nmol) was taken up in ammonium bicarbonate buffer (100 μL, 10 mM, pH 8). TPCK treated trypsin (10% by weight to analyte protein, 10 μL of 1 mg/mL in 1% acetic acid) was added and the digest left to proceed at 37°C for 24 hours. A small amount of dithiothreitol (DTT) was added to the sample. Reverse phase (Zorbax 300SB-C3) LC MS (Waters/Micromass, standard protein LC MS gradient) was used to analyse the digest. See Figure **5.10** for the diode array chromatogram at λ 440 nm and the TIC ES+ trace. ESI MS data was processed as discussed in Section **5.3**. See Table **5.1** for the ESI-MS data of this digest, and the assignment of peptide fragments.

8.5.6 HSA (Pharma Dessau, FRG) and γ-Maleimidobutyric-Gly-Phe-Leu-Gly-norhomohalichondrin B (**32**), (**63**)

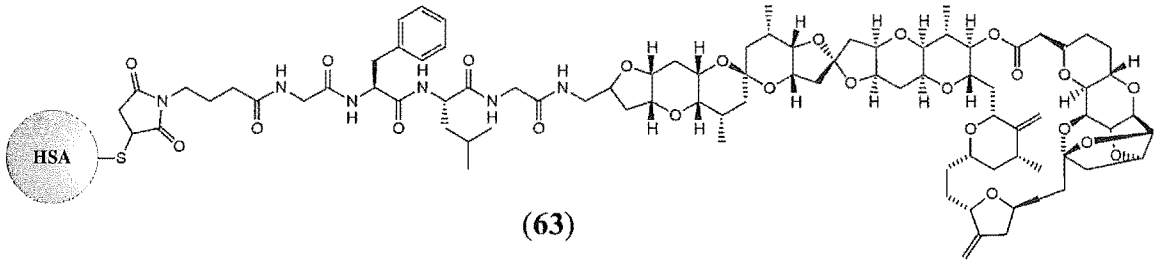

(63)

HSA (Pharma Dessau, 200 μg, 30 μL of a commercially prepared 20% solution in 16 mM sodium octanoate, 3 nmol) was diluted with borate buffer (170 μL, 0.0025 M sodium borate, 0.15 M NaCl, pH 7.2). γ-maleimidobutyric-Gly-Phe-Leu-Gly-norhomohalichondrin B (**32**, 9.8 μL of 1 mg/mL in DMF, 6 nmol) was added and the reaction was left at RT for three days. The reaction mixture was then chromatographed on a G-25 column (Sephadex®, 1 x 40 cm) with distilled water (1 mL/min) and visualised with a single beam UV detector set at 206 nm. A peak eluting at V_0 (~20 minutes) was collected and taken to dryness by evaporation under N_2 gas. The sample was reconstituted in distilled water (200 μL) and analysed by reverse phase (Zorbax 300SB-C3) LC MS (Waters/Micromass, standard protein LC MS gradient) to confirm the purity and nature of the sample. A single broad peak, with a retention time of 47-52 minutes, was visible in the TIC spectrum. MaxEnt deconvolution of the raw ESI-mass spectral data (Figure **5.12**) demonstrated that the broad peak encompassed both unreacted albumin and the conjugate product **63** (68,144 Da, approximately 33% yield) (Figure **5.13**). Unreacted protein and the conjugate product could not be separated. The remaining sample containing **63** was taken to dryness by evaporation with nitrogen and stored at 3°C until further analyses took place.

8.5.7 HSA (Pharma Dessau, FRG) and γ-Maleimidobutyric-Gly-Phe-Leu-Gly-doxorubicin (**35**), (**64**)

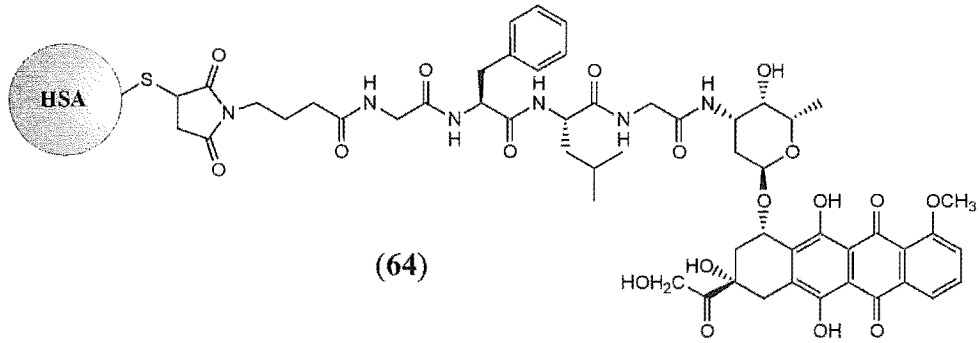

(64)

HSA (Pharma Dessau, 200 μg, 30 μL of a commercially prepared 20% solution in 16 mM sodium octanoate, 3 nmol) was diluted with borate buffer (170 μL, 0.0025 M sodium borate, 0.15 M NaCl, pH 7.2). γ-maleimidobutyric-Gly-Phe-Leu-Gly-doxorubicin (**35**, 6.5 μL of 1 mg/mL in DMF, 6 nmol) was added and the reaction was left for 24 hours at RT. A G-25 column (Sephadex®, 1 x 40 cm) was used to separate unreacted **35** from the protein component. The sample was eluted with distilled water (1 mL/min) and visualised with a diode array detector set at 206 nm. The pink fraction that eluted after 20 minutes was collected and taken to dryness by evaporation with N_2. This fraction was then redissolved in distilled water (200 μL). The sample was analysed by LCMS (Waters/Micromass, Zorbax, 300SB-C3, standard protein LC MS gradient). Figure **5.15** illustrates the single peak visible in the diode array chromatograms at λ 254 nm and λ 480 nm, and the TIC ES+ trace. The ESI-mass spectrum of this peak can be seen in Figure **5.16**, and the MaxEnt deconvoluted, neutral-scale mass spectrum is presented in Figure **5.17**. The broad peak included both unreacted albumin and the conjugate product **64** (67,531 Da). A further component eluting at the same retention time was identified as being a degradation product of the conjugate (67,115 Da). This product represented the loss of the anthracycline portion of doxorubicin (see Chapter **4**). A small aliquot of the sample (50 μL) was left for 48 hours at RT, then reanalysed by LC MS. Conjugate **64** was no longer present and the aforementioned degradation component remained. The remaining sample containing **64** was immediately taken to dryness by evaporation with nitrogen and stored at 3°C, in the dark, until further analyses took place.

8.5.8 Tryptic Digest of HSA-Doxorubicin (**64**)

Conjugate **64** (100 μg) was taken up in ammonium bicarbonate buffer (100 μL, 10 mM, pH 8). TPCK treated trypsin (10 μg in 10 μL 1% acetic acid) was added. The digest was left at 37°C for 12 hours and monitored by LC MS (Waters/Micromass, Zorbax, 300SB-C3, standard protein LC MS gradient). See Figure **5.18** for the diode array (λ 480 nm) and TIC ES+ chromatograms. The ESI-MS data was processed as discussed in Section **5.5**. The relevant ESI-MS data of this digest, and the assignment of peptide fragments can be seen in Table **5.2**.

8.5.9 HSA (Pharma Dessau, FRG) and γ-Maleimidobutyric-Gly-Phe-Leu-Gly-tyrosinamide (**37**), (**65**)

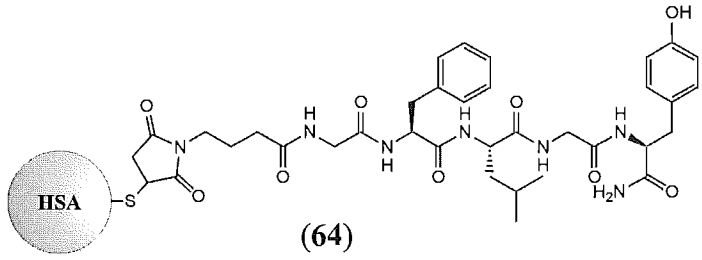

(64)

HSA (Pharma Dessau, 200 μg, 30μL of a commercially prepared 20% solution in 16 mM sodium octanoate, 3 nmol) was diluted with borate buffer (170 μL, 0.0025 M sodium borate, 0.15 M NaCl, pH 7.2) and combined with γ-maleimidobutyric-Gly-Phe-Leu-Gly-tyrosinamide (**37**, 4.3 μL of 1 mg/mL in DMF, 6 nmol). After 24 hours at RT the reaction mixture was chromatographed on a G-25 column (Sephadex®, 1 x 40 cm). The sample was eluted with distilled water (1 mL/min) and visualised with a diode array detector (λ 206 nm). The peak that eluted after 20 minutes was collected and taken to dryness by evaporation with N_2. The sample was then reconstituted in distilled water (200 μL) and analysed by reverse phase (Zorbax, 300SB-C3) LC MS (Waters/Micromass, standard protein LC MS gradient). A single broad peak, eluting at 47-51 minutes, was represented by the mass spectral data presented in Figures **5.20** and **5.21**. The peak encompassed unreacted HSA and the HSA-tyrosinamide conjugate (**65**, 67,079 Da). The sample containing **65** was again taken to dryness by evaporation under nitrogen gas flow and stored at 3°C until further analyses took place.

8.5.10 Tryptic Digest of HSA-Tyrosinamide (**65**)

Conjugate **65** (100 μg) was taken up in ammonium bicarbonate buffer (100 μL, 10 mM, pH 8). TPCK treated trypsin (10 μg) was added in 1% acetic acid (10 μL). After 24 hours at 37°C the digest was analysed by LC MS (Waters/Micromass, Zorbax, 300SB-C3). The ESI-MS data was processed as discussed in Section **5.6**. The relevant ESI-MS data of this digest, and the assignment of peptide fragments can be seen in Table **5.3**.

8.6 Work Described in Chapter 6

8.6.1 Cathepsin B Digest of **54**

Conjugate **54** (1 μg, 15 μL of stock solution prepared in Section **8.4.5**) was diluted with phosphate buffer (82 μL, 0.05 M KH_2PO_4, 0.001 M EDTA, 0.005 M glutathione, pH 6.0) and was incubated with cathepsin B (3 μg, 3 μL of 1 mg/mL in phosphate buffer from above, commercial supply of cathepsin ~30% protein) at 37°C. The degradation of **64** was monitored by LC MS after 5, 24 and 48 hours of incubation with cathepsin B. An analytical reverse phase (Zorbax C18, 2.1 x 150 mm) HPLC system was used at a flow rate of 200 μL/min. A solvent gradient comprising the following steps was used: a slow linear gradient from 0-60% CH_3CN/H_2O (5% acetic acid) over 60 minutes; a linear gradient to 100% CH_3CN over two minutes; isocratic at 100% CH_3CN for five minutes; a return to 100% H_2O over five minutes; and finally an isocratic hold on 100% H_2O for two minutes. The progress of the digestion can be seen in the LC MS traces pictured in Figure **6.1**. Analysis of the LC MS data is discussed in Section **6.2.1**.

8.6.2 ELISA Assay of **52** and **54**

A general outline of the principle and procedure of the gp120-mediated ELISA is discussed in Section **6.2**. The exact methodology is outlined below.

The ELISA assays were performed in a 96-well plate. 100 μL Dulbecco's phosphate buffered saline (D-PBS) was added to the outermost wells and gp120 (8.3 nM, 100 μL of a 0.5 μg/mL solution) in PBS was added to the central wells. The plates were incubated for two hours at room temperature (no rocking). The plates were then washed three times (200 μL) wash buffer (Tween 20, 0.02% D-PBS (without Ca and Mg)). Incubation with D-PBS (200 μL, without Ca and Mg), 1% bovine serum albumin (BSA), and 0.05% NaN_3 overnight at 4°C blocked any unused space in the wells. All wells were then washed three times with D-PBS (200 μL). The appropriate wells (shown in Figure **6.4**) were incubated (rocking) with 100 μL/well of variable concentrations of either the CV-N

mutant (**54**) or the CV-N conjugate (**52**) for one hour at room temperature. The plate was again washed three times with D-PBS (200 μL) and further incubated (rocking) with Rabbit-anti-CV-N antibodies (Rab-2-d-CV-N-Ig, 100 μL/well) for one hour at room temperature. After a further three washes the plate was incubated (rocking) with anti-Rabbit antibodies with a terminal alkaline phosphatase (anti-[rab-IgG]-Ab-AP, 100 μl/well) for one hour at room temperature. The plates were washed three times with D-PBS and incubated (rocking) with substrate buffer (pH 9.2, 10% diethanolamine, 1 mM $MgCl_2$, 4 mg/mL *p*-nitrophenyl phosphate (pNPP), 100 μL) for 15 minutes. The final step was to add EDTA (0.5 M, pH 8.0, 100 μL) to each well (without washing off the buffer). The plates were read at 405 nm in a plate reader. A graphical representation of the results is presented in Figure **6.5**.

8.6.3 Biological Assays

8.6.3.1 Anti-HIV XTT Assay

The anti-HIV assay is a relatively simple method to determine the ability of a drug to protect cells against the cytopathic effects of HIV. T-lymphocyte-derived CEM-SS cells are added to 96-well microtitre plates along with cell-free HIV and the test agent at ½-log dilutions over a multi-dose range. Six days after infection, a tetrazolium reagent, XTT, is added to the wells. In the presence of viable cells, XTT is metabolized to an orange coloured formazan, such that the quantity of viable cells, and thus, the protective ability of the test agent, is proportional to the depth of the colour. Uninfected cells are also treated with drug in order to determine the cytotoxicity of the drug, if any, to the CEM cells. For further detailed information see Weislow *et al.*[235] and Gulakowski *et al.*[236] These assays were carried out by the MTDP, NCI-Frederick, Frederick, MD, USA.

The CV-N: K3R, K48R, K74R, K84R-norhomohalichondrin B conjugate (**54**) and the free norhomohalichondrin B amine (**31**) were submitted for the above HIV cytotoxicity assay. Graphical and tabular representations of the assay results are presented in Figure **6.6**, and Table **6.1**, respectively.

8.6.3.2 P388 Biological Assay[237]

This is an anti-tumour assay, which involves incubating a dilution series of a sample with P388 murine leukaemia cells for 72 hours. The concentration of the sample required to reduce the P399 cell growth by 50%, compared to the control cells, is determined using the absorbance values obtained at 540 nm when the yellow MTT tetrazolium is reduced by healthy cells to produce purple coloured MTT formazan. The result is expressed as an IC_{50} in ng/mL. These assays were carried out in the Chemistry Department, University of Canterbury, Christchurch, New Zealand.

γ-Maleimidobutyric-Gly-Phe-Leu-Gly-OH (**30**), norhomohalichondrin B amine (**31**), γ-maleimidobutyric-Gly-Phe-Leu-Gly-norhomohalichondrin B (**32**), the HSA-norhomohalichondrin B conjugate (**63**), doxorubicin (**34**), γ-maleimidobutyric-Gly-Phe-Leu-Gly-doxorubicin (**35**) and the HSA-doxorubicin conjugate (**64**) were submitted for assay against the P388 murine leukaemia cell line. The doxorubicin samples were prepared immediately before analysis. A tabular representation of the results is presented Table **6.2**.

REFERENCES

REFERENCES

(1) Thomas, M. "AIDS Explained"; Mark G Thomas: Auckland, **1999**, 47 pp.

(2) "Rising Numbers of People Diagnosed with HIV in New Zealand", AIDS - New Zealand, Ministry of Health New Zealand, **2004**.

(3) UNAIDS/WHO. "AIDS Epidemic Update: 2003", **2003**.

(4) Berger, E. A., Doms, R. W., Fenyo, E. M., Korber, B. T. M., Littman, D. R., Moore, J. P., Sattentau, Q. J., Schuitemaker, H., Sodroski, J. and Weiss, R. A. "A New Classification for HIV-1", *Nature*, **1998**, *391*, 240.

(5) Holodniy, M. and Miller, V. "Practical Guidelines in Antiviral Therapy", Boucher, C., Galasso, G., Eds., Elsevier Science, **2002**.

(6) Levy, J. A. "HIV and the Pathogenesis of AIDS", 2nd ed.; American Society for Microbiology: Washington, DC, **1998**, 588 pp.

(7) Vaishnav, Y. N. and Wong-Staal, F. "The Biochemistry of AIDS", *Annu. Rev. Biochem*, **1991**, *60*, 577-630.

(8) Kalichman, S. C. "Understanding AIDS: Advances in Research and Treatment", 2nd ed.; American Psychological Association: Washington, DC, **1998**, 509 pp.

(9) Haase, A. T. "Pathogenesis of Lentivirus Infections", *Nature*, **1986**, *322*, 130-6.

(10) Bailes, E., Gao, F., Bibollet-Ruche, F., Courgnaud, V., Peeters, M., Marx, P. A., Hahn, B. H. and Sharp, P. M. "Hybrid Origin of SIV in Chimpanzees", *Science*, **2003**, *300*, 1713.

(11) Gao, F., Bailes, E., Robertson, D. L., Chen, Y., Rodenburg, C. M., Michael, S. F., Cummins, L. B., Arthur, L. O., Peeters, M., Shaw, G. M., Sharp, P. M. and Hahn, B. H. "Origin of HIV-1 in the Chimpanzee *Pan troglodytes* troglodytes", *Nature*, **1999**, *397*, 436-41.

(12) Weiss, R. A. "Getting to Know HIV", *Trop. Med. Int. Health*, **2000**, *5*, A10-A15.

(13) Leonard, C. K., Spellman, M. W., Riddle, L., Harris, R. J., Thomas, J. N. and Gregory, T. J. "Assignment of Intrachain Disulfide Bonds and Characterization of Potential Glycosylation Sites of the Type-1 Recombinant Human Immunodeficiency Virus Envelope Glycoprotein (gp120) Expressed in Chinese Hamster Ovary Cells", *J. Biol. Chem.*, **1990**, *265*, 10373-82.

(14) Wyatt, R., Kwong, P. D., Desjardins, E., Sweet, R. G., Robinson, J., Hendrickson, W. A. and Sodroski, J. G. "The Antigenic Structure of the HIV gp120 Envelope Glycoprotein", *Nature*, **1998**, *393*, 705-11.

(15) Kwong, P. D., Wyatt, R., Robinson, J., Sweet, R. W., Sodroski, J. and Hendrickson, W. A. "Structure of an HIV gp120 Envelope Glycoprotein in Complex with the CD4 Receptor and a Neutralizing Human Antibody", *Nature*, **1998**, *393*, 648-59.

(16) McMichael, A. "HIV: T-cell Responses to HIV", *Curr. Opin. Immun.*, **2000**, *12*, 367-9.

(17) Picker, L. J. and Maino, V. C. "The CD4+ T-Cell Response to HIV-1", *Curr. Opin. Immun.*, **2000**, *12*, 381-6.

(18) Dettin, M., Ferranti, P., Scarinci, C., Picariello, G. and Di Bello, C. "Is the V3 Loop Involved in HIV Binding to CD4?" *Biochemistry*, **2003**, *42*, 9007-12.

(19) O'Hara, B. M. and Olson, W. C. "HIV Entry Inhibitors in Clinical Development", *Curr. Opin. Pharmacol.*, **2002**, *2*, 523-28.

(20) Wainberg, M. A. and Margolese, R. G. "Strategies in the Treatment of AIDS and Related Diseases: the Lessons of Cancer Chemotherapy", *Cancer Invest.*, **1992**, *10*, 143-53.

(21) Berger, E. A., Murphy, P. M. and Farber, J. M. "Chemokine Receptors as HIV-1 Coreceptors: Roles in Viral Entry, Tropism, and Disease", *Annu. Rev. Immunol.*, **1999**, *17*, 657-700.

(22) Wyatt, R. and Sodroski, J. "The HIV-1 Envelope Glycoproteins: Fusogens, Antigens, and Immunogens", *Science*, **1998**, *280*, 1884-8.

(23) He, J., Chen, Y., Farzan, M., Choe, H., Ohagen, A., Gartner, S., Busciglio, J., Yang, Z., Hofmann, W., Sodroski, J. and Gabuzda, D. "CCR3 and CCR5 are Co-Receptors for HIV-1 Infection of Microglia", *Nature*, **1997**, *385*, 645-9.

(24) Pierson, T. C. and Doms, R. W. "HIV-1 Entry Inhibitors: New Targets, Novel Therapies", *Immun. Lett.*, **2003**, *85*, 113-8.

(25) Boyd, M. R., Gustafson, K. R., McMahon, J. B., Shoemaker, R. H., O'Keefe, B. R., Mori, T., Gulakowski, R. J., Wu, L., Rivera, M. I., Laurencot, C. M., Currens, M. J., Cardellina, J. H., II, Buckheit, R. W., Jr, Nara, P. L., Pannell, L. K., Sowder, R. C., II and Henderson, L. E. "Discovery of Cyanovirin-N, a Novel Human Immunodeficiency Virus-Inactivating Protein That Binds Surface

Envelope Glycoprotein gp120: Potental applications to Microbicide Development", *Antimicrob. Agents Chemother.*, **1997**, *41*, 1521-30.

(26) Sleasman, J. W. and Goodenow, M. M. "HIV-1 Infection", *J. Allergy Clin. Immunol.*, **2003**, *111*, S582-S592.

(27) Brooks, D. G., Hamer, D. H., Arlen, P. A., Gao, L., Bristol, G., Kitchen, C. M. R., Berger, E. A. and Zack, J. A. "Molecular Characterization, Reactivation, and Depletion of Latent HIV", *Immunity*, **2003**, *19*, 413-23.

(28) Pierson, T., McArthur, J. and Siliciano, R. F. "Reservoirs for HIV-1: Mechanisms for Viral Persistence in the Presence of Antiviral Immune Responses and Antiretroviral Therapy", *Annu. Rev. Immunol.*, **2000**, *18*, 665-708.

(29) Wallace, R. G. "Projecting the Impact of HAART on the Evolution of HIV's Life History", *Ecol. Model.*, **2004**, *Article in Press, In Press*.

(30) Touloumi, G. and Hatzakis, A. "Natural History of HIV-1 Infection", *Clinics in Dermatol.*, **2000**, *18*, 389-99.

(31) Steinhart, C. R. "Pathogenesis of HIV Infection and Implications for Clinical Practice", *Clin. Immun.*, **1999**, *19*, 125-31.

(32) Pantaleo, G., Graziosi, C. and Fauci, A. S. "The Immunopathogenesis of Human Immunodeficiency Virus Infection", *N. Engl. J. Med.*, **1993**, *328*, 327-35.

(33) De Clercq, E. "Antiviral Drugs in Current Clinical Use", *J. Clin. Virol.*, **2004**, *30*, 115-33.

(34) Pani, A., Loi, A. G., Mura, M., Marceddu, T., La Colla, P. and Marongiu, M. E. "Targeting HIV: Old and New Players", *Current Drug Targets: Infectious Disorders*, **2002**, *2*, 17-32.

(35) Miller, M., D. and Hazuda, D., J. "HIV Resistance to the Fusion Inhibitor Enfuvirtide: Mechanisms and Clinical Implications", *Drug Resistance Updates*, **2004**.

(36) De Clercq, E. "HIV-Chemotherapy and -Phophylaxis: New Drugs, Leads and Approaches", *Int. J. Biochem. Cell Biol.*, **2004**.

(37) Vella, S. and Palmisano, L. "Antiretroviral Therapy: State of the HAART", *Antiviral Res.*, **2000**, *45*, 1-7.

(38) Shafer, R. W. and Vuitton, D. A. "Highly Active Antiretroviral Therapy (HAART) for the Treatment of Infection with Human Immunodeficiency Virus Type-1", *Biomed. Pharmaco.*, **1999**, *53*, 73-86.

(39) Berger, E. A., Moss, B. and Pastan, I. "Reconsidering Targeted Toxins to Eliminate HIV Infection: You Gotta Have HAART", *Proc. Natl. Acad. Sci. USA*, **1998**, *95*, 11511-3.

(40) Bonfanti, P., Capetti, A. and Rizzardini, G. "HIV Disease Treatment in the Era of HAART", *Biomed. Pharmaco.*, **1999**, *53*, 93-105.

(41) Mansky, L. M. "Forward Mutation Rate of Human Immunodeficiency Virus Type-1 in a T-Lymphoid Cell Line", *AIDS Res. Hum. Retroviruses*, **1996**, *12*, 307-14.

(42) Menendez-Arias, L. "Targeting HIV: Antiretroviral Therapy and Development of Drug Resistance", *Trends Pharmacol. Sci.*, **2002**, *23*, 381-8.

(43) Kaufmann, G. R. and Cooper, D. A. "Antiretroviral Therapy of HIV-1 Infection: Established Treatment Strategies and New Therapeutic Options", *Curr. Opin. Microbiol.*, **2000**, *3*, 508-14.

(44) Wodarz, D. and Nowak, M. A. "HIV Therapy: Managing Resistance", *Proc. Natl. Acad. Sci. USA*, **2000**, *97*, 8193-5.

(45) Butera, S. T. "Therapeutic Targeting of Human Immunodeficiency Virus Type-1 Latency: Current Clinical Realities and Future Scientific Possibilities", *Antiviral Res.*, **2000**, *48*, 143-76.

(46) Bocklandt, S., Blumberg, P. M. and Hamer, D. H. "Activation of Latent HIV-1 Expression by the Potent Anti-Tumor Promoter 12-Deoxyphorbol 13-phenylacetate", *Antiviral Res.*, **2003**, *59*, 89-98.

(47) Cohen, P. "Nowhere to Hide", *New Scientist*, **2004**, *182*, 24-39.

(48) Quivy, V., Adam, E., Collette, Y., Demonte, D., Chariot, A., Vanhulle, C., Berkhout, B., Castellano, R., De Launoit, Y., Burny, A., Piette, J., Bours, V. and Van Lint, C. "Synergistic Activation of Human Immunodeficiency Virus Type-1 Promoter Activity by NF-kB and Inhibitors of Deacetylases: Potential Perspectives for the Development of Therapeutic Strategies", *J. Virol.*, **2002**, *76*, 11091-103.

(49) Lisziewicz, J., Bakare, N. and Lori, F. "Therapeutic Vaccination for Future Management of HIV/AIDS", *Vaccine*, **2003**, *21*, 620-3.

(50) Amara, R. R. and Robinson, H. L. "A New Generation of HIV Vaccines", *Trends in Molecular Medicine*, **2002**, *8*, 489-95.

(51) Newman, P. A., Duan, N., Rudy Ellen, T. and Johnston-Roberts, K. "HIV Risk and Prevention in a Post-Vaccine Context", *Vaccine*, **2004**, *22*, 1954-63.

(52) Johnston, M. I. and Flores, J. "Progress in HIV Vaccine Development", *Curr. Opin. Pharmacol.*, **2001**, *1*, 504-10.

(53) Bostrom, A.-C., Hejdeman, B., Matsuda, R., Fredriksson, M., Fredriksson, E.-L., Bratt, G., Sandstrom, E. and Wahren, B. "Long-Term Persistence of Vaccination and HAART to Human Immunodeficiency Virus (HIV)", *Vaccine*, **2004**, *22*, 1683-91.

(54) Stratov, I., DeRose, R., Purcell, D. F. J. and Kent, S. J. "Vaccines and Vaccine Strategies Against HIV", *Current Drug Targets*, **2004**, *5*, 71-88.

(55) Morris, K. "First Phase-3 HIV Vaccine Trial--Hype or Hope?" *Lancet Infectious Diseases*, **2003**, *3*, 186.

(56) Cohen, J. "Shots in the Dark: The Wayward Search for an AIDS Vaccine"; W. W. Norton: New York, **2001**, 440 pp.

(57) Cragg, G. and Newman, D. "Nature's Bounty", *Chem. in Britain*, **2001**, *37*, 22-6.

(58) Stanitski, C., Eubanks, L., Middlecamp, C. and Stratton, W. "Chemistry in Context: Applying Chemistry to Society", 3rd ed.; McGraw-Hill Higher Education: Boston, **2000**, 535 pp.

(59) Williams, D. H., Stone, M. J., Hauck, P. R. and Rahman, S. K. "Why are Secondary Metabolites (Natural Products) Biosynthesized?" *J. Nat. Prod.*, **1989**, *52*, 1189-208.

(60) de Vries, D. J. and Hall, M. R. "Marine biodiversity as a source of chemical diversity", *Drug Dev. Res.*, **1994**, *33*, 161-73.

(61) MarinLit. Christchurch, New Zealand: University of Canterbury, **2004**.

(62) Fay, P. "The Blue-Greens (Cyanophyta-Cyanobacteria)"; Edward Arnold Ltd: London, **1983**, 88 pp.

(63) Humm, H. J. and Wicks, S. R. "Introduction and Guide to the Marine Bluegreen Algae"; John Wiley and Sons: New York, **1980**, 194 pp.

(64) Burja, A. M., Banaigs, B., Abou-Mansour, E., Grant Burgess, J. and Wright, P. C. "Marine Cyanobacteria: A Prolific Source of Natural Products", *Tetrahedron*, **2001**, *57*, 9347-77.

(65) Shimizu, Y. "Microalgae as a Drug Source", *Drugs from the Sea*, **2000**, 30-45.

(66) Edgar, G. J. "Marine Biology - Australia"; Reed Books: Kew, **1997**, 544 pp.

(67) Munro, M. H. G., Blunt, J. W., Lake, R. J., Litaudon, M., Battershill, C. N. and Page, M. J. "From Seabed to Sickbed: What are the Prospects?" *Sponges Time Space, Proc. Int. Porifera Congr., 4th*, **1994**, 473-84.

(68) Kobayashi, M. "Search for Biologically Active Substances from Marine Sponges", *Drugs from the Sea*, **2000**, 46-58.

(69) Haygood, M. G., Schmidt, E. W., Davidson, S. K. and Faulkner, D. J. "Microbial Symbionts of Marine Invertebrates: Opportunities for Microbial Biotechnology", *J. Mol. Microbiol. Biotechnol.*, **1999**, *1*, 33-43.

(70) Hirata, Y. and Uemura, D. "Halichondrins-Antitumor Polyether Macrolides from a Marine Sponge", *Pure Appl. Chem.*, **1986**, *58*, 701-10.

(71) Uemura, D., Takahashi, K., Yamamoto, T., Katayama, C., Tanaka, J., Okumura, Y. and Hirata, Y. "Norhalichondrin A: an Antitumor Polyether Macrolide from a Marine Sponge", *J. Am. Chem. Soc.*, **1985**, *107*, 4796-8.

(72) Pettit, G. R., Herald, C. L., Boyd, M. R., Leet, J. E., Dufresne, C., Doubek, D. L., Schmidt, J. M., Cerny, R. L., Hooper, J. N. and Rutzler, K. C. "Isolation and Structure of the Cell Growth Inhibitory Constituents from the Western Pacific Marine Sponge *Axinella sp*", *J. Med. Chem.*, **1991**, *34*, 3339-40.

(73) Pettit, G. R., Gao, F., Doubek, D. L., Boyd, M. R., Hamel, E., Bai, R., Schmidt, J. M., Tackett, L. P. and Rutzler, K. "Antineoplastic Agents. CCLII. Isolation and Structure of Halistatin 2 from the Comoros Marine Sponge *Axinella carteri*", *Gazz. Chim. Ital.*, **1993**, *123*, 371-7.

(74) Pettit, G. R., Ichihara, Y., Wurzel, G., Williams, M. D., Schmidt, J. M. and Chapuis, J.-C. "Isolation and Structure of Halistatin 3 from the Western Pacific (Chuuk) Marine Sponge *Phakellia sp*", *J. Chem. Soc., Chem. Commun.*, **1995**, 383-5.

(75) Pettit, G. R., Tan, R., Gao, F., Williams, M. D., Doubek, D. L., Boyd, M. R., Schmidt, J. M., Chapuis, J. C., Hamel, E. and et al. "Isolation and Structure of Halistatin 1 from the Eastern Indian Ocean Marine Sponge *Phakellia carteri*", *J. Org. Chem.*, **1993**, *58*, 2538-43.

(76) Litaudon, M., Hart, J. B., Blunt, J. W., Lake, R. J. and Munro, M. H. G. "Isohomohalichondrin B, a New Antitumor Polyether Macrolide from the New Zealand Deep-Water Sponge *Lissodendoryx sp*", *Tetrahedron Lett.*, **1994**, *35*, 9435-8.

(77) Litaudon, M., Hickford, S. J. H., Lill, R. E., Lake, R. J., Blunt, J. W. and Munro, M. H. G. "Antitumor Polyether Macrolides: New and Hemisynthetic Halichondrins from the New Zealand Deep-Water Sponge Lissodendoryx sp", *J. Org. Chem.*, **1997**, *62*, 1868-71.

(78) Hart, J. B., Lill, R. E., Hickford, S. J. H., Blunt, J. W. and Munro, M. H. G. "The Halichondrins: Chemistry, Biology, Supply and Delivery"; Karger: Basel, **2000**, 134-53 pp.

(79) Aicher, T. D., Buszek, K. R., Fang, F. G., Forsyth, C. J., Jung, S. H., Kishi, Y., Matelich, M. C., Scola, P. M., Spero, D. M. and Yoon, S. K. "Total Synthesis of Halichondrin B and Norhalichondrin B", *J. Am. Chem. Soc.*, **1992**, *114*, 3162-4.

(80) Fang, F. G., Kishi, Y., Matelich, M. C. and Scola, P. M. "Synthetic Studies Towards Halichondrins: Synthesis of the Left Halves of Norhalichondrins and Homohalichondrins", *Tetrahedron Lett.*, **1992**, *33*, 1557-60.

(81) Hart, J. B., Blunt, J. W. and Munro, M. H. G. "Acid-Catalyzed Reactions of Homohalichondrin B, a Marine Sponge-Derived Antitumor Polyether Macrolide", *J. Org. Chem.*, **1996**, *61*, 2888-90.

(82) Fodstad, O., Breistoel, K., Pettit, G. R., Shoemaker, R. H. and Boyd, M. R. "Comparative Antitumor Activities of Halichondrins and Vinblastine Against Human Tumor Xenografts", *J. Exp. Therapeut. Oncol.*, **1996**, *1*, 119-25.

(83) Paull, K. D., Lin, C. M., Malspeis, L. and Hamel, E. "Identification of Novel Antimitotic Agents Acting at the Tubulin Level by Computer-Assisted Evaluation of Differential Cytotoxicity Data", *Cancer Res.*, **1992**, *52*, 3892-900.

(84) Bai, R., Paull, K. D., Herald, C. L., Malspeis, L., Pettit, G. R. and Hamel, E. "Halichondrin B and Homohalichondrin B, Marine Natural Products Binding in the Vinca Domain of Tubulin. Discovery of Tubulin-Based Mechanism of Action by Analysis of Differential Cytotoxicity Data", *J. Biol. Chem.*, **1991**, *266*, 15882-9.

(85) Munro, M. H. G., Blunt, J. W., Dumdei, E. J., Hickford, S. J. H., Lill, R. E., Li, S., Battershill, C. N. and Duckworth, A. R. "The Discovery and Development of Marine Compounds with Pharmaceutical Potential", *J. Biotechnol.*, **1999**, *70*, 15-25.

(86) Stamos, D. P. and Kishi, Y. "Synthetic Studies on Halichondrins: A Practical Synthesis of the C.1-C.13 Segment", *Tetrahedron Lett.*, **1996**, *37*, 8643-6.

(87) Norcross, R. D. and Paterson, I. "Total Synthesis of Bioactive Marine Macrolides", *Chem. Rev.*, **1995**, *95*, 2041-114.

(88) Towle, M. J., Salvato, K. A., Budrow, J., Wels, B. F., Kuznetsov, G., Aalfs, K. K., Welsh, S., Zheng, W., Seletsky, B. M., Palme, M. H., Habgood, G. J., Singer, L. A., DiPietro, L. V., Wang, Y., Chen, J. J., Quincy, D. A., Davis, A., Yoshimatsu, K., Kishi, Y., Yu, M. J. and Littlefield, B. A. "*In vitro* and *In vivo* Anticancer Activities of Synthetic Macrocyclic Ketone Analogues of Halichondrin B", *Cancer Res.*, **2001**, *61*, 1013-21.

(89) Lill, R. E. PhD Thesis, University of Canterbury, **1999**.

(90) Bringans, S. PhD Thesis, University of Canterbury, **2001**.

(91) Gustafson, K. R., Sowder II, R. C., Henderson, L. E., Cardellina II, J. H., McMahon, J. B., Rajamani, U., Pannell, L. K. and Boyd, M. R. "Isolation, Primary Sequence Determination, and Disulfide Bond Structure of Cyanovirin-N, an Anti-HIV(Human immunodeficiency Virus) Protein from the Cyanobacterium *Nostoc ellipsosporum*", *Biochem. Biophys. Res. Commun.*, **1997**, *238*, 223-8.

(92) Botos, I. and Wlodawer, A. "Cyanovirin-N: a Sugar-Binding Anti-viral Protein with a New Twist", *Cell. Mol. Life Sci.*, **2003**, *60*, 277-87.

(93) Mori, T., Gustafson, K. R., Pannell, L. K., Shoemaker, R. H., Wu, L., McMahon, J. B. and Boyd, M. R. "'HIV-Inhibitory Natural Products' Recombinant Production of Cyanovirin-N, a Potent Human Immunodeficiency Virus-Inactivating Protein Derived from a Cultured Cyanobacterium", *Prot. Express. Purif.*, **1998**, *12*, 151-8.

(94) Mori, T., Shoemaker, R. H., Gulakowski, R. J., Krepps, B. L., McMahon, J. B., Gustafson, K. R., Pannell, L. K. and Boyd, M. R. "Analysis of Sequence Requirements for Biological Activity of Cyanovirin-N, a Potent HIV (Human Immunodeficiency virus)-Inactivating Protein", *Biochem. Biophys. Res. Commun.*, **1997**, *238*, 218-22.

(95) Mori, T., Shoemaker, R. H., McMahon, J. B., Gulakowski, R. J., Gustafson, K. R. and Boyd, M. R. "Construction and Enhanced Cytotoxicity of a [Cyanovirin-N]-[*Pseudomonas* exotoxin] Conjugate Against Human Immunodeficiency Virus-Infected Cells", *Biochem. Biophys. Res. Commun.*, **1997**, *239*, 884-8.

(96) Bewley, C. A., Gustafson, K. R., Boyd, M. R., Covell, D. G., Bax, A., Clore, G. M. and Gronenborn, A. M. "Solution Structure of Cyanovirin-N, a Potent HIV-inactivating Protein", *Nat. Struct. Bio.*, **1998**, *5*, 571-8.

(97) Yang, F., Bewley, C. A., Louis, J. M., Gustafson, K. R., Boyd, M. R., Gronenborn, A. M., Clore, G. M. and Wlodawer, A. "Crystal Structure of Cyanovirin-N, a Potent HIV-inactivating Protein, Shows Unexpected Domain Swapping", *J. Molec. Biol.*, **1999**, *288*, 403-12.

(98) Clore, G. M. and Bewley Carole, A. "Using Conjoined Rigid Body/Torsion Angle Simulated Annealing to Determine the Relative Orientation of Covalently Linked Protein Domains from Dipolar Couplings", *J. Mag. Res.*, **2002**, *154*, 329-35.

(99) Mariner, J. M., McMahon, J. B., O'Keefe, B. R., Nagashima, K. and Boyd, M. R. "The HIV-Inactivating Protein, Cyanovirin-N, Does Not Block gp120-Mediated Virus-to-Cell Binding", *Biochem. Biophys. Res. Commun.*, **1998**, *248*, 841-5.

(100) O'Keefe, B. R., Shenoy, S. R., Xie, D., Zhang, W., Muschik, J. M., Currens, M. J., Chaiken, I. and Boyd, M. R. "Analysis of the Interaction Between the HIV-Inactivating Protein Cyanovirin-N and Soluble Forms of the Envelope Glycoproteins gp120 and gp41", *Mol. Pharmacol.*, **2000**, *58*, 982-92.

(101) Esser, M. T., Mori, T., Mondor, I., Sattentau, Q. J., Dey, B., Berger, E. A., Boyd, M. R. and Lifson, J. D. "Cyanovirin-N Binds to gp120 to Interfere with CD4-Dependent Human Immunodeficiency Virus Type-1 Virion Binding, Fusion, and Infectivity but Does Not Affect the CD4 Binding Site on gp120 or Soluble CD4-Induced Conformational Changes in gp120", *J. Virol.*, **1999**, *73*, 4360-71.

(102) Dey, B., Lerner, D. L., Lusso, P., Boyd, M. R., Elder, J. H. and Berger, E. A. "Multiple Antiviral Activities of Cyanovirin-N: Blocking of Human Immunodeficiency Virus Type-1 Gp120 Interaction with CD4 and Coreceptor and Inhibition of Diverse Enveloped Viruses", *J. Virol.*, **2000**, *74*, 4562-9.

(103) Bolmstedt, A. J., O'Keefe, B. R., Shenoy, S. R., McMahon, J. B. and Boyd, M. R. "Cyanovirin-N Defines a New Class of Antiviral Agent Targeting N-linked, High-Mannose Glycans in an Oligosaccharide-Specific Manner", *Mol. Pharmacol.*, **2001**, *59*, 949-54.

(104) Shenoy, S. R., O'Keefe, B. R., Bolmstedt, A. J., Cartner, L. K. and Boyd, M. R. "Selective Interactions of the Human Immunodeficiency Virus-Inactivating Protein Cyanovirin-N with High-Mannose Oligosaccharides on Gp120 and Other Glycoproteins", *J. Pharmacol. Exp. Ther.*, **2001**, *297*, 704-10.

(105) Bewley, C. A. and Otero-Quintero, S. "The Potent Anti-HIV Protein Cyanovirin-N Contains Two Novel Carbohydrate-Binding Sites that Selectively Bind to Man-

8 D1D3 and Man-9 with Nanomolar Affinity: Implications for Binding to the HIV Envelope Protein Gp120", *J. Am. Chem. Soc.*, **2001**, *123*, 3892-902.

(106) Bewley, C. A. "Solution Structure of a Cyanovirin-N:Manα1-2Manα Complex: Structural Basis for High-Affinity Carbohydrate-Mediated Binding to Gp120", *Structure*, **2001**, *9*, 931-40.

(107) Chang Leng, C. and Bewley Carole, A. "Potent Inhibition of HIV-1 Fusion by Cyanovirin-N Requires Only a Single High Affinity Carbohydrate Binding Site: Characterization of Low Affinity Carbohydrate Binding Site Knockout Mutants", *J. Molec. Biol.*, **2002**, *318*, 1-8.

(108) Botos, I., O'Keefe, B. R., Shenoy, S. R., Cartner, L. K., Ratner, D. M., Seeberger, P. H., Boyd, M. R. and Wlodawer, A. "Structures of the Complexes of a Potent Anti-HIV Protein Cyanovirin-N and High Mannose Oligosaccharides", *J. Biol. Chem.*, **2002**, *277*, 34336-42.

(109) Han, Z., Simpson, J. T., Fivash, M. J., Fisher, R. and Mori, T. "Identification and Characterization of Peptides that Bind to Cyanovirin-N, a Potent Human Immunodeficiency Virus-Inactivating Protein", *Peptides*, **2004**, *25*, 551-61.

(110) O'Keefe, B. R., Smee, D. F., Turpin, J. A., Saucedo, C. J., Gustafson, K. R., Mori, T., Blakeslee, D., Buckheit, R. and Boyd, M. R. "Potent Anti-Influenza Activity of Cyanovirin-N and Interactions With Viral Hemagglutinin", *Antimicrob. Agents Chemother.*, **2003**, *47*, 2518-25.

(111) Barrientos, L. G., O'Keefe, B. R., Bray, M., Sanchez, A., Gronenborn, A. M. and Boyd, M. R. "Cyanovirin-N Binds to the Viral Surface Glycoprotein, $GP_{1,2}$ and Inhibits Infectivity of Ebola Virus", *Antiviral Res.*, **2003**, *58*, 47-56.

(112) Bokesch, H. R., Charan, R. D., Meragelman, K. M., Beutler, J. A., Gardella, R., O'Keefe, B. R., McKee, T. C. and McMahon, J. B. "Isolation and Characterization of Anti-HIV Peptides from *Dorstenia contrajerva* and *Treculia obovoidea*", *FEBS Lett.*, **2004**, *567*, 287-90.

(113) Boyd, M. R. "Cyanovirin Conjugates, Matrix-Anchored Cyanovirin, and Anti-Cyanovirin Antibodies and Related Compositions for Removal of Viruses from Samples", 2000-US6247, **2000**, 93 pp.

(114) Boyd, M. R. "Anti-Cyanovirin Antibody with an Internal Image of gp120, a Method of Use Thereof, and a Method of Using a Cyanovirin to Induce an

Immune Response to gp120", 98-136594, **2001**, 38 pp, Cont-in-part of US 5,998,587.

(115) Gandhi, M. J., Boyd, M. R., Yi, L., Yang, G. G. and Vyas, G. N. "Properties of Cyanovirin-N (CV-N): Inactivation of HIV-1 by Sessile Cyanovirin-N (sCV-N)", *Develop. Biol.*, **2000**, *102*, 141-8.

(116) Tsai, C.-C., Emau, P., Jiang, Y., Agy, M. B., Shattock, R. J., Schmidt, A., Morton, W. R., Gustafson, K. R. and Boyd, M. R. "Cyanovirin-N Inhibits AIDS Virus Infections in Vaginal Transmission Models", *AIDS Res. Hum. Retroviruses*, **2004**, *20*, 11-8.

(117) Tsai, C.-C., Emau, P., Jiang, Y., Tian, B., Morton, W. R., Gustafson, K. R. and Boyd, M. R. "Cyanovirin-N Gel as a Topical Microbicide Prevents Rectal Transmission of SHIV89.6P in Macaques", *AIDS Res. Hum. Retroviruses*, **2003**, *19*, 535-41.

(118) Giomarelli, B., Provvedi, R., Meacci, F., Maggi, T., Medaglini, D., Pozzi, G., Mori, T., McMahon, J. B., Gardella, R. and Boyd, M. R. "The Microbicide Cyanovirin-N Expressed on the Surface of Commensal Bacterium *Streptococcus gordonii* Captures HIV-1", *AIDS*, **2002**, *16*, 1351-6.

(119) Kratz, F. and Beyer, U. "Serum Proteins as Drug Carriers of Anti-Cancer Agents: A Review", *Drug Deliv.*, **1998**, *5*, 281-99.

(120) Duncan, R. "Polymer Therapeutics into the 21st Century", *ACS Symp. Ser.*, **2000**, *752*, 350-63.

(121) Duncan, R. "Drug-Polymer Conjugates: Potential for Improved Chemotherapy", *Anti-Cancer Drugs*, **1992**, *3*, 175-210.

(122) Duncan, R., Dimitrijevic, S. and Evagorou, E. G. "The Role of Polymer Conjugates in the Diagnosis and Treatment of Cancer", *S.T.P. Pharma Sciences*, **1996**, *6*, 237-63.

(123) Kabanov, A. V., Batrakova, E. V. and Alakhov, V. Y. "Pluronic Block Copolymers as Novel Polymer Therapeutics for Drug and Gene Delivery", *J. Controlled Release*, **2002**, *82*, 189-212.

(124) Duncan, R., Connors, T. A. and Meada, H. "Drug Targeting in Cancer Therapy: The Magic Bullet, What Next?" *J. Drug Target.*, **1996**, *3*, 317-19.

(125) Duncan, R. and Spreafico, F. "Polymer Conjugates: Pharmacokinetic Considerations for Design and Development", *Clin. Pharmacokinet.*, **1994**, *27*, 290-306.

(126) Duncan, R. "Polymer Conjugates for Tumour Targeting and Intracytoplasmic Delivery. The EPR Effect as a Common gateway?" *PSTT*, **1999**, *2*, 441-49.

(127) Ringsdorf, H. "Structure and Properties of Pharmacologically Active Polymers", *J. Polymer Sci.*, **1975**, *51*, 135-53.

(128) Duncan, R., Lloyd, J. B. and Kopecek, J. "Degradation of Side Chains of *N*-(2-hydroxypropyl)methacrylamide Copolymers by Lysosomal Enzymes", *Biochem. Biophys. Res. Commun.*, **1980**, *94*, 284-90.

(129) Drobník, J., Kopecek, J., Labský, J., Rejmanová, P., Exner, J., Saudek, V. and Kálal, J. "Enzymatic Cleavage of Side Chains of Synthetic Water-Soluble Polymers", *Makromol. Chem.*, **1976**, *177*, 2833-48.

(130) Sinn, H., Schrenk, H. H., Friedrich, E. A., Schilling, U. and Maier-Borst, W. "Design of Compounds Having an Enhanced Tumor Uptake, Using Serum Albumin as a Carrier. Part I", *Nucl. Med. Biol.*, **1990**, *17*, 819-27.

(131) Matsumura, Y. and Maeda, H. "A New Concept for Macromolecular Therapeutics in Cancer Chemotherapy: Mechanism of Tumoritropic Accumulation of Proteins and the Antitumor Agent Smancs", *Cancer Res.*, **1986**, *46*, 6387-92.

(132) Brock, J. H. "Metalloproteins, Part 2: Metal Proteins with Non-Redox Roles", Harrison, P. M., Ed., Macmillan Press Ltd.: London, **1985**.

(133) Vitols, S. "Uptake of Low-density Lipoprotein by Malignant Cells - Possible Therapeutic Applications", *Cancer Cells*, **1991**, *3*, 488-95.

(134) Kratz, F., Beyer, U., Roth, T., Schütte, M. T., Unold, A., Fiebig, H. H. and Unger, C. "Albumin Conjugates of the Anti-Cancer Drug Chlorambucil: Synthesis, Characterisation, and *In Vitro* Efficacy", *Arch. Pharm. Pharm. Med. Chem.*, **1998**, *331*, 47-53.

(135) Kratz, F., Beyer, U., Roth, T., Tarasova, N., Collery, P., Lechenault, F., Cazabat, A., Schumacher, P., Unger, C. and Falken, U. "Transferrin Conjugates of Doxorubicin: Synthesis, Characterization, Cellular Uptake, and *In Vitro* Efficacy", *J. Pharm. Sci.*, **1998**, *87*, 338-46.

(136) Kratz, F. "Antineoplastic transferrin and albumin conjugates of cytostatic compounds selected from anthracyclines, alkylating agents, antimetabolites, and cisplatin analogs", 19636889, **1998**, 18 pp.

(137) Wels, W., Biburger, M., Mueller, T., Daelken, B., Giesuebel, U., Tonn, T. and Uherek, C. "Recombinant Immunotoxins and Retargeted Killer Cells: Employing Engineered Antibody Fragments for Tumor-Specific Targeting of Cytotoxic Effectors", *Cancer Immun. Immuno.*, **2004**, *53*, 217-26.

(138) Pincus, S. H. "Targeting HIV-Infected Cells", *Meth. Molec. Med.*, **2000**, *25*, 193-214.

(139) Pincus, S. H. "Therapeutic Potential of Anti-HIV Immunotoxins", *Antiviral Res.*, **1996**, *33*, 1-9.

(140) Hoste, K., De Winne, K. and Schacht, E. "Polymeric Prodrugs", *Int. J. Pharm.*, **2004**, *277*, 119-31.

(141) Duncan, R. "The Dawning Era of Polymer Therapeutics", *Nature Rev. Drug Discov.*, **2003**, *2*, 347-60.

(142) Vasey, P. A., Kaye, S. B., Morrison, R., Twelves, C., Wilson, P., Duncan, R., Thomson, A. H., Murray, L. S., Hilditch, T. E., Murray, T., Burtles, S., Fraier, D., Frigerio, E. and Cassidy, J. "Phase I Clinical and Pharmacokinetic Study of PK1 [*N*-(2-hydroxypropyl)methacrylamide Copolymer Doxorubicin]: First Member of a New Class of Chemotherapeutic Agents - Drug-Polymer Conjugates", *Clin. Cancer Res.*, **1999**, *5*, 83-94.

(143) Seymour, L. W., Ferry, D. R., Anderson, D., Hesslewood, S., Julyan, P. J., Poyner, R., Doran, J., Young, A. M., Burtles, S. and Kerr, D. J. "Hepatic Drug Targeting: Phase I Evaluation of Polymer-Bound Doxorubicin", *J. Clin. Oncol.*, **2002**, *20*, 1668-76.

(144) Kratz, F., Warnecke, A., Scheuermann, K., Stockmar, C., Schwab, J., Lazar, P., Drueckes, P., Esser, N., Drevs, J., Rognan, D., Bissantz, C., Hinderling, C., Folkers, G., Fichtner, I. and Unger, C. "Probing the Cysteine-34 Position of Endogenous Serum Albumin with Thiol-Binding Doxorubicin Derivatives. Improved Efficacy of an Acid-Sensitive Doxorubicin Derivative with Specific Albumin-Binding Properties Compared to that of the Parent Compound", *J. Med. Chem.*, **2002**, *45*, 5523-33.

(145) Brocchini, S. and Duncan, R. "Encycl. Control. Drug Del." Mathiowitz, E., Ed., John Wiley & Sons, Inc.: New York, **1999**; Vol. 2.

(146) Pechar, M., Ulbrich, K., Subr, V., Seymour, L. W. and Schacht, E. H. "Poly(ethylene glycol) Multiblock Copolymer as a Carrier of Anti-Cancer Drug Doxorubicin", *Bioconj. Chem.*, **2000**, *11*, 131-9.

(147) Pechar, M., Strohalm, J., Ulbrich, K. and Schacht, E. "Biodegradable Drug Carriers Based on Poly(ethylene glycol) Block Copolymers", *Macromol. Chem. Phys.*, **1997**, *198*, 1009-20.

(148) Rejmanova, P., Kopecek, J., Duncan, R. and Lloyd, J. B. "Stability in Rat Plasma and Serum of Lysosomally Degradable Oligopeptide Sequences in N-(2-hydroxypropyl)methacrylamide Copolymers", *Biomaterials*, **1985**, *6*, 45-8.

(149) Duncan, R., Cable, H. C., Lloyd, J. B., Rejmanova, P. and Kopecek, J. "Polymers Containing Enzymically Degradable Bonds. 7. Design of Oligopeptide Side-Chains in Poly[N-(2-hydroxypropyl)methacrylamide] Copolymers to Promote Efficient Degradation by Lysosomal Enzymes", *Makromol. Chem.*, **1983**, *184*, 1997-2008.

(150) Rejmanova, P., Kopecek, J., Pohl, J., Baudys, M. and Kostka, V. "Polymers Containing Enzymically Degradable Bonds. 8. Degradation of Oligopeptide Sequences in N-(2-hydroxypropyl)methacrylamide Copolymers by Bovine Spleen Cathepsin B", *Makromol. Chem.*, **1983**, *184*, 2009-20.

(151) Otto, H.-H. and Schirmeister, T. "Cysteine Proteases and Their Inhibitors", *Chem. Rev.*, **1997**, *97*, 133-71.

(152) Berdowska, I. "Cysteine Proteases as Disease Markers", *Clinica Chimica Acta*, **2004**, *342*, 41-69.

(153) MacKenzie, J. R., Mason, S. L., Hickford, J. G. H., Kohonen-Corish, M. R. J. and Bickerstaffe, R. "A Polymorphic Marker for the Human Cathepsin B Gene", *Molec. Cell. Probes*, **2001**, *15*, 235-7.

(154) Hermanson, G. T. "Bioconjugate Techniques"; Academic Press: San Diego, **1995**, 786 pp.

(155) Jue, R., Lambert, J. and Pierce, L. "Addition of Sulfhydryl Groups to *Escherichia coli* Ribosomes by Protein Modification with 2-Iminothiolane (Methyl 4-Mercaptobutyrimidate)", *Biochemistry*, **1978**, *17*, 5399-406.

(156) Lambert, J., Jue, R. and Traut, R. "Disulfide Cross-Linking of *Escherichia coli* Ribosomal Proteins with 2-Iminothiolane (Methyl 4-Mercaptobutyrimidate): Evidence That the Cross-Linked Protein Pairs are Formed in the Intact Ribosomal Subunit", *Biochemistry*, **1978**, *17*, 5406-16.

(157) Beyer, U., Roth, T., Schumacher, P., Maier, G., Unold, A., Frahm, A. W., Fiebig, H. H., Unger, C. and Kratz, F. "Synthesis and *In Vitro* Efficacy of Transferrin Conjugates of the Anti-Cancer Drug Chlorambucil", *J. Med. Chem.*, **1998**, *41*, 2701-8.

(158) Wetzel, R. and Halualani, R. "A General Method for Highly Selective Crosslinking of Unprotected Polypeptides via pH-Controlled Modification of N-Terminal α-Amino Groups", *Bioconj. Chem.*, **1990**, *1*, 114-22.

(159) Merrifield, R. B. "Solid Phase Peptide Synthesis. I. The Synthesis of a Tetrapeptide", *J. Am. Chem. Soc.*, **1963**, *85*, 2149-54.

(160) Atherton, E. and Sheppard, R. C. "Solid Phase Synthesis: A Practical Approach"; Oxford University Press: Oxford, **1989**, 203 pp.

(161) Jones, J. "Amino Acid and Peptide Synthesis"; Oxford University Press: Oxford, **1992**, 86 pp.

(162) Wang, S.-S. "*p*-Alkoxybenzyl Alcohol Resin and *p*-alkoxybenzyloxycarbonylhydrazide Resin for Solid Phase Synthesis of Protected Peptide Fragments", *J. Am. Chem. Soc.*, **1973**, *95*, 1328-33.

(163) Sieber, P. "An Improved Method for Anchoring of 9-Fluorenylmethoxycarbonyl-Amino Acids to 4-Alkoxybenzyl Alcohol Resins", *Tetrahedron Lett.*, **1987**, *28*, 6147-50.

(164) Kaiser, E., Colescott, R. L., Bossinger, C. D. and Cook, P. I. "Color Test for Detection of Free Terminal Amino Groups in the Solid-Phase Synthesis of Peptides", *Anal. Biochem.*, **1970**, *34*, 595-8.

(165) Duncan, R. "Polymer Therapeutics for Tumour Specific Delivery", *Chem. Ind.*, **1997**, 262-4.

(166) Devenish, S. PhD, University of Canterbury, **2004**.

(167) Borch, R. F., Bernstein, M. D. and Dupont Durst, H. "The Cyanohydridoborate Anion as a Selective Reducing Agent", *J. Am. Chem. Soc.*, **1971**, *93*, 2897-904.

(168) Baxter, E. W. and Reitz, A. B. "Reductive Aminations of Carbonyl Compounds with Borohydride and Borane Reducing Agents", *Organic Reactions*, **2002**, *59*, 1-714.

(169) Krueger, M., Beyer, U., Schumacher, P., Unger, C., Zahn, H. and Kratz, F. "Synthesis and Stability of Four Maleimide Derivatives of the Anticancer Drug Doxorubicin for the Preparation of Chemoimmunoconjugates", *Chem. Pharm. Bull.*, **1997**, *45*, 399-401.

(170) Mazzini, S., Mondelli, R. and Ragg, E. "Structure and Dynamics of Intercalation Complexes of Anthracyclines with d(CGATCG)2 and d(CGTACG)2. 2D-^{1}H and ^{31}P NMR Investigations", *J. Chem. Soc., Perkin Trans.*, **1998**, 1983-92.

(171) Loadman, P. M., Bibby, M. C., Double, J. A., Al-Shakhaa, W. M. and Duncan, R. "Pharmacokinetics of PK1 and Doxorubicin in Experimental Colon Tumor Models with Differing Responses to PK1", *Clin. Cancer Res.*, **1999**, *5*, 3682-8.

(172) Garsky, V. M., Lumma, P. K., Feng, D.-M., Wai, J., Ramjit, H. G., Sardana, M. K., Oliff, A., Jones, R. E., DeFeo-Jones, D. and Freidinger, R. M. "The Synthesis of a Prodrug of Doxorubicin Designed to Provide Reduced Systemic Toxicity and Greater Target Efficacy", *J. Med. Chem.*, **2001**, *44*, 4216-24.

(173) Říhová, B., Jelinkova, M., Strohalm, J., Subr, V., Plocova, D., Hovorka, O., Novak, M., Plundrova, D., Germano, Y. and Ulbrich, K. "Polymeric Drugs Based on Conjugates of Synthetic and Natural Macromolecules. II. Anti-Cancer Activity of Antibody or (Fab')2-Targeted Conjugates and Combined Therapy with Immunomodulators", *J. Controlled Release*, **2000**, *64*, 241-61.

(174) Ulbrich, K., Etrych, T., Chytil, P., Pechar, M., Jelinkova, M. and Rihova, B. "Polymeric Anticancer Drugs with pH-Controlled Activation", *Int. J. Pharm.*, **2004**, *277*, 63-72.

(175) McLennan, I. J., Lenkinski, R. E. and Yanuka, Y. "A Nuclear Magnetic Resonance Study of the Self-Association of Adriamycin and Daunomycin in Aqueous Solution", *Can. J. Chem.*, **1985**, *63*, 1233-8.

(176) Tamura, T., Wadhwa, M. S., Chiu, M. H., Da Silva, M. L., McBroom, T. and Rice, K. G. "Preparation of Tyrosinamide-Oligosaccharides as Iodinatable Glycoconjugates", *Methods Enzymol.*, **1994**, *247*, 43-55.

(177) Thomson, J. J. "Ionization by Moving Electrified Particles", *Philos. Mag.*, **1912**, *23*, 449-57.

(178) Fenn, J. B., Mann, M., Meng, C. K., Wong, S. F. and Whitehouse, C. M. "Electrospray Ionization for Mass Spectrometry of Large Biomolecules", *Science*, **1989**, *246*, 64-71.

(179) Tanaka, K., Waki, H., Ido, Y., Akita, S., Yoshida, Y. and Yohida, T. "Protein and Polymer Analyses up to m/z 100,000 by Laser Ionisation Time-of-Flight Mass Spectrometry", *Rapid Commun. Mass Spectrom.*, **1988**, *2*, 151-3.

(180) Chapman, J. R. "Protein and Peptide Analysis by Mass Spectrometry"; Humana Press: Totowa, **1996**, 350 pp.

(181) Mann, M., Hendrickson, R. C. and Pandey, A. "Analysis of Proteins and Proteomes by Mass Spectrometry", *Annu. Rev. Biochem*, **2001**, *70*, 437-73.

(182) Mann, M. and Wilm, M. "Electrospray Mass Spectrometry for Protein Characterization", *Trends Biochemical Sci.*, **1995**, *20*, 219-24.

(183) Aebersold, R. "A mass spectrometric journey into protein and proteome research", *J. Am. Soc. Mass Spectrom.*, **2003**, *14*, 685-95.

(184) Fenn, J. B. "Electrospray Wings for Molecular Elephants (Nobel Lecture)", *Angew. Chem. Int. Ed.*, **2003**, *42*, 3871-94.

(185) Muddiman, D. C., Bakhtiar, R., Hofstadler, S. A. and Smith, R. D. "Matrix-Assisted Laser Desorption/Ionization Mass Spectrometry: Instrumentation and Applications", *J. Chem. Educ.*, **1997**, *74*, 1288-92.

(186) Howard, G. C., Brown, W. E. and Editors. "Modern Protein Chemistry: Practical Aspects"; CRC Press: London, **2002**, 257 pp.

(187) Snyder, A. P. "Interpreting Protein Mass Spectra. A Comprehensive Resource"; Oxford University Press, Inc.: New York, New York, USA, **2000**, 522 pp.

(188) Kamp, R. M., Kyriakidis, D., Choli-Papadopoulou, T. and Editors. "Proteome and Protein Analysis"; Springer-Verlag: Berlin, **2000**, 372 pp.

(189) Shields, S. J., Oyeyemi, O., Lightstone, F. C. and Balhorn, R. "Mass Spectrometry and Non-covalent Protein-Ligand Complexes: Confirmation of Binding Sites and Changes in Tertiary Structure", *J. Am. Soc. Mass. Spectrom.*, **2003**, *14*, 460-70.

(190) Doroshenko, V. M., Laiko, V. V., Taranenko, N. I., Berkout, V. D. and Lee, H. S. "Recent Developments in Atmospheric Pressure MALDI Mass Spectrometry", *Int. J. Mass Spectrom.*, **2002**, *221*, 39-58.

(191) Dole, M., Mack, L. L., Hines, R. L., Mobley, R. C., Ferguson, L. D. and Alice, M. B. "Molecular Beams of Macroions", *J. Chem. Phys.*, **1968**, *49*, 2240-9.

(192) Mann, M., Meng, C. K. and Fenn, J. B. "Interpreting Mass Spectra of Multiply Charged Ions", *Anal. Chem.*, **1989**, *61*, 1702-8.

(193) Ferrige, A. G., Seddon, M. J., Green, B. N., Jarvis, S. A. and Skilling, J. "Disentangling Electrospray Spectra with Maximum Entropy", *Rapid Commun. Mass Spectrom.*, **1992**, *6*, 707-11.

(194) Redfield, C. and Dobson, C. M. "Proton NMR Studies of Human Lysozyme: Spectral Assignment and Comparison with Hen Lysozyme", *Biochemistry*, **1990**, *29*, 7201-14.

(195) Chen, Y., Mehok, A. R., Mant, C. T. and Hodges, R. S. "Optimum Concentration of Trifluoroacetic Acid for Reversed-Phase Liquid Chromatography of Peptides Revisited", *J. Chromatog. A*, **2004**, *1043*, 9-18.

(196) Mokotoff, M., Mocarski, Y. M., Gentsch, B. L., Miller, M. R., Zhou, J. H., Chen, J. and Ball, E. D. "Caution in the Use of 2-Iminothiolane (Traut's reagent) as a Cross-Linking Agent for Peptides. The Formation of N-peptidyl-2-iminothiolanes with Bombesin (BN) Antagonist (D-Trp6,Leu13-.psi.[CH_2NH]-Phe14)BN6-14 and D-Trp-Gln-Trp-NH_2", *J. Peptide Res.*, **2001**, *57*, 383-9.

(197) Singh, R., Kats, L., Blattler, W. A. and Lambert, J. M. "Formation of N-Substituted 2-Iminothiolanes When Amino Groups in Proteins and Peptides are Modified by 2-Iminothiolane", *Anal. Biochem.*, **1996**, *236*, 114-25.

(198) Rick, W. "Trypsin", *Methoden Enzym. Anal.*, **1974**, *1*, 1052-63.

(199) Kostka, V. and Carpenter, F. H. "Inhibition of Chymotrypsin Activity in Crystalline Trypsin Preparations", *J. Biol. Chem.*, **1964**, *239*, 1799-803.

(200) Pannell, L. K. "Peptide and Protein Software" http://sx102a.niddk.nih.gov/peptide.html

(201) Katritzky, A. R., Yao, J., Qi, M., Chou, Y., Sikora, D. J. and Davis, S. "Ring Opening Reactions of Succinimides", *Heterocycles*, **1998**, *48*, 2677-91.

(202) Okada, Y. and Iguchi, S. "Amino Acids and Peptides. Part 19. Synthesis of β-1- and β-2-Adamantyl Aspartates and their Evaluation for Peptide Synthesis", *J. Chem. Soc., Perkin Trans. 1*, **1988**, *8*, 2129-36.

(203) Kostidis, S., Stathopoulos, P., Chondrogiannis, N.-I., Sakarellos, C. and Tsikaris, V. "Aspartyl Methyl Ester Formation *via* Aspartimide Ring Opening: a Proposed Modification of the Protocols Used in Boc- and Fmoc-based Solid-Phase Peptide Synthesis", *Tetrahedron Letters*, **2003**, *44*, 8673-6.

(204) Xie, M., Vander Velde, D., Morton, M., Borchardt, R. T. and Schowen, R. L. "pH-Induced Change in the Rate-Determining Step for the Hydrolysis of the Asp/Asn-Derived Cyclic-Imide Intermediate in Protein Degradation", *J. Am. Chem. Soc.*, **1996**, *118*, 8955-6.

(205) O'Keefe, B. R. Personal Communication, **2002**.

(206) Arcamone, F., Franceschi, G., Penco, S. and Selva, A. "Adriamycin (14-hydroxydaunomycin), a Novel Antitumor Antibiotic", *Tetrahedron Lett.*, **1969**, *13*, 1007-10.

(207) Arnone, A., Fronza, G., Mondelli, R. and Vigevani, A. "Carbon-13 NMR Analysis of the Antitumor Antibiotics Daunorubicin and Adriamycin", *Tetrahedron Lett.*, **1976**, 3349-50.

(208) O'Hare, K. B., Duncan, R., Strohalm, J., Ulbrich, K. and Kopeckova, P. "Polymeric Drug-Carriers Containing Doxorubicin and Melanocyte-Stimulating Hormone: *In Vitro* and *In Vivo* Evaluation Against Murine Melanoma", *J. Drug Target.*, **1993**, *3*, 217-29.

(209) Seymour, L. W., Ulbrich, K., Steyger, P. S., Brereton, M., Subr, V., Strohalm, J. and Duncan, R. "Tumour Tropism and Anti-Cancer Efficacy of Polymer-Based Doxorubicin Prodrugs in the Treatment of Subcutaneous Murine B16F10 Melanoma", *Br. J. Cancer*, **1994**, *70*, 636-41.

(210) Drevs, J., Hofmann, I., Marme, D., Kratz, F. and Unger, C. "*In Vivo* and *In Vitro* Efficacy of an Acid Sensitive Albumin Conjugate of Adriamycin Compared to the Parent Compound in Murin Renal-Cell Carcinoma", *Drug Deliv.*, **1999**, *6*, 89-95.

(211) Duncan, R., Gac-Breton, S., Keane, R., Musila, R., Sat, Y. N., Satchi, R. and Searle, F. "Polymer-Drug Conjugates, Polymer-Directed Enzyme Prodrug Therapy (PDEPT) and (Polymer-Enzyme Liposome Therapy) PELT: Basic Principles for Design and Transfer from the Laboratory to Clinic", *J. Controlled Release*, **2001**, *74*, 135-46.

(212) Maniez-Devos, D. M., Baurain, R., Lesne, M. and Trouet, A. "Degradation of Doxorubicin and Daunorubicin in Human and Rabbit Biological Fluids", *J. Pharm. Biomed. Anal.*, **1986**, *4*, 353-65.

(213) Beijnen, J. H., Van der Houwen, O. A. G. J. and Underberg, W. J. M. "Aspects of the Degradation Kinetics of Doxorubicin in Aqueous Solution", *Int. J. Pharm.*, **1986**, *32*, 123-31.

(214) Janssen, M. J. H., Crommelin, D. J. A., Storm, G. and Hulshoff, A. "Doxorubicin Decomposition on Storage. Effect of pH, Type of Buffer and Liposome Encapsulation", *Int. J. Pharm.*, **1985**, *23*, 1-11.

(215) Subr, V., Strohalm, J., Ulbrich, K., Duncan, R. and Hume, I. C. "Polymers Containing Enzymically Degradable Bonds, XII. Effect of Spacer Structure on the Rate of Release of Daunomycin and Adriamycin from Poly[N-(2-hydroxypropyl)methacrylamide] Copolymer Drug Carriers *In vitro* and Antitumor Activity Measured *In vivo*", *J. Controlled Release*, **1992**, *18*, 123-32.

(216) Sharman, W. M., van Lier, J. E. and Allen, C. M. "Targeted Photodynamic Therapy *via* Receptor Mediated Delivery Systems", *Adv. Drug Deliv. Rev.*, **2004**, *56*, 53-76.

(217) Kragh-Hansen, U., Chuang, V. T. G. and Otagiri, M. "Practical Aspects of the Ligand-binding and Enzymatic Properties of Human Serum Albumin", *Biol. Pharm. Bull.*, **2002**, *25*, 695-704.

(218) Kratz, F., Müller-Driver, R., Hofmann, I., Drevs, J. and Unger, C. "A Novel Macromolecular Prodrug Concept Exploiting Endogenous Serum Albumin as a Drug Carrier for Cancer Chemotherapy", *J. Med. Chem.*, **2000**, *43*, 1253-6.

(219) Babson, A. L. and Winnick, T. "Protein Transfer in Tumor-Bearing Rats", *Cancer Res.*, **1954**, *14*, 606-11.

(220) Maeda, H., Ueda, M., Morinaga, T. and Matsumoto, T. "Conjugation of Poly(styrene-co-maleic acid) Derivatives to the Antitumor Protein Neocarzinostatin: Pronounced Improvements in Pharmacological Properties", *J. Med. Chem.*, **1985**, *28*, 455-61.

(221) Kratz, F., Drevs, J., Bing, G., Stockmar, C., Scheuermann, K., Lazar, P. and Unger, C. "Development and *in vitro* Efficacy of Novel MMP2 and MMP9 Specific Doxorubicin Albumin Conjugates", *Bioorg. Med. Chem. Lett.*, **2001**, *11*, 2001-6.

(222) Trouet, A., Masquelier, M., Baurain, R. and Deprez-De Campaneere, D. "A Covalent Linkage Between Daunorubicin and Proteins that is Stable in Serum and Reversible by Lysosomal Hydrolases, as Required for a Lysosomotropic Drug-Carrier Conjugate: *In Vitro* and *In Vivo* Studies", *Proc. Natl. Acad. Sci. USA*, **1982**, *79*, 626-629.

(223) Bures, L., Bostik, J., Motycka, K., Spundova, M. and Rehak, L. "The Use of Protein as a Carrier of Methotrexate for Experimental Cancer Chemotherapy. III. Human Serum Albumin-Methotrexate Derivative, its Preparation and Basic Testing", *Neoplasma*, **1988**, *35*, 329-42.

(224) Warnecke, A. and Kratz, F. "Maleimide-oligo(ethylene glycol) Derivatives of Camptothecin as Albumin-Binding Prodrugs: Synthesis and Antitumor Efficacy", *Bioconj. Chem.*, **2003**, *14*, 377-87.

(225) Crowther, J. R. "ELISA: Theory and Practice"; Humana Press: Totowa, **1995**, 223 pp.

(226) Boyd, M. R. and Paull, K. D. "Some Practical Considerations and Applications of the National Cancer Institute *in vitro* Anticancer Drug Discovery Screen", *Drug Develop. Res.*, **1995**, *34*, 91-109.

(227) Northcote, P. T., Blunt, J. W. and Munro, M. H. G. "Pateamine: a Potent Cytotoxin from the New Zealand Marine Sponge, *Mycale* sp", *Tet. Lett.*, **1991**, *32*, 6411-4.

(228) Rzasa, R. M., Shea, H. A. and Romo, D. "Total Synthesis of the Novel, Immunosuppressive Agent (-)-Pateamine A from *Mycale* sp. Employing a β-Lactam-Based Macrocyclization", *J. Am. Chem. Soc.*, **1998**, *120*, 591-2.

(229) Pattenden, G., Critcher, D. J. and Remuinan, M. "Total Synthesis of (-)-Pateamine A, a Novel Immunosuppressive Agent from *Mycale* sp." *Can. J. Chem.*, **2004**, *82*, 353-65.

(230) Nichifor, M., Schacht, E. H. and Seymour, L. W. "Polymeric Prodrugs of 5-Fluorouracil", *J. Controlled Release*, **1997**, *48*, 165-78.

(231) Putnam, D. and Kopecek, J. "Enantioselective Release of 5-Fluorouracil from N-(2-Hydroxypropyl)methacrylamide-Based Copolymers *via* Lysosomal Enzymes", *Bioconjugate Chem.*, **1995**, *6*, 483-92.

(232) Moore, K. S., Wehrli, S., Roder, H., Rogers, M., Forrest Jr, J. N., McCrimmon, D. and Zasloff, M. "Squalamine: An Aminosterol Antibiotic from the Shark", *Proc. Natl. Acad. Sci. USA*, **1993**, *90*, 1354-8.

(233) Choucair, B., Dherbomez, M., Roussakis, C. and El Kihel, L. "Synthesis of 7α- and 7β-Spermidinylcholesterol, Squalamine Analogues", *Bioorg. Med. Chem. Lett.*, **2004**, *14*, 4213-6.

(234) Barthwal, R., Srivastava, N., Sharma, U. and Govil, G. "A 500 MHz Proton NMR Study of the Conformation of Adriamycin", *J. Mol. Struct.*, **1994**, *327*, 201-20.

(235) Weislow, O. S., Kiser, R., Fine, D. L., Bader, J., Shoemaker, R. H. and Boyd, M. R. "New Soluble-Formazan Assay for HIV-1 Cytopathic Effects: Application to High-Flux Screening of Synthetic and Natural Products for AIDS-Antiviral Activity", *J. Natl. Cancer Inst.*, **1989**, *81*, 577-86.

(236) Gulakowski, R. J., McMahon, J. B., Staley, P. G., Moran, R. A. and Boyd, M. R. "A Semiautomated Multiparameter Approach for Anti-HIV Drug Screening", *J. Virol. Meth.*, **1991**, *33*, 87-100.

(237) Alley, M. C., Scudiero, D. A., Monks, A., Hursey, M. L., Czerwinski, M. J., Fine, D. L., Abbott, B. J., Mayo, J. G., Shoemaker, R. H. and Boyd, M. R. "Feasibility of Drug Screening with Panels of Human Tumor Cell Lines Using a Microculture Tetrazolium Assay", *Cancer Res.*, **1988**, *48*, 589-601.

"Life should NOT be a journey to the grave with the intention of arriving safely in an attractive and well preserved body, but rather to skid in sideways, Champagne in one hand - oysters in the other, body thoroughly used up, totally worn out, and screaming WOO HOO - What a Ride!"